HEALTH MONITORING OF SUBMERGED PLATES USING ULTRASONIC GUIDED WAVES

A

Thesis

Submitted in fulfillment of the requirement

For the award of degree of

DOCTOR OF PHILOSOPHY

By

SANDEEP KUMAR SHARMA

Regd. No 90608503

SUPERVISOR

Dr. Abhijit Mukherjee

Professor, Civil Engineering Department

Curtin University, Bentley, WA 6102, Australia

DEPARTMENT OF MECHANICAL ENGINEERING

THAPAR UNIVERSITY, PATIALA-147004

2014

CERTIFICATE

Certified that the work presented in the thesis titled, **"HEALTH MONITORING OF SUBMERGED PLATES USING ULTRASONIC GUIDED WAVES"** which is being submitted by **Mr. Sandeep Kr. Sharma**, **Regd. No 90608503**, in fulfillment of the requirement for the award of the degree of 'Doctor of Philosophy' in the Department of Mechanical Engineering, Thapar University, Patiala, is an authentic record of the candidate's own work carried out from May- 2008 to June- 2014 in this university under my supervision. The matter presented in this thesis has not been submitted for the award of any other degree in any other university.

(Dr. Abhijit Mukherjee)

Professor

Civil Engineering Department

Curtin University, Bentley, WA 6102

Australia

ACKNOWLEDGEMENTS

Time has provided me cherished opportunity to express feelings of gratefulness and submit my acknowledgements for those who helped me earning this day in my life. First and foremost, I wish to express my deep sense of gratitude with reverence towards my supervisor **Prof. Abhijit Mukherjee**, Professor, Department of Civil Engineering, Curtin University, Bentley, Australia, for his valuable guidance and inspiring encouragement in pursuance of this work. Despite his busy schedule, he always spared time for me and his guidance, precious and genial, which always kept me on the right track. I shall remain grateful to him for providing valuable and remarkable support throughout my research work. I am indeed highly indebted to him for his support and thought provoking suggestions during many exigent circumstances. His systematic approach and unconditional co-operation made me work hard. It was a great pleasure working with him and for me; it is the beginning of research. I shall remain grateful to him forever.

I am also very thankful to Dr. Ajay Batish, Prof. & Head, Department of Mechanical Engineering for providing excellent academic environment and encouragement throughout my work. I have no words to express my sincere gratitude to Dr. Naveen Kwatra, Associate Professor and Head, Civil Engineering Department for providing me laboratory facilities for experimentation in the Structural Dynamics Laboratory and Concrete Structures Laboratory of the Civil Engineering Department. I am also extremely thankful to the staff of these laboratories. Without their active support and enthusiasm, it would not have been possible to carry out the experimental work. I am extremely thankful to Sh. Ram Sumiran and Sh. Varinder Kumar and all other manpower for their support and much needed help.

Constructive suggestions and help of my students, Mr. Raghuram, Mr. S. Arjun, Mr. Sameer Sharma and Mr. Gurjot Singh Dhaliwal towards amelioration of this work are deeply acknowledged. I am highly obliged to them for their support in carrying out present research work.

Thanks are also due to my senior colleagues Dr. S.K. Mohapatra, Dean of Academic Affairs and Dr. S.P. Nigam, Visiting Professor Mechanical Engineering Deptt. whose motivating words and encouragement always kept me rolling. I am also grateful to the Dr.

P.K. Bajpai, Dean (RSP) for giving me the opportunity, co-operation and support in pursuing this work. I also thank all my fellows, friends, colleagues at Thapar University and relatives who directly or indirectly helped me carry out this research.

I am indeed indebted to my parents, Sh. Hari Om Sharma and Ms. Darshana Sharma and my parent in-laws, Dr. V.R Sharma and Ms. Sneh Sharma without whose encouraging words and timely support this would not have been possible. I am also thankful to my brother, Mr. Mandeep Sharma for providing emotional support and help whenever required. Thanks are also due to my brother in-laws, Sh. Munish Kaushal, Dr. Paras Khullar, Dr. Sumit Bedi & Er. Mayank for their encouraging words. My sisters, Dr. Ritu Kaushal, Dr. Smriti Khullar, Dr. Sonali Bedi and Ms. Deepti Sharma also require a special mention for providing cheerful support during the tenure of my work.

I owe special thanks to my sons, Sanyam and Satyam for patiently bearing inattentiveness towards them during my doctoral work. I acknowledge my heartiest gratitude to my wife and best colleague, Dr. Shruti Sharma, without whose untiring support, enduring patience and valuable suggestions, I would ever have been able to complete this work successfully.

Last but not the least, I wish to express my thanks to all those who remained behind the screen but whose work has been quoted and consulted in the present research. In the end, I am thankful and grateful to the Almighty for bringing this day in my life.

(Sandeep K. Sharma)

ABSTRACT

Several offshore and marine infrastructural systems involve plate like members in submerged condition and are often subjected to extreme service and environmental conditions leading to deterioration in the form of corrosion loss, fatigue cracking and other mechanical degradations. Submerged condition of such structures often makes them inaccessible for various established non-destructive technologies. Most of these conventional techniques approaches require interruption of normal service and removal of the subject structure from submerged condition. The prohibitive out-of-service inspection costs restrict the frequency of such investigations, thus exposing them to a great risk of unnoticed fatal damages. Hence, there is a need to supplement or replace these methods with an efficient, reliable, in-situ, non-contact and non-destructive monitoring technique for submerged plate assemblies. The present work reports a laboratory study using a pair a mobile non-contact probes arranged in pitch-catch orientation employing immersion coupling utilizing Leaky Lamb waves for assessing and characterizing notch and corrosion damages in submerged plates.

The propagation characteristics of the different Lamb wave modes in a submerged plate are studied. The longitudinal wave excited by cylindrical transducer falls obliquely on the submerged plate using surrounding water as natural couplant. The transmitted signal is received by other transducer after it has traversed through the length of the plate. Use of water coupled transducers makes the system non-contact and non-invasive. Interaction of propagating waves with the simulated damages in the form of machined notches has been studied. By comparing the transmitted signals of the healthy plate with that of the notched plate, damage monitoring technique is developed. Specific Lamb wave modes sensitive to near surface and sub-surface damages have been identified. These modes are further exploited for non-contact scanning of the plates to identify and quantify the presence as well as extent of damage. Effective combination of specific Lamb wave modes leads to comprehensive inspection of the submerged plate structures. Exact location of the damage is ascertained by pulse echo monitoring of the plate. Post processing of the ultrasonic data generated from scanning the plate has been pictorially represented in the form of defect maps.

The developed methodology is further successfully applied for monitoring progressive accelerated corrosion in submerged plates. It is observed that corrosion in submerged plates is discernible using ultrasonic guided waves. Through a judicious selection of different Lamb wave modes, not only the corrosion phenomenon can be monitored but also different effects and mechanisms of corrosion can be successfully identified. Combination of the selected guided wave modes could also discern uniform and pitting corrosion in submerged plates. Along with the ultrasonic signals, mass loss, stress-strain behavior and tensile strength of the plates at different stages of corrosion have been monitored. Semi-empirical relationships between the ultrasonic readings and other parameters have been developed. This investigation should be useful in developing a non-contact, non-invasive and non-destructive technique for monitoring progressive corrosion in plates and assessing their deterioration in strength, stiffness and mass loss that would help in the estimation of residual life. The methodology has the potential to develop into a commercially viable real time, non-invasive and in-service corrosion monitoring and evaluation tool for large submerged structures as in marine installations.

LIST OF PUBLICATIONS

- Sharma S., Mukherjee A., "*Damage detection in submerged plates using ultrasonic guided waves*", Sadhana, October 2014, Volume 39, Issue 5, pp 1009-1034 **DOI 10.1007/s12046-014-0255-4**.
- Sharma S., Mukherjee A., *" A Non-Contact Technique for Damage Detection in Submerged Plates using Guided Waves"*, Journal of Testing And Evaluation, Volume 43, Issue 4 (July 2015), **DOI:10.1520/JTE20120357**
- Sharma S., Mukherjee A., "*Ultrasonic Guided Wave for Corrosion Monitoring in Submerged Plates*", Structural Control and Health Monitoring, DOI **10.1002/stc.1657.**
- Mukherjee A., Sharma S. and Sharma, S., "*Corrosion Monitoring in Infrastructures Using Ultrasonic Wave Propagation*", 23rd Australian Conference on Mechanics of Structures and Materials ACMSM23, 9-12th December, 2014, Byron Bay, Australia, **Accepted for Publication.**
- Sharma S., Sharma, S. and Mukherjee A., "*Discovering Hidden Structural Degradations*", Proceedings of the International Symposium on Engineering under Uncertainty: Safety Assessment and Management (ISEUSAM - 2012), ISBN: 978-81-322-0756-6 (Print) 978-81-322-0757-3 (Online) DOI 10.1007/978-81-322-0757-3, pp179-193, 2013
- Sharma S., Mukherjee A., "*Ultrasonic Guided wave approach for damage monitoring in plate structures*" SMIRT-2011, International Association for structural Mechanics in Reactor Technology, ISBN: 978-1-62276-343-6, 2011, pp. 3463-70
- Sharma S., Sharma, S.K. and Mukherjee A., "*Ultrasonic Investigations of Embedded and Submerged Components"*, International Conference on Theoretical, Applied, Computational and Experimental Mechanics, ICTACEM , December 27-29, 2010, IIT Kharagpur, India, pp 25-28
- Sharma S., Mukherjee A., "*Defect Detection In Plated Structures Using Ultrasonic Guided Waves*", Journal of Pure and Applied Ultrasonics, ISSN 0256- 4637, Vol. 31 (No. 3), October-Dec, 2009
- Mukherjee A., Sharma S., Sharma S., "*Health Monitoring of Steel Structures using Ultrasonic Waves*", INSDAG Year Book-2009.

CONTENTS

ABBREVIATIONS AND SYMBOLS USED

DOF	Degree Of Freedom
D_P	Propagation distance
DPR	Defect Reflection Peak
DRO	Digital Read Out
D_w	Water path
f	Frequency of sound waves
f_t	Tensile Strength
ML	Mass Loss
NDE	Non-Destructive Evaluation
PC	Pitch Catch
PE	Pulse Echo
PR	Pulse Receiver
PT	Pulse Transmission
SHM	Structural Health Monitoring
T_t	Time of arrival of transmitted pulse in PT signature
t_w	Time of flight in water
t_w`	Average time of flight in water for both transmitter and receiver probes
$t_{w\ left}$	Time of flight in water for left probe

$t_{w\ right}$	Time of flight in water for right probe
v	Velocity of sound waves
V_{gr}	Group velocity
V_n	Normalized peak to peak amplitude ratio
V_p	Peak to peak voltage amplitude
V_{ph}	Phase velocity
V_w	Longitudinal velocity of sound in water
θ	Angle of the probe with the vertical
λ	Wavelength of sound waves

LIST OF FIGURES

LIST OF TABLES

CHAPTER 1

INTRODUCTION

1.1 BACKGROUND AND MOTIVATION

Several offshore and marine infrastructural systems involve plate like members in submerged condition and are often subjected to extreme service and environmental conditions leading to deterioration in the form of corrosion loss, fatigue cracking and other mechanical degradations. Submerged condition of such structures often makes them inaccessible for various established non-destructive technologies. If the deteriorations remain unnoticed they may result in catastrophic failures causing huge loss to human life and property. In order to avoid any severe loss of integrity of such structures, real time health monitoring is very important.

Several non-destructive evaluation (NDE) techniques have been used over the years to identify damages in structures involving plate like members. These include dye penetrant, magnetic particle inspection, magnetic resonance imagery, laser interferometry, pressure testing, infrared thermography, eddy currents, acoustic emission and radiography. Most of the approaches require interruption of normal service and removal of the subject structure from submerged condition. For example, to inspect a ship it needs to be in dry dock. The prohibitive out-of-service inspection costs restrict the frequency of such investigations, thus exposing them to a great risk of unnoticed fatal damages. Hence, there is a need to supplement or replace these methods with an efficient, reliable, in-situ, non-contact and non-destructive monitoring technique for submerged plate assemblies.

Traditionally, ultrasonic bulk waves have been used as a reliable means to monitor the state of health of structures. But the use of ultrasonic bulk waves is limited due to its inability to quickly scan large domains. For applications involving large area inspection in a quick way, ultrasonic guided waves have been suggested by various researchers as an effective and viable tool especially in discovering hidden anomalies. Ultrasonic guided waves have the characteristic ability to propagate over long distances and hence may quickly provide global information. They have low attenuation even when propagating in water loaded structures. Due to their unique propagation characteristics, guided waves have been used for damage detection and inspection in a variety of applications like strips and plates, boiler and heat

exchanger pipes, K-joints in offshore structures and plate assemblies, spot welds, cylindrical embedded reinforcing bar systems as in concrete applications etc. (Lehfeldt and Holler, 1967; Ball and Shewring, 1976; Manfield, 1975; Silk and Bainton, 1979; Rokhlin and Bendec, 1983 ; Alleyne and Cawley 1991, Alleyne and Cawley 1992; Ditri and Rose 1994; Ghosh et al. 1998; Sharma and Mukherjee 2011 a,b; 2013). But in all these works, the subject structure is placed in air and transducers are required to be in contact with the structure being monitored. Owing to the several practical limitations in direct contact approach and to exploit mode specific behavior of guided waves to advantage, some researchers have suggested local water column as an effective means to couple the structure with the transducer (Ghosh et al. 1998, Na and Kundu, 2002a, b). Although guided waves in plates, called Lamb waves, offer a quick and effective means of health monitoring but they are difficult to interpret. So it is very important to understand the key impediments of using the Lamb waves as potential health monitoring tool viz. - dispersive behavior of various modes and presence of multiple modes for a given frequency and plate thickness especially in submerged systems.

Literature of last three decades has established the capability of guided waves for damage detection in plates. However, a fast, in-situ and non-contact health monitoring methodology for real time damage assessment of submerged plate structures as in marine installations is still not developed. In this work, a non-contact inspection technique utilizing ultrasonic guided waves for damage monitoring in submerged plates is presented. The propagation characteristics of ultrasonic guided waves in healthy submerged plates are first investigated. Signals are then obtained in immersed plate having notches of varying depths. By comparing the signals of the notched plate with that of the healthy plate the damage monitoring technique is developed. Specific guided Lamb wave modes sensitive to near-surface and sub-surface defects are identified. These modes are further exploited for non-contact scanning of the plates to identify and quantify the presence as well as extent of damage. Effective combination of specific Lamb wave modes leads to comprehensive inspection of the submerged plate structures. Post processing of the data generated from scanning the plate defects has been pictorially represented in the form of defect maps. Proposed technique has the potential to develop into real time health monitoring and evaluation tool for submerged structures.

Another issue in marine infrastructural installations as in ships is that they have a propensity to travel globally and as such they experience the extremes of oceanic environments. Marine conditions combine the catastrophic effects of saline seawater, rain,

dew, condensation, salt laden air, localized high temperature and the corrosive effects of combustion gases and constitute one of the most insidious environments. Tropical marine environments as experienced in Indian conditions are far more corrosive than cold European climates because the temperature has a significant impact on the rate of corrosion. Hence, there is an urgent need for developing a corrosion monitoring and assessment technique for marine structures. The developed methodology for notches in plates is further successfully applied for monitoring progressive corrosion in submerged plates. Along with the ultrasonic signals, mass loss, stress-strain behavior and tensile strength of the plates at different stages of corrosion have been monitored. Semi-empirical relationships between the ultrasonic readings and other parameters have been developed. This investigation should be useful in developing a non-destructive technique for monitoring progressive corrosion in plates and assessing their deterioration in strength, stiffness and mass loss that would help in the estimation of residual life. The present work will pave the way for developing an efficient non-destructive technique for monitoring corrosion in submerged, especially marine infrastructural installations.

1.2 EXISTING DAMAGE/CORROSION MONITORING METHODOLOGIES

A non-contact and real time health monitoring of plate assemblies as in case of ship hulls and other marine components for damages like cracks, dents and corrosion is very important to avoid any compromise to the integrity of these structures. At the same time, “out of service “costs are highly punitive to go in for frequent inspections. Various non-destructive techniques to assess in- service damages and corrosion in marine structures are listed below:

- Visual Inspection
- Magnetic particle inspection
- Magnetic flux leakage technique
- Eddy currents
- Pressure testing
- Magnetic resonance imagery
- Laser interferometry
- Acoustic Emission (AE) technique
- Penetrating gamma and X-rays
- Thermo graphic imaging or time-resolved thermography

- Holographic interferometry
- Sensors such as galvanic thin film, electrochemical sensors, chemical sensor etc.

However, implementation of these techniques requires the interruption of normal service and removal of the subject structure from submerged condition which is very uneconomical. These techniques provide only idea about the initiation and presence of damage but the quantification still remains a vital issue. The infrastructure involved in measurement is bulky. They are either too expensive or they require highly skilled personnel or have limited practical applications like in radiography, thermography and acoustic tomography. So the health monitoring of plates in marine infrastructures needs a method which can determine simply, accurately, and non-destructively not only whether or not deterioration is taking place but also the extent of damage and its characterization.

Hence, there is a need to develop a non-destructive damage monitoring technique for plates in submerged conditions typically for corrosion induced damages that can replace or supplement the prevalent techniques. Present work is an attempt to develop a complete damage monitoring methodology for steel plate structures in submerged state using ultrasonic guided waves.

1.3 ULTRASONIC GUIDED WAVES – A POTENTIAL SOLUTION

Currently used methods for non-destructive testing and damage evaluation of submerged plates assemblies as discussed above are indirect indicators of likelihood of damage or corrosion. These cannot be used for large structures either due to scale up problems or huge costs associated with their implementation and maintenance. Corrosion, if undiscovered can cause catastrophic failure of the structure. A wide range of techniques have been reported in the literature that may be suitably employed for the monitoring of corrosion in marine structure for diagnosing the cause and extent of corrosion. But all these techniques suffer from various practical limitations. Therefore, it is imperative to develop a non-intrusive and a non-contact technique for monitoring state of health of plates forming marine infrastructure.

Ultrasonic bulk waves have been used in the past as an effective method to monitor the health of various kinds of structures. Bulk wave's travel within the interior of a material away from any boundaries, exhibit a finite number of wave modes and have small wavelengths compared to the dimensions of the object being inspected. The state of health of the structure is judged on the basis of parameters like transmission amplitudes, traveling time,

and attenuation of received signals. Time of flight can also be used to locate the damage and quantify the amplitude of the reflected signal so as to assess the severity of the damage. But the bulk waves have limited scanning capabilities which is mainly attributed to rapid loss of energy due to bulk material attenuation. Guided waves have come up as a promising option for effective and reliable monitoring of relatively larger domains. Guided waves exhibit strong penetration, fast propagation, omni-directional dissemination, convenience of activation and acquisition, inexpensive implementation and most importantly, high sensitivity to structural damage and material in-homogeneities even when they are small in size or lie beneath the surface. Due to these unique propagation characteristics, guided waves have been effectively used for damage detection in a variety of applications involving plate, pipe and rod geometries. In most of these applications the subject structure is placed in air and transducers are required to be in direct contact with the structure being monitored.

Guided waves in the plates called Lamb waves can be predominantly excited (while subduing other modes) by offering the longitudinal incident ultrasonic wave obliquely to the plate at a particular angle of incidence. This can be accomplished by using – 'Variable Angle Probes' and ‘Immersion Coupling’. Former technique is a contact type arrangement, in which a variable angle probe riding on lateral surface of a Perspex semi-cylinder transmits energy into the subject plate. Perspex block is coupled to the plate by a thin layer of gel. But this contact system is not suitable for submerged applications. Moreover, measurements are unreliable mainly due to the inadvertent variations in the contact pressure and couplant thickness. Owing to the several practical limitations in direct contact approach and to exploit mode specific behavior of Lamb waves to advantage, some researchers have suggested to use immersion coupling by employing local water column as an effective means to couple the structure with the transducer. However, in case of submerged structures, presence of water makes the situation unique and challenging as it acts as a natural couplant. A quick, in-situ and non-contact health monitoring methodology for real time damage assessment of submerged plate structures as in marine installations is still not reported .

Present work is focused on developing a non-contact inspection technique utilizing ultrasonic guided waves for damage monitoring in submerged plates. The proposed technique has the potential to develop into real time health monitoring and evaluation tool for submerged structures. A pair of mobile transducers placed in ‘pitch catch’ orientation employing Immersion coupling has been used. The surrounding water acts as a carrier of incident ultrasonic energy from the probe to the plate. In order to excite a specific Lamb wave

mode, a transmitter probe inclined at a specific angle injects incident energy in the plate. Receiver is also placed in the same orientation as the transmitter. It makes the receiver most sensitive to the wavelength of the mode being input. It results in the receiver highlighting the preferred mode and suppressing the others. This set-up has been used to generate and acquire the propagating guided Lamb waves through the healthy submerged plate. Subsequently, plates with damages in the form of machined notches of varying depths inflicted on them have been tested. Specific Lamb wave modes sensitive to near surface and sub-surface damages have been identified. Experimental data captured using pulse echo and pulse transmission techniques has been used effectively in combination to identify, locate and quantify the various kinds of notch damages oriented in different configuration, i.e. notches place normal and obliquely to the direction of propagation, multiple notches, notches of varying depths etc. Ultrasonic signal data is further used to generate defect maps. The technique is also successfully applied to submerged plates undergoing progressive corrosion. After exposure to different corrosive environments for specified durations, the plates are subjected to destructive tests to determine mass loss, tensile strength and stress-strain characteristics. Calibration of ultrasonic test data is done with destructive tests to relate the ultrasonic voltages measured at a particular instant to the physical condition of the plate in terms of residual mass and tensile strength. An attempt has been made to facilitate non-destructive evaluation of plates undergoing corrosion and estimate the residual life of structures.

1.4 AIMS AND OBJECTIVES

The aim of the present work is to develop a damage monitoring methodology for steel plates as in marine structures using guided wave propagation. The developed technique should detect, localize and finally quantify the extent of deterioration in submerged steel plates. However, key technologies must be established before the Lamb waves are effectively utilized in the monitoring submerged steel plates. A large number of specimens must be investigated with different amounts and rates of damage, different extents and locations of damages etc. and characterization of the same needs to be done. Hence, the objectives of the present work can be outlined as:

- Investigation of propagation of guided Lamb waves through healthy and damaged submerged plate specimens
- Map the wave signatures with the defects
- Determination of sensitivity of waves to typical damages

- Post processing of the data to develop defect maps
- Application of the developed methodology to plates undergoing corrosion
- Calibration of the ultrasonic signals with physical parameters and development of semi-empirical relationships.
- Recommend a non-invasive, non-contact and in-situ damage monitoring methodology for submerged plates.

1.5 LAYOUT OF THE THESIS

From the study carried out in this work, the thesis is organized in the following chapters:

In **Chapter 1,** the significance and need for a non-invasive and in-situ damage monitoring technique for submerged plate assemblies is established by highlighting the drawbacks of the existing methods and introduction to ultrasonic guided waves is established.

Chapter 2 highlights the theory and background of ultrasonic guided waves in plates called Lamb waves and discusses the key issues in the use of Lamb waves for damage detection in infrastructures. It also outlines the brief corrosion mechanism in submerged structures plates and reviews the various methods for monitoring the same.

Chapter 3 brings out the review of the latest works done till date in the use of Lamb waves for damage detection in plate structures and corrosion monitoring in structures have been compiled.

A detailed non-invasive and non-contact experimental set-up is developed for generation and propagation of guided waves in submerged plates and the experimental study on propagation characteristics of various ultrasonic guided wave modes in submerged plates is presented in **Chapter 4.**

The investigated Lamb wave modes in submerged plates are utilized for damage detection using pulse transmission method of Ultrasonic Testing. The damages are inflicted in the form of machined notches in plates and typical modes sensitive to surface and sub-surface damages are identified to develop a defect detection strategy in plates in **Chapter 5.**

In **Chapter 6,** damage detection methodology developed above is extended to plates undergoing accelerated corrosion. Ultrasonic nondestructive testing data is calibrated with destructive test parameters of tensile strength and mass loss to facilitate a correlation between the two.

Chapter 7 establishes the non-contact and non-invasive technique for damage investigations in submerged system using combination of Pulse Transmission and Pulse Echo Techniques to

generate defect maps. Various case studies involving normal and oblique notches, corroded plates etc. have been presented.

Chapter 8 summarizes the entire work and conclusions derived from the study are reported. Future scope of work in the area is also highlighted.

CHAPTER 2

GUIDED WAVES FOR DAMAGE MONITORING IN PLATES

2.1 INTRODUCTION

Although many NDE (Non-Destructive Evaluation) techniques such as liquid penetrant dye, radiography, holography, thermography, X-ray, eddy current, magnetic flux, are available but elastic wave based techniques have found more acceptability for Structural Health Monitoring (SHM) applications. This regime involves use of active or passive wave propagation through the subject structure to evaluate the state of health.

Active wave propagation techniques require high-frequency external excitation. A very low energy level, high frequency 'stress pulse' or 'wave packet' is injected into a structure and its wave propagation parameters (like reflection, transmission, attenuation etc.) are observed and employed for evaluating state of health of the structure. Generation and detection of the stress waves is generally based on piezoelectric effect. Passive wave propagation health monitoring techniques does not require any external excitation and rely on structure borne noticeable sonic and ultrasonic waves that are generated during crack initiation and propagation which propagate fairly large distances through the structure under investigation and can be detected by a structure mounted sensors. Presence, extent and location of damage in the structure can be ascertained by analyzing the received signal.

Reliability and availability are the key features of these techniques. The Acousto-Ultrasonic approach combines the both; Ultrasonic Inspection (active) and Acoustic Emission (passive). In the present work, ultrasonic wave propagation has been considered. Ultrasonic waves are of vibrational waves having frequencies greater than 20 kHz, the human audible range. Though, the range of frequency of these waves can be as high as 15-20 GHz, but for practical SHM applications, frequency rarely exceeds 20MHz. SHM using ultrasonic guided waves does not result into geometric modification of the subject structure as the applied loading of the propagating waves is within elastic limits. Employing ultrasonic wave propagation as a means for monitoring the soundness/ health of structure involves the propagation of acoustic waves through structures. The wave characteristics change due to the deterioration in the structure and they are sensitive to the location, extent and character of

damage. However, for successful monitoring a prior knowledge of the effect of various types of damage on the wave characteristic is imperative.

In this work, it is proposed to use ultrasonic guided waves for damage monitoring in submerged plates as in case of offshore and marine applications. Various kinds of defects in the form of machined notches and plates undergoing actual corrosion in submerged conditions are considered. This chapter presents a brief overview of the use of ultrasonic waves for damage monitoring. Various types of ultrasonic waves, basic testing principles and types of ultrasonic testing procedures is outlined to understand the basics of ultrasonic wave propagation based methods for SHM. A brief overview of the corrosion mechanism in marine structures is also presented to understand its effect and implications for successfully developing a corrosion monitoring methodology in the following chapters.

2.2 ULTRASONIC WAVES

Ultrasonic waves are structured mechanical vibrations which can propagate through solid, liquid, or gas. For a given medium, these waves will have unique propagation characteristics and when they encounter a boundary with a different medium they will be reflected or transmitted. This is the principle of physics that underlies ultrasonic flaw detection.

Elastic waves of all frequency ranges viz. ultrasonic, sonic and subsonic that propagate in a medium -can be broadly categorized into two groups: Body waves or Bulk waves and Surface waves or Guided waves **(Figure 2.1)**. Body or bulk waves travel through the interior of a structure without interaction with edges or boundaries. So bulk waves travel in any elastic structure acting as an infinite extent of material. Velocity of waves in materials depends on the elastic properties and can be calculated by measuring the time of flight between the two given points. Defects like discontinuities, cracks and voids can be detected by signal attenuation or change in time of flight. Surface waves are generated only in presence of a free boundary. These are also called as guided waves and have long range inspection potential. Guided waves require boundaries for their existence. Guided waves propagate through a structure while boundary or surface guides the propagating waves with minute loss in energy resulting in longer propagation distances.

Some of the commonly used terms related to ultrasonic wave propagation used in the thesis have been explained as below:

1. **Wave Velocity (v):** The speed of a sound wave varies depending on the medium through which it is traveling. It is affected by the medium's density and elastic properties. Sound waves travel at different velocities in different media.

2. **Wavelength (λ):** It is the distance between any two corresponding points in the wave cycle as it travels through a medium. Wavelength is related to frequency and velocity by the simple equation Wavelength (λ) = Velocity (v)/frequency (f). In ultrasonic flaw detection, the generally acceptable lower limit of size of flaw is one-half wavelength, and anything smaller than that will be invisible. In ultrasonic thickness gauging, the theoretical minimum measurable thickness is one wavelength.

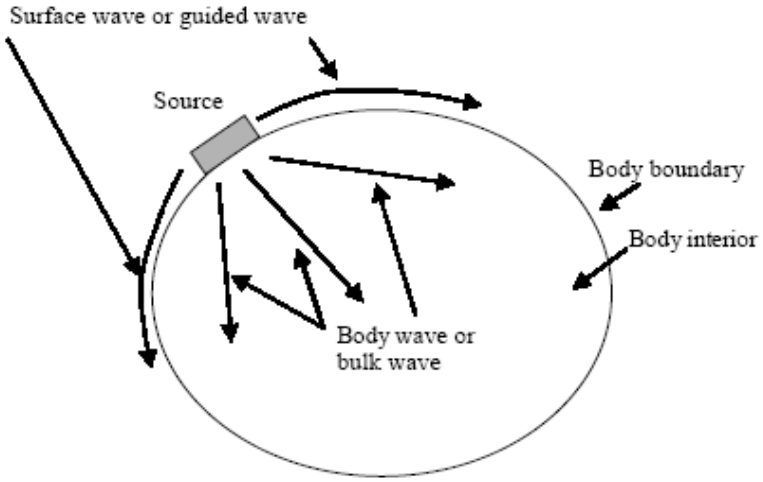

Figure 2.1: Body waves and Surface waves generated by an ultrasonic source (Kundu, 2007)

3. **Attenuation:** Normally the distance that a wave at a given frequency and energy level travel depends on the material through which it is travelling. Hard and homogeneous materials transmit sound waves more efficiently than soft, heterogeneous or granular materials. When sound propagates through a medium, its intensity reduces with distance. Attenuation is measure of loss of wave amplitude (or ‘‘signal’’) due to all propagation related mechanisms like beam spreading, absorption, scattering etc. Ultrasonic attenuation is the decay rate of the wave as it propagates through material. It is largely dependent on natural properties and loading conditions. For idealized medium, sound pressure (signal amplitude) is only reduced by the spreading of the wave.

As the beam travels, the leading edge grows, the energy associated with the wave is spread over a larger area, and eventually the energy dissipates. Attenuation is energy loss

associated with sound transmission through a medium, essentially the degree to which energy is absorbed as the wave front moves forward. However, natural materials, exhibit further weakening due to scattering and absorption. Absorption is the conversion of the sound energy to other forms of energy. Scattering is the reflection of the sound in directions other than its original direction of propagation like random reflection from grain boundaries and similar microstructure. As frequency goes up, beam spreading decreases but the effects of attenuation and scattering are increased. For a given application, transducer frequency should be selected to optimize these variables.

4. **Acoustic impedance (Z):** Sound travels through materials under the influence of sound pressure. Since molecules or atoms of a solid are bound elastically to one another, the excess pressure results in a wave propagating through the solid. Acoustic impedance (Z) of a material is defined as the product of its density (ρ) and acoustic velocity (v).

$$Z = \rho v \tag{2.1}$$

Acoustic impedance is important in determination of acoustic transmission and reflection at the boundary of two materials having different acoustic impedances.

5. **Reflection and transmission coefficients:** Ultrasonic waves are reflected at boundaries where there is a difference in acoustic impedances (Z) of the materials on each side of the boundary as shown in the **Figure 2.2**. This difference in 'Z' is commonly referred to as the impedance mismatch. The greater the impedance mismatch, the greater the percentage of energy that will be reflected at the interface or boundary. The fraction of the incident wave intensity that is reflected can be derived since particle velocity and local particle pressure are continuous across the boundary.

When the acoustic impedances of the materials on both sides of the boundary are known, the fraction of the incident wave intensity that is reflected can be calculated **(Equation 2.2)** and is known as the reflection coefficient.

$$R = \left[\frac{Z_2 - Z_1}{Z_2 + Z_1} \right]^2 \tag{2.2}$$

Since the amount of reflected energy plus the transmitted energy must equal the total amount of incident energy, the transmission coefficient is calculated by simply subtracting the reflection coefficient from one.

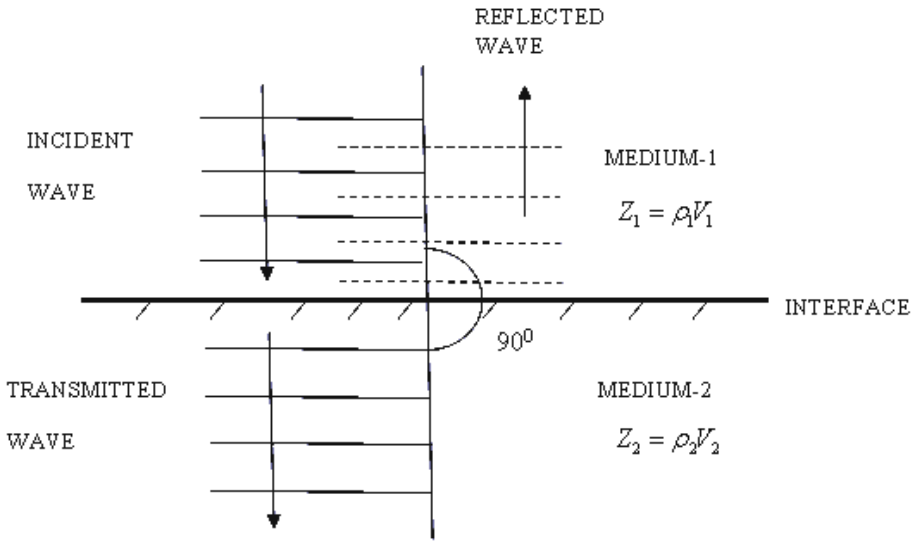

Figure 2.2: Reflection and Transmission of sound wave at normal incidence

(Bindal, 1999)

6. **Mode Conversion:** When sound propagates through a solid material, one form of wave energy can be transformed into another form due to its interaction with interface. For example, when a longitudinal wave hits an interface at an angle, it can result into particle movement in the transverse direction to start a shear (transverse) wave. Mode conversion occurs when a wave encounters an interface between materials of different acoustic impedances and the incident angle is not normal to the interface and it can result into very confusing and very hard to interpret ultrasonic signals.

When incident sound waves encounters an interface between materials having different acoustic velocities, at angle other than right angle, some portion of the incident energy is reflected (medium 1) and some portion is refracted (medium 2) depending upon the acoustic impedance mismatch at the interface **(Figure 2.3)**. Incident longitudinal wave undergoes mode conversion in both reflection and refraction. Larger the difference in acoustic longitudinal velocities between the two materials, the more the sound is refracted. The shear wave is not refracted as much as the longitudinal wave due to lower acoustic velocity. Similarly in reflection, the reflected shear wave is reflected at a smaller angle than the longitudinal wave. This is also due to the fact that the shear wave velocity is less than the longitudinal wave velocity within a given material. Snell's Law holds true for shear waves as well as longitudinal waves and can be written as follows:

$$\frac{Sin\theta_1}{V_{L1}} = \frac{Sin\theta_2}{V_{L2}} = \frac{Sin\theta_3}{V_{S3}} = \frac{Sin\theta_4}{V_{S4}} \quad (2.3)$$

where:

V_{L1} - is the longitudinal wave velocity in medium 1

V_{L2} - is the longitudinal wave velocity in medium 2

V_{S1} - is the shear wave velocity in medium1

V_{S2} - is the shear wave velocity in medium 2

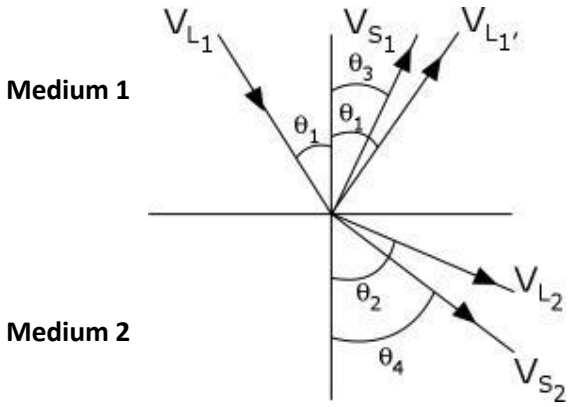

Figure 2.3: Reflection and Refraction at the boundary of two media

(Bindal, 1999)

2.2.1 Modes of Wave Propagation

Propagation of sound wave in air takes place in the form of compressions and rarefactions of air molecules along the direction of wave propagation. However, in solids, molecules can afford to vibrate in other directions as well. Different types of sound wave propagation styles characterized by oscillatory patterns, that are capable of maintaining their shape and propagating in a stable manner, are called wave modes. On the basis of the mode of particle displacement, these wave modes can be classified as:

- Longitudinal or Compression waves (L-waves)
- Transverse or Shear waves (S-waves)
- Surface or Rayleigh waves
- Lamb or Plate waves

Longitudinal or Compression waves

In longitudinal waves, the molecules oscillate in the longitudinal direction or the direction of wave propagation **(Figure 2.4)**. Liquids, solids and gases can support compression waves because the energy propagates via atomic structure by a series of compression and expansion (rarefaction) movements. These are also termed as **density waves** because their movement of particles results into fluctuation of density.

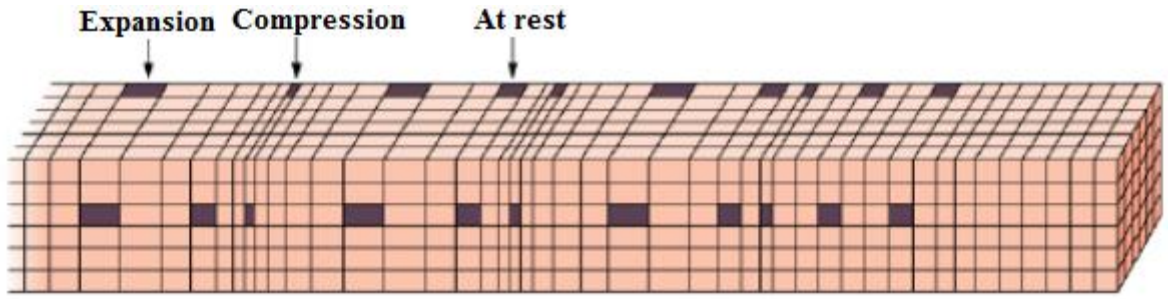

Figure 2.4: Propagation of Longitudinal waves (www.ndt.org)

Transverse or Shear waves

In the transverse or shear wave, the molecules oscillations take place in a direction normal to the direction of wave propagation **(Figure 2.5)**. Transverse waves necessitate material that can withstand shear load. Therefore, this mode of wave propagation is supported by solids only and not by liquids or gasses. Shear waves are relatively weak as compared to longitudinal waves. Shear waves can be classified as SH (Shear Horizontal) and SV (Shear vertical) waves depending upon the polarization in horizontal plane or vertical plane

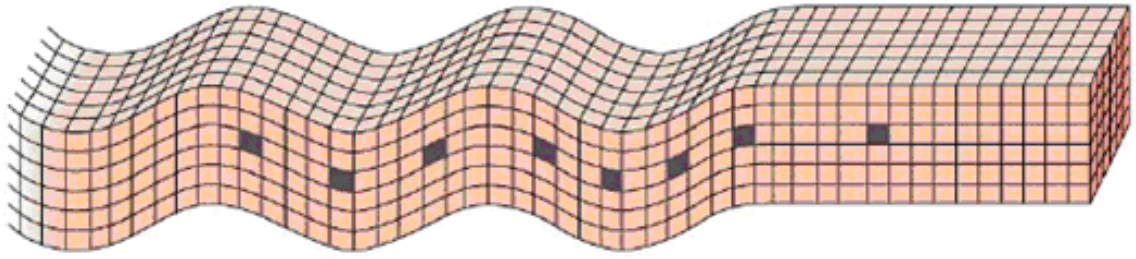

Figure 2.5: Propagation of Transverse or Shear waves (www.ndt.org)

Surface (or Rayleigh) waves

Surface (or Rayleigh) waves travel the surface of a relatively thick solid material and are effective up to a depth of nearly one wavelength. In this case particles undergo a combination of a longitudinal and transverse motion to create an elliptic orbit motion **(Figure**

2.6) with major axis of the ellipse normal to the surface of the solid. As the depth of an individual atom from the surface increases, the horizontal swing of the elliptical motion decreases. These waves are generated by a longitudinal wave interacting with an interface at an angle of incidence near the second critical angle. Velocity of surface waves is approximately 85% to 95% of a shear wave velocity. Rayleigh waves are useful because they are very sensitive to surface defects and they follow the surface around curves. Because of this, Rayleigh waves can be used to inspect areas that other waves might find difficult to reaching.

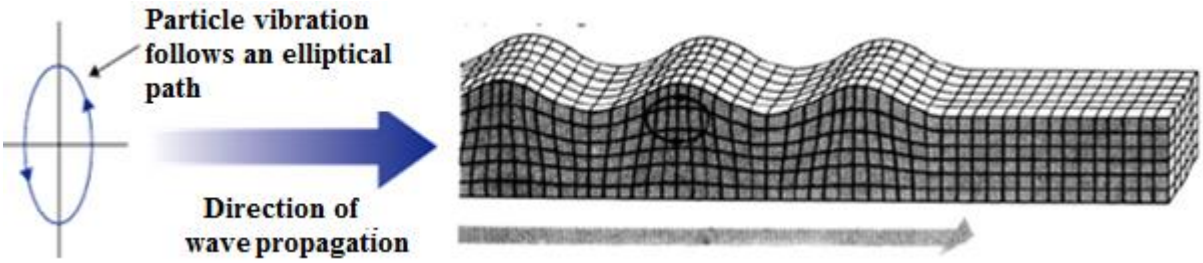

Figure2.6: Propagation of Surface or Rayleigh waves (www.ndt.org)

Plate waves or Lamb waves

Plate waves are similar to surface waves except they can only be generated in materials that are few wavelengths thick. Lamb waves are the most commonly used plate waves in NDT. These are complex vibrational waves that travel through the entire thickness of a plate. Propagation of Lamb waves depends on excitation frequency and plate thickness apart from material properties like density and the elastic constant.

2.3 ULTRASONIC TESTING

2.3.1 Basic Principles

Ultrasonic non-destructive testing employs short duration, low energy, high frequency stress pulse that is introduced into a test object in order to obtain information about the structural integrity of the specimen without altering or damaging it in any way. Typical Ultrasonic Testing (UT) system includes several functional units like pulser/receiver system, piezoelectric patches or transducers, data acquisition and display devices etc. Pulser/receiver system produces and feeds high voltage electrical pulses to the active transducer. Transducer converts electric input energy to high frequency ultrasonic energy, which is injected to the

structure being investigated. Interaction of propagating energy with flaws/ defects results in reflection, scattering of the energy. The reflected wave signal is picked up by passive transducer and is transformed into electrical signal. The received signal is duly conditioned by receiver module of PR system and is displayed/ stored for further analysis **(Figure 2.7)**.

Two basic parameters measured during ultrasonic testing are: - time of flight of sound waves through the sample, and amplitude of received signal.

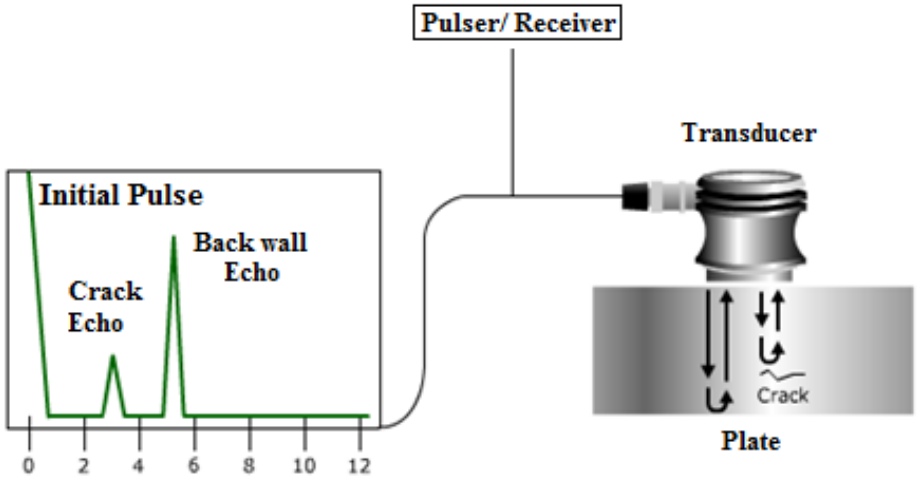

Figure 2.7: General ultrasonic inspection principle (www.ndt.net)

Measurement and interpretation of these parameters can effectively reveal information about the size, location and orientation of the flaw.

2.3.2 Methods of Ultrasonic Testing

Most commonly used methods of ultrasonic testing are:

- Pulse Echo method
- Pulse Transmission/ Through Transmission method
- Pitch Catch method
- **Pulse Echo (PE) method**

In this method only one piezoelectric transducer is used that acts as both active as well as passive transducer. Transducer is positioned normal to and mounted on or near the surface of the subject specimen **(Figure 2.8).** It introduces ultrasonic energy into test piece. The ultrasonic waves are reflected at different interfaces present in the specimen. These interfaces may be formed by the opposite face of the material or by discontinuities, layers, voids, or inclusions etc. in the material. Energy reflected form various interfaces is captured

by the same transducer (acting as receiver) and is converted into an electrical signal, which is further conditioned in a computer and digitized for display. Various testing parameters like relative thickness of the material, location of the defect etc. may be divulged using time of flight information from PE data.

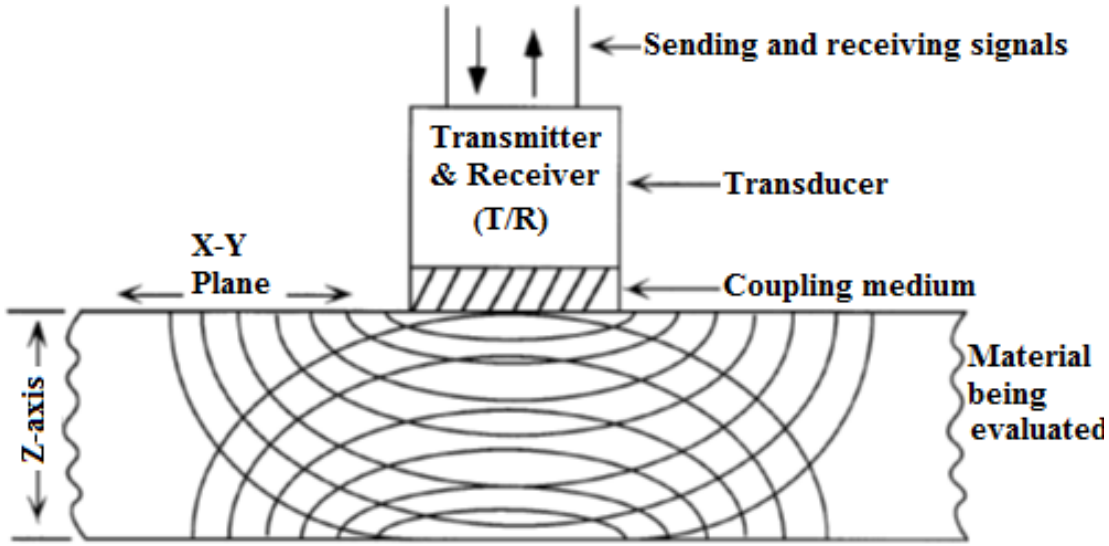

Figure 2.8: Pulse Echo method of testing

(Source: NASA Guidelines for Ultrasonic testing of Aerospace Materials)

The pulse-echo technique allows testing when access to only one side of the material is possible.

- **Pulse Transmission (PT)/ Through Transmission method**

PT method uses two transducers placed on opposite sides of the specimen. One transducer acts as transmitter and the other as receiver. The beam from the transmitter (T) propagates through the material to opposite surface where the receiving transducer (R) is placed **(Figure 2.9).** PE is ideally used for detecting and localizing the defect in specimen. PT is employed for sizing the defect. By measuring the relative change of the amplitudes of the input and the received signals, the relative severity of the flaw can be assessed.

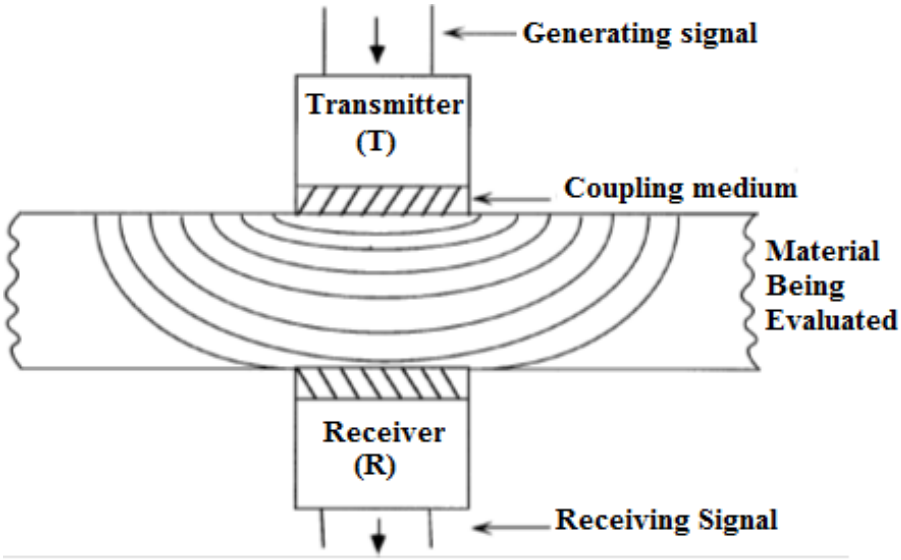

Figure 2.9: Pulse Transmission method of testing

(Source: NASA Guidelines for Ultrasonic testing of Aerospace Materials)

- **Pitch Catch (PC) method**

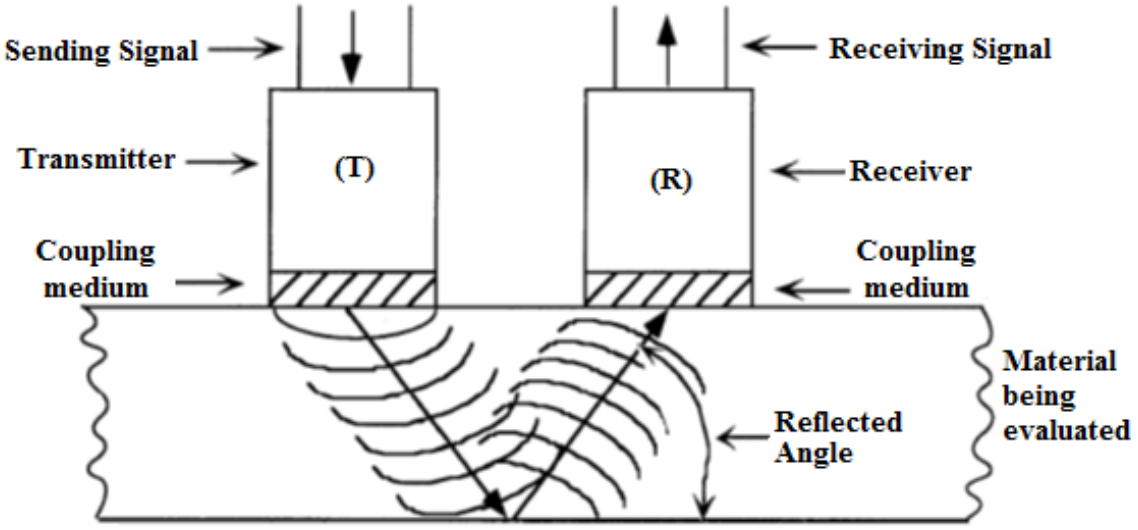

Figure 2.10: Pitch catch method of testing

(Source: NASA Guidelines for Ultrasonic testing of Aerospace Materials)

Like pulse transmission method, this methods also employs two transducers. However, in this case the both the transducers are placed on the same side of the specimen. In PE and PT methods, transducer is usually oriented normally to the specimen surface. However, in PC method, ultrasonic energy may be transmitted at an angle and received as reflected energy returning at reflected angle. PC method is usually employed for inspecting

tubular or plane geometries with parallel opposite surfaces where both sides of the specimen are not accessible.

2.4 ULTRASONIC GUIDED WAVES

2.4.1 Introduction

These waves are characterized by the fact that a boundary (like tube, cylinder or plate etc.) as a guiding surface is required for wave propagation. When ultrasonic wave is constrained and guided within the geometric boundaries of the structure, it becomes a guided wave. Key benefits of using guided waves over conventional ultrasonic testing are their ability to inspect over long distances with excellent sensitivity and to inspect hidden structures with limited accessibility.

Guided waves exist in structures that do not behave as an infinite mass of material, and the sound propagation is constrained by one or more material boundaries. In such cases, sound propagation is complex and sound can travel in a large number of 'modes' that can be determined by the solution of the wave propagation equation using given boundary conditions. The complications arise from the fact that these guided waves are dispersive, and the frequency dependence of their propagation characteristics (like velocity and attenuation) must be known so that test results can be accurately interpreted. Use of guided ultrasonic waves is more complicated than bulk waves and has relatively limited use in NDT. It is still in research phase and has not developed into a full-fledged practical method.

Various structures that guide the propagating waves are also known as waveguides. **Figure 2.11** shows the different types of guided waves supported by corresponding natural wave guides. Ultrasonic guided waves are generated by constructive interference of longitudinal and shear bulk waves. The bulk stress waves generated by conventional transducer interact with the boundaries of the wave guide. Multiple reflections and mode conversions take place until their superposition form wave packets i.e. ultrasonic guided waves. Different types of guided waves depending upon their wave guide are given below:

Lamb waves: Waves propagating through a plate type structure with two parallel stress-free boundaries are known as Lamb waves, named after Horace Lamb who first discovered them. These waves are also known as plate waves because they propagate through plates (**Figure 2.11a)**.

Bar waves: When guided waves propagate through a rod or bar they are known as bar waves (**Figure 2.11b and c)**.

Cylindrical Guided Waves: Elastic waves propagating through a hollow cylinder or pipe are called cylindrical guided waves (**Figure 2.11d)**. Since for a cylinder the two stress-free surfaces- inner and outer surfaces are parallel to each other as in a plate, sometimes the cylindrical guided waves are also called Lamb waves.

Rayleigh wave: If the structure is a homogenous half space, then the guided wave propagating along the surface of the half space is called Rayleigh wave, named after its inventor (**Figure 2.11e)**.

Rayleigh-Lamb waves: Waves propagating parallel to the free surface of a multilayered solid half-space are known as generalized Rayleigh-Lamb waves or simply Rayleigh waves (**Figure 2.11f)**.

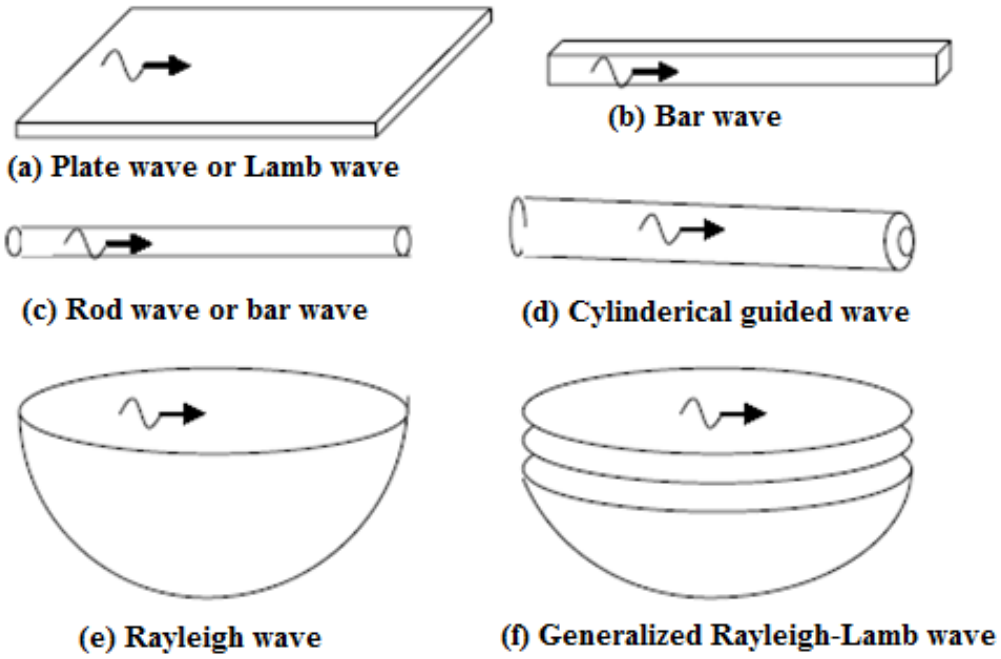

Figure 2.11: Different types of guided waves in various wave guides (Kundu, 2007)

2.4.2 Guided Waves in Plates

Plate waves are a particular mode of propagation which is established by two parallel traction free boundary surfaces. These are also called as Lamb waves, named after the Horace Lamb who originally developed the theory describing the propagation characteristics of plate waves in 1916. Plate forms a natural waveguide which directs the propagating waves along the structure. Since the waves can propagate in the plane of a plate, and as the material used

here has very little damping, the energy of the waves is practically not absorbed. This result in longer scanning spans from a single location.

In plate structures these waves are usually generated by impinging the plate obliquely with a ultrasonic signal from a relatively large transducer as a result of which variety of different waves reflecting and mode converting inside a structure are generated and superimposing with areas of constructive and destructive interference leading to the nicely behaved guided wave packets that can travel in the structure. Plate specimen can be offered obliquely to the incident longitudinal waves by using angle probes or immersion coupling technique. Another approach to generate Lamb waves is to use a comb probe which relies on matching of desired Lamb wave mode wavelength with the comb pitch. Piezoelectric wafer active sensors (PWAS) have also been employed in applications where bulky setups involving conventional transducers are unaffordable. In addition to this Lamb waves can also be excited by optical, electromagnetic and magneto-strictive means.

Lamb waves, like surface waves, propagate parallel to the test surface and have elliptical particle motion that occurs throughout the thickness of the Plate. Lamb waves propagate only in thin plate geometries (plate thickness <= 3λ). These are two dimensional stress waves that penetrate the entire thickness of the plate and propagate parallel to the surface. Particle displacements and stresses in the Lamb waves occur throughout the thickness of the plate. Longitudinal wave, polarized in the direction perpendicular to the surface called as shear vertical (SV) wave, are combined with L waves form **Lamb Waves (Figure 2.12).**

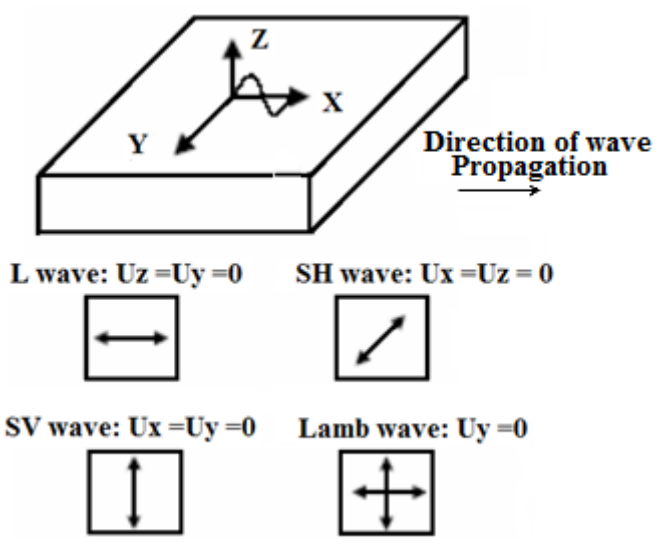

Figure 2.12: Lamb waves propagation (Edalati et al., 2005)

The propagation characteristics of Lamb waves depend on the material properties (density, elastic modulus of the plate), geometrical properties (thickness of plate, angle of incidence, boundary conditions) and the frequency of vibrations. The resulting refection and refraction at the interfaces produces many new signal packets. If angle of incidence and frequency is adjusted properly, the reflected and refracted energy within the plate interferes constructively to form a Plate Wave.

Lamb waves exhibit infinite number of possible modes of particles with in plate for a given excitation frequency and plate thickness each mode has its unique propagation characteristics. But the most commonly used modes are Symmetrical and Anti-symmetrical. These are labelled as S_i and A_i, where S and A indicates symmetrical and anti-symmetrical nature respectively and '*i'* is the order of the mode. In symmetrical mode, particles displace in symmetrical fashion about the mid plane of the plate so that crest on near side surface coincides with a trough on far side surface **(Figure 2.13a)**. It is also termed as longitudinal mode or extensional mode because the wave is "stretching and compressing" the plate in the direction of wave propagation and the average displacement over the thickness of the plate or layer is along the direction wave motion. In anti-symmetric modes, particles displace in anti-symmetric fashion about the mid plane so that crests of the wave on the near and far surfaces coincide **(Figure 2.13b)**.It results in average displacement to be in a normal direction to the plate thickness. Anti-symmetrical Lamb wave mode is often called the "flexural mode" because the plate bends as the two surfaces move in the same direction **(Figure 2.13b).**

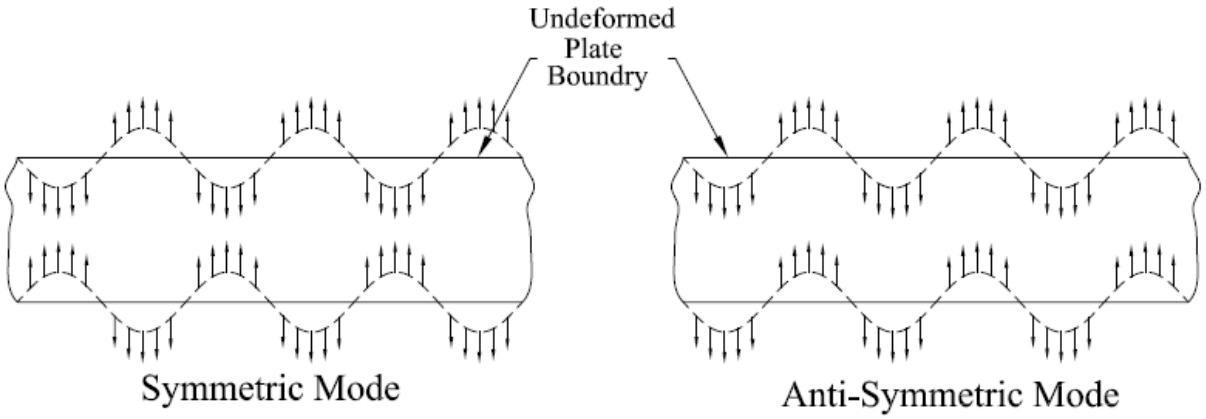

(a) **(b)**

Figure 2.13: Lamb wave propagation (a) Symmetrical mode (Dilatational)

(b) Anti-symmetrical mode (Bending) waves

2.4.3 Key Characteristics of Lamb waves

2.4.3.1 Wave Propagation in Plate in Vacuum

Although using Lamb waves is quicker and effective means of health monitoring as compared to bulk waves, but they are notoriously difficult to interpret. So it is very important to highlight and understand some of the important characteristics of Lamb waves for use as a potential health monitoring tool viz. - Dispersive behavior of various modes and presence of multiple modes for a given frequency and plate thickness (Alleyne and Cawley, 1991). Dispersion curves for 1mm thick steel plate in vacuum modeled using DISPERSE software (Pavlakovic and Cawley, 2000) are shown in **Figure 2.14.** Symmetric and anti-symmetric modes are shown in red and blue color respectively. **Figure 2.14a** shows the dispersion curves as phase velocity against frequency. It describes the rate at which an individual crest of the wave travels. **Figure 2.14b** displays the group velocity projections with frequency. It indicates the speed at which a guided wave packet travels. This can be seen as the velocity of the energy of the wave travelling through isotropic non-attenuative media. Because the system is elastic, the material has very little damping, so energy does not leak into a surrounding medium resulting in no attenuation. It can be seen from **Figure 2.14** that the number of modes increases with the frequency and an infinite number of symmetric or anti-symmetric modes can exist at higher frequencies.

The phase velocity shown in **Figure 2.14a** shows characteristics of Lamb wave dispersion curves. The two fundamental modes, A_0 and S_0, are available from zero frequency. The fundamental symmetric mode, S_0, propagates with a phase and group velocity equal to Young's velocity at zero frequency. In this case, the mode is purely extensional, the motion along the direction of propagation, and the energy is evenly distributed across the thickness of the plate. As the frequency increases, the S_0 mode begins to take on more complex characteristics. In addition to the "in-plane" displacements, that are parallel to the direction of propagation, the mode experiences many "normal" displacements that are normal to the plate (perpendicular to the direction of propagation). As the frequency continues to increase, the S_0 mode begins to act more and more like a pair of Rayleigh waves propagating on the top and bottom surfaces of the plate. The energy and displacement of the Rayleigh mode is concentrated in the outer portions of the plate, primarily in the first wavelength in depth.

The fundamental anti-symmetric mode, A_0, also exhibits unique characteristics. The mode begins at zero frequency and zero phase velocity as a pure bending mode but the phase

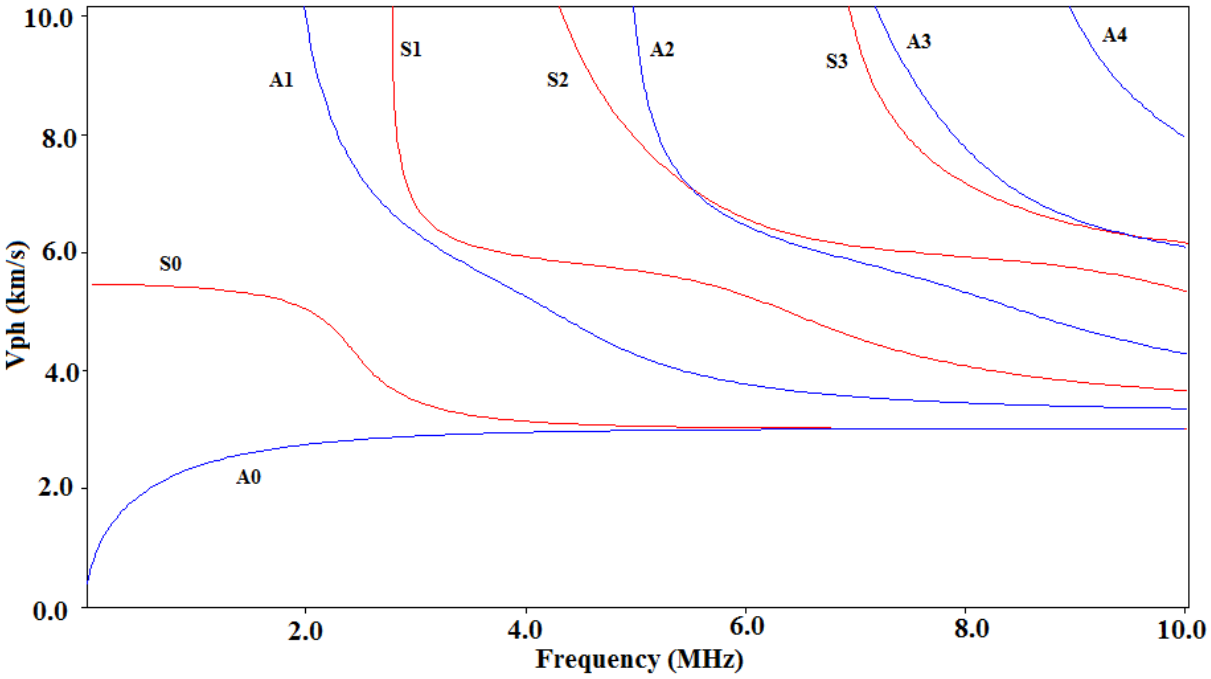

(a) Phase Velocity Vs Frequency

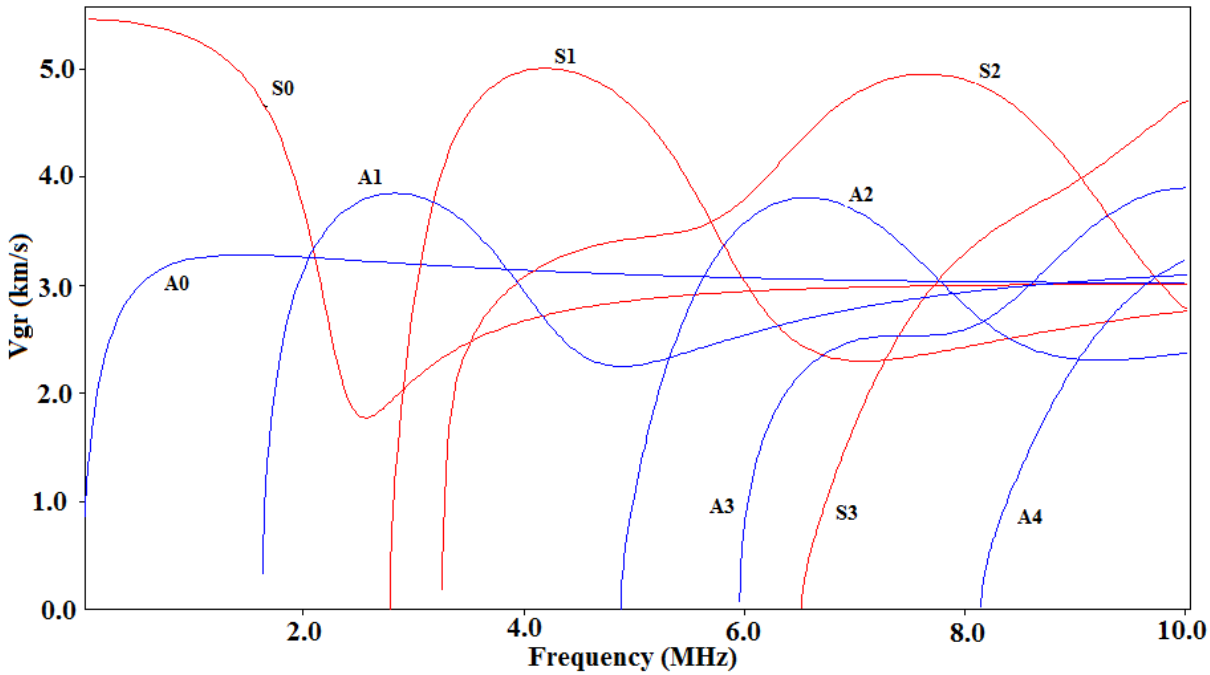

(b) Group Velocity Vs Frequency

Figure 2.14: Dispersion curves for 1mm steel plate in vacuum

and group velocity quickly increases. Because of the sudden change in group velocity at low frequencies, the mode is very dispersive in this region, indicating that wave packets will tend to spread out as different frequency components travel at different speeds. Like the phase

velocity of the S_0 mode, the phase velocity of the A_0 mode tends to the Rayleigh velocity as the frequency increases.

The higher order modes are the modes that do not propagate at zero frequency. The numerical index that follows a mode indicates the order of the modes in increasing frequency of their "cut-off" frequencies. The cut-off frequency of a mode is its low-frequency limit where the phase velocity tends to infinity. The higher the index of the mode, the more maxima and minima will be present in the mode shape of the displacements of the mode.

2.4.3.2 Leaky Lamb Waves

In the present work, leaky Lamb waves will be used for developing damage detection in plates completely submerged in water. Leaky Lamb waves refer to guided waves that exist in a single elastic, isotropic layer that is immersed in a surrounding liquid. The Leaky Lamb case uses the same analytical functions as the Lamb wave case. However, an extra term appears in the characteristic equation that accounts for the liquid loading on the surface of the plate. As the wave propagates down the isotropic layer, bulk waves are generated in the surrounding fluid layers. These bulk waves carry energy away from the system and cause attenuation. Therefore, in order to find a valid wave propagation solution, the attenuation value must be found in addition to the frequency and real wave number. Thus the search for the roots of the dispersion curves is a search in three variables.

The dispersion curves for Leaky Lamb waves in case of a 1mm thick plate submerged in water are shown in **Figure 2.15**. In general, phase velocity dispersion curves for leaky Lamb waves shown in **Figure 2.15a** are very similar to the phase velocity curves for a Lamb wave shown in **Figure 2.14a**. For a material such as steel, which has high acoustic impedance, the water loading (with much lower acoustic impedance) does not have much effect on the phase velocity of the modes. However one difference is immediately evident in this case. For the water loaded case, there is another low frequency, anti-symmetric mode that does not appear in the Lamb case. This mode, called the Scholte wave. It is a wave that propagates at the interface of the steel and the water. At lower frequencies, its phase velocity is less than the bulk velocity in the fluid and it experiences no attenuation. Its phase velocity tends towards the bulk velocity in the water as the frequency increases.

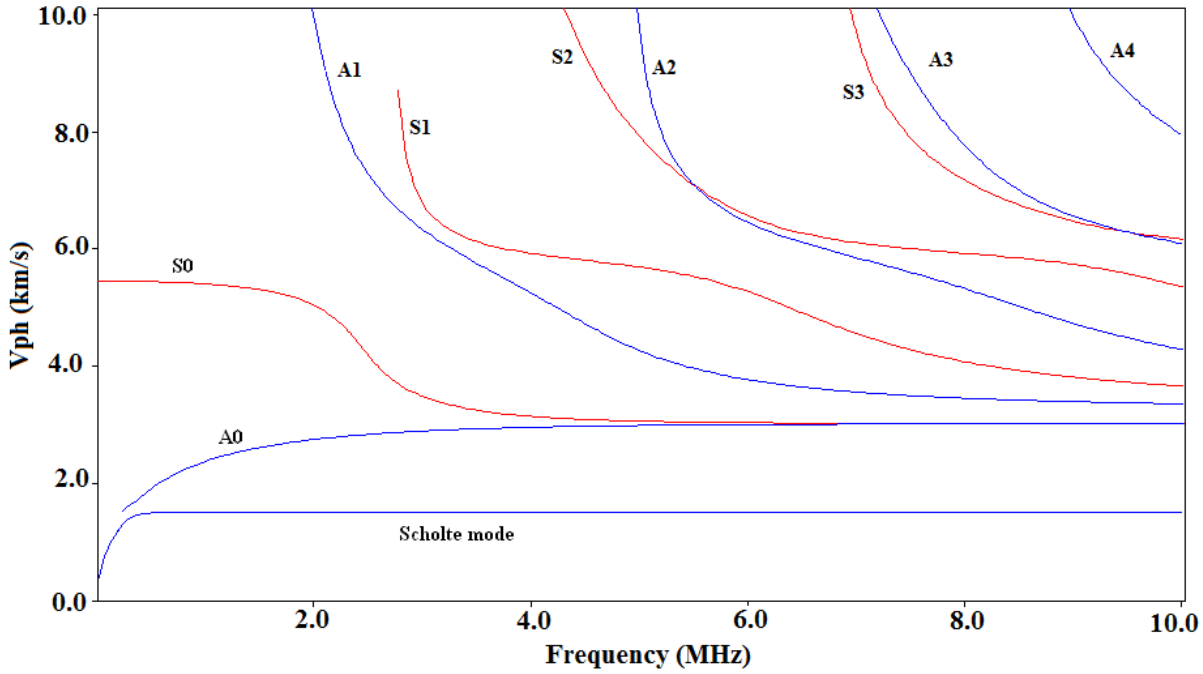

(a) Phase Velocity Vs Frequency

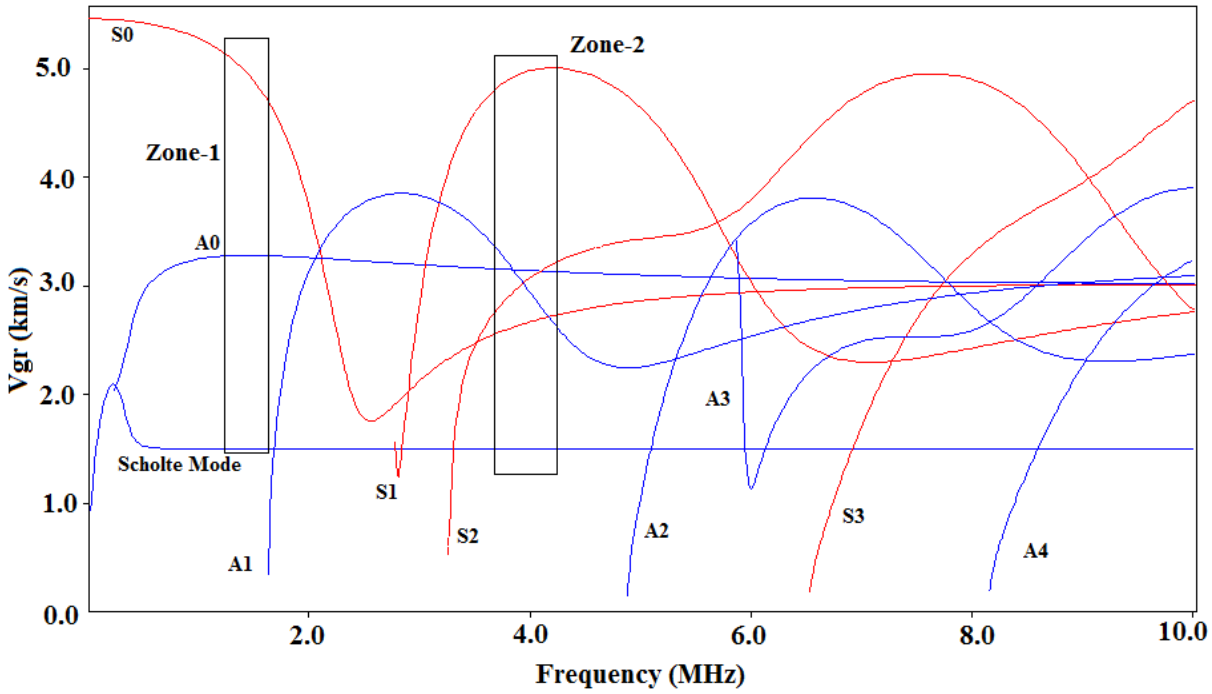

(b) Group Velocity Vs Frequency

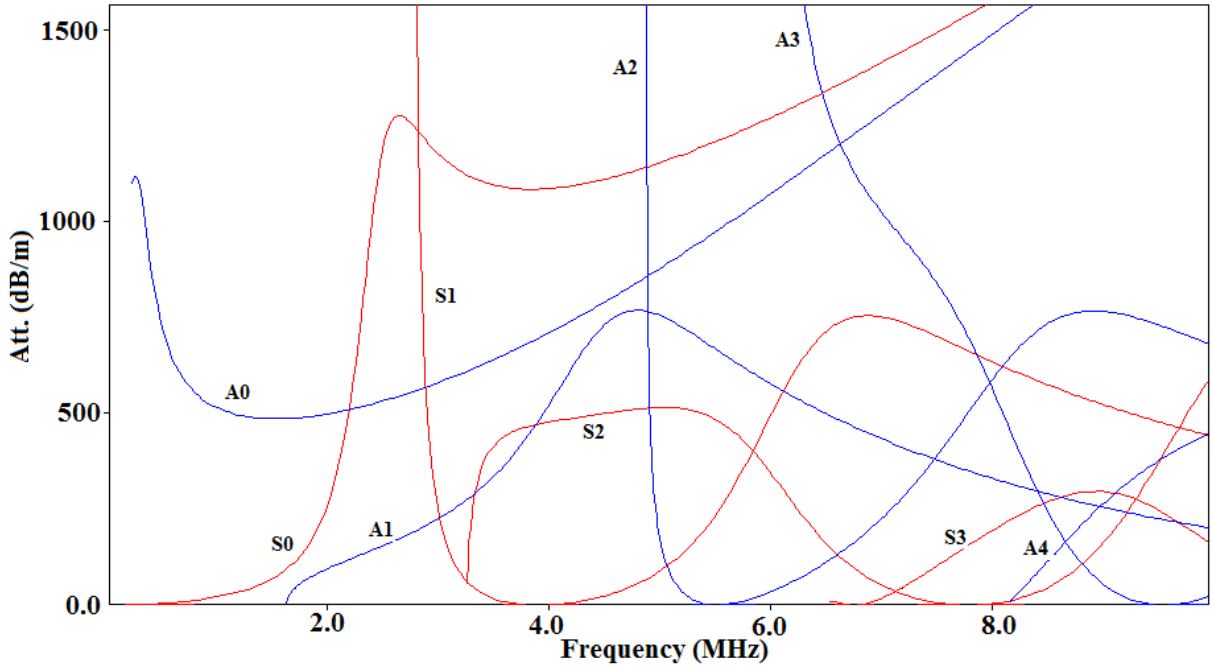

(c) Attenuation Vs Frequency

Figure 2.15: Dispersion curves for 1mm steel plate in water (Pavlakovic and Cawley, 2000)

Although the dispersion curves are very similar between a steel plate in vacuum and one in water, the attenuation which is caused by the leakage into the water provides a significant difference between the two cases. The attenuation (in decibels per meter) is shown in **Figure 2.15 c**. The attenuation characteristics of the two fundamental modes provide a great deal of insight into the behaviour of the leaky waves. The fundamental symmetric mode, S_0, behaves entirely as an extensional mode at zero frequency. Since practically all of the displacement is in the direction along the interface between the steel and the water, and since this tangential motion does not couple between the two materials, the wave in the plate takes no notice of the liquid loading and the attenuation remains effectively zero. However, as the frequency increases and the mode adopts also some lateral motion, the attenuation increases dramatically. At high frequencies, the attenuation of the fundamental mode becomes asymptotic to the attenuation value for a leaky Rayleigh wave.

The fundamental anti-symmetric mode, A_0, behaves in a different fashion. This mode has significant bending motion over its entire frequency range, which means that it always has significant lateral motion and so we should expect that it should always transmit energy into the surrounding liquid. Indeed this is true for most of its range. However, this mode does not behave this way at low frequencies. As the phase velocity of the A_0 mode drops below the

bulk velocity of the surrounding liquid, the attenuation drops to zero. This phenomenon is caused by the matching of the wavenumbers at the interface of the two materials.

2.4.3.3 Main issues for Lamb Wave Mode Selection for Damage Detection

Although guided waves have distinguishing benefits over bulk waves, they are characterized by dispersive nature, multi-mode behavior and frequency dependent wave structure. This results in a complex signal which impedes their practical implementation. The key issues to be taken care of while utilizing them for health monitoring purposes are discussed below.

Group velocity (the velocity at which energy propagates along the plate) depends on frequency-thickness product **(Figure 2.15b)** and it is important to understand its implications. When the transducer is excited with a broad band pulse different frequency components (range of frequencies as shown by width of box showing Zone-1) having different group velocities travel in the plate and reach the receiver at different times showing a spread in time domain for the received pulse. When the span of inspection is increased, this spread also increases resulting in arrival of set of peaks giving rise to received pulse which has a tail like appearance rather than a sharp pulse. This phenomenon is called as *dispersion* and it leads to low signal to noise ratio and is a main stumbling block in interpretation of the received pulse in large span inspection.

The physical manifestation of dispersion is that when a particular Lamb wave mode is generated by an excitation with a finite duration (referred to as the incident signal), the energy in the Lamb wave spreads out in both space and time as it propagates away from the source. To avoid it, attempts should be made to select the product of excitation frequency and plate thickness such that group velocity curve is as flat as possible (non-dispersive range) and secondly the bandwidth of the excitation pulse is as limited as possible. However, theoretically speaking, no non-dispersive point exists on a Lamb wave dispersion curve. Even if the group velocity is stationary with respect to frequency at some point, no incident signal of a finite duration can have an infinitely narrow bandwidth. Although this problem is less prominent when the span of inspection is not too large, resulting in limited temporal spread of different frequency components propagating in the plate. In case both the factors are not favorable i.e.- range of inspection is large and group velocity is also in dispersive range; then symmetric modes should be preferred as their propagation velocities are higher than the other

modes propagating at the same frequency, thus making their separation in time domain in received pulse (Alleyne and Cawley, 1992).

The other key issue with the use of Lamb wave is existence of more than one mode at any given frequency, as shown in *Zone 2* of **Figure 2.15b**. For plates immersed in water, at low frequency-thickness products only S_0 and A_0 modes can propagate. For a given plate thickness, as frequency content increases, more modes begin to appear. Each of these modes has their own group velocity and results in to a complex received pulse which is very difficult to comprehend. Thus practically as far as possible, it is preferable to operate in single mode zone. Otherwise if multimode zone is inevitable, modes having well separated group velocities should be preferred so that the various modes in the received signal can be resolved in time domain.

In addition to this, another important factor related to use of Lamb wave modes is wave structure. Wave structure of guided wave mode describes the distribution of particle displacement pattern, stresses and the energy density distributions through the thickness of the layer. It provides important information for understanding the eventual interaction of Lamb waves with a specific defect in a plate structure. Wave structure determines the sensitivity of the mode as different Lamb wave modes interact with flaws differently because of their different through-thickness displacement properties. Some modes have large particle motion amplitudes near the surface while others have more intense motion near the mid-plane of the plate. For multi-layers structures like composites, the wave structure may become even more complex. For evaluating surface defects the preferred mode shall have significant particle displacement or energy distribution near the surface. The wave structure changes from point to point along all modes in phase velocity-frequency space on a dispersion curve. Frequency dependent wave structure provides versatility to Lamb waves to scan for variety of defects in terms of geometry and location across thickness.

If the phase velocity of the guided wave in submerged plate is higher than the bulk longitudinal velocity in the surrounding liquid, energy is radiated in to liquid as bulk waves even if the liquid is inviscid. This provides an energy radiating mechanism causing attenuation of the guided waves leading to relatively shorter inspection spans. Degree of attenuation is dependent on the out of plane displacement of the guided wave at the surface. Particularly anti-symmetric modes, having particle displacement in the thickness direction, generate wave modes that couple efficiently with surrounding liquid causing strong attenuation of these modes. Fundamental symmetric mode (S_0) at low frequencies exhibits in

plane particle displacement, thus having reasonably low attenuation. However, at higher frequencies, particle displacement for S_0 mode is dominantly in the thickness direction, resulting in steep rise in attenuation.

These observations are experimentally validated in the following chapters along with the confirmation of the signal fidelity for further use in defect detection. Any one of the modes shown in **Figure 2.15** can be predominantly excited (while subduing other modes) by offering the longitudinal incident ultrasonic wave obliquely to the plate at angle of incidence (θ) given by Snell`s law as –

$$\theta = sin^{-1}\left(\frac{V_L}{V_{Ph}}\right) \tag{2.4}$$

Where V_{Ph} = Phase velocity of the desired Lamb wave mode

V_L =Longitudinal velocity of the incident wave in the coupling media.

Specific Guided Lamb wave modes can be predominantly produced either by using – 'Variable Angle Probes' or ‘Wedge Probes’ or ‘Immersion Coupling’. The former technique is a contact type arrangement, in which a variable angle probe riding on lateral surface of a Perspex semi-cylinder transmits energy into the subject structure. The Perspex block is coupled to the plate by a thin layer of gel. But the measurements can be unreliable due to the inadvertent variations in the contact pressure and couplant thickness. However, immersion coupling avoids these issues and enables contact free data acquisitions.

However, in case of submerged structures, presence of water makes the situation unique and challenging as it acts as a natural couplant. Studies on a non-contact health monitoring methodology for submerged plate geometries are scant. In this study, it is proposed to use immersion coupling which uses a continuous column of water as a carrier of incident energy from the probe to the plate. In order to excite a specific Lamb wave mode, a transmitter probe inclined at a specific angle injects incident energy in the plate. It is important to note that in pitch catch (PC) configuration, the receiver transducer in the same orientation as the transmitter becomes most sensitive to the wavelength of the mode being input as compared to other modes. It results in the receiver either not detecting or severely underestimating the amplitudes of other modes. So, this configuration improves fidelity of the received signal.

The objective of the present research is to study the propagation of ultrasonic guided waves through a submerged plate simulating marine /offshore applications and develop a non-contact, non-invasive damage monitoring methodology for detecting simulated defects like machined notches and actual corrosion in the plates. The guided waves are generated using the submerged transducer that is not in contact with the plate. The signal is received by another non-contact transducer in pitch-catch configuration after wave has traversed through the length of the plate.

2.4.4 Closing Remarks – Ultrasonic Guided waves

In the preceding section, the basics of ultrasonic waves and the principal issues associated with it to be adopted as a NDT tool for engineering purposes have been elaborated. Ultrasonics can be exploited as bulk waves or guided waves for health monitoring. They have normally been employed as bulk waves since the use of guided ultrasonic waves is more complicated, thus limiting its use in NDT. It is still in research phases and has not developed into a full- fledged practical method because of its complex propagation characteristics. Guided waves can travel in a large number of 'modes', which can be determined by the solution of the wave propagation equation with given boundary conditions. The complications arise from the fact that these guided waves are dispersive and exhibit multi-mode behavior. Thus, frequency dependence of their properties such as velocity and attenuation must be properly understood so that test results can be accurately interpreted.

Review of the prominent and latest works using Lamb waves for damage monitoring in plates in the form of simulated defects and corrosion damages is presented in the following Chapter 3. It establishes the capability of Lamb wave modes for damage detection in plate geometries. But rarely any study has focused on real time damage monitoring of plates structures in submerged state to investigate the onset and propagation of corrosion. A brief overview of corrosion and its effect in submerged marine structures is presented below to understand its mechanism and facilitate the development of a suitable monitoring technique.

2.5 CORROSION IN MARINE ENVIRONMENT

2.5.1 Effect of corrosion and its financial implications

Marine and offshore structures are often exposed to extreme loading and corrosive environments during service. This may result in age related deterioration such as corrosion wastage, fatigue cracking or mechanical damage (e.g., local denting) (Guang et al., 2002) which can further lead to significant issues in terms of safety, health, environment and

financial expenditures. It has been recognized that such deteriorations almost always result in the catastrophic failures of structures including total losses (Bayliss et al., 1988). It is thus of great importance to develop advanced inspection technologies which can allow for proper management and control of such damages. Submerged stage of such structures makes them inaccessible to various established non-destructive technologies, thus subjecting them to high risk of unnoticed damage.

Ships including naval warships travel globally and experience the extremes of marine environments which have often been noted to accelerate the decline in the material state of the operating ship. Marine environment combines the effects of saline seawater, salt laden air, rain, dew, condensation, localised high temperature and the corrosive effects of combustion gases is the most corrosive of environments. India has 3000 km of coastline and tropical marine environments as in Indian scenarios are far more corrosive than cold European climates because the temperature has a significant impact on the rate of corrosion.

Corrosion is prevalent throughout a ship and it manifests as mainly as degradation of the material and rust staining **(Figure 2.16)**. It generally occurs in two forms as *Uniform or General Corrosion* and *Pitting Corrosion* (Titcomb, 1982) besides many other types of corrosion like galvanic corrosion, crevice corrosion etc. which are limited to only specific and certain areas.

Uniform or general corrosion is typified by uniform rusting of steel when the metal surface is exposed for extended periods of time in saline water. Uniform or general corrosion usually occurs in stagnant or low flow seawater at a rate of approximately 5 – 10 microns per year on mild and low-alloy steels. The rust generally has a constant thickness and similar consistency over the surface. Another form of hazardous corrosion in naval ships is *pitting corrosion*. It is a form of extremely localized corrosion that leads to the creation of small holes in the metal. It is a very serious type of corrosion damage due to its rapid growth following an initial delay time. It is also self-generating, i.e. autocatalytic, starting from irregularities in the metal surface, under scale or other deposits, or from some in-homogeneities in the metal. This kind of corrosion is extremely insidious, as it causes little loss of material with small effect on its surface, while it damages the deep structures of the metal. The pits on the surface are often obscured by corrosion products. It can be initiated by a small surface defect, being a scratch or a local change in composition, or damage to protective coating. Polished surfaces display higher resistance to pitting, provided the polishing is carried out correctly. Poor quality polishing can accelerate corrosion. The

presence of chlorides, e.g. in sea water, significantly aggravates the conditions for formation and growth of the pits through an auto catalytic process. It is mostly favoured by stagnant water. A brief chemistry of the corrosion mechanism in saline environments is discussed below:

Figure 2.16: Effect of Corrosion on Ship Hull showing Pits

Corrosion is an electrochemical process and both anode and cathode in case of submerged ship hulls takes place on the same plate surface. Corrosion of steel in marine environments in the presence of chlorides takes place in several steps as below:

At the anode, iron is oxidized to ferrous state and releases electrons:

***Anodic Reaction*:** $Fe \rightarrow Fe^{2+} + 2e^-$ (2.5)

***Cathodic Reaction*:** $2e^- + H_2O + \frac{1}{2}O_2 \rightarrow 2OH^-$ (2.6)

Both the anodic and cathodic reactions are necessary for corrosion to occur and they need to take place simultaneously. The hydroxyl ions combine with the ferrous ions to form ferrous hydroxide:

$Fe^{2+} + 2OH^- \rightarrow Fe(OH)_2$ (2.7)

In the presence of water and oxygen, the ferrous hydroxide is further oxidized to form Fe_2O_3.

$4Fe(OH)_2 + O_2 + 2H_2O \rightarrow 4Fe(OH)_3$ (Ferric Hydroxide) (2.8)

$2Fe(OH)_3 \rightarrow Fe_2O_3.3H_2O$ (Hydrated Ferric Oxide- Rust) (2.9)

Whenever spontaneous reaction occurs, all the electrons released in the anodic reaction are consumed in the cathodic reaction; no excess or deficiency is found. Therefore, no net current can be measured externally. Moreover the metal normally takes up more or

less uniform electrode potential often called corrosion or mixed potential (E_{corr}). The corresponding rate of metal dissolution at this potential is called corrosion rate (I_{corr}). The manifestation of corrosion is in the formation of these corrosion products or rust on the surface of the submerged plate.

Corrosion of steel in plates in the presence of chlorides, but with no oxygen (at the anode) and referred to as ***Chloride Corrosion (CC)*** takes place in several steps. At the anode, iron reacts with chloride ions to form an intermediate soluble iron-chloride complex:

Anodic Reaction: $Fe + 2Cl^- \rightarrow (Fe^{2+} + 2Cl^-) + 2e^-$ (2.10)

When the iron-chloride complex diffuses away to an area with higher pH and concentration of oxygen, it reacts with hydroxyl ions to form $Fe(OH)_2$. This complex reacts with water to form ferrous hydroxide:

Cathodic Reaction: $(Fe^{2+} + 2Cl^-) + 2e^- + 2H_2O \rightarrow Fe(OH)_2 + 2H^+ 2Cl^-$ (2.11)

This ferrous hydroxide is oxidized to rust in the presence of oxygen and water. Corrosion leads to the formation of rust product and dissolution of the metal surface leads to local weakening, pitting and loss of strength and ductility of the ship hulls which can be very catastrophic if, not monitored and maintained regularly.

Mitigating unexpected corrosion can be very expensive in terms of direct cost and it also impacts heavily on platform availability. If an offshore structure and its systems were designed with corrosion resistance built-in, this would result in less planned and unplanned maintenance and a substantial saving in through life costs would accrue.

"At US$1.8 trillion, the annual cost of corrosion worldwide is over 3% of the world's GDP. Yet, governments and industries pay little attention to corrosion except in high-risk areas like aircraft and pipelines": George F Hays: Director World Corrosion Organization (2006).

This unpredictability of the extent and cost of corrosion can be mitigated by considering the appropriate choice of materials, fabrication and assembly processes, coatings and coating application thus leading to minimization of the life costs. Some rough estimates have been made of the cost of corrosion and are rather intangible, but they do however, provide an indication of the magnitude of the costs. Recently the World Corrosion Forum estimated the world wide cost of corrosion to be between 1.3 and 1.4 trillion Euros or 3.1 % to 3.5 % of a nation`s GDP. These figures only reflect the direct cost of corrosion –

essentially materials, equipment, and services involved with repair, maintenance, and replacement. It does not include the environmental damage, waste of resources, loss of production, or personal injury resulting from corrosion and in 2001 a US Department of Defence study estimated that corrosion cost the department at least $20 billion a year. The primary cost of corrosion in ships structure can be divided into two major parts (Johnson, 1992):

- The cost for the new construction of the ships. These costs include corrosion-resistant materials, coatings, and cathodic protection systems installed during construction.
- The cost of repairs and maintenance. These costs include the replacement of ship hull plates, the removal and re-application of coatings, and the cost of additional cathodic protection. The down time cost due to corrosion maintenance will be included according to the revenue lost due to the ship being out of service while repairs and maintenance are being performed. The estimated annual cost of corrosion in the U.S. marine shipping industries was $2.7 billion.

Hence, there is an urgent need for developing a corrosion monitoring system for marine vessels so that an idea of initiation of corrosion can be had much before it reaches to a catastrophic level. To avoid any severe compromise to the integrity of the structure, periodic and continuous health monitoring of these structures and other components for corrosion damages is very important. In such cases the integrity of the structure cannot be compromised and at the same time "out of service "costs are highly punitive/prohibitive to go in for frequent inspections. So in such situations, it is necessary to have in-situ health monitoring systems that can inspect the integrity of these members while in service. It requires a health monitoring tool which is non-invasive, in-situ and non-contact.

2.5.2 Existing Wastage Assessment Technologies

There are many of non-destructive evaluation techniques to assess the corrosion in marine structures that have been used in the last few decades. The review of these methods have been reported **(**Agarwala and Ahmad, 2000) and discussed in brief in this section.

Visual Methods

Visual methods have been accepted for ship inspection for a long time. Different devices and techniques have been developed. *Sentry holes* are the technique that uses liquid leakage to ascertain the allowance thickness of the ship structure. When the depth of corrosion meets the thickness allowance, the leakage of liquid inside will provide an early

warning. Another commonly used procedure is the use of *Charge coupled dev*ices which are relatively inexpensive and utilize optical scanning devices to record the images. These images are then processed through computer programs to indicate the state of health of the ship structure. But this technique is complicated and requires skill of the operators. Also this technique suffers from the drawback that though it can scan large areas such as ships and pipelines but the use is limited to open surfaces only.

Visual methods give an indication of damage state or level of deterioration only when it is visible and has already reached an alarming level. Need of the hour is to develop damage detection methodology which can assess the initiation of damage mush before it reached to alarming levels.

Acoustic Emission Method

The use of a continuous acoustic monitoring system to detect and locate corrosion-induced failures has been considered as a favourable alternative in NDT. It involves the listening of acoustic events in a structure through permanently attached transducers. The characteristics of the signals can be correlated to identify failure event. Use of many transducers allows the events to be located accurately. The ability of acoustic emission (AE) equipment to monitor an entire vessel, metal or fiberglass-reinforced plastic for structural integrity establishes AE detection as a valuable non-destructive inspection technique. The technique was successfully used to detect development of pitting corrosion in vertical walls of oil storage tanks and a good correlation was observed between AE activity and pitting rate (Guang et al. 2002)**.**

But the method is limited in use due to its very typical and difficult data interpretation.

Radiographic Methods

Radiographic techniques use high frequency electromagnetic radiation in the form of X-rays and gamma rays to gain detailed images of the internal structure of installations. Despite the highly specialized equipment and safety precautions, radiography produces the most desirable results. The principle behind radiography involves the measurement of attenuation of these rays as it passes through the material under investigation. Penetrating gamma and X-rays are used to provide images of the variation in thickness of metallic components in ship structures. These methods require the access to both sides of the structure. Ship operators usually place films inside the large tanks or ships and radiation

sensors are placed outside. The images obtained can be compared with relatively good condition areas.

But the major drawback in the use of X-Ray or radiographic methods is that they have low resolution and require radiation safety measures and are mostly now banned in most of the countries.

Thermal Imaging or Thermography

All objects naturally emit infrared radiation in proportion to their surface temperature. Thermography measures the emitted radiation and displays the information as a visual image. Today's state-of-the-art equipment can measure radiation from 490,000 points every second and display the information as a TV picture. This can then be recorded for subsequent analysis to provide a permanent record of heat loss and surface temperature. With a temperature range of –30°C to 2000°C and a sensitivity of 0.05°C, there are very few applications beyond the reach of this hi-tech technique. By combining infrared and computer technologies, it is possible to generate thermograms (heat pictures), having up to 256 colors, that clearly show thermal profiles and temperature measurements. The images generated change with deteriorations in the structures due to its usage and other effects and hence, can relate to degradations.

Thermographic imaging, or time-resolved thermography, has been developed for the detection of hidden corrosion. Thermographic imaging can scan large areas to provide a macro view of an uncomplicated structure. Although fast, safe, and non-intrusive, this method is not yet a cost-effective way to quantify low levels of corrosion damage. Because of the difficulty of thermographic image interpretation, precision and reliability are dependent on the skill and experiences of the operator. The resolution of IR cameras is affected also. Vavilov, 2003 used a non-contact one-sided evaluation of hidden corrosion in metallic constructions by using transient infrared thermography.

Galvanic Thin Film Micro Sensors

When two dissimilar metallic elements of the sensor are exposed to the corroded environment but kept isolated from each other, they corrode at their respective corrosion rates. But when they are electrically short-circuited through a zero resistance ammeter, they become galvanically coupled. A current is developed when an electrolyte, such as saline water in marine conditions condenses on the sensor elements and electrically connects the

gap between the two electrodes. The magnitude of this galvanic current is directly proportional to the corrosivity of the condensed environment and its film thickness.

By considering the electrochemical dissimilarity in metals, the method for in-situ corrosion monitoring has been developed. The sensors have been evaluated for environmental corrosivity characterization, coating performance, properties of sealant and adhesives, hidden corrosion detection, and composite degradation (Agarwala and Fabiszewski, 1994). Among the various combinations of metals used for galvanic couple, the best combination was Au-Cd. This couple was found most sensitive and reproducible for environments which can detect even slight corrosion in materials. In marine atmosphere, Au-Ni was found to be best suited for long term testing.

Electrochemical Sensors

Electrochemical sensors involving electrochemical measurements of corrosion kinetics, types and rates have been developed successfully. Most common among these is the use of potentiodynamic measurements of pitting potential which vary with chloride ion concentration, pH of water, dissolved oxygen content, temperature and flow velocity in marine conditions. The influence of these parameters on the pitting potential has been successfully evaluated and the technique demonstrates stable convergence and results in an empirical equation facilitating the forecast of pitting potential within the investigated parameter field (Agarwala and Ahmad, 2000).

Electrochemical Noise Technique

Electrochemical Emission Spectroscopy (EES) has been developed for non-destructive, real-time corrosion rate measurements. The measurement of the corrosion is made using signals generated by the corroding system as passive sensors. EES can detect the onset and re-passivation of a previously localized corrosion site. EES offers several advantages over other corrosion monitoring techniques, such as linear polarization resistance and electrochemical impedance spectroscopy (EIS). EES requires no external perturbation of measuring the corrosion rate and may have significant potential in industrial corrosion monitoring applications according to Davis et al. 2002.

Chemical Sensors

Colour Change or Fluorescent Type: There are compounds that change their optical signature when they undergo oxidation-reduction behavior. The compounds, which show colour change in the visible spectrum range, show intense color shift from very light blue to

dark purple when reacting with ferric iron ions during corrosion. However, these compounds have not proven to be very practical in the cosmetic sense; when put into coatings as indicators, they show up as blotches in visible light. The compounds, which show fluorescence in the ultraviolet to near infrared region, were investigated for their corrosion sensing when subjected to the effects of temperature, pH, reduction and re-oxidation behavior. These studies show that fluorescent methods appear to have potential as early warning sensors for the detection of corrosion (Agarwala and Ahmad, 2000). Various smart coatings utilizing electrochemical properties of color change coatings have been developed.

Fiber Optic-Color Changing sensor array (Panova et al., 1997) capable of both visualizing remote corrosion sites and measuring local chemical concentrations at these sites was applied to real-time corrosion monitoring. Heterogeneous fluorescence signals were observed due to both pH increases at cathodic surface sites and pH decreases at anodic surface sites. These fluorescence signals showed both localization and rates of corrosion activity.

Holographic Interferometry

This method is an optical corrosion meter used to measure the corrosion density of copper in sea water (Habib and Al-Sabti, 1997). The meter was developed to test and evaluate materials in relation to different corrosion phenomena. It is based on the principle of holographic interferometry for measuring micro-surface dissolution and on the principles of electrochemistry for measuring bulk electronic current of metallic samples in aqueous samples. Results suggest that the technique is very useful for monitoring pitting at the initiation stage for different metals in aqueous solutions.

Ultrasonic Methods

Ultrasonic bulk waves have been used for the detection of a variety of material defects. By sending ultrasonic waves through substrate and measuring reflection and transmission amplitudes, traveling time, and attenuation, the discontinuities or internal defects can be detected, and the residual plate thickness can be calculated. But the major disadvantage is the time consumed to thoroughly test a large structure in ultrasonic bulk wave's measurements because of point-by-point examination. Furthermore, preparation of the surface and coupling mediums are required. They have limited scanning capabilities and range of inspection is small. For large area inspection, ultrasonic guided waves have been suggested by various researchers as a potential tool. The advantage of guided waves is the ability to travel along the surface and make measurements faster than the use of bulk waves.

Guided wave techniques have proven to provide more information about damage type, severity and location than other SHM methods and are suitable for structural health monitoring applications since they travel long distances and can be applied with simple and easy to operate piezoelectric actuators and sensors that require little power. Although these techniques have been in different stages of development in the aerospace and automotive research, investigations on marine and naval structures have been scanty. The present research proposes to investigate the application of guided waves in submerged structures involving plate geometries to study and investigate corrosion and develop a non-contact, in-situ and in-service corrosion monitoring technology.

2.6 CLOSING REMARKS

Although considerable progress has been made in understanding the propagation of ultrasonic Lamb waves in damaged plates immersed in fluid, for practical application of the technology several advancements are imperative. Lamb wave modes sensitive to different kinds of corrosion need to be identified. The technology needs to be demonstrated in structures undergoing progressive corrosion in marine environments. Moreover, the ultrasonic readings must be calibrated with actual degradations such as mass loss, loss of strength and stiffness in order to evaluate the residual life of a structure. The present work will pave the way for developing an efficient non-destructive technique for monitoring corrosion in submerged, especially marine infrastructural installations.

CHAPTER 3

REVIEW OF LITERATURE

3.1 GENERAL

There is a growing trend of the use of ultrasonic guided waves for damage detection in civil, mechanical, offshore and marine infrastructures. This chapter presents a brief review of the literature utilizing guided waves for damage monitoring in plate geometries used in various kinds of such structures. First part of the review focusses on the applications of Lamb waves for detecting various types of damages in plates. Second part presents a brief account of the important studies utilizing guided waves for corrosion detection in structures.

3.2 GUIDED WAVES FOR DAMAGE DETECTION IN PLATES

Theory for wave propagation in multi layered media for waves propagating along the free surface of a semi-infinite elastic half-space was presented by Lord Rayleigh's derivation **(Rayleigh, 1885)**. The derivation provides a third order expression whose roots determine the velocity of the propagating surface wave.

Stoneley (1924) provided solution for the single interface problem, wherein waves propagating along the interface between two different elastic solids was considered. Subsequently this work was carried forward by **Scholte, (1947)** wherein the conditions were presented when these waves may travel without leaking into either of the solids (true modes). **Pilant, (1972)** further extended this work to obtained solution for leaky waves that attenuate as they propagate.

In **1917 Lamb** extended Rayleigh's work by considering additional interface to present the model of wave propagation through a flat layer of finite thickness. This derivation was for plates in vacuum. Roots of his two equations, one for symmetric modes and one for anti-symmetric modes, yielded the well-known Lamb wave dispersion curves. Although Lamb produced the dispersion equation for acoustic wave propagation in plates in 1917, it became possible in 1961 when **Worlton** experimentally verified the propagation of Lamb waves at megacycle frequencies. This paved the way for application of Lamb waves to be used as a viable means for non-destructive testing purposes.

Love (1911) presented the possibility of shear horizontal waves propagating in the plane of a finite thickness layer. Discussions of these and other specific layer geometries may be found in references **(Ewing and Jardetzky, 1957; Viktorov, 1970; Farnell and Adler,**

1972; Achenbach, 1973; Brekhovskikh, 1980; Brekhovskikh and Goncharov, 1985) The developments of equations of motion for an infinite elastic solid is presented in many texts and is now available and has therefore not been reproduced here **(Kolsky, 1963; Grafff, 1973; Krautkramer and Krautkramer, 1983; Auld, 1990 and Rose, 1999)**. This section outlines the latest works done in experimental investigations in which Lamb waves have been exploited for damage detection in plate geometries due to their unique characteristics.

Guided waves have the characteristic ability to propagate over long spans and quickly provide global information. These waves are characterized by the fact that it requires a boundary (like tube, cylinder or plate etc.) as a guiding surface for wave propagation. In plate like geometries the guided waves called Lamb waves have emerged as a promising candidate in NDE regime. They have low attenuation even when propagating in water loaded structures. Various researchers have recognized the benefits of employing Lamb waves for quick investigation of structures. Thus Lamb waves resulted in faster inspections which reasonably compensated the drop in sensitivity and resolution attainable otherwise with high standard frequency inspection procedures.

Lamb waves have been used to carry out coarse, quick inspection on a variety of different strips and plates by **Lehfeldt and Holler (1967), Ball and Shewring (1976)** and **Mansfield (1975). Silk and Bainton (1979)** explored the application of guided waves to localize the defects in boiler and heat exchanger piping. **Rokhlin (1979)** presented sensitivity of Lamb waves to detect elongated delaminations. **Rokhlin and Bendec (1983)** also studied the interaction of Lamb waves with spot welds. They reported transmission of the first order symmetric (S_1) mode through a spot weld may be linearly related to the cube of the diameter of the spot weld. **Rose et al. (1983)** have reported investigations on suitability of Lamb waves to investigate K-joints in marine structures. Several reported works have used Lamb waves to obtain the elastic properties of materials. **Nayfeh and Chimenti (1983) and Mal and Bar-Cohen (1990)** determined the elastic constants of composite materials. **Okada (1986)** has used Lamb wave techniques to measure the anisotropy of cold rolled metals. Earlier efforts to use Lamb waves for damage detection in plate assemblies include works by **Chimenti and Nayef (1985), Nagy et al. (1986), Perason and Murri (1986), Rose et al. (1986), Nayyef (1986), Tang and Henneke (1989), Bridge and Ramli (1990), Atalar et al. (1990, 1992), Challis and Bork (1993) and Ditri and Rose (1992, 1994)**. Lot of research has been carried out on the application of Lamb waves for damage analysis and monitoring. Prominent works related to the use of Lamb waves in plate structures have been briefed below:

Alleyne and Cawley (1991, 1992) suggested two dimensional Fourier transformation techniques for ease of interpretation of signals obtained in Lamb waves non-destructive testing. These signals are generally complex due to several mode conversion and dispersion that take place during propagation of Lamb waves **(Alleyne et al. 1991)**. Authors used time records from a series of uniformly spread out locations along the surface and applied two dimensional Fourier transform. It resulted into three-dimensional plot of amplitude versus frequency and wavenumber. This transformation provides the amplitudes of various modes traveling at any given frequency. This methodology was extended to both experimental and numerically predicted data. Various interactions of Lamb modes with defects were considered in different frequency-thickness ranges.

Alleyne et al. (1992) elaborated the criteria for selection of appropriate Lamb wave mode and corresponding frequency. Authors reviewed various excitation methods, response measurement and signal processing in plate structures. The authors emphasized the need to transmit a solo non-dispersive Lamb wave mode and explained methods for generating the same. Authors also presented a variety of signal processing techniques, ranging from simple time domain to relatively complex two-dimensional Fourier analysis. Authors emphasized that in low frequency-thickness regions, time domain processing suffices because only fundamental modes are present. But as the higher order modes begin to appear in high frequency-thickness range, this technique is not dependable. Authors presented design of a Lamb wave testing regime through an example. It consisted of a set of tests carried out on a butt-welded steel plate with simulated weld defects of varying depths. Results showed that by avoiding multiple mode regime and judicious selection of testing technique, variations in shape of the received waveform can effectively mapped to the defects present on the plate.

Guo and Cawley (1993) proposed to use Lamb waves for long span investigations of multi-layered composite plates. Authors studied interaction of fundamental symmetric mode with delamination in composite plate. It was reported that reflections of propagating S_0 mode from the delamination defect in composite plate was controlled by its location along thickness direction. Uni-directional and cross laminates specimens with full width delamination defects planted in different layers were tested using wedge transducer at 0.5 MHz mm frequency thickness combination. Experimental results were successfully matched with the analytical results.

Rose et al. (1995) presented a rather sophisticated guided wave technique for NDE of adhesively bonded joints. Proposed guided wave technology was aimed to address aging aircraft issues related with delaminations and corrosion defect detection in lap splice joint and

tear strap. Lot of experimentation were reported in this work including the field trial on a Boeing aircraft. A special Double Spring Hopping Probe (DSHP) was designed in order to have proper contact with the aircraft structures. This work established adaptability of the Lamb wave technique by implementation of the DSHP to tackle varied specimen geometries. It was shown that painted structures rapidly attenuate higher order modes, but the fundamental symmetric mode has penetration power and good sensitivity to defect detection. Plate thinning due to corrosion and cracks in the first and second layer was also detected using the S_0 mode.

Cawley and Alleyne (1996) emphasized the importance of Lamb waves for quick inspection of large structures. Authors discussed main limitation of Lamb wave inspection like, multimode behaviour and dispersive nature resulting into complicated received signals. Authors suggested appropriate choice of frequency-thickness range for exciting Lamb wave modes in non-dispersive region as the key to the successful application of Lamb waves. The paper discussed the selection of an appropriate mode, its excitation and reception for detection of delaminations in composite materials and corrosion in pipes.

Datta and Kishore (1996) presented a two-dimensional plane strain finite element model with absorbing boundary condition to investigate the ultrasonic wave propagation in isotropic and orthotropic media. Model simulated the experimental pulse echo technique to obtain A-scan data, when a short duration pulse propagated through the domain with or without a flaw. Flaws in the form of a crack or an inclusion of different material such as a Teflon insert or a resin rich zone were considered. Frequency domain feature analysis was also performed on A-scan data. This work provided a guideline regarding the suitability of certain harmonics sensitive to certain types of flaw. The simulation exhibited mode conversion and scattering due to the presence of flaws.

Rose et al. (1997) developed a comb transducer model that can be used to study the influence of transducer design parameter on the resulting guided wave field for inspection purposes. Various methods of achieving a dominant mode were discussed in this work.

Ghosh et al. (1998) presented non-contact technique using Lamb wave propagation in large plates for detecting internal defects. Steel plate (9.9. mm thick), aluminum plates (13 mm & 26 mm thick) were used in the experiment. Simulated defect in the form of horizontal holes along central plane and vertical hole on the top of plate were drilled. Local water pools (12 inches apart) with broad band transducers (500 kHz frequency) immersed in water were used for generating selected Lamb wave modes in large plate. Interaction of selected Lamb wave modes (S_0, S_1, A_1) with different types of defects was presented. Voltage –frequency

plots of the received signal have been used to study efficacy of Lamb wave modes to detect internal defect in different orientations. Authors reported that symmetric and anti-symmetric modes did not exhibit same sensitivity to the defects present at center plane. Sensitivity of a Lamb wave mode to horizontal defect in plate is largely dependent on stress distribution corresponding to that mode. However energy distribution curves are better suited for detecting of vertical defects.

Yang and Kundu (1998) carried out similar study in elastic, homogenous but anisotropic multilayered plates. Numerically it was established that different Lamb wave modes generate displacement and stress fields of varying strengths in different layers of composite plates. Different Lamb wave modes were exploited for assessing the extent of damage in different layers of a composite. Subsequently, theoretical predications were verified experimentally.

Kishore et al. (2000) developed a two-dimensional finite element model with absorbing boundary conditions to investigate the scattering of ultrasonic waves in infinite isotropic solids. The model was capable of showing a complex mode-conversion, when a short duration sinusoidal pulse interacted with a flaw like; narrow crack-like defects, cylindrical and spherical holes of size equal to the wavelength of the incident wave. Results in the form of snapshots and scattering cross-sections provided good understanding wave–flaw interaction, especially mode-conversion of the incident field due to interaction with flaw.

Dalton et al. (2001) investigated the potential of guided waves for monitoring large areas of metallic aircraft fuselage structures. The potential for long-range propagation of ultrasonic guided waves through metallic aircraft fuselage structure was investigated using dispersion analysis and numerical modelling, validated by experiments.

Kundu et al. (2001) studied the importance of near lamb wave imaging in multilayered composite plates. Researchers in this work reported defects in any two layers of mirror symmetry in a multilayered composite can be effectively imaged by fine tuning the incident angle / frequency in the neighborhood of Lamb wave mode.

Lowe and Diligent (2001) compared analytical and experimental results of reflection of low-frequency S_0 Lamb wave mode from surface-breaking rectangular notches in isotropic plates. Authors have also explained the periodic variations in reflection coefficients of S_0 mode as a function of notch width and related it to the interference between the reflections from both sides of the notch. In practical NDE applications, perfect square notches may not

be encountered but characterization of notch aspect ratio with reflection coefficient is still important to understand the interaction of guided waves with defects.

Fromme and Sayir (2002 a, b) compared the change in scattered displacement field of A_0 mode around a rivet hole due to presence of defects like crack. A_0 mode in plate was excited selectively by means of a piezoelectric transducer driven below the cut off frequencies of the higher wave modes. The scattered field around a circular cavity was measured point wise using a heterodyne laser interferometer. Simulated damages like, notch cut with a very fine saw blade, and a fatigue grown crack was studied. Good agreement between measurements and analytical results obtained by using Mindlin`s theory of plates was found.

Guo & Kundu (2001) reported the design and fabrication of a new transducer holder mechanism for inspection of pipes using cylindrical guided waves. The holder employed commercially available ultrasonic transducers. It generated compressional waves which were converted into cylindrical waves in pipes using this specially designed holding mechanism. It could detect various kinds of anomalies in copper and aluminium pipes. The preliminary results showed that a number of Lamb modes, when generated properly by the new coupling mechanism, were very sensitive to the pipe defects. **Na & Kundu (2002)** used the fabricated holding mechanism to detect different types of mechanical defects in underwater pipes like dents, gouges and removed metal etc. With the help of this device, the incident angle adjustment and frequency sweeping could be carried out.

Song et al. (2002) presented application of guided waves to obtain size and location of the damage in the form of approximate image using defect locus map technique. Experiment used PE technique in which guided waves excited from one position propagate through plate and reflections form the discontinuity /defect were recorded. Knowing the group velocity and time of flight of reflected waves, approximate distance of defect was determined. An arc of radius equal to calculated distance of defect was drawn. This procedure was repeated for all test positions and arcs drawn. Intersection of the arcs simulated the approximate location, size and topology of the defect. Plates with different thickness and having defects in the form of elliptical and circular cavities were used in the experiment. Authors also compared the effectiveness of using Lamb waves and shear horizontal waves for generating the defect map. Shear horizontal waves produced better results due to non-dispersive nature, better penetration and less mode conversions

Lee and Staszewski (2003 a, b) discussed the modelling of Lamb waves for damage detection using Local Interaction Simulation Approach (LISA) in one-dimensional and two

dimensional cases for homogeneous and heterogeneous materials. LISA approach is particularly suitable for modelling interfaces and discontinuities. Its key advantage was use of sharp interface model (SIM) for imposing the continuity resulting in perfect contact, of displacement and stresses at interfaces and discontinuities. Key point of the analysis was the two-dimensional wave interactions with slot-type defects. Authors reported that however amplitude of the simulated Lamb wave response increased locally due to reflections from damage and boundaries, but overall signal amplitude dropped significantly due to wave attenuation and damage. Amplitude reduction due to damage was more severe for the small width of damage slot. Large widths of damage slots did not cause significant amplitude change.

Benz et al. (2003) suggested automated methodology for localization of notches using Lamb waves. The experimental setup used a laser source and a dual-probe laser interferometer. Time domain Lamb waves were transformed to the time–frequency domain; using time frequency representation (TFR) and individual modes are resolved. TFR data was normalized with respect to propagation distance to obtain slowness-frequency representation (SFR). Reflected and transmitted contributions of each Lamb mode were identified considering the notch to be secondary source. These results were then used to develop a quantitative understanding of the interaction of an incident Lamb and then serve as a basis for a correlation technique to locate the notch.

Fromme et al. (2004) developed a prototype of ultrasonic array of transducers capable of generating ultrasonic guided waves for SHM of large, plate like structures. Proposed set up had a ring of 32 transducers which were permanently bonded to the plate structure with a protective membrane, encompassing necessary multiplexing electronics. Laboratory measurements on a 5 mm thick steel plate were performed containing various machined defects simulating corrosion defects using A_0 Lamb wave mode. Sensitivity of the array device for defect detection was established by comparing the results for standard defects to theoretical predictions. Simulated corrosion pitting and a defect cut with an angle grinder simulating general corrosion were easily and effectively detected. An approximate indication of the severity of a defect could be obtained from the amplitude of the reflected signal.

Leduc et al. (2004) studied sensitivity of Lamb waves to the plate roughness experimentally using an air-coupling transducer system. Plate surface topographies acquired by an optical surface profiler were compared with the acoustic characteristics viz. wave phase velocity and amplitude attenuation. It was reported that amplitude attenuation was strongly

affected by the surface roughness and thus is a strong parameter to discriminate between different levels of roughness.

Edalati et al. (2005) investigated two ultrasonic lamb wave techniques of pulse-echo (A_1 mode emitter) and emission (S_1 mode emitter) for interpretation of notch defects with depths of 10%, 30% and 60% of plate thickness. Thickness of plate was 2 mm and the nominal central frequency of transducers was 2MHz. Angle probe and normal contact probes were employed for Pulse echo and emission techniques respectively. It was observed that these techniques were sensitive to evaluate notch defects, especially in short probe to defect distances.

Santos and Perdiga (2005) used Leaky Lamb waves for the detection and sizing of defects in bonded aluminium lap joints using probes in pitch catch configuration. The scattering of the fundamental symmetric mode S_0 from through holes in plates were analysed and compared with the results obtained by analytical model. The same approach was used for the scattering evaluation from defects localized in the bond line of aluminum lap joints.

Banerjee and Kundu (2006) studied elastic wave propagation in sinusoidally corrugated waveguides. The authors developed semi-analytical technique called Distributed Point Source Method (DPSM) to model the ultrasonic field in sinusoidally corrugated waveguides immersed in water where the interface curvature changes rapidly. The ultrasonic field is computed both inside the plate and in the surrounding fluid medium. Theoretical predictions were compared with experimental results generated by reflecting a bounded 2.25 MHz ultrasonic beam by a fabricated corrugated plate. It is observed that the reflected beam strength is weaker for the corrugated plate in comparison to that from the flat plate. The backward scattering is found to be stronger for the corrugated plate in comparison to the flat plate. However, in waveguides with small corrugation the wave propagates in the forward direction. The forward and backward propagation phenomenon is found to be independent of the signal frequency and depends on the degree of corrugation**.**

Drinkwater and Wilcox (2006) presented a review of use of ultrasonic arrays for damage detection. According to the authors, arrays offered great potential to increase inspection quality and reduce inspection time and their main advantages were their increased flexibility over traditional single element transducer methods, meaning that one array could be used to perform a number of different inspections, and their ability to produce immediate images of the test structure was better. Reported advantages had led to the rapid uptake of arrays by the engineering industry.

Lu et al. (2007) investigated numerically and experimentally the forward and back-scattering of Lamb waves by through-thickness cracks of different lengths and orientations in aluminium plates. Array of surface-bonded piezoelectric discs were arranged as actuators and sensors to generate and collect Lamb waves, respectively, and the effect of crack orientation on Lamb wave propagation was evaluated.

Mijarez et al. (2007) reported the possibility of using permanently attached PZT sensors for real time monitoring of sub-sea cross beam members in offshore oilrigs. Proposed approach improved the limitation of flood member detection (FMD) and made the monitoring more automated. Experimental set up comprised of single PZT transducer permanently attached to the lower end of subsea crossbeam, powered by seawater battery; receiver transducer with signal amplifier , fitted at the top end of the cross beam. The transmitted signal propagated through two channels viz. through the seawater (TSA) or through the steel structure (TSW) wave guide. Axisymmetric L (0, 7) mode at a frequency of 38.5 kHz was used with nominal attenuation through the steel. TWA approach using underwater communication faced certain problems like noise and signal attenuation, resulting in poor SNR.

Banerjee and Kundu (2008) applied DPSM technique to model ultrasonic fields in solids with internal anomalies immersed in a fluid generated by finite size transducers. A general formulation for both isotropic and anisotropic solids was presented in this paper.

Benmeddour (2008 a, b) studied the fundamental Lamb modes interaction with symmetrical and asymmetrical notches. In this work, using FEM and modal decomposition techniques, power reflection and transmission coefficients were computed. The key point was to decompose the symmetrical notch into two elementary abrupt changes in the plate section. The power reflection and transmission coefficients were computed, using finite element and the well-known average power flow equation. An experimental device was built to launch an individual A_0 or S_0 mode and to study their sensitivity to symmetrical notches. This technique facilitated a faster analysis and a direct comparison between the numerical and the experimental results.

Bingham et al. (2009) described the use of ultrasonic guided waves for identifying the mass loading due to underwater limpet mines on ship hulls. Authors used Dynamic Wavelet Fingerprint Technique (DWFT) to extract the guided wave mode information in two-dimensional binary images because raw time domain waveform features are too complex to understand. Signal processing using wavelets retained both time and scale features. 500 kHz transducers were placed on the ship hull in longitudinal and transverse direction. Plate

thickness of the hull was 18.25 mm and S_2 lamb wave mode was excited by using 15.53^o angle of incidence. Authors were able to capture the leaky Lamb wave with transducer placed 1 meter apart. Despite leakage of energy in the surrounding fluid, propagating Lamb wave modes were reported to be sensitive to the mass loading on plate.

Ledesma et al. (2009) presented a case study about a partially underwater gas pipeline approximately 1km long.

Santos and Faia (2009) investigated the propagation of ultrasonic Lamb waves in aluminium adhesively bonded lap joints and in single plates. Authors analysed the propagation of Lamb waves in multi- layered systems by characterising their behaviour in the bonded region. Immersion probes with central frequency of 500 kHz were employed in pitch catch orientation to generate desired Lamb wave mode in aluminium bonded plates. Peak to peak amplitude of S_0 mode in case of single and bonded plates was used to determine the attenuation due to bonding region. Comparison of experimental attenuation of the single and bonded confirmed the dominant propagation modes existing in the bonded region. Longitudinal and the transversal attenuations in aluminium plates was also determined using guided waves propagation parameters which is usually difficult, especially in thin plates by using the conventional pulse-echo technique.

Rizzo et al. (2010) presented application of hybrid laser/immersion transducer system for long range inspection of underwater structures. Elastic waves were generated in a submerged aluminum plate (1200 x900 x 1.5875 mm^3) using pulsed laser. A pair of conventional immersion transducers was used to detect the propagating waves. Transmission of lowest order symmetric, anti-symmetric leaky Lamb modes and quasi-Scholte wave mode were studied. Time domain signal were processed using the Gabor wavelet transform to obtain ultrasonic energy transmission coefficients. Two simulated damages, a rectangular notch (30 x 1 x 1 mm^3) and a circle (diameter 4mm and 1 mm depth), were machined on the specimen. Authors reported that the selected modes were significantly modified by the presence of these defects. Authors suggested to use small lift off distance for Scholte mode because the amplitude of particle motion reduced significantly away from the interface. This work provided an effective non-contact approach to inspect underwater structures.

Mohan and Mitra (2011) presented an experimental study on Lamb wave based tomography for damage detection in thin aluminium plates. Lamb wave were employed for the purpose of tomography for creating an image of the test specimen using the propagation parameters of wave passing through the specimen. The array of patches required for the experiment was studied and modified cross-hole geometry was used. Prior to the

experimental study, a FE simulation was carried for defect-less plate and is validated with the experimental results. Later, the experiments were conducted for different forms of damages, namely, lumped masses of different sizes and orientations, and notch. The experiments proved that the method was successful in predicting the presence of defects, orientation and size using time-of-flight (ToF) data of the propagating Lamb wave.

Poddar et al. (2011) experimentally studied application of time reversibility of a Lamb wave for baseline-free damage detection in an aluminum plate where in reconstruction of the original signal was achieved at the source location by a time reversed form of the received signal at the receiver and presence of damage in the path of the signal was ascertained by observing the change in reconstructed signal. Authors used PZT wafer transducers to explore the effect of frequency, pulse frequency band width, transducer size and the influence of tuning these parameters on the quality of a reconstructed input signal. Authors concluded that narrower frequency band width and selection of proper actuator size resulted in lesser amplitude dispersion leading to better reconstruction of input signals for enhanced damage sensitivity. Time reversal process (TRP) was also implemented to detect various defects like block mass, notch and surface erosion in an aluminum plate and these defects could be effectively discerned by quantification of reconstructed signals.

Deng and Yang (2011) studied the scattering of S_0 Lamb mode in plate with multiple damages. Plate theory and wave function expansion method were used to derive the analytical solutions for the scattering wave field in plate with a single damage, and by using the addition theorems of Bessel functions, interference phenomena between scattering wave fields from different damage were successfully investigated.

Singh et al. (2011) used guided waves for sizing strip-like defects in plates. This paper dealt with developing a parametric 2D finite-element technique, which can size strip-like defects in elastic or viscoelastic, isotropic or anisotropic material plates. A pure incident Lamb wave mode is sent towards the defect and reflection and transmission coefficients produced by mode conversion phenomenon were used as input data for the inversion process, which consisted in quantifying two unknown parameters representing the geometry of the defect.

Bijudas et al. (2013) used time reversed Lamb wave (TRLW) technique for baseline independent damage detection of stiffened aluminum plate. Authors used fundamental anti symmetric Lamb wave mode to establish the efficacy this technique in identifying the damage in a stiffened plate. Damage in the form of disbanding and cracking of the stiffeners

in plane and T-stiffeners configurations were considered. Desired Lamb wave mode was excited and captured by using piezoelectric wafer transducers through specific transducer placement and amplitude tuning. Effects of mode splitting and conversion at the entry and exit of the stiffening member were considered in reconstruction of time reversed Lamb modes. Samples with T-stiffeners posed a complex interaction of Lamb wave mode in reconstruction process but due to low amplitudes of converted and secondary reflected modes the results were not much affected.

Leleux et al. (2013) used a low frequency, multi-element matrix probe driven by phased array principle for exciting and capturing pure Lamb wave modes in large plates. Selected modes propagating were launched and detected in specific directions for which phase and group velocities are collinear. Authors experimentally evaluated the directivity of the launched guided beams and the possibility of detecting, locating and sizing acoustic sources like placed at various positions around a receiving probe. Defects like 3D shaped delamination, impact damages in composites plates and corrosion-like defects in metallic plates were detected using the proposed setup prototype.

Pistone et al. (2013) presented an automated non-contact damage detection technique for monitoring of immersed metallic plate by using leaky Lamb waves. Authors used hybrid setup comprising of laser-induced ultrasound exciters with array of immersion transducers as detectors. Time domain signal were processed to obtain damage-sensitive features and were subsequently used in a multivariate outlier analysis. Results were related to the simulated defects inflicted on the specimen. FE model was developed to simulate the propagation of the guided waves in plate and pressure field in the liquid. Authors used monitoring system for the automated inspection of immersed structures that was designed by the research group and its repeatability was ensured by comparing the signals recorded at same point and by inspecting the test object many times. Signal processing algorithm adopted in this study was able to capture an artificial notch clearly and was partially able to detect a through-thickness hole that was as small as few millimeters. A dent and a simulated corrosion (plate thinning) were not detected probably due to their small size. Results could be further improved by rearranging the spatial direction of the detectors and by selecting other features from the time, time–frequency and frequency domains.

In most of these reported works, the subject structure is placed in air and transducers are required to be in direct contact with the structure being monitored. Owing to the several practical limitations in direct contact approach and to exploit mode specific behavior of Lamb waves to advantage, some researchers have also suggested to use local water column as an

effective means to couple the structure with the transducer. **Ghosh et al, 1998; Na and Kundu, 2002a, b** designed setups using specialized coupler mechanism and transducer holder capable of generating desired Lamb wave for inspecting defects in large plate structure and underwater pipes, however in these studies the structure not in submerged state.

In case of completely submerged structures, presence of water makes the situation unique and challenging as it acts as a natural couplant. Studies on a non-contact health monitoring methodology for submerged plate geometries are scant. Prominent works regarding the application of guided waves for monitoring submerged structures include **(Mijarez et al. (2007), Ledesma et al. (2009), Chen et al. (2010), Bingham et al. 2010, Rizzo et al. (2010), Pistone et al. (2013)**. Although considerable progress has been made in understanding the propagation of ultrasonic Lamb waves in damaged plates immersed in fluid, for practical application of the technology several advancements are required. Lamb wave modes sensitive to different kinds of damages and corrosion need to be identified. The technology needs to be demonstrated in structures undergoing progressive corrosion in marine environments. Moreover, the ultrasonic readings must be calibrated with actual degradations for predicting residual strength. The objective of the present research is to study the propagation of ultrasonic guided waves through a submerged plate and develop a non-contact, non-invasive damage monitoring methodology for submerged plates simulating ship hulls in marine environment with notches and corrosion defects.

3.3 GUIDED WAVES FOR CORROSION MONITORING

Corrosion in marine infrastructure is particularly challenging mainly due to factors viz.; highly insidious, limited access for monitoring, relatively higher cost of corrosion damage and associated risk to human life and property. Variety of techniques have been developed and implemented to detect corrosion in marine structures. A lot of research effort is still on to develop automatic system for data acquisition and interpretation for evaluating health of marine infrastructures. Use of ultrasonic guided waves is one of the promising options that provide good penetration power as guided waves have long propagation distance. Some of the latest works related to application of guided waves for detection of corrosion are presented below:

Lowe et al. (1998) used guided waves for corrosion detection in insulated pipes in chemical and oil industry. Presented method replaced the current practice of point by point investigations which necessitated removal of protective insulation at the each point of testing. Authors used propagation of ultrasonic guided waves in pipe walls using pulse echo

configuration. Access to the pipe surface was provided by removing insulation at just one location. Signals were then transmitted and reflections from received using a single transducer unit. This work mainly focused on selection of the optimum guided wave modes and the formulating the relationships between the reflection signal amplitude vis-à-vis the defect size. Dry-coupled piezo-electric patches distributed around the circumference of a ring were employed to generate and receive an axially symmetric mode. Arrival times of reflections reveal the presence and axial location of defects. Authors reported that a span of 50 meter pipe length could be done in one set up. Key feature of this work was generation of a selected single mode despite the possibility of number of other modes within the used frequency bandwidth. Reflection coefficients of L(0,2) and F(1,3) modes were successfully related to the extent of damage on the pipes. The results provided a basis for predicting the strengths of L(0,2) and F(1,3) reflections from defects for any combination of circumferential and radial extent and it was generalized for pipes of other sizes.

Alleyne et al. (2001) addressed the issues related with inspection of corrosion on pipe network in industrial and civil applications. Main problem in such situations is the accessibility of the structure for inspection and cost of inspection. Authors suggested use of Guide waves for quick investigation of longer span of pipes. Guided waves were launched from one location on the pipes and reflections if any from the corrosion or other discontinuity were analyzed for its location. Authors used dry coupled piezeo electric transducer system **(Figure 3.1)** and an inspection span of up to 25 meters on pipelines with 2 to 24 inches

Guided Ultrasonics Ltd Wavemaker 16 instrument and transducer rings for 3 inch pipe

Flexible, pneumatically clamped transducer rings for larger diameter pipe

Figure 3.1: Guided Ultrasonics Ltd. Wavemaker for corrosion detection in pipes (Alleyne et al., 2001)

diameter was reported. L(0,2) mode was employed due to factors viz. non-dispersive nature, particle motion largely in axial direction and uniform distribution of strain through pipe wall. Circumferential and radial extents of the depth were correlated with the reflection coefficients. The system yielded good field results also. Cross sectional area loss up to 5-10% could be detected at any given axial position.

Jenot et al. (2001) demonstrated the use of Lamb waves for measurements for thickness of plate undergoing corrosion. In this work, researchers measured group velocity of S_0 mode propagating through plate. Variations in the measured group velocities were related to the progressively reduced thickness of the plate exposed to successive chemical attacks. Dispersive nature of Lamb waves, which is otherwise considered to be an impediment in guided wave health monitoring applications, was used to advantages in this work. A pair of Perspex wedge was employed to excite desired Lamb wave modes through a copper plate (0.45 mm thick) which was successively exposed to concentrated nitric acid. Experimental and numerical results indicated that the group velocity can be very sensitive to the reduction in thickness; however it depended upon the Lamb wave mode used for monitoring. This technique yielded satisfactory results when the erosion of the surface was uniform and there were small variations in thickness. Results were found be independent of the side (corroded or on the un-corroded) on which the Lamb wave generation and detection for group velocity measurements were made. Authors recommended wavelet signal processing to resolve the signals, when several modes overlap because of strong dispersion or limited propagation distance. Thus it was possible to track the desired Lamb wave mode for which the variation in group velocity Vis-a Vis thickness of plate was considered.

Tuzzeo and Scalea (2001) used micro machined air coupled capacitive transducers nondestructive detection of thinning in aluminum plates due to corrosion. Author exploited dispersive nature of selected Lamb waves. Mode cutoff, frequency shift, group velocity and time of flight measurements were used for estimating the severity and extent of material loss in the form of corrosion.

Saidarasamoot et al. (2003) presented a broad review of the state of the art non-destructive evaluation techniques used for ensuring the integrity of the coatings on marine structures and meticulously examine the corrosion wastage. Authors compiled review of developments in important nondestructive techniques like electromagnetic wave sensors for eddy current, elastic wave sensors for advanced ultrasonic practices, electrochemical sensors and time-resolved thermography techniques etc. The authors emphasized the necessity of using methodologies for convenient and quick assessment of corrosion loss on coated marine

structures despite tough spatial locations. Each one of the available nondestructive technologies was evaluated on the basis of a set of requirements obligatory to be a suitable marine corrosion wastage testing tool.

Sicard et al. (2003) presented the possibility of using phase velocity variations in A_1 mode as an investigation parameter for detection of corrosion in the form of thinning of plates in airframe structure. For a corroded patch if the thinning is relatively constant in depth, the phase velocity curve of a Lamb wave propagating through this area can be exploited to evaluate the residual thickness. In this work a Comb array and a wedge transducer were employed as emitter and receiver respectively. Mode selection was based on the criteria: mode should be highly dispersive and should be isolated form other modes in phase velocity dispersion curves. 11.5 % thinning was reported to be measured with an accuracy of 2%.

Sicard et al. (2004) presented Lamb Synthetic Aperture Focusing Technique (L-SAFT) for detecting and obtaining images of corrosion defects with defect to wavelength ratio as small as 2/11. This technique proposed to overcome the limitation of Lamb wave investigations like; low SNR due to dispersive nature, inaccuracy in time of flight measurement for long span inspections. L-SAFT algorithm generated defect images of corrosion pitting using pulse-echo data in frequency domain. Authors demonstrated the application of this technique in imaging of simulated defects (5 holes of diameter 1.5mm on 1.82 mm thick stainless steel 304 plate) and simulated defects (real corrosion pit of 0.25 mm diameter and 0.25 mm deep on 1.87 mm thick stainless steel 304 plate) using 2 MHz transducer. Simulated defect was detected using A_1 and S_1 modes, whereas as corrosion defect was detected using S_1 mode.

Yeo and Fromme (2006) investigated pilot Finite Element (FE) study on Lamb wave propagation and reflection characteristics in plates resembling part of a ship hull. The hull of ships is reinforced using longitudinal and transverse stiffeners, web frames. These zones are acknowledged to be safety sensitive area and prone to fatigue as well crevice and pitting corrosion. In this work a two dimensional FE model a ship hull has been idealized as a stiffener on a plate. Corrosion damage introduced as localized thickness reduction at different locations relative to the stiffener and excitation and monitoring locations. Authors studied wave propagation, reflection, transmission and mode conversion characteristics with A_0 mode pulses and predicted sensitivity of defect detection. Reasonably good sensitivity for the detection of defects at a stiffener and lying masked behind a stiffener were predicted. Special emphasis was placed on the quantification of the A_0 mode pulses reflected back to the

excitation location, which could be measured using a guided wave array monitoring approach. However, due to the large number of structural features, the authors concluded that the observed time signal was quite complicated and the exact determination of defect location and severity from a measured time trace would require further investigation.

Mazeika et al. (2007) investigated the Lamb wave tomography for inspection of tank floors for corrosion deposits where circumferential access is available. Proposed technique did not require draining and cleaning of the tank, thus ensuring in-service inspection. Authors presented the pilot study carried out on a prototype small sized tank and results of *in situ* experiments were reported. Authors found that significant losses take place due to loading conditions and lap weld present on the floor plate. These losses are comparatively lesser for fundamental symmetric mode as compared to fundamental anti symmetric mode and hence this mode is not recommended for scanning longer spans. Authors proposed prediction technique of the informative signal which considered propagation characteristics like attenuation, frequency dependent leakage losses and appropriate phase velocity dispersion, so as to improve the quality of transmission tomography.

Volker et al. (2008) presented a permanent corrosion monitoring system using guided waves with a focus on real time quantitative evaluation of ageing infrastructure in order to improve reliability. Authors presented a methodology for evaluating the wall thickness of a plate specimen with water loading on one side using two arrays of ultrasonic transducers. Transducers in the active array were excited sequentially to generate selected Lamb wave modes in dispersive zone. All transducers in the receiver array recorded the signals. Transmitting transducers excited selective Lamb wave modes that are highly dispersive. When these modes interacted with the section of plate having thin section due to corrosion, it took longer to propagate. Inversion algorithm was invoked to invert the measured time of flights to corresponding wall thickness.

Chen et al. (2010) emphasized on the early stage detection of corrosion to prevent massive degradation to the metallic structure embedded in corrosive environment. Authors presented corrosion detection technique in terms of pulse echo measurements in submerged structures by employing A_0 mode. This mode was preferred over S_0 mode due to factors like; ease of excitation, lower wavelengths and larger signal amplitude. But coupled fluid medium drastically modulated propagation characteristics of A_0 mode resulting in erroneous identification of the damages. Authors investigated and calibrated the effect of fluid coupling of varying extents on the A_0 mode. The proposed technique was corroborated analytically numerically by assessing through-thickness hole and chemical corrosion in submerged

aluminum plates by using probability-based diagnostic imaging approach. Results proved the need to rectify and compensate medium loading effect in case of Lamb-wave-based damage identification.

3.4 CLOSING REMARKS

Review of literature since last five decades have established the capability of Lamb wave for damage detection in plate geometries with simulated damages in the form of cracks, notches and corrosion defects. But rarely any study has been focused on site application to real time damage monitoring of submerged plates undergoing actual corrosion. The objective of the present research effort is to develop a real time, non-invasive corrosion monitoring strategy for submerged plate structures using guided waves. Although considerable progress has been made in understanding the propagation of ultrasonic Lamb waves in plates immersed in fluids, for practical application of the technology several advancements are imperative. Lamb wave modes sensitive to different mechanisms of corrosion need to be identified. The technology needs to be demonstrated in structures undergoing progressive corrosion in marine environments. Moreover, the ultrasonic readings must be calibrated with actual degradations such as mass loss, loss of strength and stiffness.

CHAPTER 4

ULTRASONIC WAVE PROPAGATION IN SUBMERGED PLATES

4.1 GENERAL

A rigorous experimental study on generation of specific guided waves modes at particular frequencies in submerged plate is presented in this chapter. The idea is to develop an effective non-contact health monitoring strategy for submerged plate structures utilizing ultrasonic Lamb waves. The submerged plate is subjected to ultrasonic waves obliquely generated by a cylindrical piezoelectric transducer using the surrounding water as coupling medium. Suitable Lamb wave modes with optimum scanning capabilities have been identified in submerged plate systems. Finally, the propagation of these selected modes through submerged plates would be further utilized for damage detection in plates.

4.2 EXPERIMENTAL INVESTIGATIONS

4.2.1 Set-Up and Specimen Details

The experimental set-up consists of an acrylic tank (1500mm x 1000mm x 900 mm) filled with water up to 750 mm height to completely submerge the mild steel plates. Plate specimen is placed on wooden blocks in the water tank. To avoid the interference of unwanted reflected waves from the tank walls, water top surface and bottom of the tank, a minimum separation of about 250 mm is maintained. A pair of ultrasonic transducers arranged in pitch-catch orientation is used for generation of ultrasonic waves. These probes are fitted in holder arrangement that has four degrees of freedom (X, Y, Z, and θ) **(Figure 4.1).** These transducers can be moved along X, Y directions using a drive. The drive consists of three stepper motors with 1.8^{o} step angles controlling the translatory motions. The motors are individually controlled by a microprocessor unit operated through a user interface. Two motor drives are used for regulating the inter-probe distance along Y-direction by moving the two probes independently (Y-DOF). The third motor unit is dedicated for moving the both the probes simultaneously in X-direction, thus scanning the specimen in X-direction (X-DOF). Using XY drive all locations on the submerged plate can be approached and scanned by any of the two probes. This entire scanning set-up is fitted on top of water tank.

Another important feature of the set-up is a *Digital Read Out* (DRO) system**,** which provides the user the current X and Y coordinates of the probe with respect to the user defined origin. Both the probes can also be independently adjusted manually in Z-direction (Z-DOF). In addition to this, probes can also be set at desired angle with respect to the vertical (θ – DOF, least count 0.1 degree). It enables the probes to be placed obliquely at required angle of incidence to the specimen.

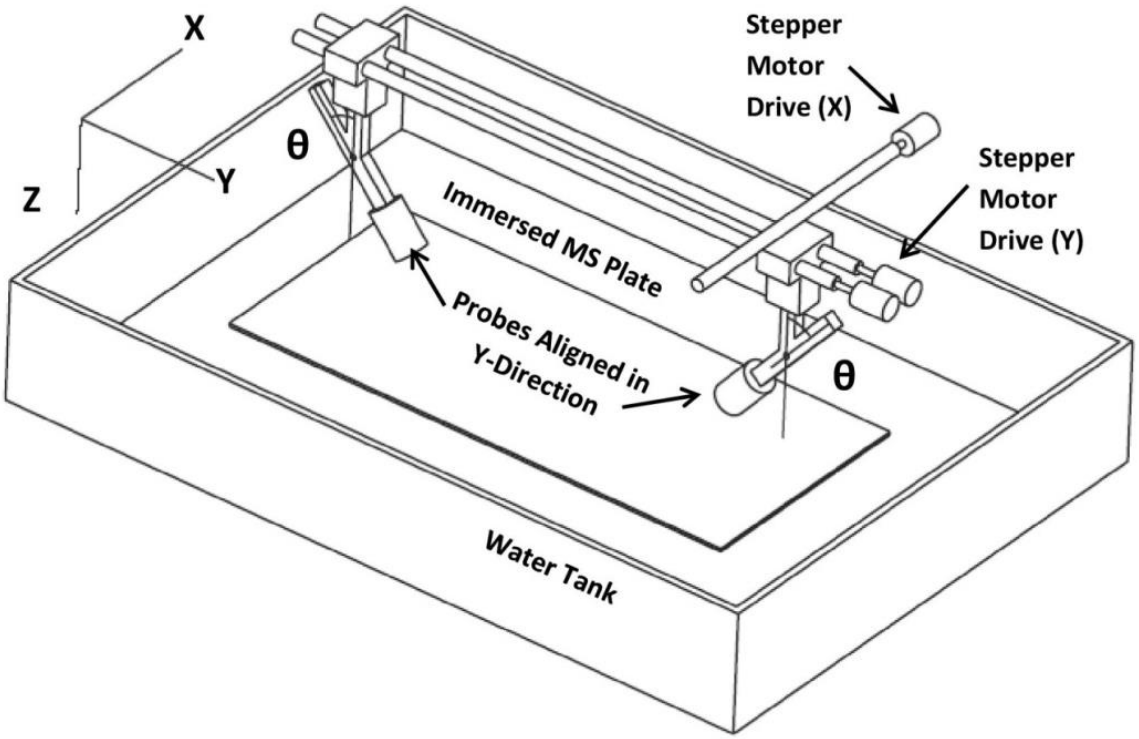

Figure 4.1: Scanning Set up

For ultrasonic testing, a typical UT system consisting of a Pulser-Receiver (PR) device (JSR make, Model DPR 300), ultrasonic transducers (Parametrics^{TM} Immersion Probes), data acquisition card (Agilent Make) and display devices have been used **(Figure 4.2 a, b)**. The subject steel plate (1065 mm x 610mm x 4mm) supported on wooden blocks is completely immersed in the water tank. Two pairs of immersion probes (Olympus Make) with rated frequencies of 0.5 MHz and 1 MHz have been used for the investigation. Selection of frequencies of 0.5 MHz and 1 MHz for initial investigation is based on the principle of lesser material attenuation, scattering and mode conversions at lower frequencies (Alleyne & Cawley, 1992; Ghosh et al., 1998; Rose 2002 (a, b); Rose 2003.

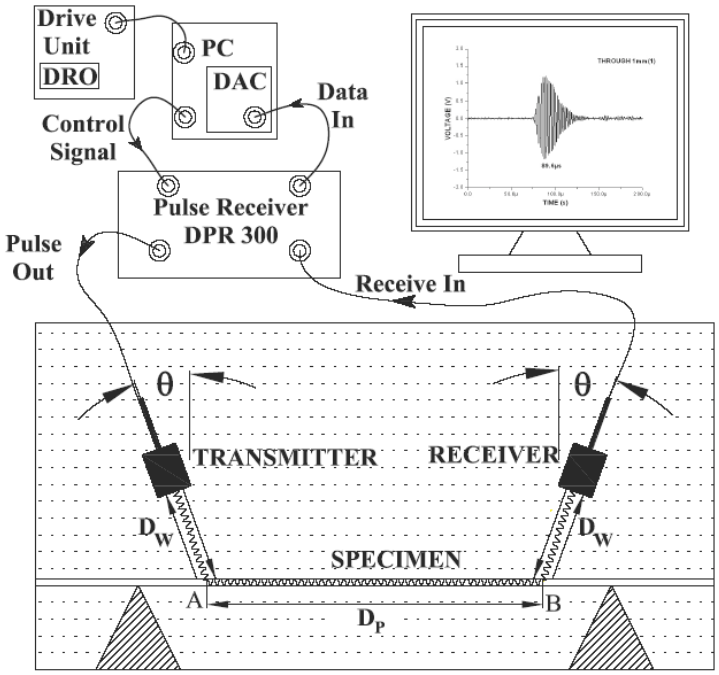

(a) Schematic Arrangement

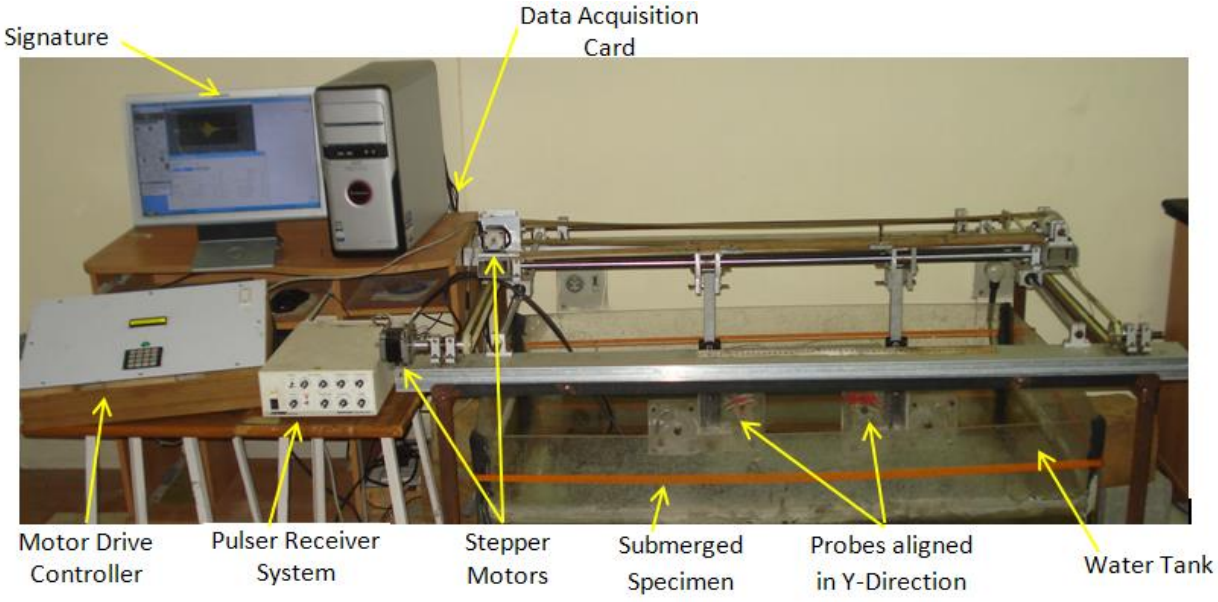

(b) Actual Photo

Figure 4.2: Experimental Set-Up

4.2.2 Ultrasonic wave propagation in submerged plates

The present study focuses on the propagation of ultrasonic waves through the immersed plate for developing a non-contact health monitoring strategy. For this purpose, the ultrasonic probes and the subject plate specimen are completely immersed in water. The probes are placed in pitch catch orientation, at a distance from the immersed plate and

making equal inclinations (θ) with vertical (**Figure 4.2a**). A vertical gap is maintained between the probes and the immersed plate so as make the system non-contact. A pulse of specific duration and amplitude is generated by the P-R The longitudinal ultrasonic waves generated by the transducers travel through the surrounding water and impinge the submerged steel plate obliquely. This input energy is partly reflected and is partly transmitted into the plate. In the pulse echo (PE) mode reflected waves are received by the probe.

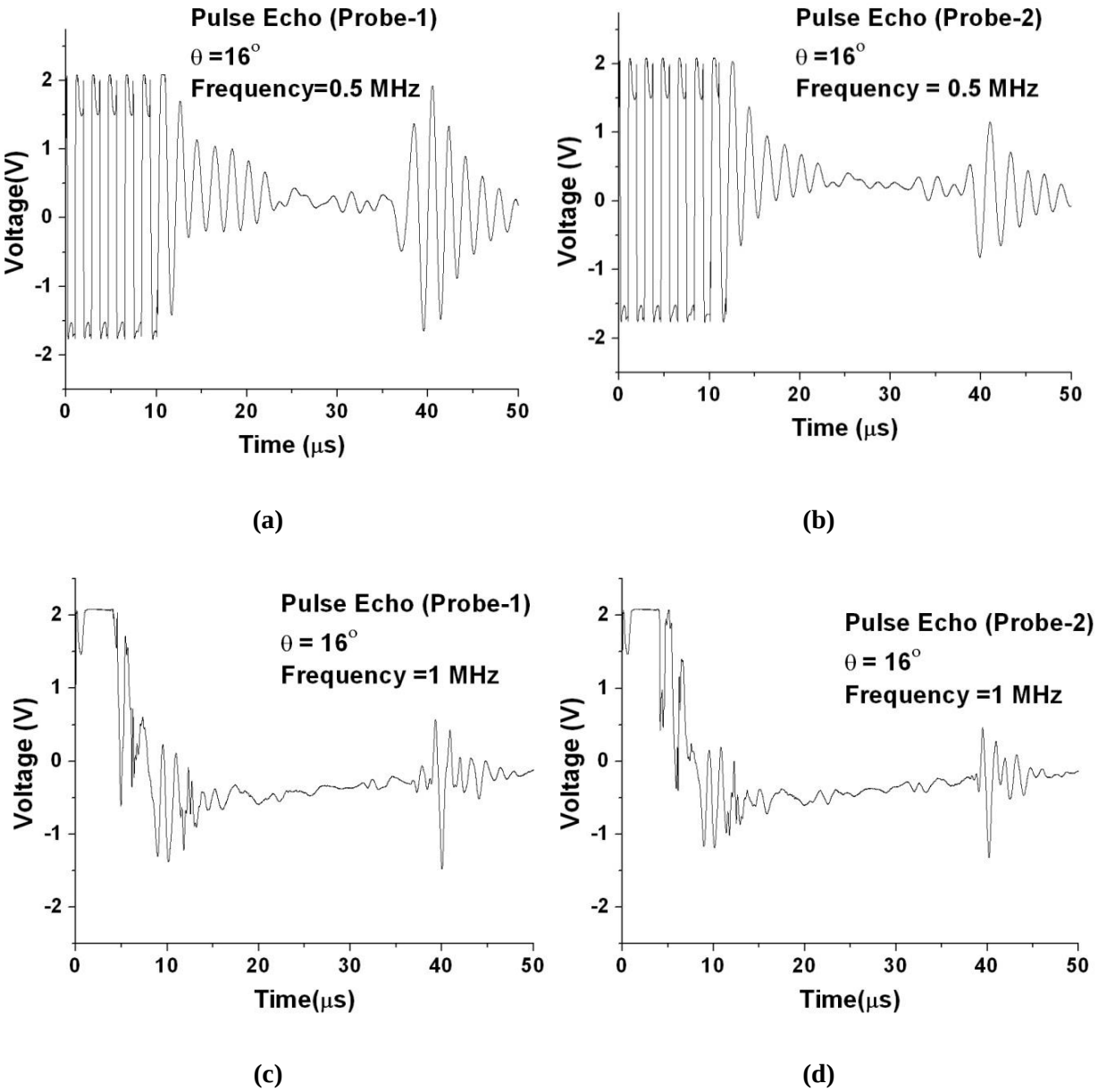

Figure 4.3: Pulse Echo Signtaures at θ=16° (a-b) 0.5 MHz, (c-d) 1 MHz

Distance of separation (D_w) of the probes from specimen is termed as *Water Path* **(Figure 4.2a)**, as it is the distance travelled by longitudinal wave in water before the wave hits the solid interface.

Figure 4.3(a-b) and **Figure 4.3(c-d)** show PE signatures for the both the probes set at a particular angle ($\theta=16^o$) for the two selected frequencies of 0.5 MHz and 1 MHz respectively. It may be noted that the time of flight in these signatures is kept the same by adjusting D_w. Water path (D_w) can be related to the time of flight in water (t_w) of the first reflection from the specimen in Pulse Echo configuration

$$D_w = \frac{t_w \times V_w}{2} \tag{4.1}$$

where

V_w is the longitudinal velocity of the sound in water.

Too large a water path results in loss of incident energy to the surrounding water. On the other hand, if the probes are placed too close to the plate, field reflections from the solid interface overlaps with the initial pulse of the transducer. Also the near field effects influence the received signal. A number of trials were undertaken to obtain the suitable water path. Time of flight in water (t_w) in the range of 40-50μs gives satisfactory results in terms of signal fidelity and repeatability. Thus, in the entire experimental investigations t_w is kept at 40μs for both the probes.

After setting the probes, ultrasonic testing of the immersed specimen has been carried out in pulse transmission (PT) mode. The input energy is transmitted into the plate and is guided by the plate geometry to propagate further in the solid media. Guided waves propagating through the immersed plate continuously loose energy to the surrounding water. These leaky guided waves are captured by the receiver probe. These pulses are further conditioned by the PR unit and are displayed on the screen. The distance traversed by the guided waves through the plate is termed here as *Propagation distance (D_p)*. **Figure 4.4 (a, b)** show the PT signatures obtained using 0.5 MHz and 1.0 MHz probes in healthy plate. PT signature at 0.5 MHz has only one clear peak **(Figure 4.4a).** But PT signature at 1 MHz **(Figure 4.4 b)** has two distinct peaks indicating arrival of two different trains of pulses at the receiver probe, traveling with different speeds.

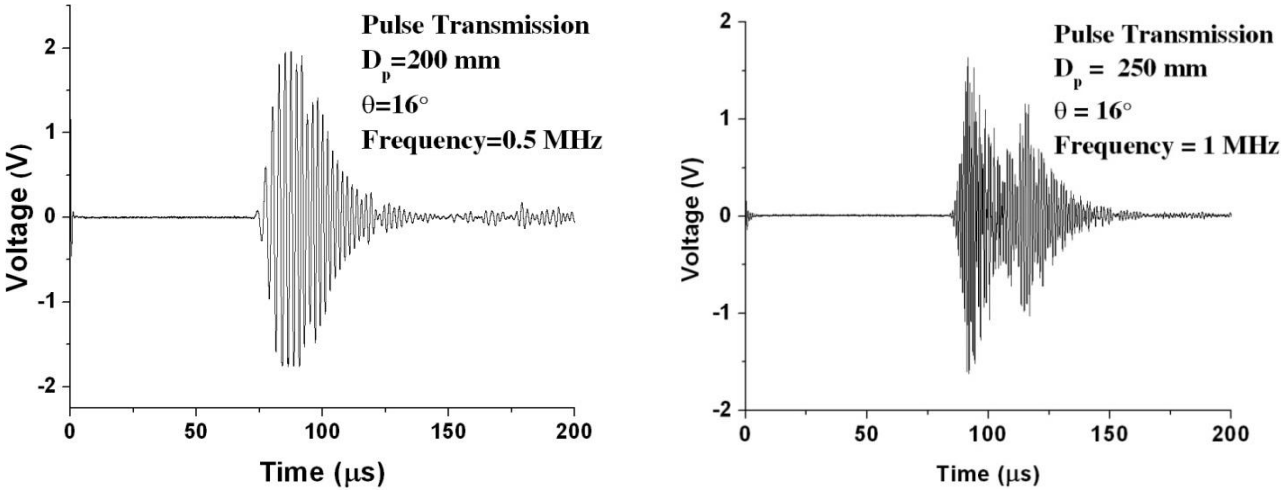

(a) **(b)**

Figure 4.4: Pulse Transmission Signatures at θ=16^o (a) 0.5 MHz, (b) 1 MHz

PT signatures are likely to get affected in the presence of damage in the plate. To investigate the feasibility and efficacy of the guided waves to detect damages in the submerged plate utilizing PT, notch damages of varying depths were inflicted on the immersed plate and PT signatures in the notched plates were compared with healthy plate signals. **Figure 4.5** shows the results of a primitive study to understand the effect of varying the notch depth on the PT signature using 0.5 MHz and 1 MHz frequencies. It is clear that as the depth of the notch increases the peak to peak voltage amplitude of the received signal drops. Hence, PT technique can successfully identify the notches and possibly quantify the extents.

Also, at 1 MHz, the left peak corresponding to the faster travelling wave train at 1 MHz is visibly more affected as compared to the peak appearing on the right. It is also evident from **Figure 4.5** that the time of arrival of the received pulse remains largely unaltered. Hence, pulse transmission testing of immersed plate obtained by using non-contact probes exhibit a great potential as a non-destructive investigation tool. A detailed study of interaction of Lamb waves with the simulated damages like notches is presented in Chapter 5. The following section describes the effect of other experimental variables like angle of inclination (θ) and propagation distance (D_P) on the transmitted wave signal. The effect of external physical obstruction on the Lamb wave propagation is also investigated.

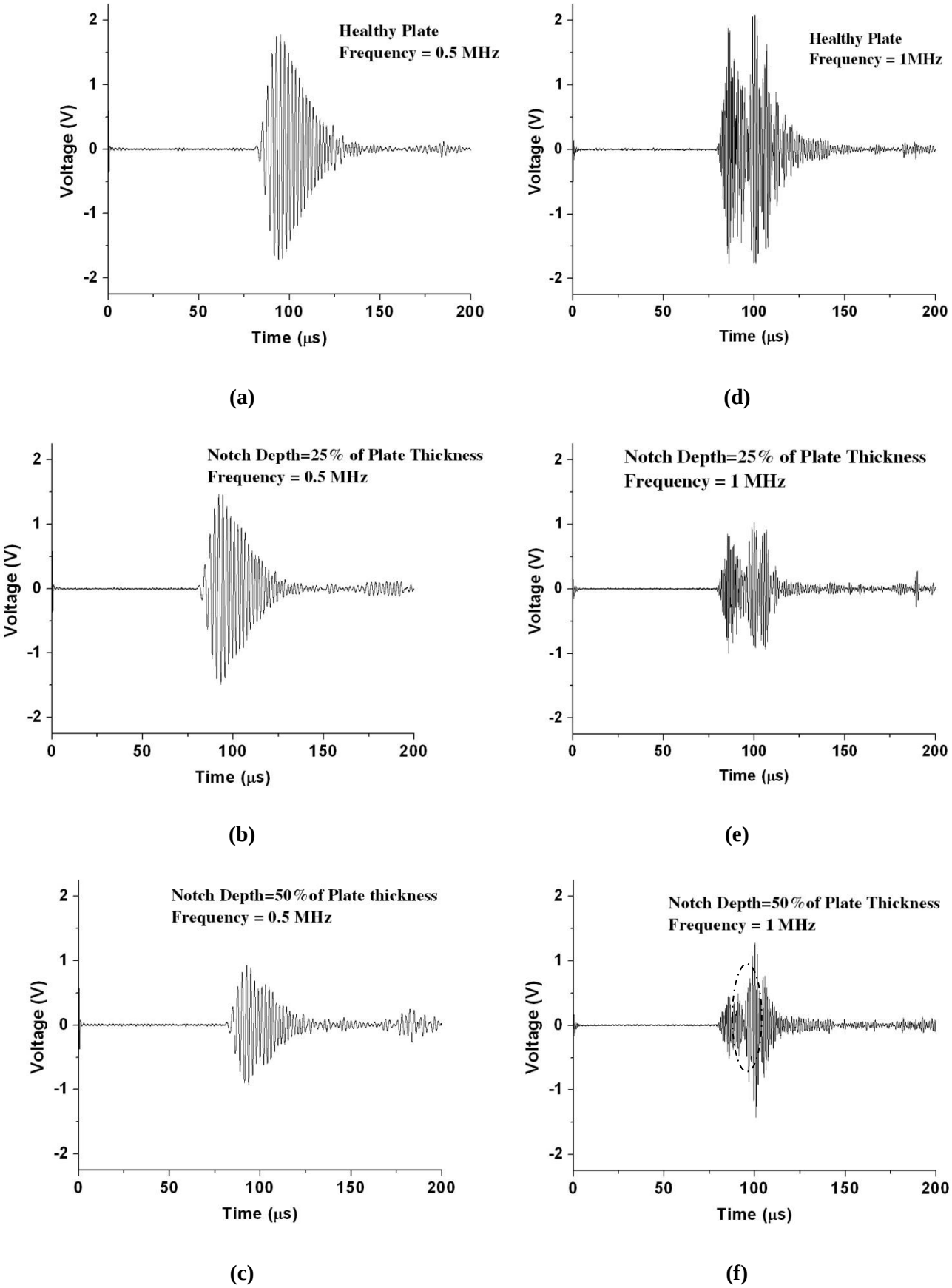

Figure 4.5: Effect of Notch on PT signatures – (a-c) 0.5 MHz, (d-f) 1 MHz

4.3 EFFECT OF INCIDENT ANGLE ON LAMB WAVE PROPAGATION

4.3.1 Experimental Details

For a selected frequency and plate thickness combination, a number of Lamb wave modes can exist in the plate geometry, each one having its unique propagation characteristics like- phase velocity, group velocity and attenuation. Particular modes can be selectively excited by keeping the transmitter and receiver probes at a specified angle of incidence (Equation 2.7). Objective of this study is to experimentally investigate the variation in propagation characteristics of the transmitted pulse with respect to the angle of incidence (θ) and determine suitable angles of incidence for damage monitoring in given submerged plates.

In this study, angles of incidence for both transmitter and receiver probes are varied simultaneously from 0° to 28° in steps of 2°. Corresponding PT signatures are recorded using frequencies of 0.5 MHz and 1.0 MHz respectively. During entire experimentation, t_w has been kept as 40μs. Propagation distance (D_p) of 200 mm and 250 mm has been used for frequencies 0.5 MHz and 1 MHz respectively. PT signatures have been recorded at different locations on the plate specimen in order to ensure consistency and repeatability of the results.

4.3.2 Observations and Discussions

4.3.2.1 Effect of varying angle

Figures 4.6 and 4.7 show the PT signatures obtained at different angles of incidence using 0.5 MHz and 1.0 MHz frequencies respectively. At 0.5 MHz frequency, when angle of incidence is in the range of 2°-6° **(Figure 4.6 a -c)**, a broad and weak signal is obtained. At 8°, a sharp peak is obtained at 107μs. For 10° and 12° angles, this peak becomes even sharper and appears at 104μs and 98μs respectively. Additionally, traces of another smaller amplitude peak on the left side can be seen at about 83μs. As θ increases to 14°, 16° and 18°, the peak on the left side gets stronger and appears at around 90μs, whereas the peak on the right side gets fainter and finally disappears. With further increase in θ (20° and beyond) all peaks gradually diminish **Figure 4.6(l)**.

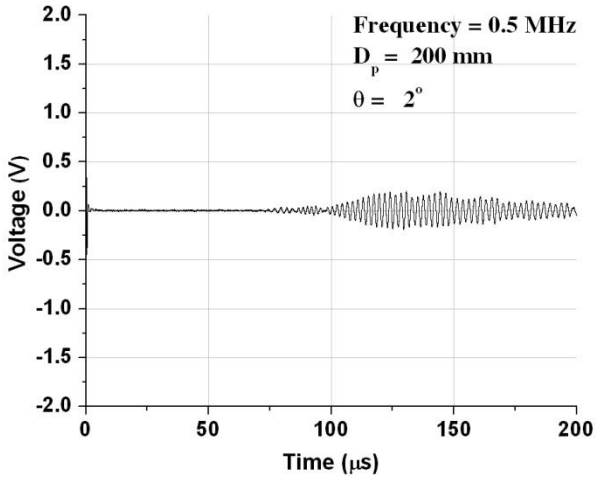
Frequency = 0.5 MHz
D_p = 200 mm
θ = 2°
Voltage (V)
Time (μs)

(a)

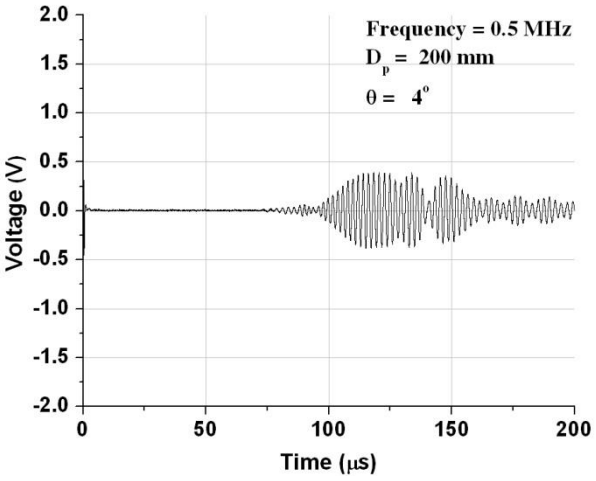
Frequency = 0.5 MHz
D_p = 200 mm
θ = 4°
Voltage (V)
Time (μs)

(b)

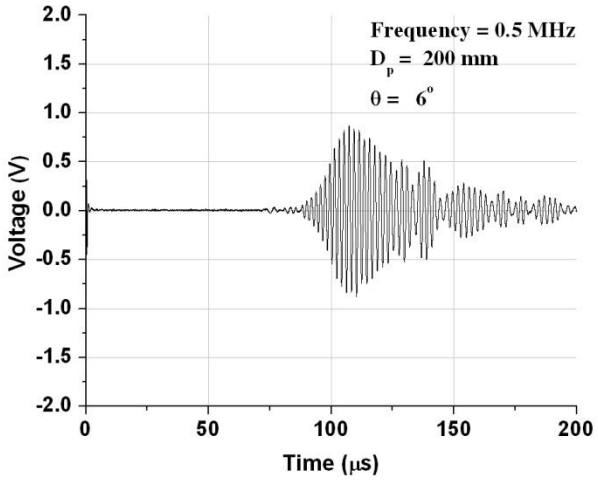
Frequency = 0.5 MHz
D_p = 200 mm
θ = 6°
Voltage (V)
Time (μs)

(c)

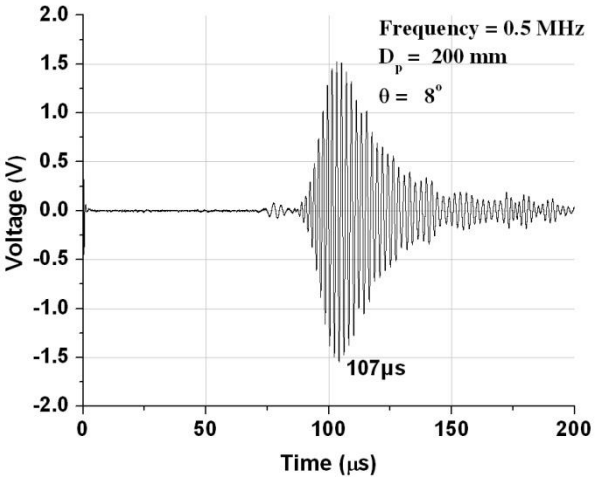
Frequency = 0.5 MHz
D_p = 200 mm
θ = 8°
107μs
Voltage (V)
Time (μs)

(d)

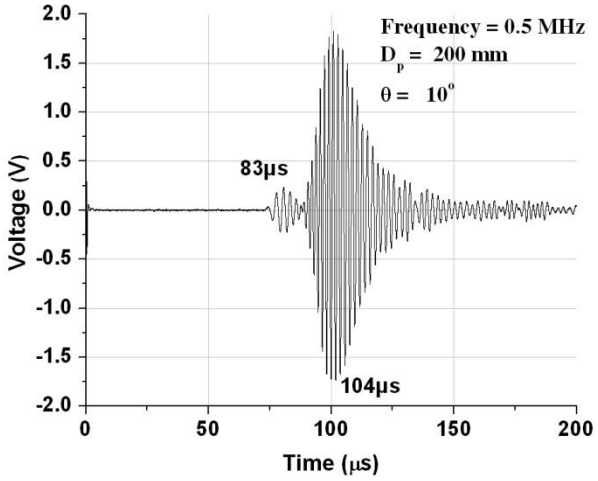
Frequency = 0.5 MHz
D_p = 200 mm
θ = 10°
83μs
104μs
Voltage (V)
Time (μs)

(e)

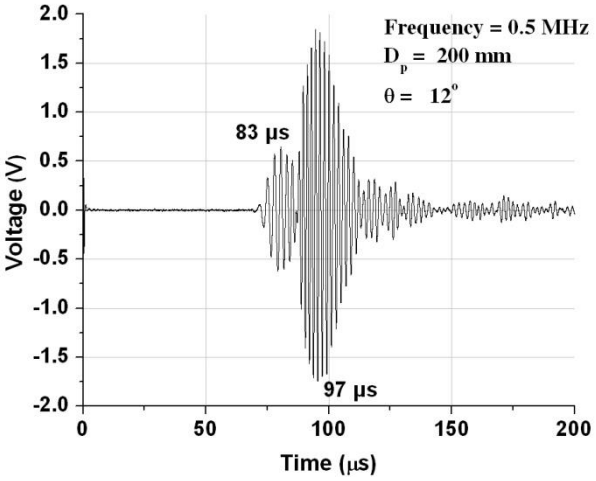
Frequency = 0.5 MHz
D_p = 200 mm
θ = 12°
83 μs
97 μs
Voltage (V)
Time (μs)

(f)

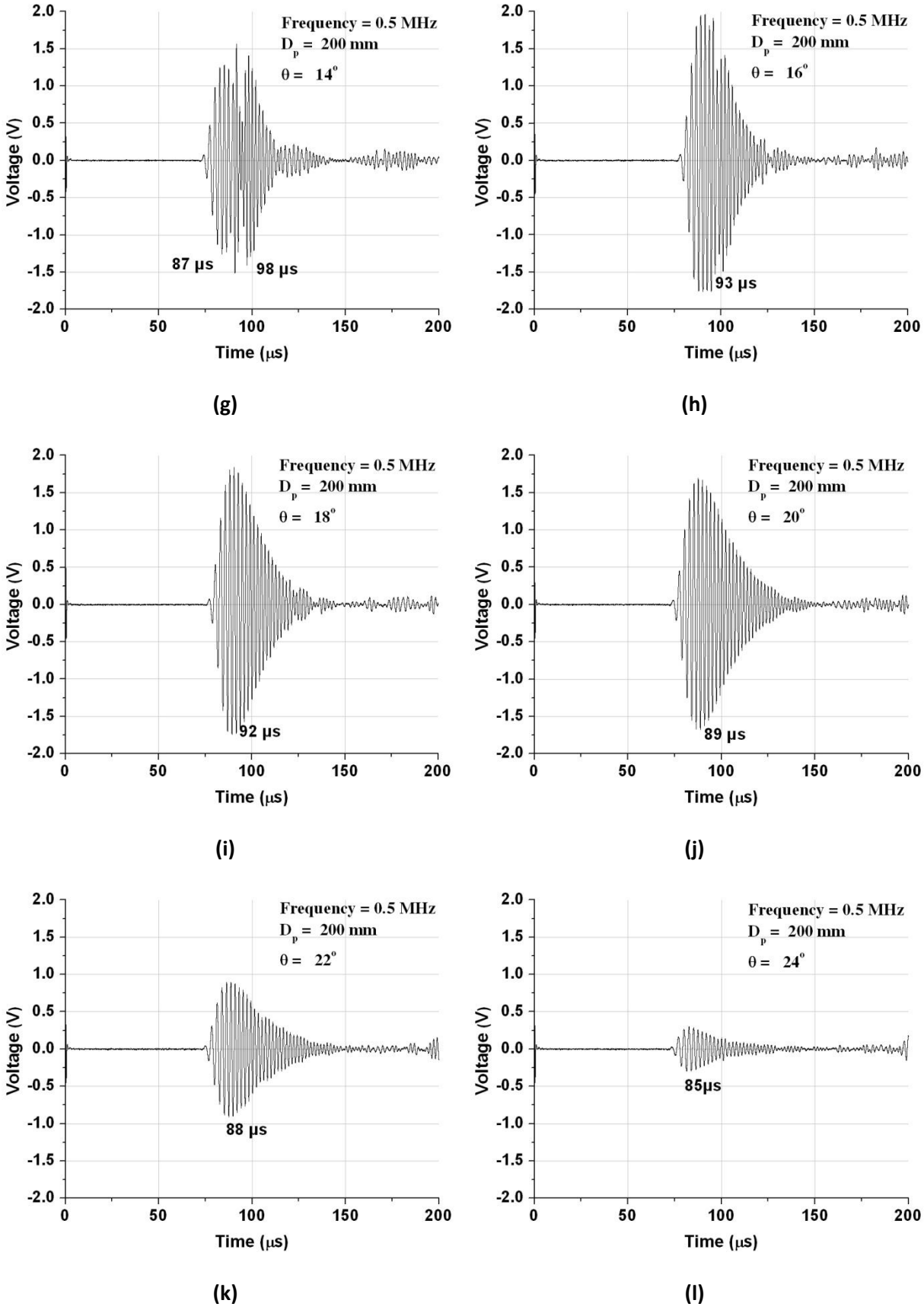

Figure 4.6: Pulse Transmission signatures at varying angles of incidence (0.5 MHz)

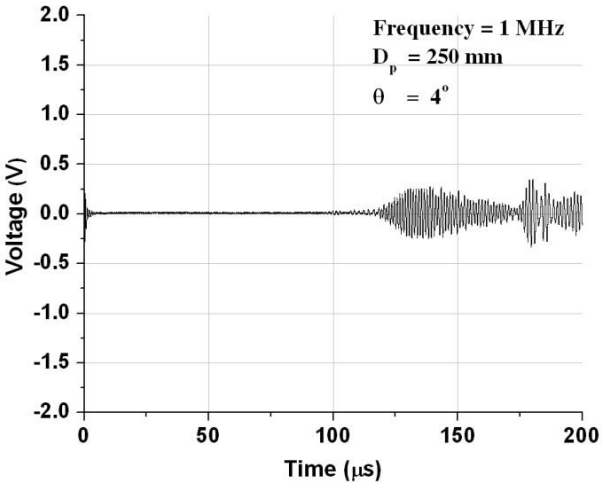
Frequency = 1 MHz
D_p = 250 mm
θ = 4°
Voltage (V)
Time (μs)

(a)

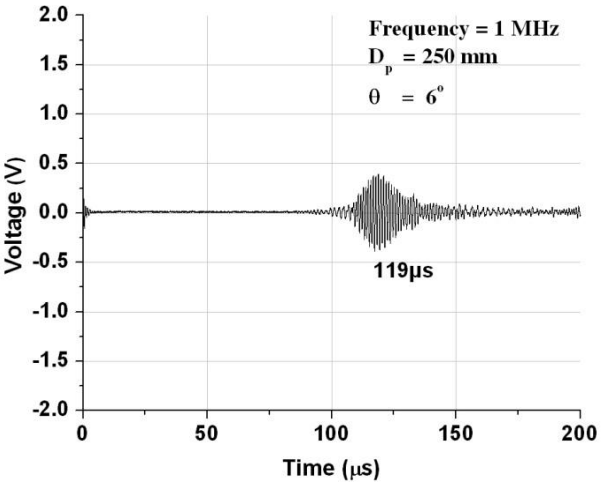
Frequency = 1 MHz
D_p = 250 mm
θ = 6°
119μs
Voltage (V)
Time (μs)

(b)

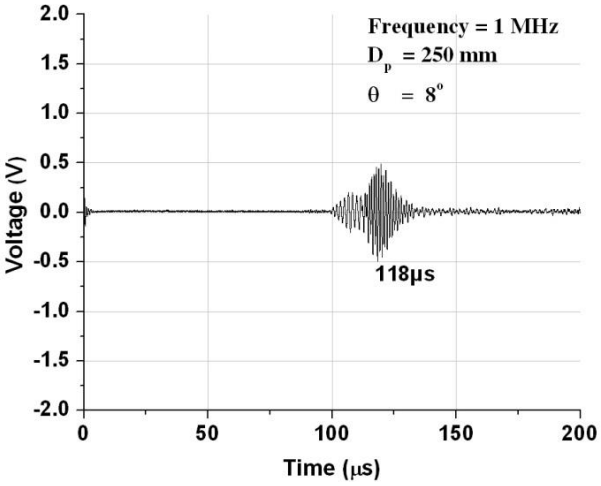
Frequency = 1 MHz
D_p = 250 mm
θ = 8°
118μs
Voltage (V)
Time (μs)

(c)

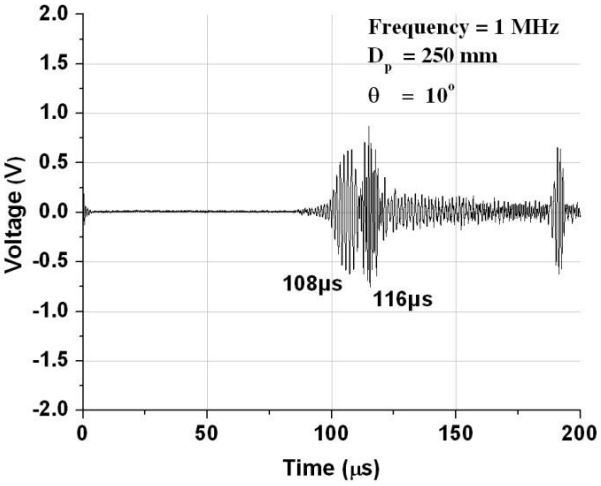
Frequency = 1 MHz
D_p = 250 mm
θ = 10°
108μs
116μs
Voltage (V)
Time (μs)

(d)

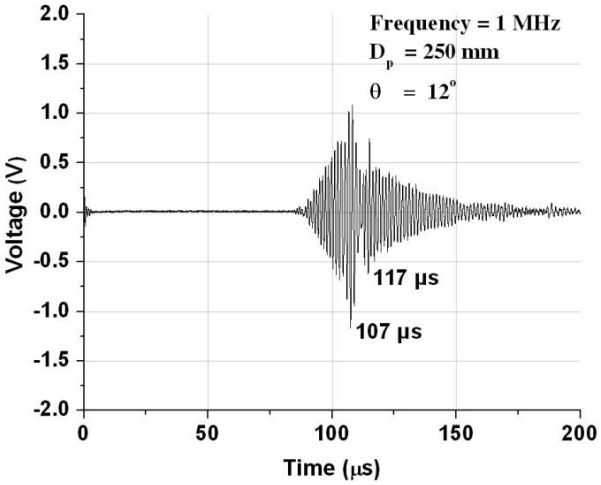
Frequency = 1 MHz
D_p = 250 mm
θ = 12°
117 μs
107 μs
Voltage (V)
Time (μs)

(e)

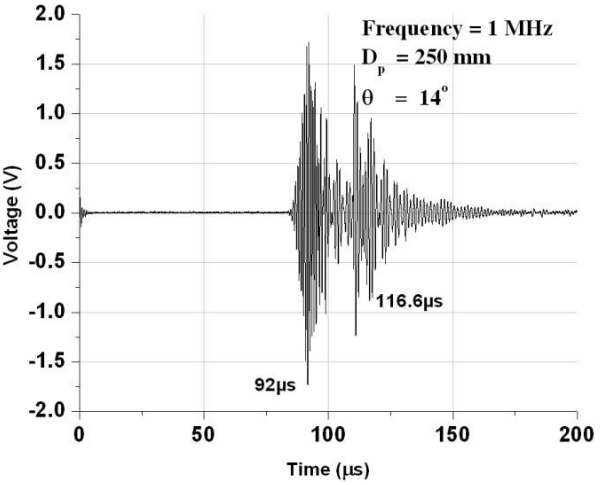
Frequency = 1 MHz
D_p = 250 mm
θ = 14°
116.6μs
92μs
Voltage (V)
Time (μs)

(f)

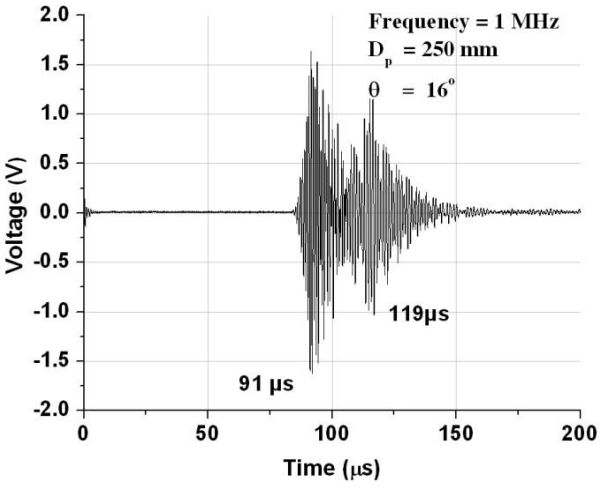
Frequency = 1 MHz
D_p = 250 mm
θ = 16°
119µs
91 µs
Voltage (V)
Time (µs)

(g)

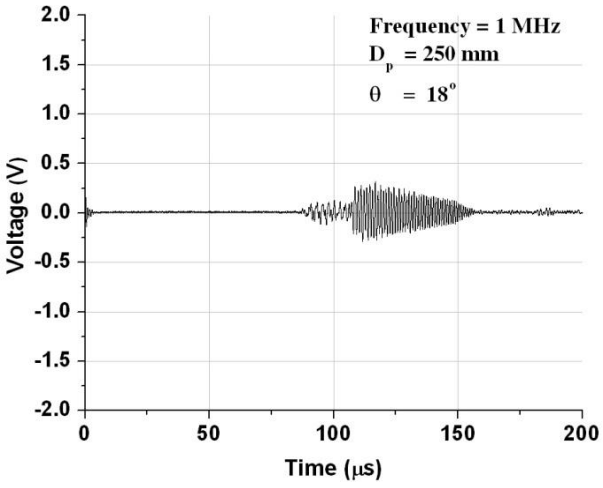
Frequency = 1 MHz
D_p = 250 mm
θ = 18°
Voltage (V)
Time (µs)

(h)

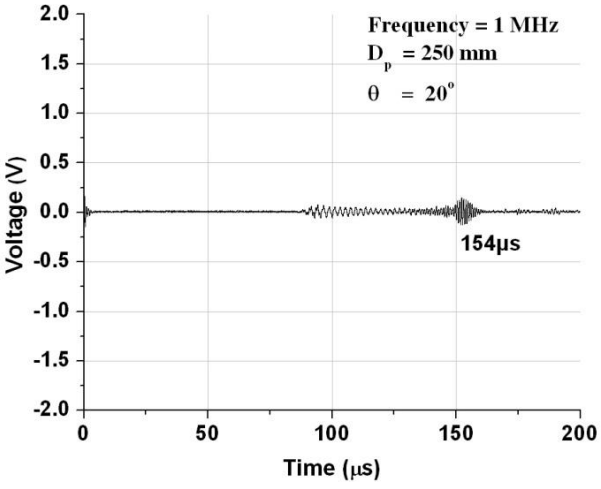
Frequency = 1 MHz
D_p = 250 mm
θ = 20°
154µs
Voltage (V)
Time (µs)

(i)

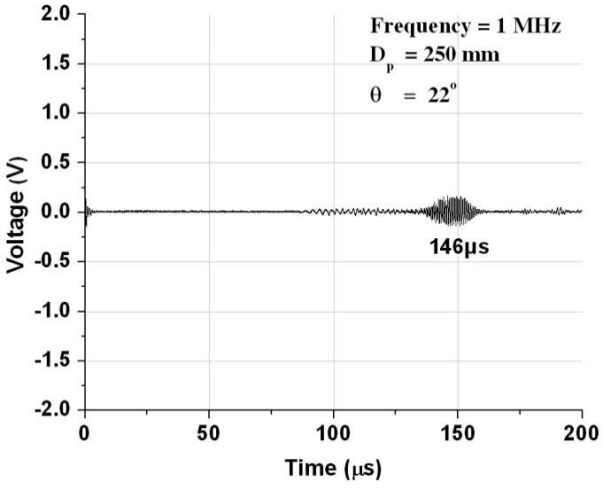
Frequency = 1 MHz
D_p = 250 mm
θ = 22°
146µs
Voltage (V)
Time (µs)

(j)

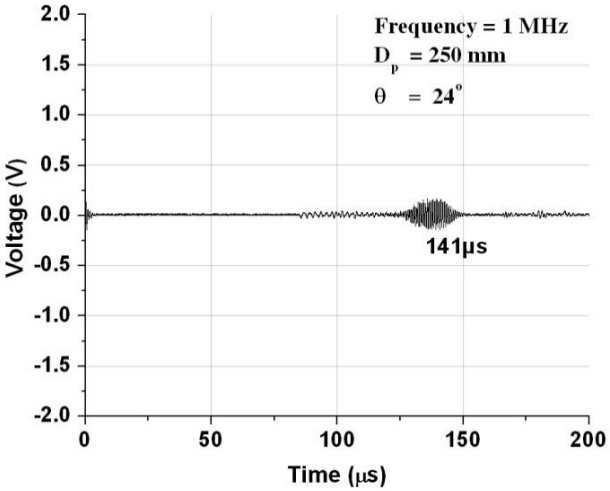
Frequency = 1 MHz
D_p = 250 mm
θ = 24°
141µs
Voltage (V)
Time (µs)

(k)

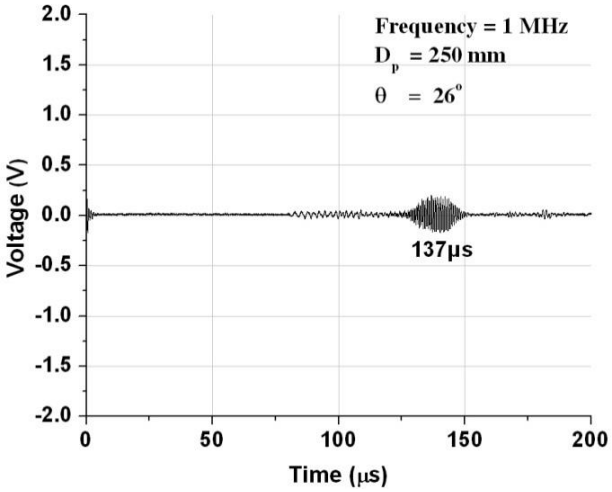
Frequency = 1 MHz
D_p = 250 mm
θ = 26°
137µs
Voltage (V)
Time (µs)

(l)

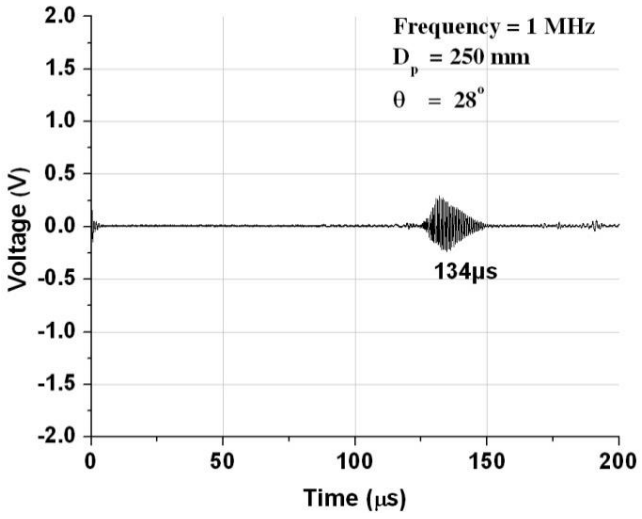

(m)

Figure 4.7: Pulse Transmission signatures at varying angles of incidence (1 MHz)

At 1 MHz frequency and angle of incidence 4° **(Figure 4.7a)**, a broad and weak signal is obtained. Subsequently at 6°, peak formation starts at 119µs. With further increase in angle of incidence (8°-12° range), the peak grows in magnitude and begins to split in to two peaks. This separation is further enhanced at 14°-16° where two distinct peaks can be clearly seen at 91µs and 117µs. At 18° these peaks vanish abruptly resulting in a broad and weak signature. At higher values of θ, a weak but relatively sharper peak appears. It grows in size and keeps shifting leftwards with increase in θ (ranging from 22° to 28°).

Variations in the PT signatures clearly indicate that for a selected frequency of excitation and plate geometry, the propagation characteristics like signal shape and its amplitude and time of arrival of the transmitted pulse are substantially influenced by varying the angle of incidence. **Figure 4.8 (a, b)** shows the plot of peak-peak voltage (V_p) of the received signal at different angles of incidence for 0.5 MHz and 1.0 MHz respectively. It clearly indicates distinctive bands in V_p-θ plots where signal fidelity is best and this range can be further exploited for investigation of submerged plates.

At 0.5 MHz frequency **(Figure 4.8a)** there are two ranges of angles of incidence (9°-11° and 15°-17°) at which V_p of the transmitted pulse is distinctively higher. It is highest at 15°-17° range. Similarly, at 1 MHz frequency **(Figure 4.8b),** for angles 12°-16°, V_p is higher.

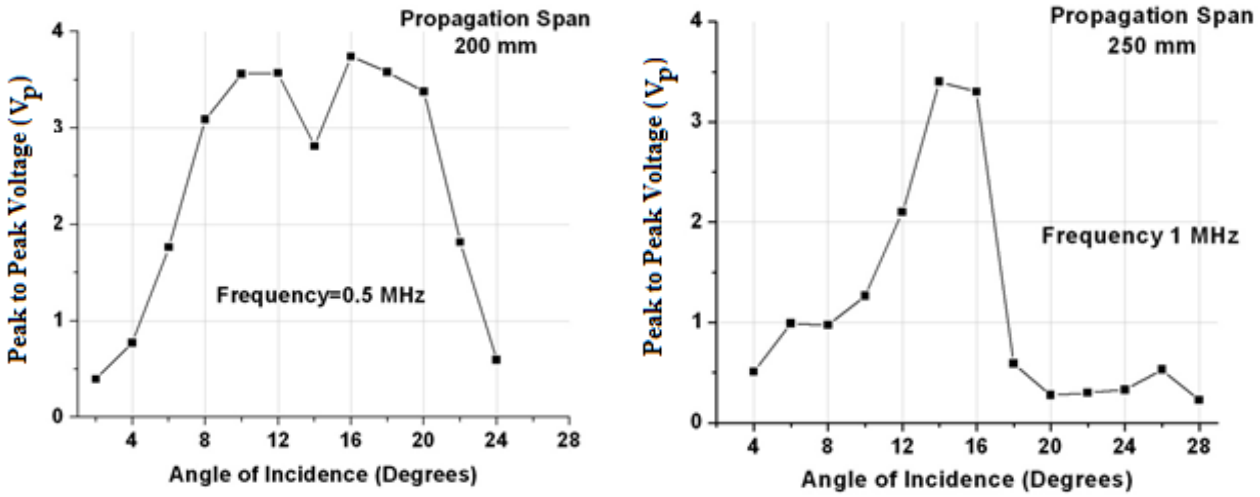

(a) 0.5 MHz **(b) 1 MHz**

Figure 4.8: Angle of incidence (θ) Vs. V_p of transmitted pulse

4.3.2.2 Mode Identification using Dispersion Curves

The variations in V_p with incidence angle can be explained theoretically by plotting dispersion curves for the submerged plate system. The dispersion curves showing the variation of phase velocities (km/s), group velocities (km/s) and attenuation characteristics (dB/m) with respect to frequency (MHz) for 4 mm steel plate completely submerged in water have been plotted using Software Disperse (Pavlakovic and Cawley, 2000) (**Figure 4.9)**. From the phase velocity dispersion curves **(Figure 4.9a)**, at 0.5 MHz, two Lamb wave modes S_0 and A_1 exist with phase velocities of 5.02 km/s and 9.75 km/s respectively. Similarly at 1 MHz, three Lamb wave modes exist, namely S_0, S_1 and A_1 with phase velocity 3.14 km/s, 5.93 km/s and 5.23 km/s respectively. Any of these desired Lamb wave modes can be selectively excited by impinging longitudinal waves from the transmitter at an appropriate angle of incidence given by Equation 2.7 and as outlined in **Table 4.1**. These values obtained from the dispersion curves can be related to the experimental observations.

In experimental studies, at 0.5 MHz frequency, when the angle of incidence is in range 8°-10° **(Figure 4.6 d-e)**, the sharp peaks appearing at 107μs and 104μs indicate the dominance of A_1 mode in this range **(Table 4.1**, θ for A_1 mode is 8.85°). Another small peak is visible at 83μs (at **θ** = 10-14°) represents the infusion of the traces of S_0 mode (**Table 4.1**, **θ for S_0 mode is 17.4°**). Presence of A_1 mode (at **θ** = 8°) can also be verified by matching the experimental arrival time i.e. 107μs with the theoretical arrival time.

Table 4.1: Angle of incidence (θ) for various Lamb wave modes

S. No.	Lamb wave mode	Phase Velocity (km/s)	Angle (θ)
1.	A_1 at 0.5 MHz	9.75	8.85 ^{o}
2.	S_0 at 0.5 MHz	5.02	17.4^o
3.	S_1 at 1 MHz	5.93	14.7 ^{o}
4.	A_1 at 1 MHz	5.23	16.7 ^{o}
5.	S_0 at 1 MHz	3.14	28.5 ^{o}

Theoretical arrival time of the transmitted pulse (T_t) in PT signature, comprises of two components namely- t_w at both transmitter (left probe) and receiver probes (right) and the time of propagation through the plate and is calculated as

$$T_t = \left[\frac{(t_w)_{left}+(t_w)_{right}}{2}\right] + \left[\frac{D_p}{V_g}\right] \quad (4.2)$$

where,

V_{gr} = Theoretical Group Velocity of the mode obtained from Dispersion curve **(Figure 4.9b)**

For t_w of 40 μs, D_p of 200 mm and with group velocity of 3 km/s (for A_1 mode), the theoretical arrival time of the transmitted pulse is 106.6μs, which matches closely with the experimentally observed time of arrival of the pulse.

With further increase in θ (12°-14°), the peak corresponding to A_1 vanishes and peak corresponding to S_0 mode grows in amplitude. At 16°-18°, there is a single sharp peak. Presence of S_0 mode appearing at 92μs in the signature can also be verified by matching with the theoretical arrival time of the mode. For t_w of 40μs, D_p of 200 mm and with group velocity of 3.75 km/s of S_0 mode, the theoretical arrival time of the transmitted pulse is 93.2μs which matches closely with the experimental arrival time of the pulse. At higher values of θ (20°-24°) this peak vanishes which is also supported by the dispersion curves that no Lamb wave mode is feasible beyond 20°.

Response of S_0 and A_1 modes at 0.5 MHz with varying probe angle is plotted in **Figure 4.10a** as peak to peak voltage amplitude in the PT signatures **(Figure 4.6 a-l)** at

corresponding time of arrival ($92\mu s$ and $107\ \mu s$ of the two modes respectively). It clearly highlights the regions of dominance of these modes at 0.5 MHz. It is clear that **Figure 4.8a** is the envelope curve encompassing the effect of all the feasible modes at 0.5 MHz.

Similarly, in PT signature of immersed plate at 1.0 MHz frequency, no clear peak is visible for angles of incidence up to 4° **(Figure 4.7a)**. At 6°, the peak starts appearing at 119μs. For 10°-16° the signal contains two well separated peaks centered at 91 μs and 119 μs. These two peaks represent the simultaneous presence of two modes in the signal viz. S_1 and A_1. It is due to the fact that angles of incidence required for S_1 and A_1 modes are 14.7° and 16.7° respectively **(Table 4.1)**. Presence of S_1 and A_1 modes in the signal can also be verified by the comparing the experimental arrival times of the transmitted pulse peaks with the theoretical arrival times. For t_w of 40μs, D_p of 250mm and with group velocities 4.98 km/s (for S_1 mode) and 3 km/s (for A_1 mode), the theoretical arrival times of the transmitted pulse are $90.5\mu s$ and $123.3\mu s$ for S_1 and A_1 modes respectively. They match reasonably with the experimentally observed times of arrival of the pulse for S_1 and A_1 modes (91μs and 119μs respectively). For higher values of angle of incidence (18° and above) both A_1 and S_1 modes disappear. This is indicated by the absence of any sharp peak in **Figure 4.7 (h-m).**

Further, at 20° there is appearance of a weaker peak at 154μs which continuously shifts leftwards with increasing values of θ. This peak exhibits highest amplitude at 28° and corresponding arrival time is 134μs. This peak is attributed to the S_0 mode as indicated by its time of arrival in PT. Theoretical time of arrival of $134.3\mu s$ matches closely with experimentally obtained time of arrival of transmitted pulse i.e. 134μs.

Voltage amplitude of the received signals (**Figure 4.7 a-m**) corresponding to the arrival times of S_1 mode (91 μs), A_1 mode (123μs) and S_0 mode (134 μs) at 1 MHz have been plotted in **Figure 4.10b**. This plot shows the regions of dominance of these modes in the V-θ plot. It is also clear that the curve in **Figure 4.8b** is the envelope curve of all the modal responses.

4.3.2.3 Criteria for guided wave mode selection

Selection of a particular mode is based on the considerations of minimum attenuation for maximizing scanning distance, good signal fidelity and the energy distribution profile across the plate thickness for maximizing the sensitivity of a mode for detection of a typical flaw/damage. In view of this, desired Lamb wave mode should exhibit well defined sharp

peak, suffer minimum attenuation and there should be ease of excitation and successful capturing of the signal.

In the present work, at 0.5 MHz, the two available modes namely symmetric mode S_0 and anti-symmetric mode A_1 have well separated phase velocities **(Figure 4.9a)** and relatively lower attenuation **(Figure 4.9c)**. But S_0 mode exhibits a well-defined sharp peak in comparison to A_1 mode. Also as outlined in Chapter 2 symmetric modes should be preferred over anti-symmetric modes because of their higher group velocities **(Figure 4.9b)** resulting in lesser dispersion. Hence, S_0 is the preferred mode for damage monitoring at 0.5 MHz.

At a frequency of excitation of 1.0 MHz, there are three available modes i.e. symmetric mode S_0, anti-symmetric mode A_1 and symmetric mode S_1. S_0 mode is out rightly rejected due to extremely high attenuation. This is also clear from **Figure 4.7 (l , m)**. Since the amplitude of the pulse received in healthy state with S_0 mode is too small that it is difficult to sense any change it may undergo after interaction with damage. A_1 mode, though has lesser attenuation than S_0 mode but its group velocity is quite close to S_0. . It results in appearance of a number of merging peaks in PT signature due to contributions of traces of S_0 mode. It results in a very broader signal with very poor signal fidelity. The signal obtained is in the form of an envelope rather than a sharp distinctive peak **(Figure 4.7h)**. It makes interpretation of results difficult.

Also phase velocities of A_1 and S_1 are very close resulting in a very close angle of incidence. It is important to note that since the diameter of the transducer is 25mm, the divergence in the longitudinal beam in water may result in inadvertent generation of neighbouring modes. However, these peaks corresponding to these modes are well separated due to difference in group velocities and this separation increases with higher values of D_p. So S_1 mode at 1.0 MHz is the least dispersive, fastest mode (V_{gr}=4.98 km/s), and exhibits minimum attenuation and thus should be preferred over S_0 and A_1 modes at the same frequency.

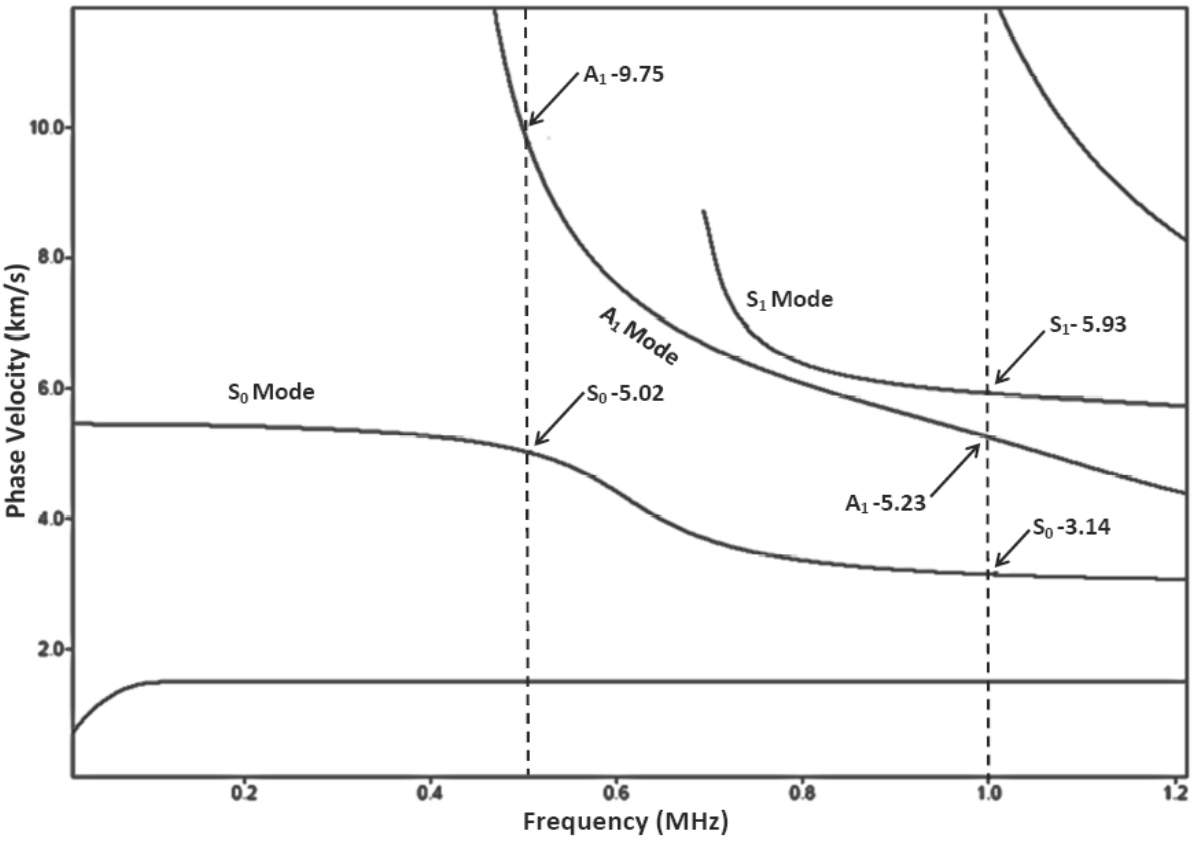

(a) Phase Velocity vs Freqency

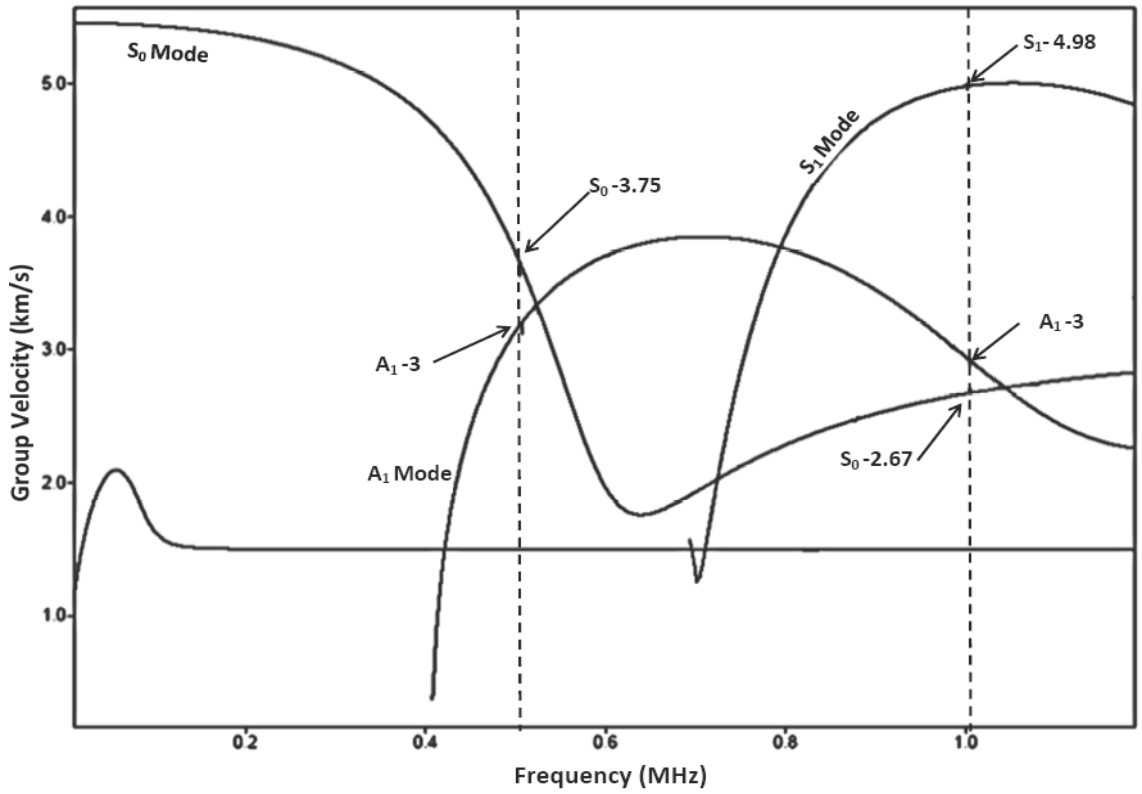

(b) Group Velocity vs Freqency

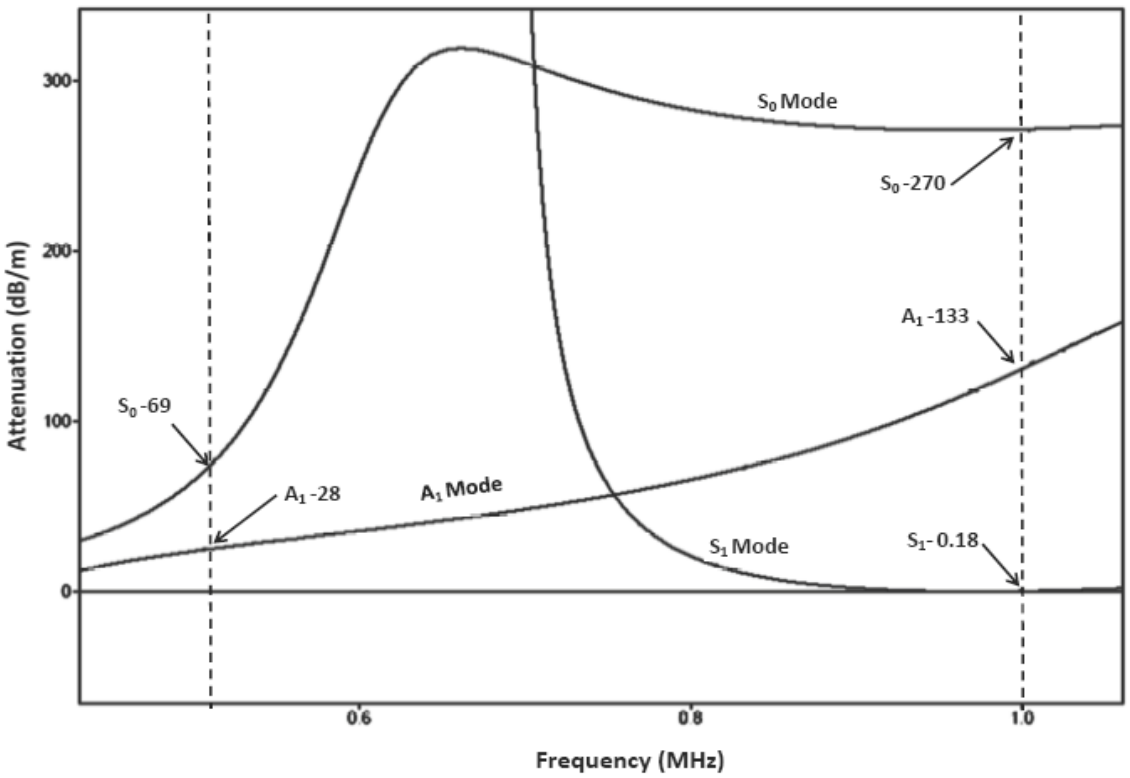

(c) Attenuation vs Freqency

Figure 4.9 : Dispersion curves for 4mm steel plate in water

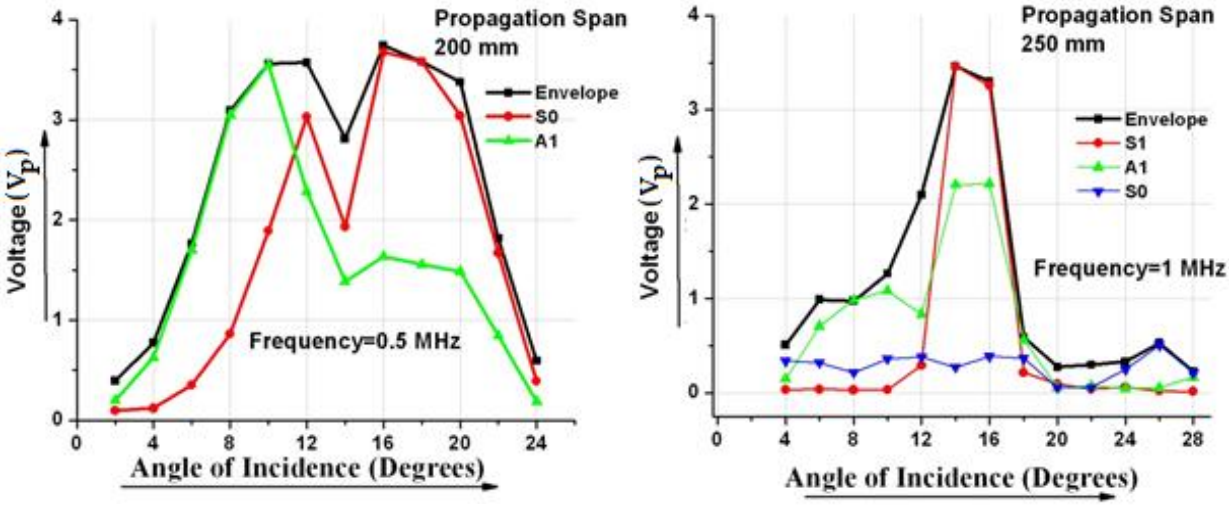

(a) 0.5 MHz **(b) 1 MHz**

Figure 4.10: V_P-θ plot for the feasible modes

4.3.2.4 Verification with Group Velocity

Presence of the various modes at corresponding frequencies of excitation is further verified by matching experimental group velocity of the modes (from PT signatures) and theoretical Group Velocity (**Figure 4.9b**).Experimental group velocity is calculated as

$$\text{Group Velocity}_{\text{Experiment}} = \frac{D_P}{(T_t - \grave{t_w})} \quad (4.3)$$

Where, D_P = Propagation Span (in mm)

T_t = Arrival time of the transmitted pulse

$\grave{t_w}$ = average of TOF in water at transmitter and receiver probes

Table 4.2: Experimental Group Velocity vs. Theoretical Group Velocity

Propagation Span (For 0.5 MHz-200 mm, For 1 MHz-250 mm)

S. No.	Lamb wave Mode	Experimental Data				Theoretical Group Velocity (km/s)*	Difference
		Pulse Echo time $t_{w\ left}$ (μs) at Transmitter	Pulse Echo time $t_{w\ right}$ (μs) at Receiver	Pulse transmission time T_t (μs)	Experimental Group Velocity (km/s)		
1.	S_0 – 0.5 MHz (θ~18°)	40	40	92	3.84	3.75	-2.4%
2.	A_1 – 0.5 MHz (θ~8°)	40	40	107	2.98	3	+0.7 %
3.	S_0 – 1.0 MHz (θ~28°)	40	40	134	2.65	2.67	+2.9%
4.	S_1 – 1.0 MHz (θ~14°)	40	40	92	4.90	4.98	+1.6%
5.	A_1 – 1.0 MHz (θ~16°)	40	40	119	3.20	3	+6.7%

***- From Dispersion Curves**

The comparison of the experimental and theoretical group velocities for all feasible Lamb wave modes at 0.5 and 1.0 MHz shows a close match between the theoretical and experimental group velocities (**Table 4.2)**. The difference may be attributed to the local variations in the plate thickness and material properties.

4.4 EFFECT OF OBSTRUCTION ON LAMB WAVE PROPAGATION

This experimental study has been undertaken to ensure that PT signatures only depict the guided Lamb waves travelling through the submerged plate. Aim of this study is to rule out any possibilities of any undesirable signals like reflections or transmission from other nearby interfaces like water surface in the tank, bottom of the tank etc. In this study, the specimen remains submerged and another steel plate 12mm thick is used as obstruction in different configurations **(Figure 4.11)**. PT signatures corresponding to various configurations have been recorded for selected S_0 mode at 0.5 MHz **(Figure 4.12a)** and S_1 mode at 1 MHz **(Figure 4.12b)**. Near identical PT signatures in **Figure 4.12** suggests that the receiver probe captures the Lamb waves traveling through the submerged plate only. Thus, the presence of the obstructing steel plate in the surrounding does not influence the propagation of Lamb waves in plate.

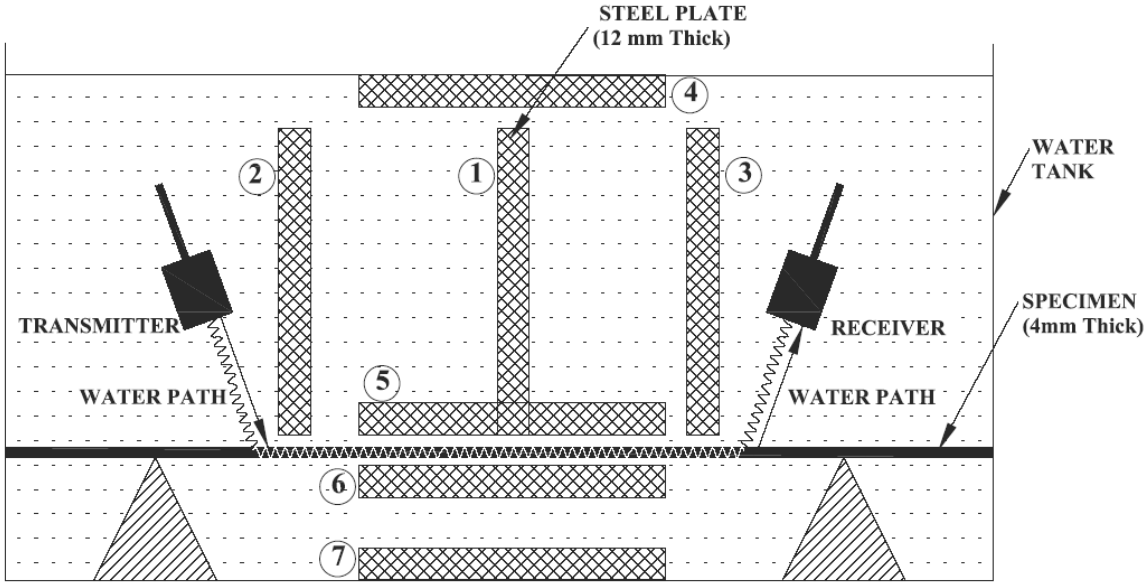

Figure 4.11: Guided wave propagation with obstruction placed in different configurations

(1)-Midway Between the probes (2)- Near left probe (3)-Near right probe (4)-Near water surface (5)-Just on top of specimen plate (6)-Just Below specimen Plate (7)- Lying on the tank Bottom

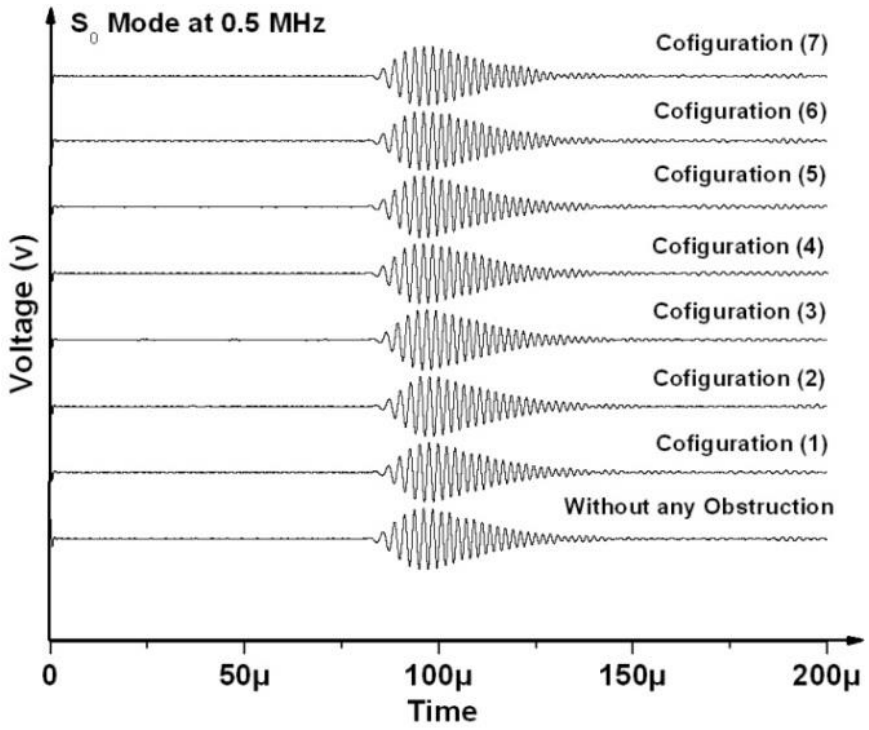

(a)

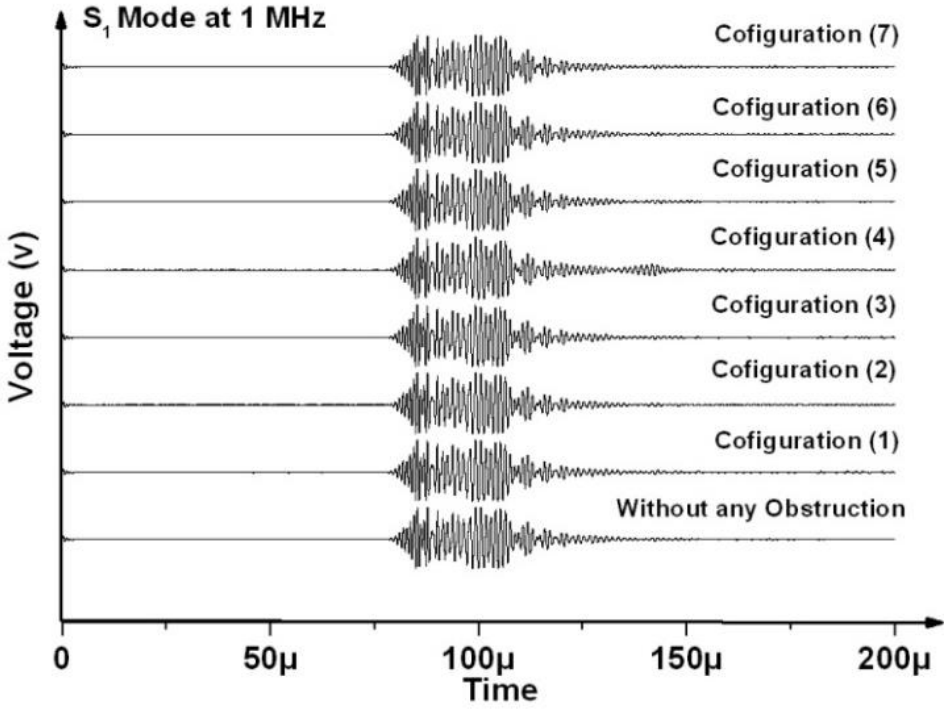

(b)

Figure 4.12: Pulse Transmission signatures for different configurations

Hence, it can be concluded that a particular Lamb wave mode with unique propagation characteristics can be selectively excited with reasonable accuracy in an immersed plate using non-contact systems by orienting the submerged longitudinal probes at suitable angles of incidence. Presence of a particular mode can be confirmed by matching its experimental arrival time (from PT signatures) with theoretical arrival time (from dispersion curves) for a given propagation distance.

4.5 EFFECT OF PROPAGATION DISTANCE

4.5.1 Signal fidelity vis- a-vis propagation distance

In this section, the effect of propagation distance on the transmitted signal strength is studied. At different angles of incidence, D_p has been varied from 200 mm to 300 mm. During this experiment, operating parameters like dB setting, Low Pass Filter (LPF), High Pass Filter (HPF) settings etc. for the PR unit are kept at the same level in order to avoid any external biasing. It has been observed that for some values of angles of incidence, Lamb waves are too weak to traverse through the given span. In such cases signal is too weak or undetectable. **Figure 4.13** shows V_p of transmitted pulse corresponding to the different angles of incidence at variable propagation distances. For a given angle of incidence, the amplitude of the transmitted pulse decreases with increase in the propagation distance. This can be primarily attributed to the more leakage of energy into the surrounding water and increased material attenuation due to increased propagation distance. It clearly suggests that change in the propagation distance has no effect on the trends of transmitted pulse amplitudes **(Figures 4.8 and 4.13**).

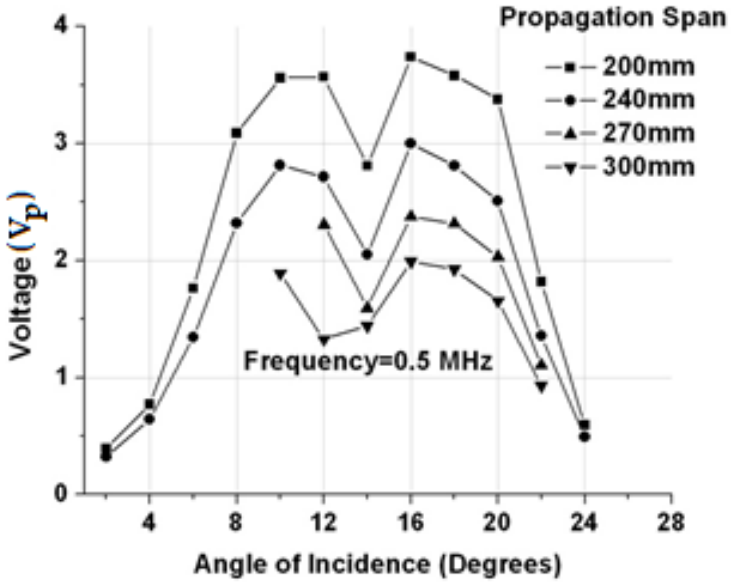

(a) At 0.5 MHz

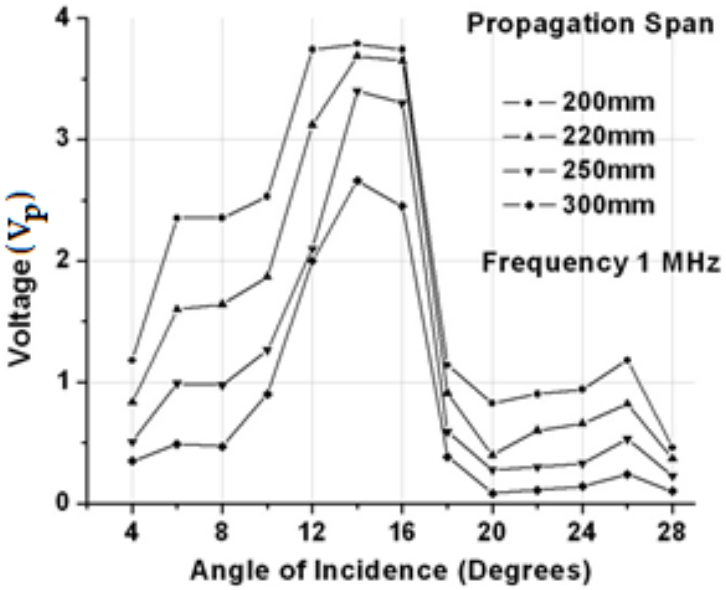

(b) At 1 MHz

Figure 4.13: Angle of incidence (θ) vs. Transmissted Pulse Amplitudes at Varying Propagation Spans

4.5.2 Effect of Propagation distance on Selected Modes

To investigate the optimum scanning capabilities of the selected symmetric Lamb wave modes (S_0 at 0.5 MHz and S_1 at 1 MHz), the transmitter and receiver probes are set at respective angles in pitch catch configuration. Initially, the probes are set to have a propagation distance (D_p) of 200 mm and the PT signatures are recorded. Subsequently, D_p is increased in steps of 20mm and the PT signatures are recorded at each incremented position

Figure 4.14 shows stack of such PT signatures recorded with increasing propagation distances for S_0 mode at 0.5 MHz and S_1 mode at 1 MHz. It is clear that the envelope of the PT signature characterizing the selected mode remains unaltered with the change in propagation distance. However, their arrival time increases as the propagation path gets longer since the group velocity of a particular mode through the steel plate is constant. Also the voltage amplitude of the transmitted pulse falls with increasing distance.

The variation in the arrival time and the normalized voltage amplitude of the transmitted pulse with increasing propagation distances for both S_0 mode at 0.5 MHz **(Figure 4.15a)** and S_1 mode at 1 MHz **(Figure 4.15b)** is plotted. Normalized voltage amplitude has been obtained by normalizing the V_p of the PT signatures with V_p obtained with D_p = 200 mm.

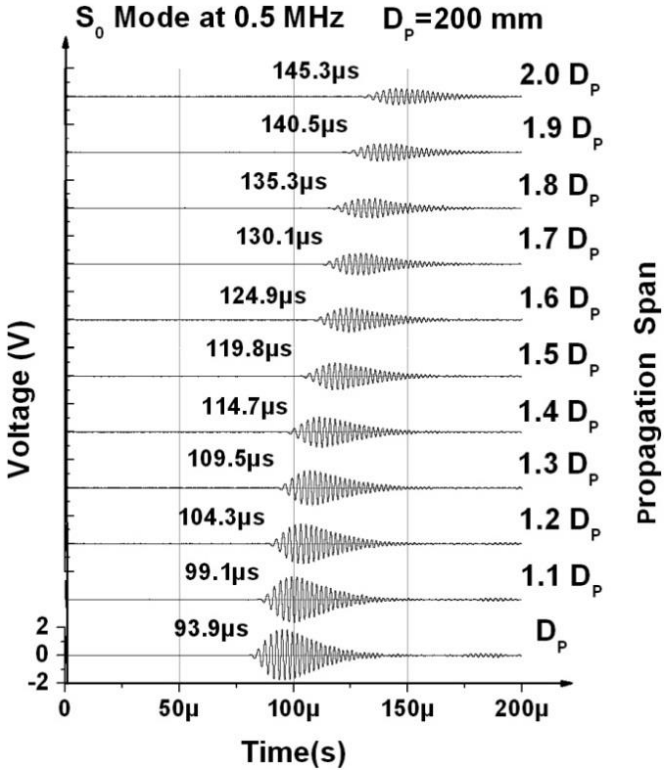

(a) S_o Mode at 0.5 MHz

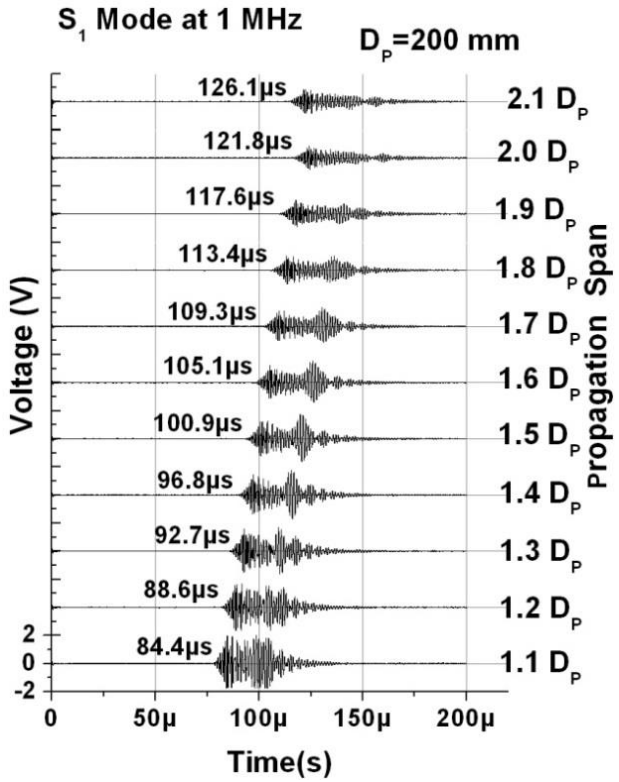

(b) S_1 Mode at 1 MHz

Figure 4.14: Pulse Transmission signatures with increasing Propagation Spans

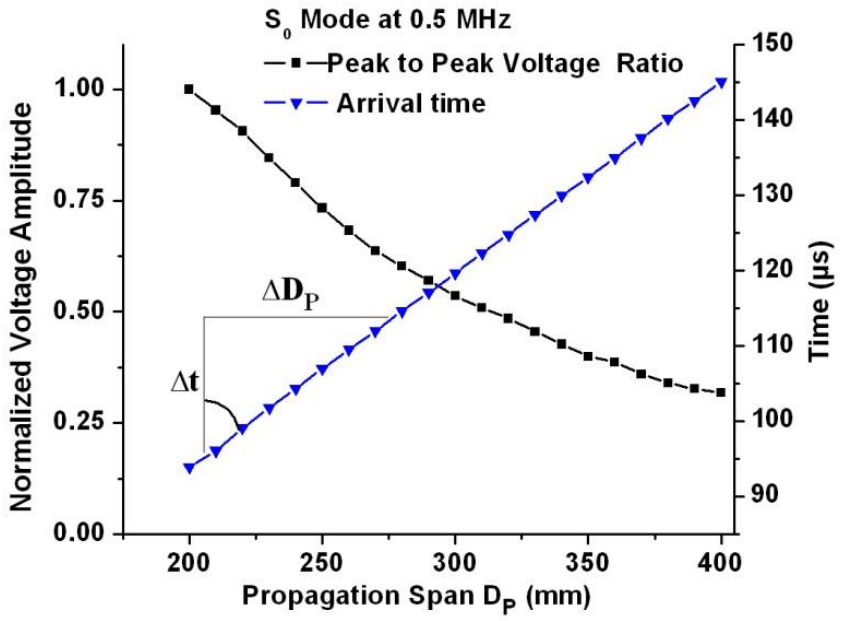

(a) S_0 Mode at 0.5 MHz

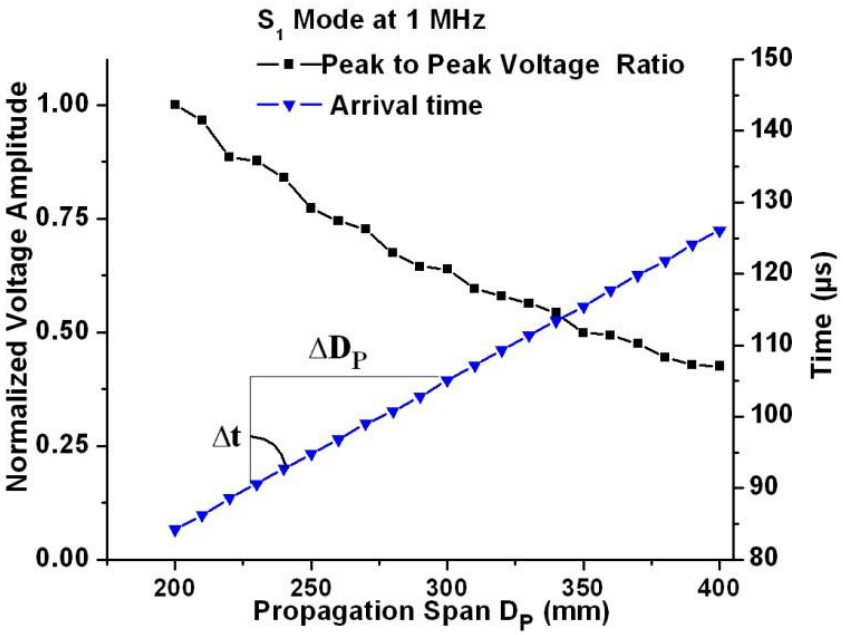

(b) S_1 Mode at 1 MHz

Figure 4.15: Variation in peak to peak voltage ratio and time of arrival with increasing propagation span

It is observed that fall in voltage amplitude with increase in D_p is relatively higher for 0.5 MHz –S_0 mode in comparison to 1 MHz-S_1 mode. This can be explained by attenuation characteristics of these Lamb wave modes as obtained from attenuation dispersion curves **(Figure 4.9c)**. Attenuation for S_1 mode at 1MHz is quite low (0.18 dB/m) as compared to S_0

mode at 0.5 MHz (69 dB/m). So voltage amplitude for S_0 mode falls more sharply as compared to S_1 mode. The variation of arrival time with D_p was found to be linear. It illustrates that the group velocity of this mode is constant irrespective of the propagation distance . The shifts in the arrival time of the pulse with increments in propagation distance can be used to determine the group velocity of the corresponding Lamb wave mode experimentally from the slope of arrival time-distance graph (**Figure 4.15**).

Table 4.3: Experimental Group Velocity by Incremental Propagation Span

Propagation Span	**Increment in position (ΔD_p)**	**S_o at 0.5 MHz**			**S_1 at 1.0 MHz**		
		Arrival Time (µs)	**Increment in Arrival time (Δt)**	**Experimental Group Velocity $\left(\frac{\Delta D_P}{\Delta t}\right)$***	**Arrival Time (µs)**	**Increment in Arrival time (Δt)**	**Experimental Group Velocity $\left(\frac{\Delta D_P}{\Delta t}\right)$ ******
200	0	93.9	--	--	--	--	--
220	20	99.1	5.2	**3.84**	84.4	--	--
240	20	104.3	5.2	**3.84**	88.6	4.2	**4.76**
260	20	109.5	5.2	**3.84**	92.7	4.1	**4.88**
280	20	114.65	5.15	**3.88**	96.8	4.1	**4.88**
300	20	119.8	5.15	**3.88**	100.9	4.1	**4.88**
320	20	124.95	5.15	**3.88**	105.1	4.2	**4.76**
340	20	130.1	5.15	**3.88**	109.3	4.2	**4.76**
360	20	135.3	5.2	**3.84**	113.4	4.1	**4.88**
380	20	140.5	5.2	**3.84**	117.6	4.3	**4.76**
400	20	145.6	5.1	**3.92**	121.8	4.1	**4.76**
420	--	--	--	**--**	126.1	4.3	**4.65**

$$\text{Group velocity} = \frac{\Delta D_P}{\Delta T} \quad (4.4)$$

***- Experimental Group velocity(3.86 km/s) matches closely with theoretical GV(3.75 km/s).**

****- Experimental Group velocity(4.98 km/s) matches closely with theoretical GV(4.8 km/s).**

Table 4.3 shows the group velocity computations for the selected modes by using Equation 4.4. The experimental group velocities of the selected modes match reasonably well with the theoretical group velocity values as indicated in dispersion curves **(Figure 4.9b)**. This study experimentally validates the propagation characteristics of the selected Lamb wave modes in 4mm thick steel plate completely submerged in water.

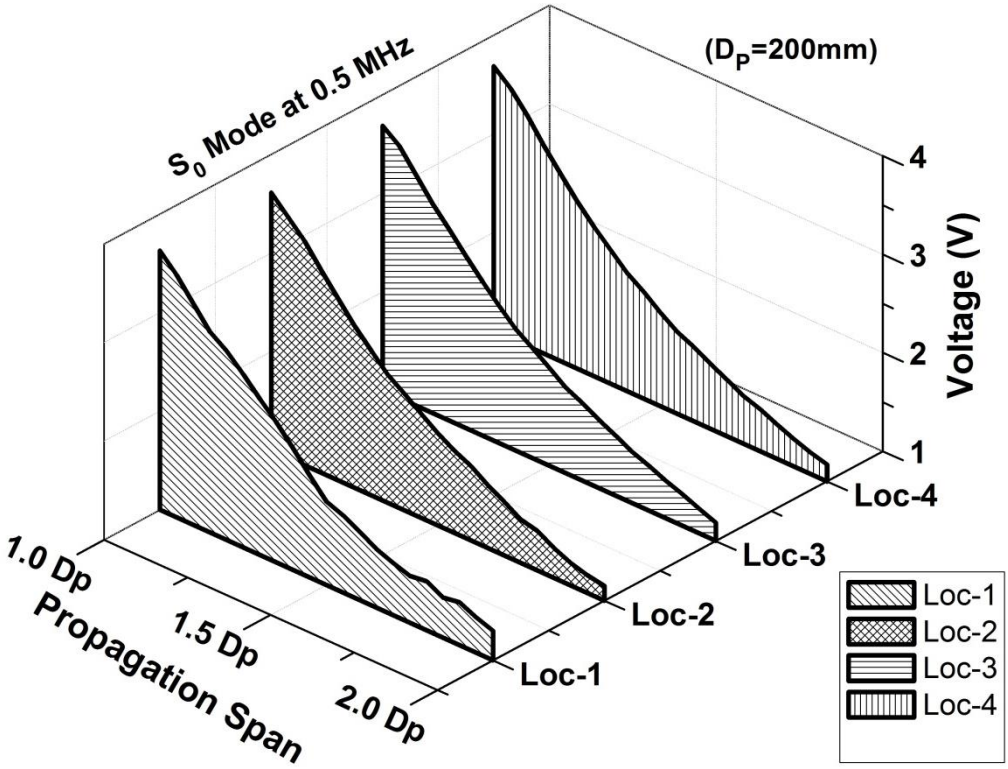

(a) S_0 Mode at 0.5 MHz

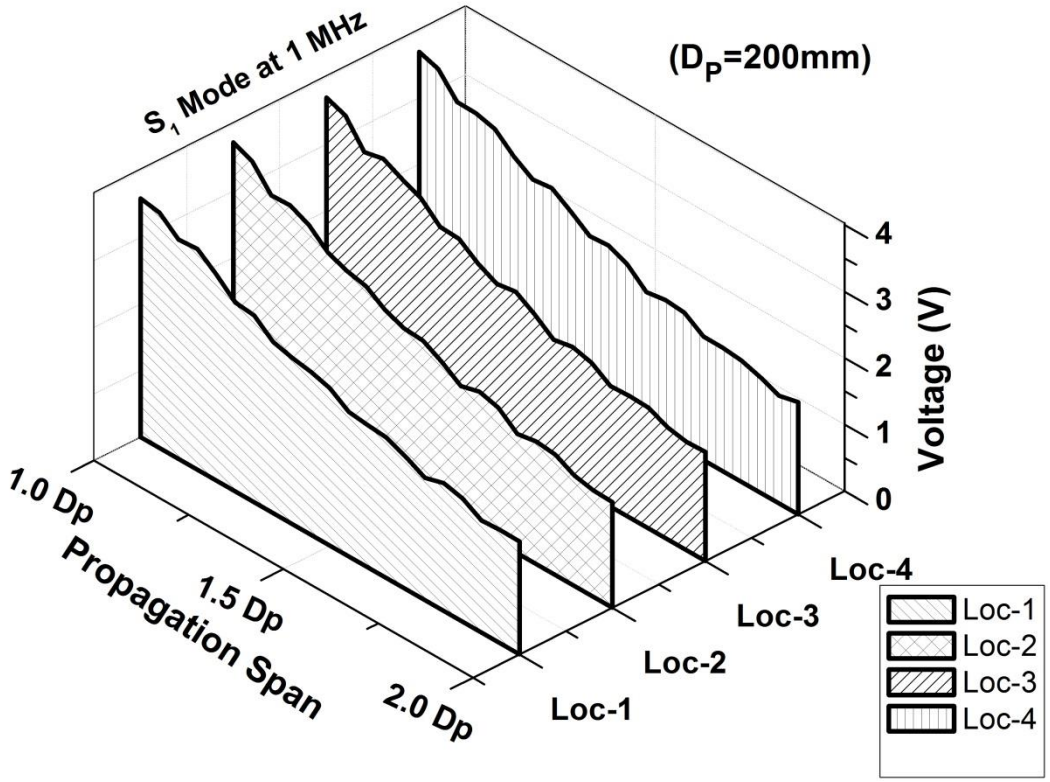

(b) S_1 Mode at 1 MHz

Figure 4.16: Variation in peak to peak voltage amplitude with increasing propagation span at different locations on the specimen

In order to ensure repeatability, the experimentation was carried out at different locations on the submerged plate. Testing parameters like t_w and PR settings were kept unaltered. Peak to peak voltages amplitudes of PT signals at these locations with increasing D_p is shown in **Figure 4.16**. Clearly the variation in V_p with increasing D_p is consistent and repeatable at various locations. The fall in voltage amplitude for S_0 mode is steeper as compared to S_1 mode. This trend is also repeated at various locations.

4.6 CLOSING REMARKS

This chapter was aimed at investigating the propagation characteristics of different guided Lamb waves in submerged plate geometries which would be further used to develop a non-contact, in-situ and non-invasive health monitoring strategy for submerged plate assemblies. In such large structures, where the principal motive is detection of defect, the propagation characteristics of different guided wave modes would eventually help to develop a damage detection strategy for immersed structures wherein a pair of immersion mobile transducers can collect the information about the health of the submerged plate. Specific

ultrasonic guided wave modes with unique scanning capabilities have been identified experimentally. The different guided wave modes were generated and excited by keeping the transmitter and receiver probes at suitable incident angles and distances in a pitch catch configuration. The selected Lamb wave modes would be further investigated for optimum scanning capabilities in submerged plates with different types of damages in the following Chapters.

CHAPTER 5

PLATES WITH NOTCHES

5.1 INTRODUCTION

The characteristics of the different Lamb wave modes in submerged plate specimen of a particular thickness investigated in the preceding chapter will be further utilized to develop a damage detection methodology. Different Lamb wave modes at frequencies of 0.5 MHz and 1 MHz will be used to obtain PT signatures of the healthy submerged plate in water in pitch –catch orientation. The change in the received pulse transmission signatures vis-à-vis increasing damages in the form of notches in the plate will lead to development to a health monitoring strategy for the submerged plates. Specific guided wave modes sensitive to different extents of notch defects have been identified and subsequently used for damage identification and its localization. Experimental data will be further processed to generate pictorial representation of the actual state of the plate specimens in the form of defect maps. Main focus of this chapter is to develop a non-contact methodology for rapid evaluation of the health of a submerged plate using specific Lamb wave modes and to generate a topographical representation of the specimen.

5.2 EXPERIMENTAL INVESTIGATIONS

5.2.1 Excitation Frequencies and Modes

Despite having several advantages over bulk waves, complexity involved in Lamb wave propagation is a challenge in their successful and correct signal interpretation for health monitoring purposes. These complications are mainly attributed to the dispersive nature, multimode behavior and frequency dependent energy distribution profile of these modes. So it is imperative to judiciously select the optimum frequency and corresponding Lamb wave mode to thoroughly evaluate the presence, extent and location of the damage. In **Chapter 4**, it has been observed that specific Lamb wave modes can be produced in submerged plates of particular thickness at particular frequencies by varying the angle of the probes in the Pitch-Catch orientation. PT signatures are obtained for various available modes at 0.5 MHz and 1 MHz frequencies in the healthy plate. These signatures are likely to get affected due to the presence of any kind of damage in the plate. Hence, PT testing of immersed plate obtained by using non-contact probes exhibits a great potential as a non-destructive investigation tool.

This chapter explores the interaction of Lamb wave modes with the simulated damages and studies the suitability of these modes to efficiently detect the extent of damage. Simulated damages in the form of notches of varying depths have been machined on a 4mm thick steel plate. Dispersion curves showing phase velocity **(Figure 4.9a)**, group velocity (**Figure 4.9b**) and attenuation characteristics (**Figure 4.9c**) of the Lamb wave modes in healthy 4mm thick submerged steel plate have been plotted using software Disperse (Pavlakovic and Cawley, 2000). The important parameters related to the propagation behavior of various modes in the specimen plate are presented in detail in **Table 5.1.** For a submerged plate, water on both sides presents a highly attenuative media for Lamb wave propagation. In order to accomplish faster scanning, it is required to inspect longer spans. This necessitates the use of lower frequencies. Two pairs of mobile immersion probes with rated frequencies of 0.5 MHz and 1.0 MHz have been used to develop damage detection methodology in submerged plates as outlined in **Chapter 4**.

Table 5.1: Propagation characteristics of modes from dispersion curves

S. No.	Frequency (MHz)	Mode	V_{ph} (km/s)	Angle (θ)	V_{gr} (km/s)	Attenuation (dB/m)
1	0.5	A_1	9.75	8.85^{o}	3.1	28
2		S_0	5.021	17.4^{o}	3.64	69
3	1.0	S_1	5.93	14.7^{o}	4.98	0.18
4		A_1	5.23	16.7^{o}	2.98	133
5		S_0	3.14	28.5^{o}	2.67	270

At these frequencies, following key observations are made from the dispersion curves **(Figure 4.9)**:

- In case of submerged plate, Scholte wave propagates at the interface of steel and water. Its phase velocity is nearly equal to the bulk velocity of wave in the liquid and it experiences no attenuation. This mode does not exist in case of plates in air.

- Anti-symmetric mode, A_0 has significant lateral motion over the entire frequency range leading to substantial loss of energy into the surrounding liquid and hence, is not discernible in the dispersion curves.
- At 0.5 MHz two modes, S_0 and A_1, are available. A_1 mode has a phase velocity significantly higher than the longitudinal bulk velocity of sound in steel and in water.
- At 1 MHz, three modes namely S_0, A_1, S_1 exist. Incident angles for A_1 Mode at 1 MHz (16.7^o) and S_1 Mode at 1 MHz (14.7^o) are close owing to nearly matching phase velocities.
- Group velocities for S_0 Mode and A_1 Mode at 1 MHz are close. When testing for short spans, these modes may interfere with each other causing overlapping of the received signal.
- S_0 Mode at 1 MHz is highly attenuative (270 dB/m). However, S_0 mode at 0.5 MHz is quite isolated and has reasonably low attenuation.

These modes at specific frequencies of 0.5 MHz and 1 MHz will be further experimentally validated in the following sections in plates with varying depths of machined notches to develop a damage detection strategy for submerged plates.

5.2.2 Experimental preparation and methodology

To develop a damage monitoring strategy in submerged plates, first scanning of the plate in Pulse Transmission mode (PT) at all selected frequencies and modes is done to obtain the baseline signatures. Then the plate is seeded with machined notch of depth of 12.5% of the plate thickness (0.5 mm) and PT signatures are again recorded. Subsequently the notch depth is increased gradually up to 75% (3mm deep) of the plate thickness in steps of 12.5% (0.5 mm depth increment) of the plate thickness each and PT signatures are recorded for each depth of notch **(Figure 5.1)**. During this testing, experimental parameters like D_w, D_p, PR settings (gain, HPF, LPF) are kept unaltered.

For experimental study on submerged plate without and with notches, the experimental Set-up and Probe and UT system characteristics are kept same as outlined in Chapter 4. To generate a specific mode, the probes are placed in pitch catch orientation, at a particular distance from the immersed plate. Both the probes are set at the same angle of inclination with vertical (θ). The ultrasonic excitation is a spike pulse obtained when PR is set at maximum input voltage amplitude of 475V. The ultrasonic energy in the form of

longitudinal waves generated by the probes traverses through the water and hits the plate obliquely. Part of this energy is transmitted into the plate in the form of Lamb waves and rest is reflected back. Probe receives this reflected energy and PE signature is obtained.

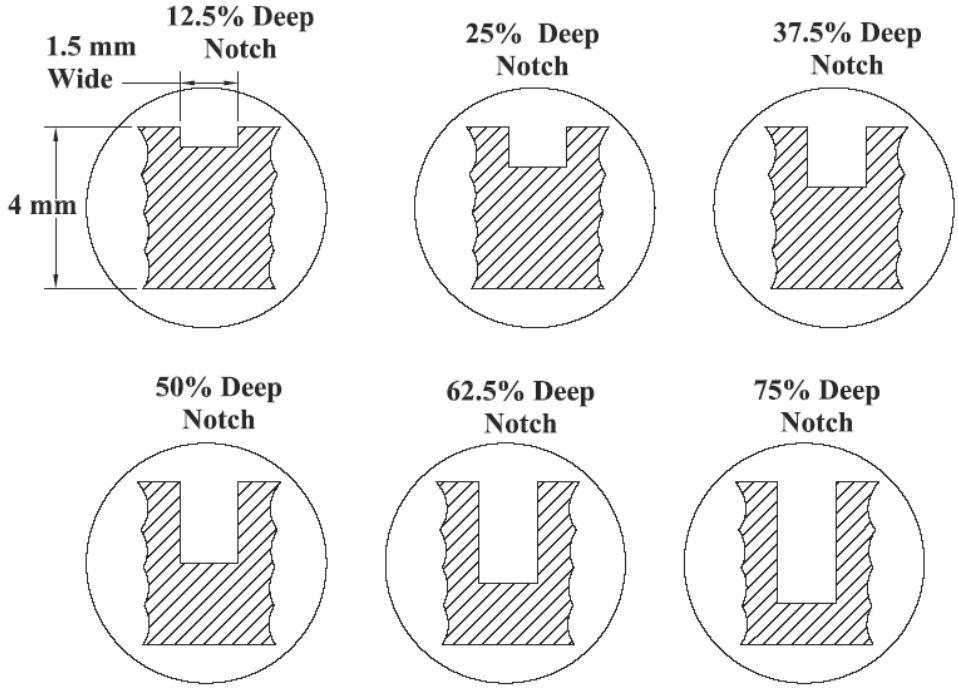

Figure 5.1: Notch Geometry Details (1.5 wide and depths varying from 0.5 mm to 3 mm with 0.5 mm increment)

The vertical placement of the probes is adjusted in terms of time of flight in water (t_w) of first reflection from the specimen in Pulse Echo (PE) mode **(Figure 5.2 a)** and is related to water path (D_w) by **Equation 4.2**. The time of flight, t_w is kept as 40µs in the entire experimental investigations for both the probes to ensure equidistant placement of the probes at a convenient location from the specimen in terms of signal clarity and repeatability. **Figure 5.2 (b –c)** shows typical PE signatures for transmitter and receiver probes obtained with S_0 mode at 0.5 MHz and S_1 at 1 MHz respectively.

After setting up the probes, the plate specimens have been tested in PT mode. PT signals in the healthy plate are recorded with all available modes at 0.5 MHz and 1.0 MHz frequencies. The desired combination of the mode and frequency is obtained by setting the probes at a corresponding angle of incidence (**Table 5.1**). **Figure 5.3 (a-e)** shows the PT signatures in the healthy plate with all modes at 0.5 MHz and 1 MHz. Time of arrival for different modes indicated in these signatures is computed using Equation 4.3, t_w, D_p and V_{gr} (**Table 5.1**).

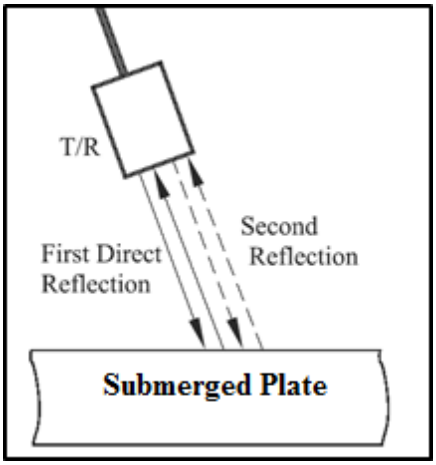

(a) PE Testing Peaks in Healthy Zone of the submerged plate

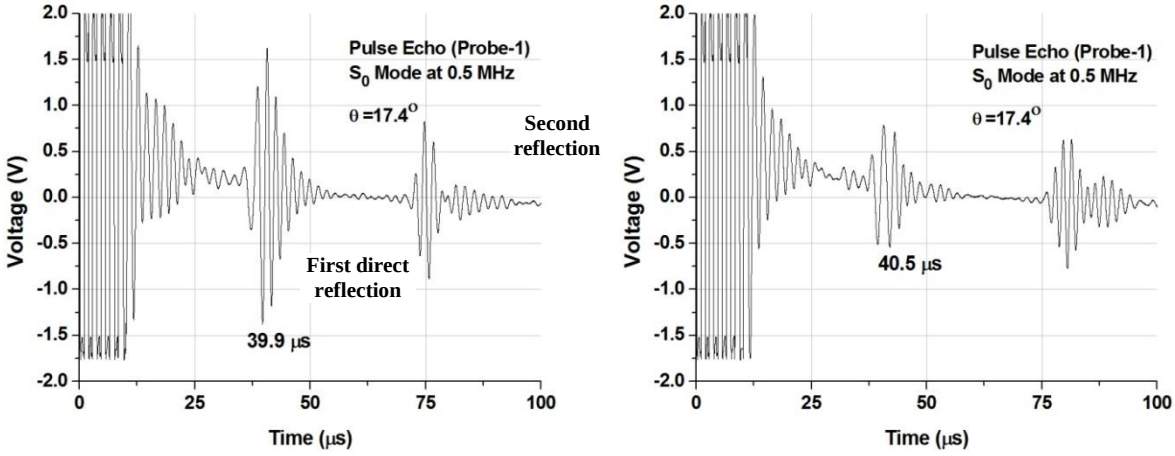

(b) S_0 mode at 0.5 MHz

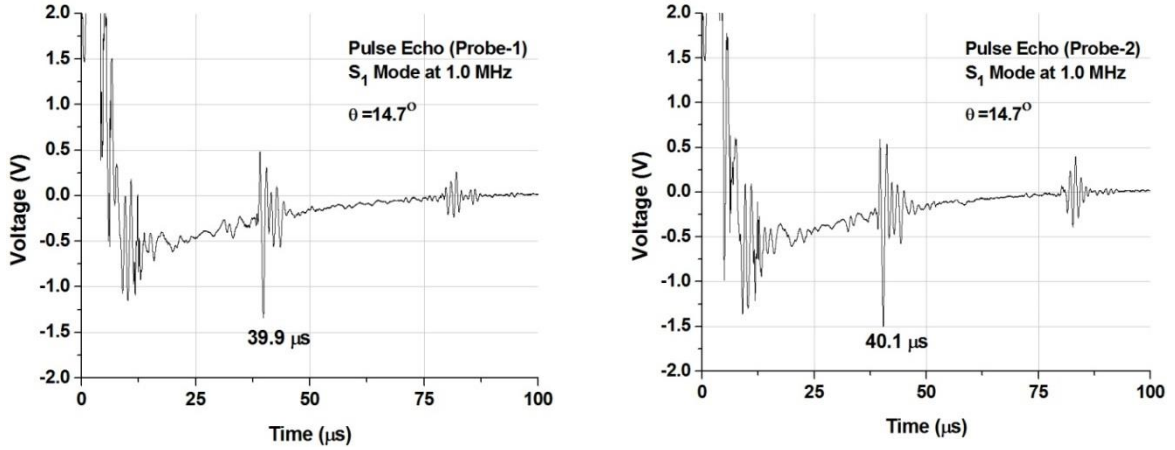

(c) S_1 Mode at 1 MHz

Figure 5.2: Pulse Echo signature of plate in water

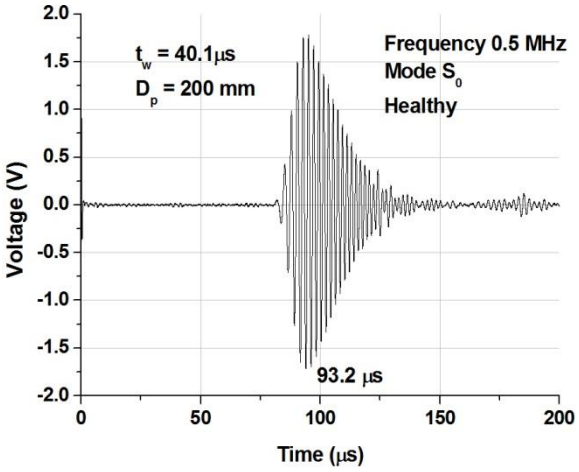

(a) S_0 Mode at 0.5 MHz

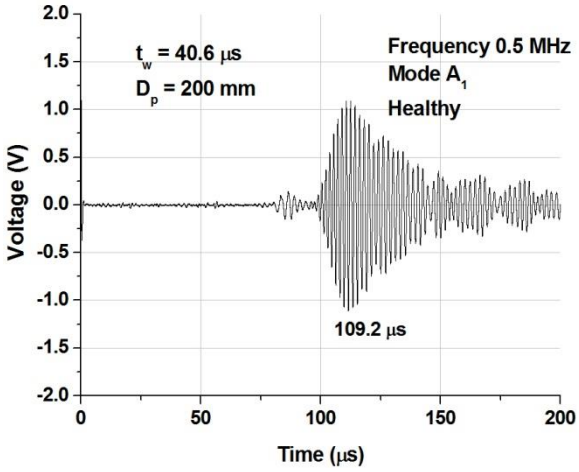

(b) A_1 Mode at 0.5 MHz

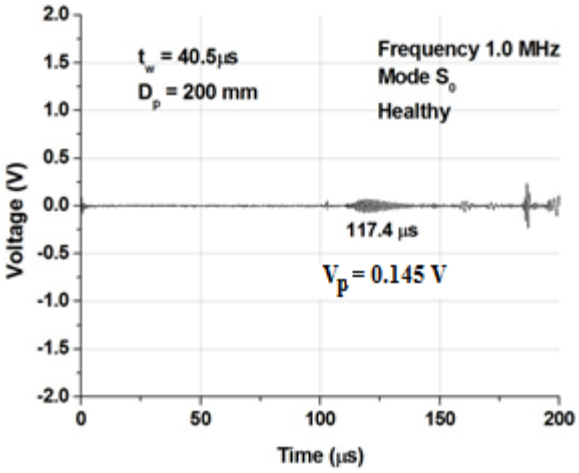

(c) S_0 Mode at 1.0 MHz

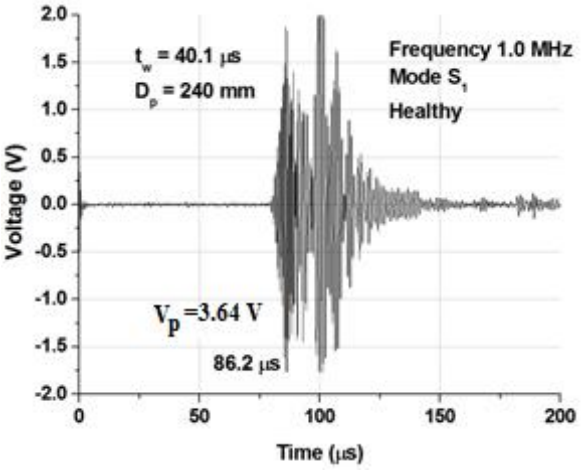

(d)) S_1 Mode at 1.0 MHz

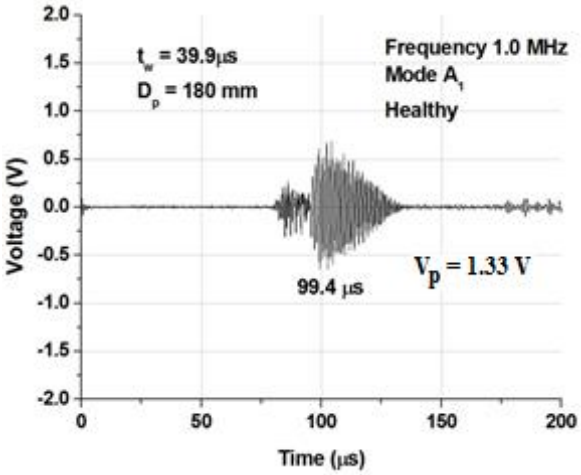

(e) A_1 Mode at 1.0MHz

Figure 5.3: PT signatures in healthy zone of plate with various modes

Experimental and theoretical time of arrival of the transmitted pulse for all the modes at 0.5 MHz and 1 MHz in the healthy plate is shown in **Table 5.2.** A close match is observed in the theoretical and experimental time of arrival of the transmitted pulses thus confirming the generation of specific Lamb wave modes experimentally. Minor deviation in the two values may be attributed to various reasons like –uneven thickness of the plate, inherent variation in material properties and small variations in incident angles.

Table 5.2: Arrival times of transmitted pulses of various modes

Mode	Frequency (MHz)	D_p (mm)	Time of arrival (μs)		% Difference
			Experimental	Theoretical	
S_0	0.5	200	93.2	93.3	-0.1%
A_1		200	109.2	106.7	+2.3%
S_0	1.0	200	117.4	114.9	+2.1%
S_1		240	86.2	88.1	-2.1%
A_1		180	99.4	100.4	-0.99%

The experimental methodology consists of scanning the plate with seeded defects in PT to identify the damaged areas in the plate. Comparison of the received PT signals in the notched plate's vis-à-vis the healthy plate would lead to the diagnosis of damage. Further for localization of damage, ultrasonic testing is carried out in PE mode and ultrasonic data gathered in PE and PT is used to generate a defect map.

5.2.3 Ultrasonic Pulse Transmission Investigations

PT signatures are likely to be modified due to presence of damage on the plate. Owing to unique distribution of particle displacement and energy across the plate thickness, each Lamb wave mode is expected to exhibit unique response to notches of varying depths. In order to exploit the Lamb waves as an effective NDE tool, it is important to select those modes which are more sensitive to the type of defects being investigated. Modes that are likely to exhibit largest variation in signal amplitude of the transmitted pulse for a notched specimen vis-à- vis healthy plate are most suitable and are preferred.

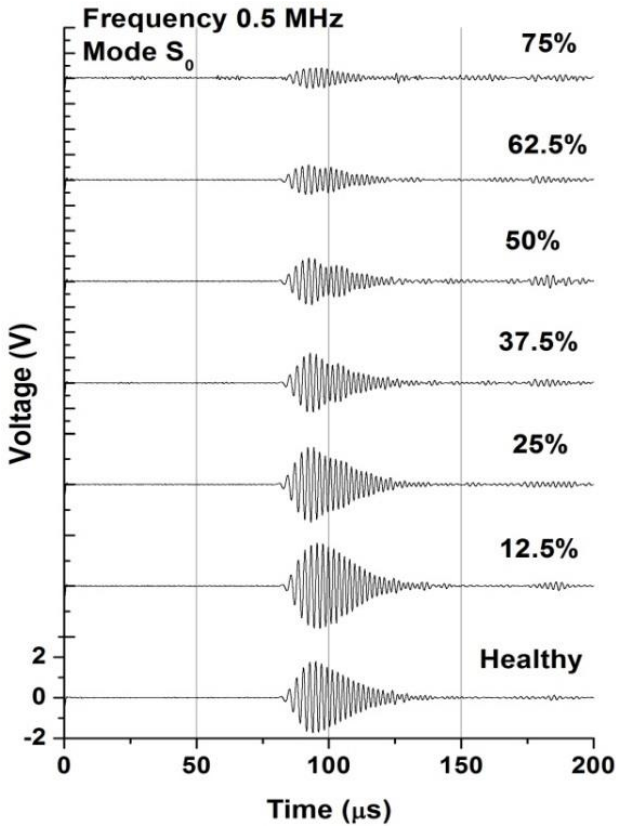

(a) S_0 mode

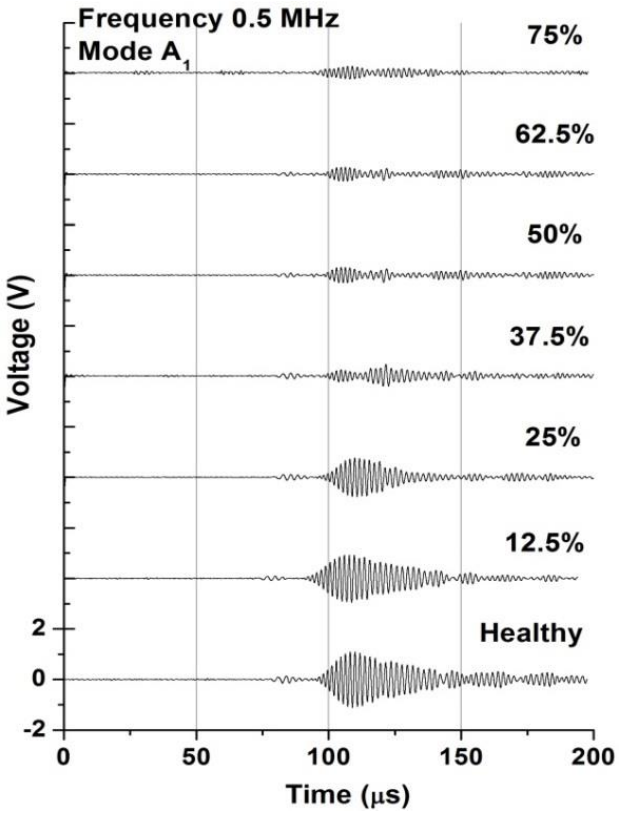

(b) A_1 mode

Figure 5.4: PT signatures Vis-a- Vis Notch Depth using all modes at 0.5 MHz

Figure 5.4 shows the PT signatures recorded using S_0 mode at 0.5 MHz for plate specimens having varying depth of notch. It is clear that as the depth of the notch increases, the signal amplitude of the received signal drops. It can be attributed to the fact that as the depth of the notch increases more of the energy is reflected back from the notch and less of it is transmitted to the receiver **(Figure 5.5)**. Hence, this technique can successfully identify the presence of notches and possibly quantify their extent.

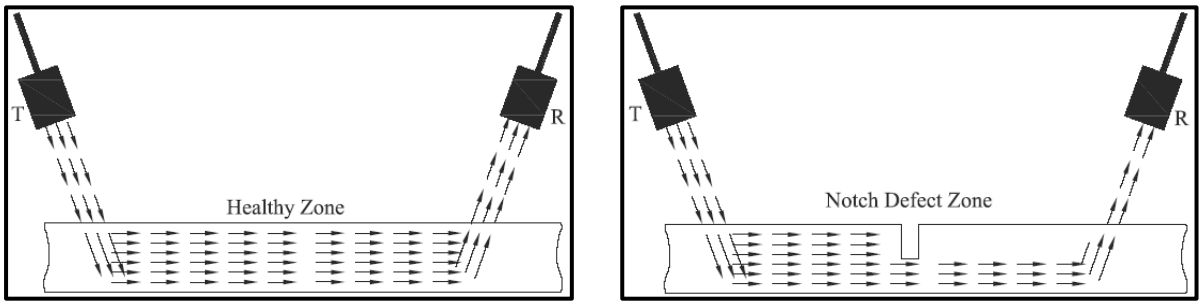

(a) **(b)**

Figure 5.5: Flow of ultrasonic energy in (a) Healthy zone (b) Defect ridden zone

Figure 5.5 (b) shows similar trends for A_1 mode at 0.5 MHz **(Figure 5.5b).** It is important to note that the time of arrival of the received pulse for both modes remains largely unaltered with the varying depths of notches. Comparison of PT signatures for these two modes at 0.5 MHz indicates that S_0 mode retains its character and sharpness even when it comes across the notch**.** But same is not true in case of A_1 mode, where the signal spreads in time domain as depth of notch increases making the signal interpretation difficult. This may be attributed to mode conversions due to interaction of A_1 mode with notch. Hence, S_0 mode at 0.5 MHz has been considered for further experimental investigations.

Figure 5.6 shows the PT signatures obtained with all three available modes of S_1, A_1 and S_0 at 1.0 MHz for healthy and notched plates. Comparison of healthy PT signatures **(Figure 5.3 c, d and e)** clearly brings out that S_0 mode at 1.0 MHz yields a very feeble PT signal with an extremely low V_p of 0.145 V whereas for other available modes i.e. A_1 mode and S_1 modes V_p is 1.33 V & 3.64 V respectively. This is due to very high attenuation of 270 dB/m (**Figure 4.9c**). Peak to peak voltage amplitude corresponding to S_0 mode is too small to be useful for monitoring any significant changes during PT scanning of healthy and as well as notched plate **(Figure 5.6a)**. Hence, S_0 mode at 1.0 MHz is discarded and not used for further study.

Similarly, anti-symmetric modes are also considered unsuitable for damage detection in submerged conditions due to their relatively higher attenuation characteristics. This is mainly attributed to the effective coupling of the out-of-plane displacement component with the surrounding medium which is well supported by the attenuation dispersion curves **(Figure 4.9c)**. At 1 MHz, A_1 mode has higher attenuation of 133 dB/m as compared to S_1 mode (0.18 dB/m). In addition to this, group velocities for modes S_0 (2.67 km/s) and A_1 (2.98 km/s) at 1MHz are very close. It results in appearance of a number of merging peaks in PT signature of A_1 mode due to contributions of S_0 mode. So the signal obtained is in the form of an envelope rather than a sharp distinct peak **(Figure 5.6b)**. It makes signal interpretation difficult and it is hard to notice any quantitative change in received signal with increase in notch depth. Owing to these factors, A_1 mode is not preferred and is also discarded. Hence, S_1 mode at 1 MHz, being the fastest and least attenuative (0.18 dB/m) and having a distinct peak (**Figure 5.6c)** has been used for subsequent investigations. It is well separated in group velocity dispersion curves **(**Figure 4.9 b) from the rest of the modes. Its peak to peak voltage (V_p=3.64 V) in healthy plate is also higher than A_1 and S_0 modes at the same frequency and it shows marked signal drop with increasing depth of the notch **(Figure 5.6).** Peak to peak voltage amplitudes of all the available modes at 0.5 MHz and 1.0 MHz for healthy and notched plates are compiled and presented in **Figure 5.7**.

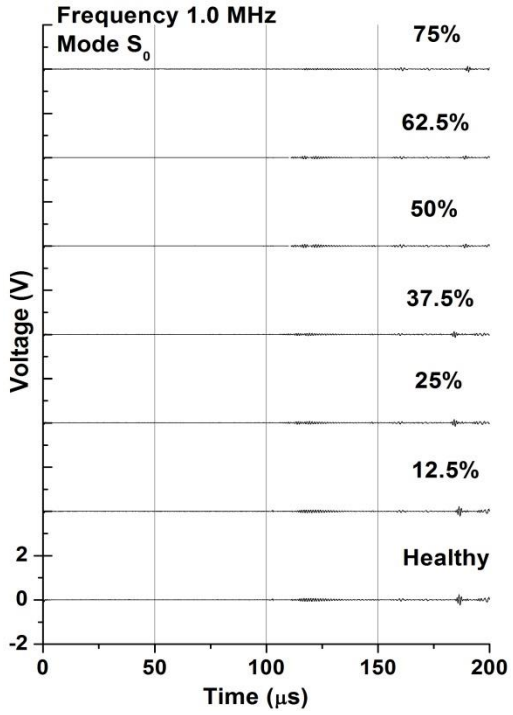

(a) S_0 mode

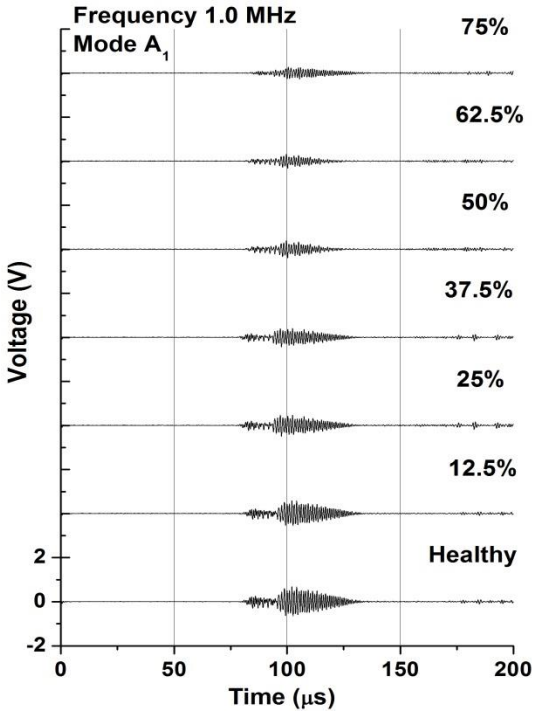

(b) A_1 mode

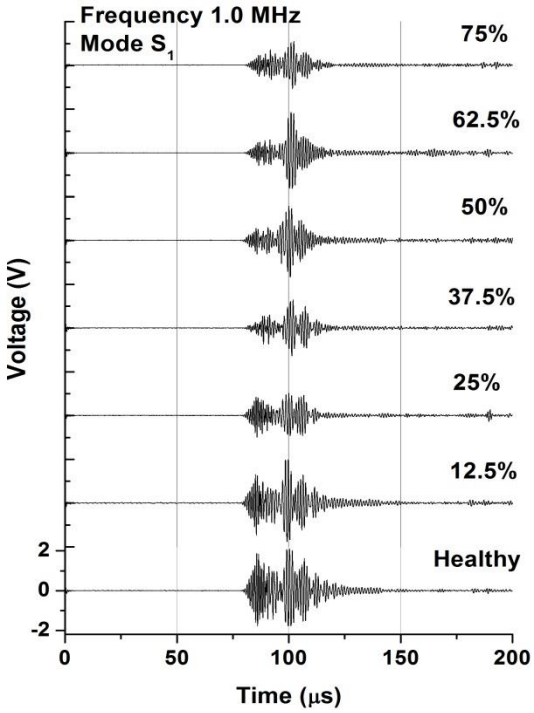

(c) S_1 mode

Figure 5.6: PT signatures Vis-a- Vis Notch Depth using all modes at 1.0 MHz

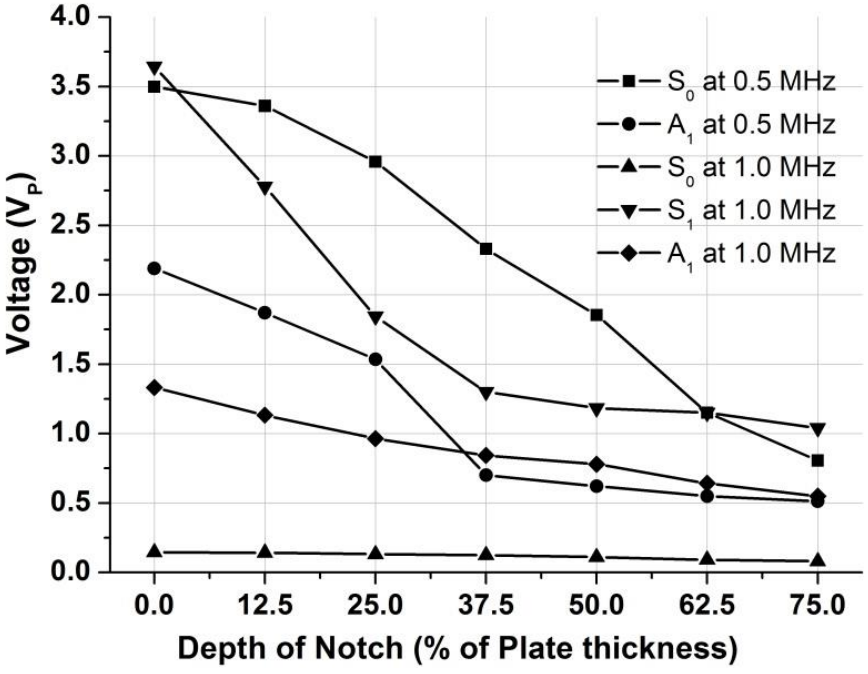

Figure 5.7: Variation in Voltage Amplitude with varying notch depths using different Lamb wave modes at 0.5MHz and 1 MHz

5.2.4 Mode Sensitivity

As discussed in the previous section, amplitude of the transmitted pulse suffers a drop when it encounters a notch. But the fall in voltage amplitudes for a given notch depth is not same for all modes. These variations in the transmitted signal strength corresponding to notched specimens suggest that each Lamb wave mode interacts uniquely with the notch defect depending on its depth. So it is important to understand the notch depth dependent behavior of these modes so that suitable mode can be exploited to investigate the extent of defect on a given specimen. The mode specific interaction has been termed here as *Mode Sensitivity*, which determines the suitability of a given mode to effectively detect near surface and deeper defects ranging up to the mid plane of the plate and beyond.

For the two selected Lamb wave modes (S_0 mode at 0.5 MHz and S_1 Mode at 1.0 MHz), normalized peak to peak voltage ratio of the transmitted pulses (V_n) are shown in **Figure 5.8**. V_n ratios for a selected mode are obtained by normalizing V_p values at different notch depth values (0% to 75% depth) with respect to the corresponding healthy V_p value. V_n is preferred over V_p amplitudes in order to compare the efficacy of the selected modes so that the extrinsic biases in the experiment (like PR settings, Propagation distance etc.) can be avoided.

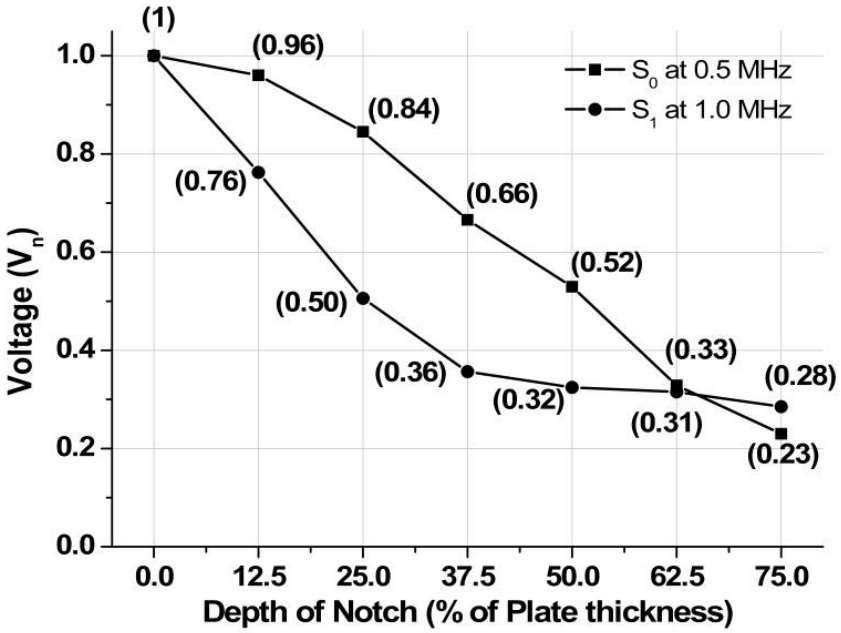

Figure 5.8: Normalized voltage amplitudes for selected modes at 0.5 MHz and 1 MHz

In healthy condition, the V_n ratio is unity for both the modes. When the notch depth is incremented to 12.5%, S_0 mode is marginally affected (V_n falls to 0.96) while S_1 mode exhibits a much greater loss (V_n falls to 0.76) for the same notch depth. Similar trend is followed at 25% notch depth where S_0 mode suffers only 16% drop in signal as compared to 50% drop observed in S_1 mode.

But the trend is reversed with further increase in depth of notch. At 37.5% depth of notch, fall in V_n is visibly higher for S_0 mode than S_1 mode. At 50% depth of notch, S_1 mode undergoes a nominal change with its V_n ratio falling from 0.36 to 0.32 whereas S_0 mode continues to yield a consistent drop in V_n ratio. With even deeper notches (62.5% -75% depths), S_1 mode continues to exhibit a sluggish fall in V_n ratio as indicated by a nearly horizontal line. However, S_0 mode shows a consistent fall in V_n ratio even in this region. The trends clearly establish that S_0 mode at 0.5 MHz is relatively insensitive to the shallow notches but is better suited for detecting deeper notches.

On the other hand, S_1 mode at 1 MHz is highly sensitive to surface modifications as indicated by sharp fall in V_n ratio for shallow notches. However, for deeper defects this mode is relatively insensitive as indicated by nearly flat V_n plot for notch depths ranging beyond mid plane of the plate. Hence, by judicious selection of specific modes, deep and shallow notches can be effectively discerned.

The variable behavior of the modes to notch defects can be attributed to the wave structure. It is observed that S_1 mode at 1 MHz **(Figure 5.9a)** has significant displacement and energy distribution near the surface as compared to the core of the plate. It is more sensitive to shallow notches. Thus, this mode would be better suited for detecting surface defects and is named as the ***Surface Sensitive Mode***. Similarly, the behavior of S_0 mode at 0.5 MHz which shows more sensitivity to deep notches can be explained from its wave structure. This mode has more of its energy concentrated at the mid plane of the plate and hence, is not suitable for detecting the surface changes **(Figure 5.9b),** but it works well for the deeper defects lying in the core. Such a mode is referred to as ***Core Sensitive Mode*.**

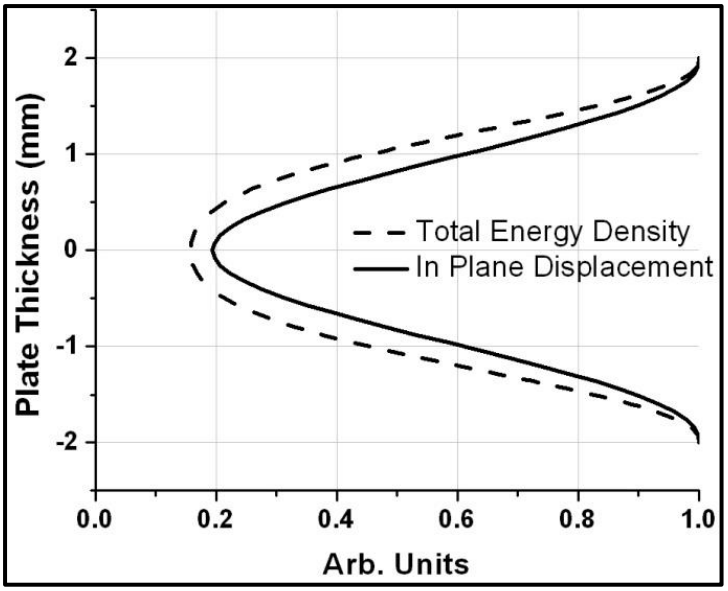

(a) S_1 mode at 1 MHz

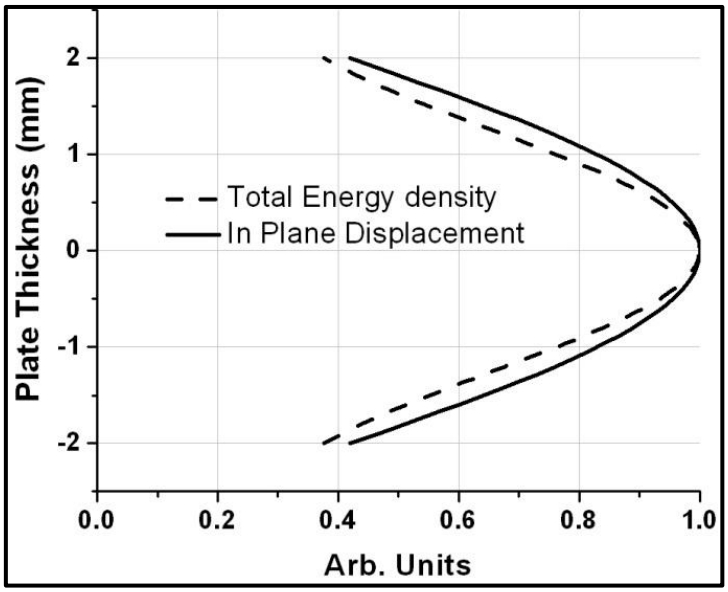

(b) S_0 mode at 0.5 MHz

Figure 5.9: Wave structure of selected Lamb wave modes

5.3 SCANNING AND GENERATING DEFECT MAPS

The selected core sensitive and surface sensitive modes have been further used for detailed scanning of the plate with notch defects and subsequently generating defect maps. For this purpose, a plate (1065mm x 610mm x 4mm) with machined notches of varying depths (25%, 50% and 75% of the plate thickness) at different locations (X_1-X_2, X_3-X_4, X_5-X_6) is scanned using pitch catch configuration (**Figure 5.10)**.

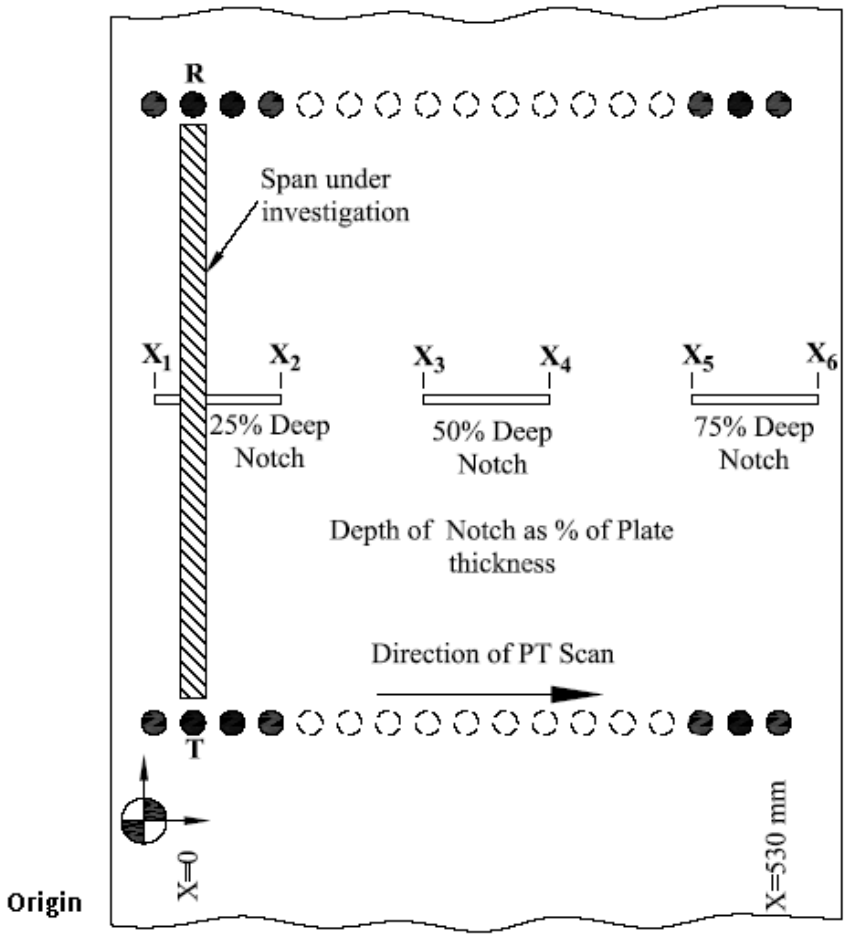

Figure 5.10: Pulse Transmission Scanning of the plate

The orientation of the notches is parallel to X-direction and normal to the direction of wave propagation. The plate is scanned using a pair of mobile probes by moving them along X-direction. The shaded area shows the zone under investigation at a sampling point. The stepper motor drive system translates the aligned probes in X-direction from X=0 to X= 530 mm, at a uniform speed (about 1mm/s) and corresponding coordinates can be read from the ***DRO***. During this scan, PT signatures are continuously recorded at regular intervals using the selected modes along with the corresponding coordinates from DRO. A drop in PT signal indicates a discontinuity in that zone and is further scanned with finer resolution. Normalized voltage amplitudes of the received signals are plotted for both core sensitive mode and surface sensitive mode (**Figures 5.11- 5.12)**. Quantitative changes can be observed in these

plots in the notched zones vis-à-vis the healthy zone. These changes can be correlated to the presence, location and depth of the notches.

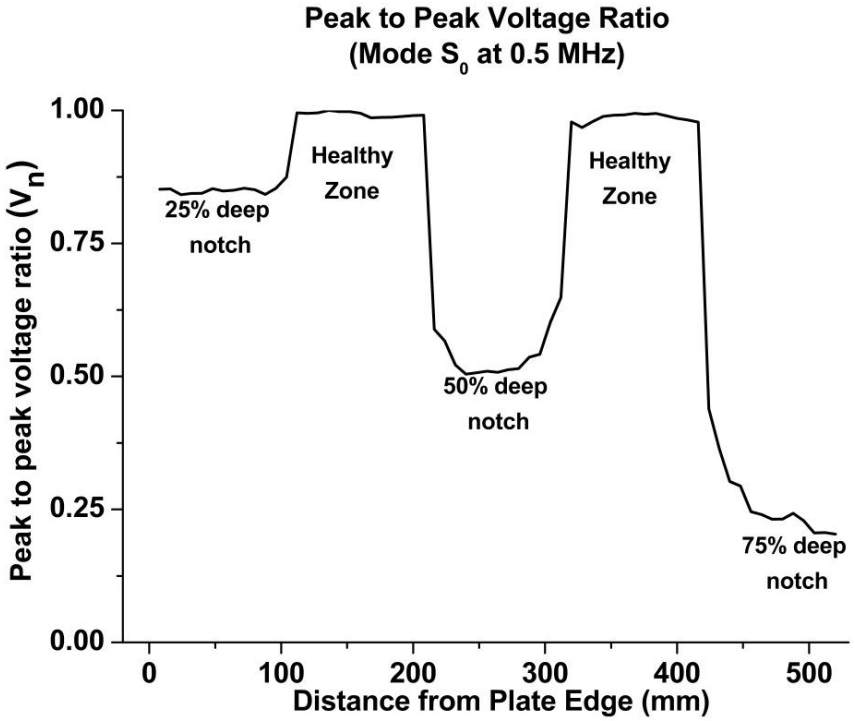

Figure 5.11: Normalized peak to peak voltage ratios using S_0 mode at 0.5 MHz

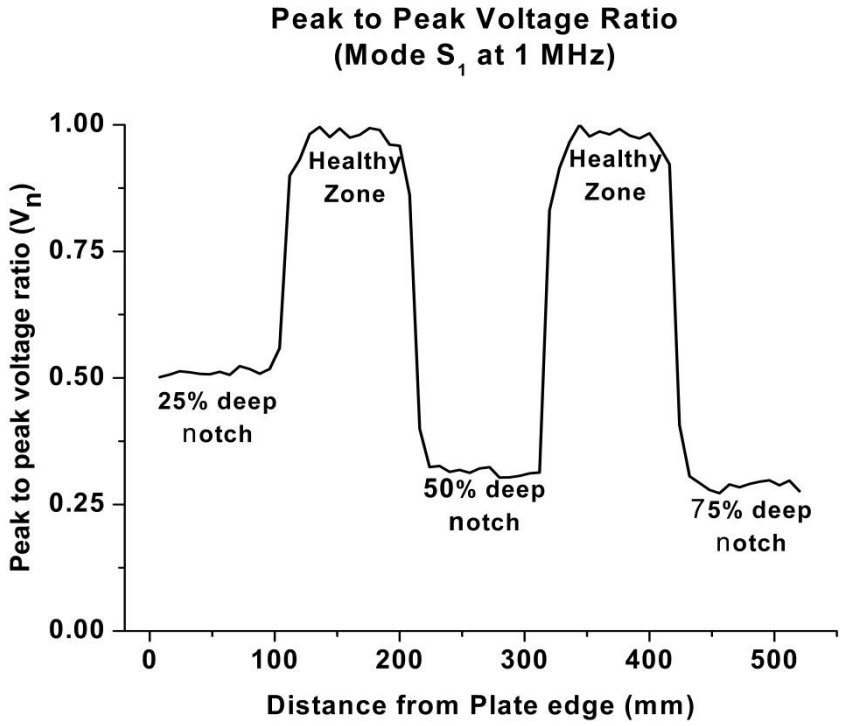

Figure 5.12: Normalized peak to peak voltage ratios using S_1 mode at 1 MHz

5.3.1 Scanning with Core Sensitive Mode

Figure 5.11 shows V_n while scanning with S_0 mode at 0.5 MHz. Presence and the extent of the notches are clearly characterized by the variation in V_n ratios. It is observed that for 25% deep notch, there is a small change in V_n (falls to 0.85). With further increase in the depth of notch, V_n falls steeply. At 50% and 75% notch depth, V_n values are 0.52 and 0.26 respectively. It is due to the core sensitive characteristic of S_0 mode at 0.5 MHz. The energy of this mode is concentrated in the center of the plate and hence it is relatively less sensitive to near surface modifications up to 25% depth of the plate. But this mode is more effective in identifying the sub surface defects lying around the mid-plane of the plate.

5.3.2 Scanning with Surface Sensitive Mode

The plate is also scanned with the surface sensitive S_1 mode at 1 MHz. Due to its significant energy distribution near the surface; this mode may be exploited for detecting surface defects. **Figure 5.12** also shows the PT scan with S_1 mode at 1MHz frequency. For 25% notch depth, drop in V_n is visibly higher as compared to corresponding drop with S_0 mode at 0.5 MHz. V_n falls to 0.5 using the surface sensitive mode as compared to 15% drop while using the core sensitive mode. Subsequently at 50% and 75% deep notches this mode does not reflect much change in the received signal. V_n falls to 0.33 and 0.28 for 50% and 75% deep notches respectively. Hence, this mode is better suited for picking up near surface irregularities and discontinuities.

PT scanning at the rate of 1mm/sec using core sensitive and surface sensitive modes is the first step for monitoring presence of defects and leads to quick identification of defect regions on the plate. Results of PT scan reveal dips in V_n while the probes are present in X_1-X_2, X_3-X_4 and X_5-X_6 zones as indicated on the plate (**Figure 5.10**), indicating presence of damage in the respective areas. Extent of damage at any location can be estimated by comparison of relative dips in the voltage ratios (V_n) in these areas (**Figure 5.11 - 5.12)**. These identified damage ridden zones are further investigated in PE configuration for the localization of the defects.

5.3.3 Defect Localization and Mapping

PE scanning is accomplished with in the damage ridden zones identified in the previous step by moving one of the probes along Y direction (**Figure 5.13**). During this translation, Y-coordinates of the probe (from DRO) and the corresponding PE signatures are recorded.

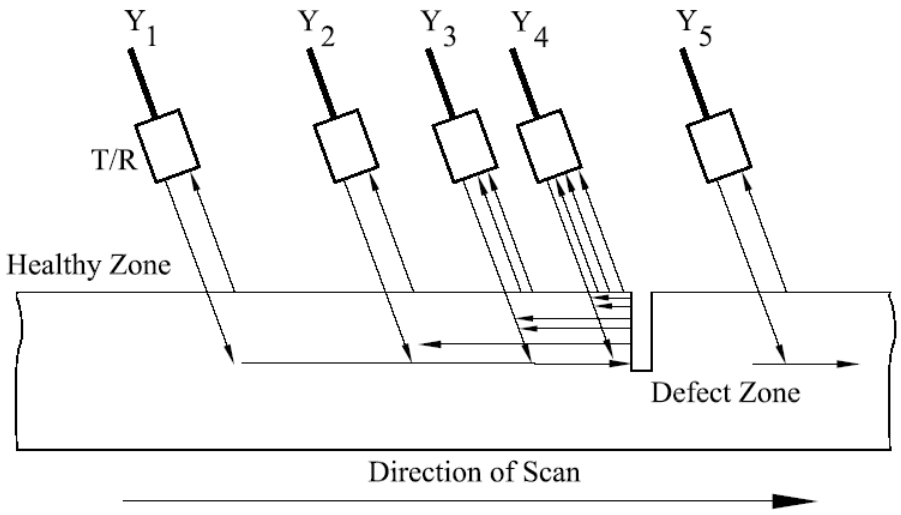

Figure 5.13: Defect Localization in Y-direction PE Scan

At a particular location (say Y_1), which is quite far from the notch, PE signature is as shown in **Figure 5.14 (a)** using S_0 mode at 0.5 MHz. This mode has been selected for PE monitoring since it exhibits a continuous and consistent drop in PT signal with increasing notch depths as against the surface sensitive mode which is sensitive to notch defects only up-to the mid plane of the plate. Two distinct peaks at around 38 µs and 76 µs can be observed in PE signature. These two peaks are first and second reflections from the plate as shown in **Figure 5.2a** for healthy plate. It has been experimentally observed that in the healthy zone, signal amplitude of first reflection peak varies within ±10%. These variations in PE signatures are mainly attributable to the inherent surface undulations present on the specimen.

As the probe approaches the notch (positions Y_2, Y_3 etc.) a third peak starts to appear in the PE signature **(Figure 5.14 b-e).** It is due to the reflection of the Lamb waves from the notch. It is referred to as *Defect Reflection Peak (DRP)*. When the distance between the probe and notch reduces to 40 mm, the defect reflection peak appears at about 60 µs (**Figure 5.14b**).

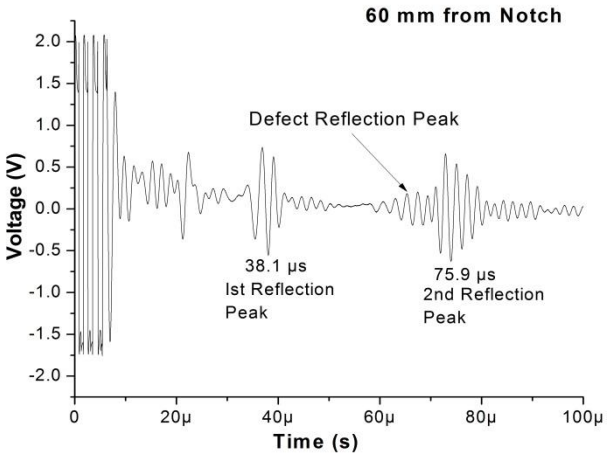
60 mm from Notch
Defect Reflection Peak
38.1 µs
Ist Reflection
Peak
75.9 µs
2nd Reflection
Peak
Voltage (V)
Time (s)

(a)

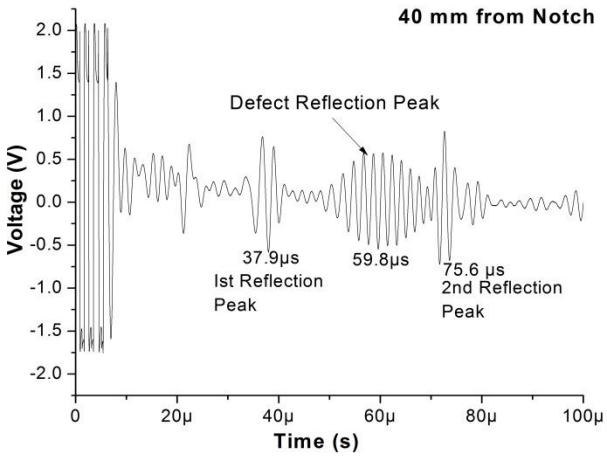
40 mm from Notch
Defect Reflection Peak
37.9µs
Ist Reflection
Peak
59.8µs
75.6 µs
2nd Reflection
Peak
Voltage (V)
Time (s)

(b)

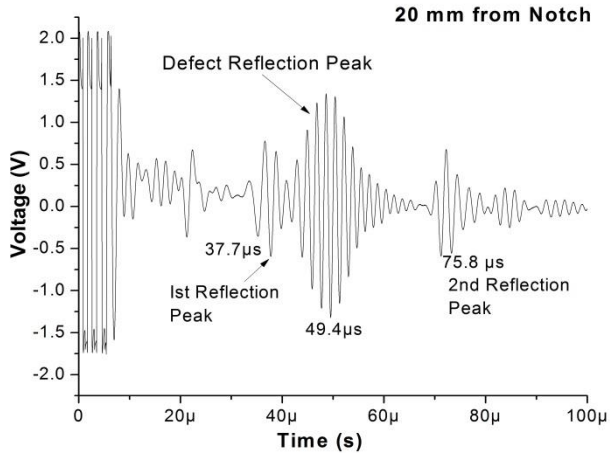
20 mm from Notch
Defect Reflection Peak
37.7µs
Ist Reflection
Peak
49.4µs
75.8 µs
2nd Reflection
Peak
Voltage (V)
Time (s)

(c)

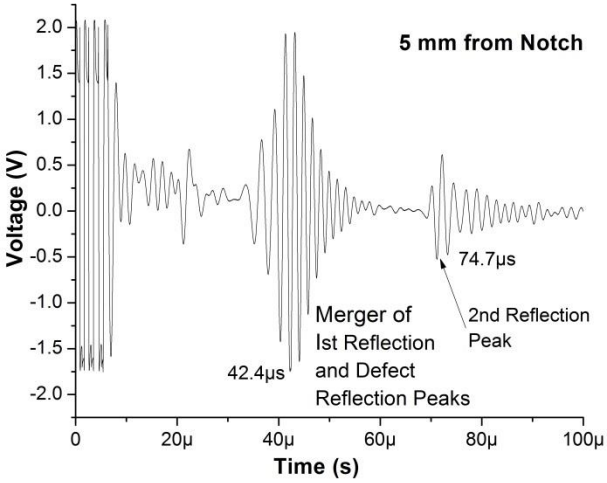
5 mm from Notch
74.7µs
Merger of
Ist Reflection
and Defect
Reflection Peaks
42.4µs
2nd Reflection
Peak
Voltage (V)
Time (s)

(d)

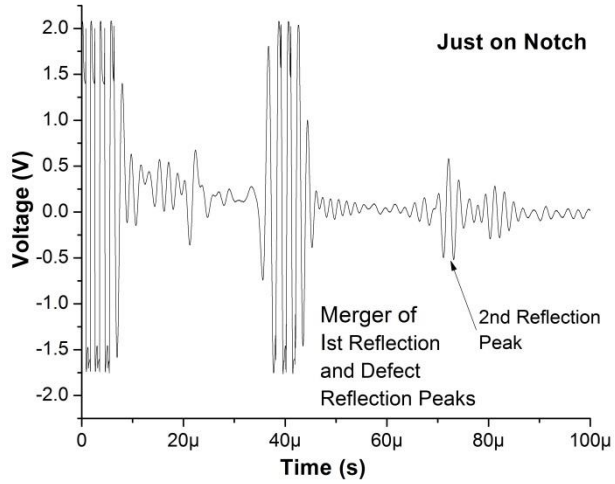
Just on Notch
Merger of
Ist Reflection
and Defect
Reflection Peaks
2nd Reflection
Peak
Voltage (V)
Time (s)

(e)

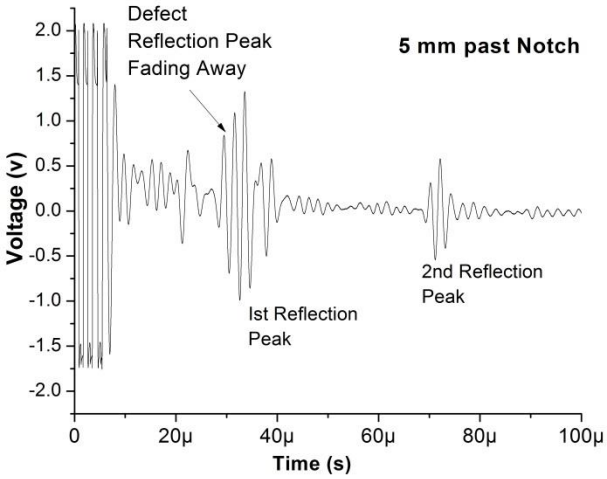
Defect
Reflection Peak
Fading Away
5 mm past Notch
2nd Reflection
Peak
Ist Reflection
Peak
Voltage (v)
Time (s)

(f)

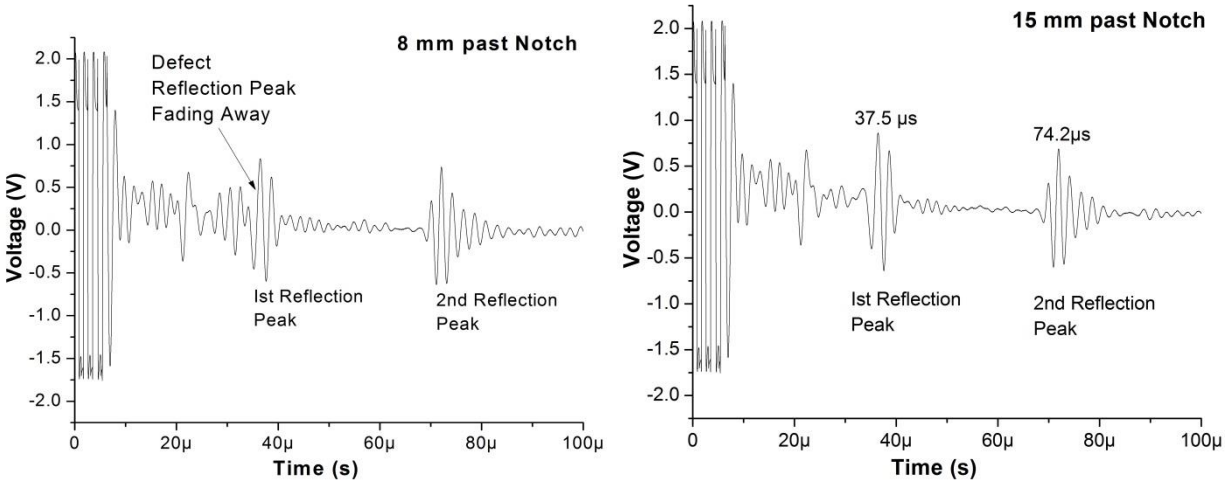

(g) **(h)**

Figure 5.14: PE signatures at different locations from the notch in Y-direction

Time of flight of DRP at this position can be correlated to the water path (38 µs), distance between probe and notch (40 mm × 2) and group velocity (3.64 km/s) of the S_0 mode at 0.5 MHz. Subsequently as the probe advances further towards notch, DRP in PE signatures progressively gets stronger and shifts to left suggesting the reducing distance between the probe and the notch. Time of flight is also found to be consistent with corresponding gap between the probe and notch. When the probe is placed very close to the notch**,** DRP merges with the first reflection peak **(Figure 5.14 d-e).** Appearance of a distinctively sharp first peak indicates that the presence of a notch in the vicinity of the probe. Peak-peak voltage amplitude of first reflection peak from PE signatures and corresponding position coordinates of the probe are simultaneously recorded and are further processed to generate the defect map. As the probe moves beyond the notch, the reflected Lamb waves start fading. It is shown by the receding PE voltage amplitude (**Figure 5.14 f-g**). When the probe completely clears the notch, the PE signature (**Figure 5.14 h**) is similar to the PE signature for healthy zone (**Figure 5.14a**).

Further, it has been experimentally observed that first reflection peak amplitude rises with increase in the depth of the notch **(Figure 5.15)**. It is due to the increase in the depth of the vertical wall of the notch that reflects the propagating Lamb wave. This data is further utilized for defect localization and quantification in the form of a defect map.

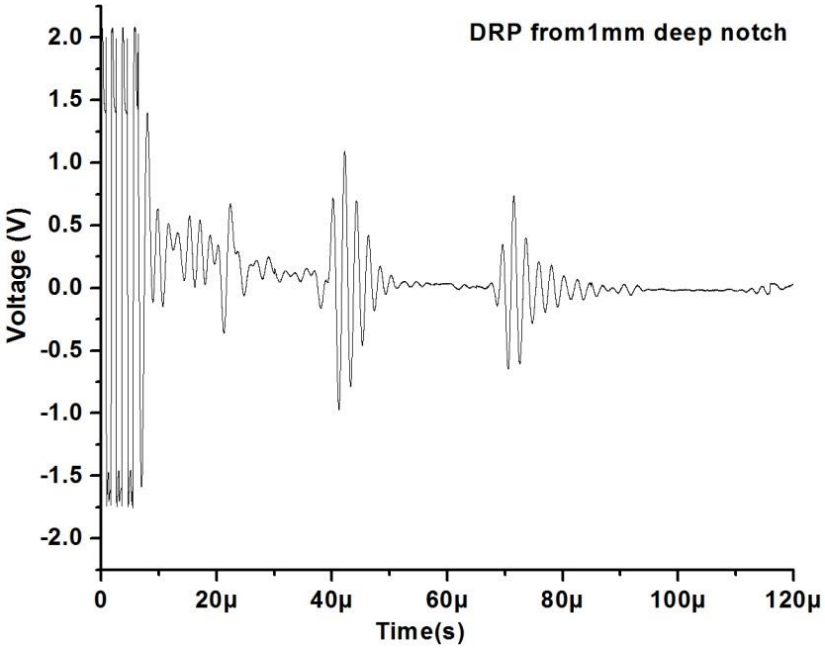
DRP from1mm deep notch
Voltage (V)
2.0
1.5
1.0
0.5
0.0
-0.5
-1.0
-1.5
-2.0
0
20µ
40µ
60µ
80µ
100µ
120µ
Time(s)

(a)

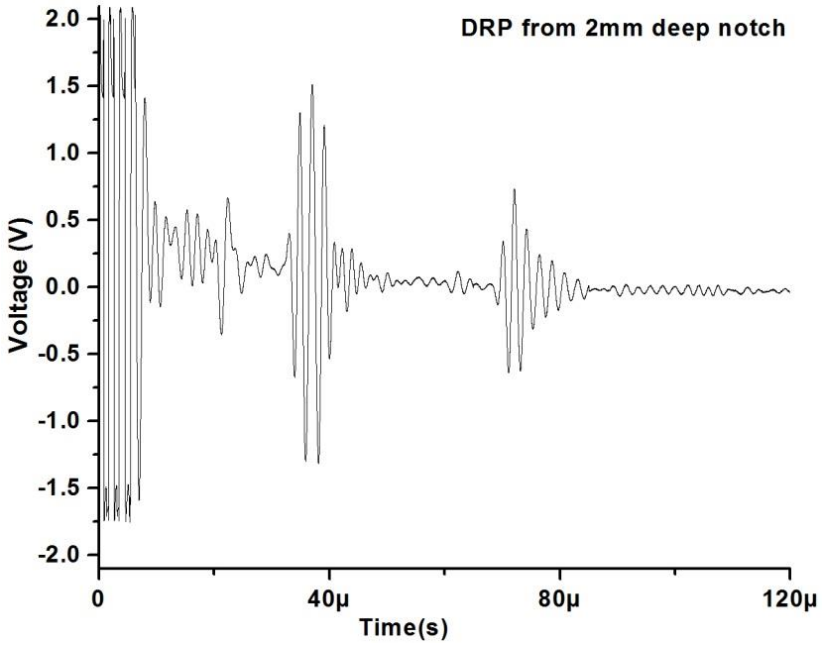
DRP from 2mm deep notch
Voltage (V)
2.0
1.5
1.0
0.5
0.0
-0.5
-1.0
-1.5
-2.0
0
40µ
80µ
120µ
Time(s)

(b)

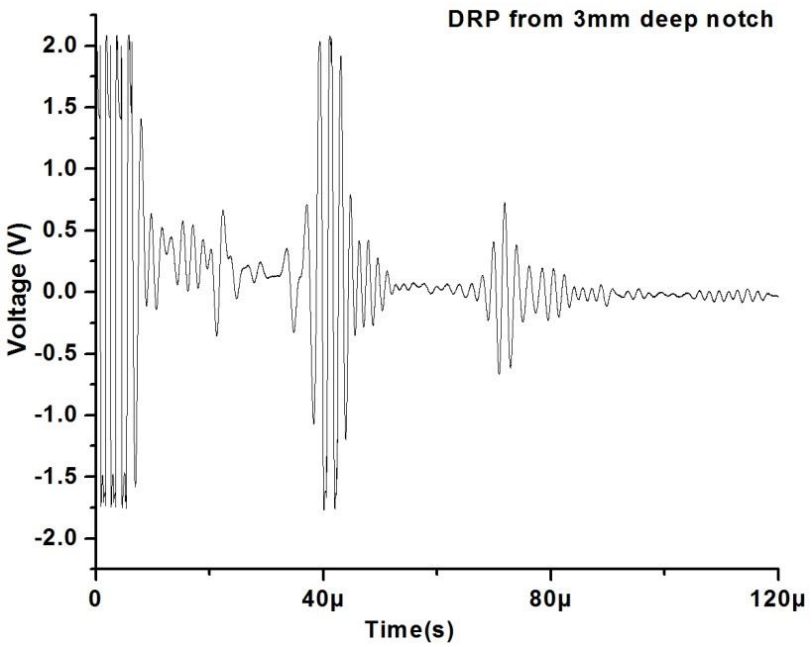

(c)

Figure 5.15: PE signatures showing variation in DRP for varying depths of notches

5.3.4 Defect Maps

For generating the defect map, peak-peak voltage amplitudes for PE signatures are tabulated in the form of a matrix M given as

$$M = [C_{ij}]$$

where i = (1, 2, 3 ……. x) and j = (1, 2, 3 ……. y) where x and y are the number of PT and PE locations considered for scanning.

Size of the defect map matrix (M) depends on the number of incremental positions in PT scanning along X-direction and PE scanning along Y-direction. **Figure 5.16a** shows the schematic layout of the actual plate specimen discretized into columns and rows. PT scan is carried out in 50 steps with an increment of 10 mm each, thus making 50 columns of matrix (**M**). Similarly PE scan has been divided in 100 steps with an increment of 2 mm each, thus making 100 rows of matrix **M**. Matrix M is initialized with averaged V_p amplitudes for PE signatures recorded at random healthy locations.

During PE scanning of the plate, wherever V_p amplitude surges, thus indicating the presence of notch, positional data from DRO along with corresponding PE signature is recorded. A code ***D-Expert*** has been developed that quickly extracts V_p values of first

reflection peak from a given PE signature and updates matrix M with the extracted V_p values and the corresponding coordinates. Updated matrix M is represented as a *contour surface plot*, and is termed as *defect map*. Hence the presence, spread (i.e. position and size) and magnitude (i.e. depth) of the notch in the plate is characterized and indicated very well by the present methodology. Defects in the form of notches with varying depths are represented in the color plots levels on the defect map (**Figure 5.16b)**. The defect map closely matches with the actual photographic image of the plate specimen (**Figure 5.16c).** The photographic image although represents the spread and location of the defect, but it does not clearly show the depth of the notch. However, the defect map generated in this study clearly depicts location, spread and depth of the defects present on the plate.

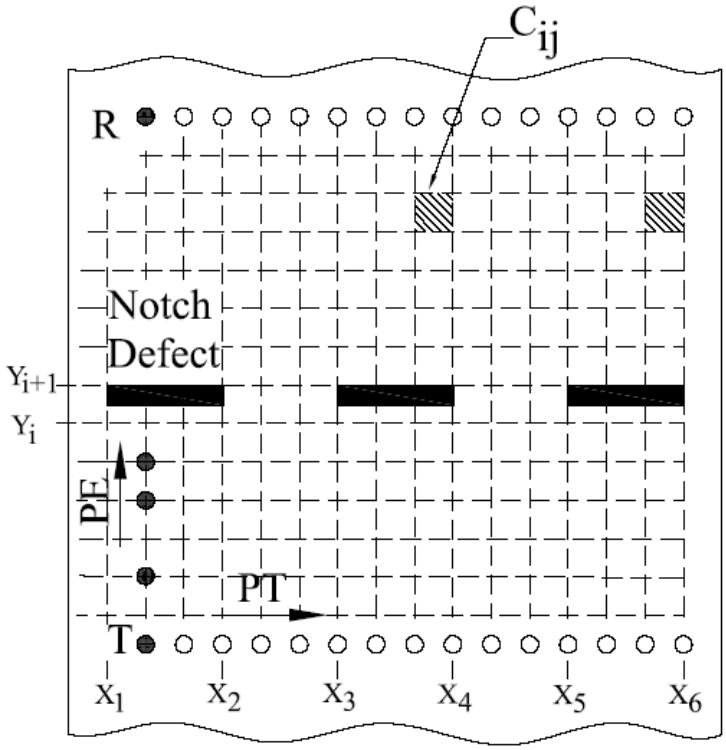

(a) Discretized Schematic layout of the Plate

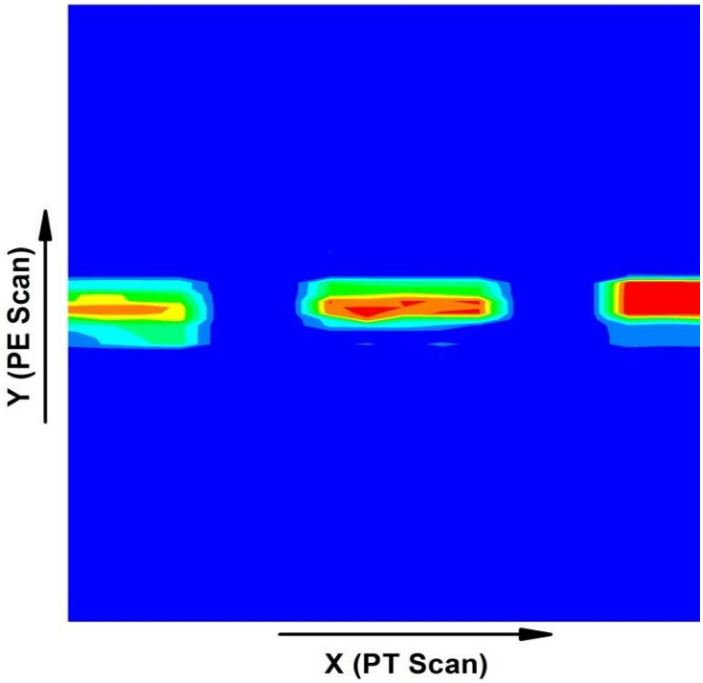

(b) Defect Map for notched plate

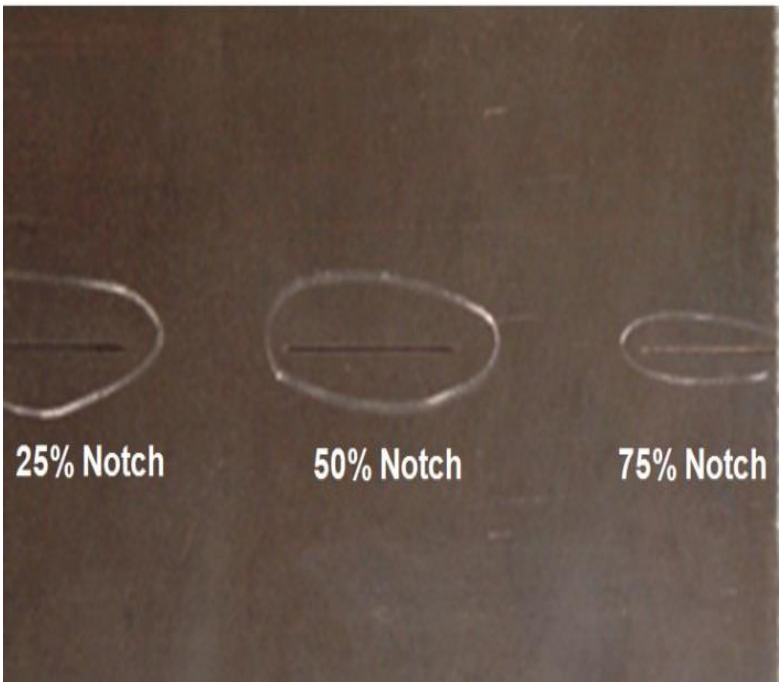

(c) Actual Plate with seeded notch defects of varying depths

Figure 5.16: PE scanning of a plate with multiple notches of varying depths

5.3.5 Plate with multiple notches

Presence of multiple notches within the investigation span of the probes can also be detected by the suggested methodology. PT scanning identifies the defect ridden zones in the plate followed by PE scanning to generate the defect map. During the PE scan, the coordinates and corresponding signatures are recorded whenever the surges in V_p are observed indicating the presence of defect. This data is plotted in the form of defect map.

Figure 5.17a shows the schematic of an actual plate **(Figure 5.17 b)** having two notches of 1mm and 2mm depth milled on it. During the PT scan (along X-direction) carried out on the marked locations using the selected Lamb wave modes, fall in V_n (**Figure 5.17 c, d)** suggested the presence of defect. Subsequently, PE scans (Y-direction) has been carried out to generate the defect map (**Figure 5.17 e**) which clearly brings out pictorial representation of the defects on the plate.

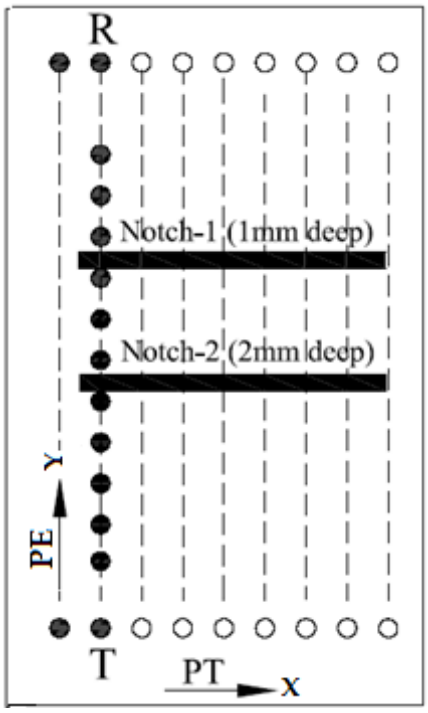

(a) Schematic

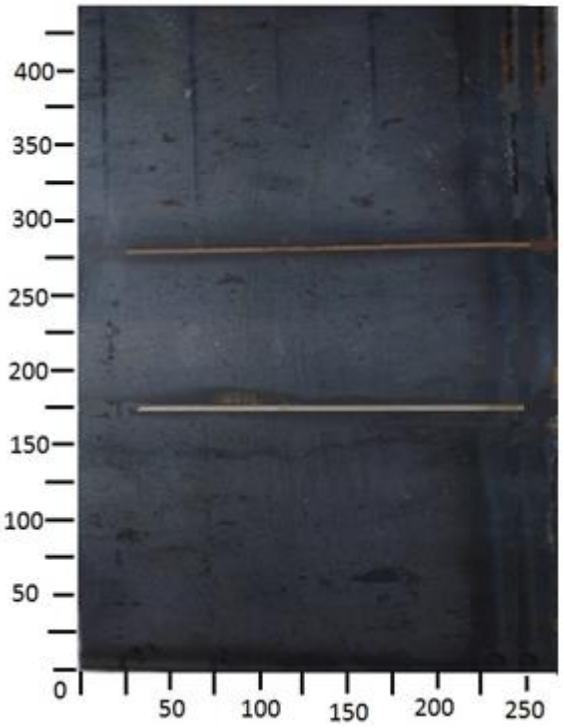

(b) Actual plate

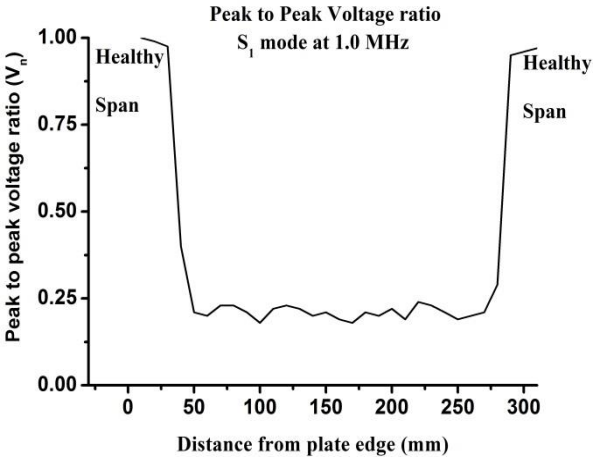

(c) PT scan using surface sensitive mode

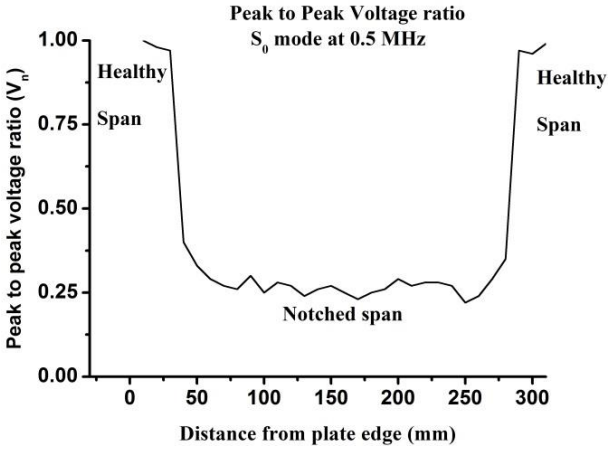

(d) PT scan using core sensitive mode

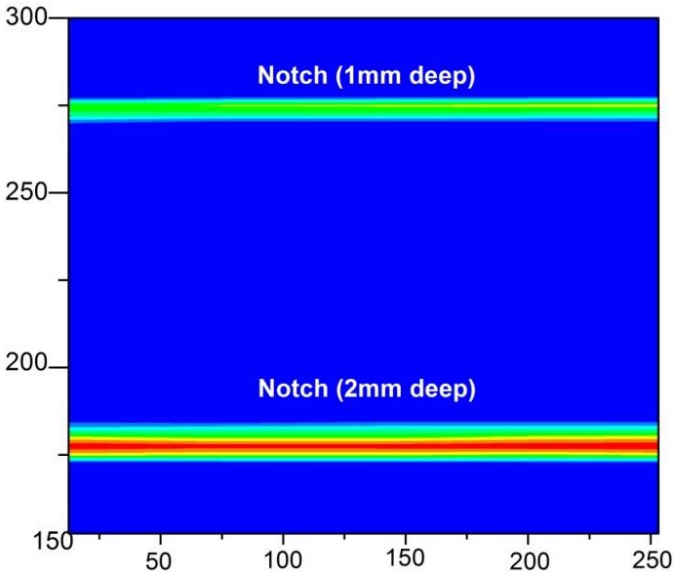

(e) Defect map

Figure 5.17: PE scanning of a plate with twin notches

5.4 CLOSING REMARKS

This chapter discusses a non-contact and in-situ damage monitoring methodology in the form of simulated notch defects in submerged plates using ultrasonic guided waves. The application of ultrasonic guided waves for detecting, localizing and quantifying defects in submerged plates is investigated. Pair of mobile immersion transducers is used to collect the information about the health of the submerged plate and yield defect maps while it is in service.

Surface sensitive and core sensitive Lamb wave modes are identified. These modes are further used for non-contact scanning of the plates in pitch catch configuration to identify, locate and quantify the extent of damage. Pulse transmission scanning of the specimen helps in identifying the problem areas in the plate due to the damage. Attenuation of the transmitted signal could relate to the extent of the damage in the form of notch. The defect reflection peaks obtained in pulse echo indicated the exact position of the notch. Post processing of the information generated from pulse echo scanning of the plate is pictorially represented in the form of defect maps. The methodology is successfully applied to plates with single as well as with multiple notches and corresponding defect maps clearly highlight the defect terrain on the specimen.

CHAPTER 6

PLATES UNDERGOING ACCELERATED CORROSION

6.1 INTRODUCTION

Most of the marine infrastructure is exposed to extreme conditions that are highly conducive to corrosion. If material wastage in the form of corrosion goes unnoticed it may result into massive loss to human life and property. Due preventive measures are also effective if corrosion damage is detected in early stages of inception. A variety of corrosion detection techniques are commercially available, but they have associated limitations like high downtime cost, sophisticated and costlier infrastructure, need of higher degree of operator skill. Hence, there is a need for developing an in service, real time corrosion monitoring and wastage assessment technique for marine structures.

In the preceding Chapter 5, the methodology is developed for damage monitoring in submerged plates inflicted with machined notches. The efficacy of different Lamb wave modes in monitoring notches of different depths in immersed plates was demonstrated using a combination of pulse transmission and pulse echo techniques. The present chapter explores the application of this methodology for corrosion monitoring in plates undergoing actual accelerated corrosion. Proposed methodology also attempts to predict the residual life of the corroding infrastructural component.

6.2 COMMON CORROSION TYPES IN MARINE ENVIRONMENTS

Marine structures generally experience uniform or general corrosion and pitting corrosion besides many other types of corrosion like galvanic corrosion, crevice corrosion, in limited extents (**Titcomb, 1982**). Marine environments cause corrosion on metal surfaces exposed for extended periods of time. Uniform or general corrosion usually occurs in stagnant or low flow seawater at a rate of approximately 5 – 10 microns per year on mild and low-alloy steels. The corrosion product appears as non-protective rust which can also occur on uncoated internal surfaces of a ship. The rust generally has a constant thickness and similar consistency over the surface.

Another form of corrosion prevalent in marine structures is pitting. It is a localized form of corrosion that leads to the creation of small holes in the metal. It is self-generating, i.e. autocatalytic, starting from irregularities in the metal surface, under scale or other

deposits, or from some in-homogeneities in the metal. This kind of corrosion is extremely insidious, as it causes little loss of material with small effect on its surface, while it damages the deep structures of the metal leading to catastrophic failures. The pits on the surface are often obscured by corrosion products. An ultrasonic technique developed for detecting shallow and deep notches in submerged plates is demonstrated in Chapter 5. This chapter extends the concept to detect corrosion in submerged structures.

6.3 GUIDED WAVE MODES FOR CORROSION MONITORING

The experimental study involves development of ultrasonic guided wave methodology for monitoring corrosion in mild steel plates of 4mm thickness. Similar set-up as used for damage detection in plates with machined notches is used **(Figure 4.2).** Two pairs of probes with rated central frequencies of 0.5 MHz and 1.0 MHz will be used for monitoring corrosion. In Chapter 5, efficacy of using the specific guided wave modes of S_0 at 0.5 MHz and S_1 at 1 MHz for detecting notches in submerged plates has been demonstrated. It has been established that each Lamb wave mode interacts uniquely with the notch defects. S_0 mode at 0.5 MHz is relatively insensitive to the shallow notches and is better suited for detecting deeper notches that reach close to the mid plane of the plate. On the other hand, S_1 mode at 1 MHz is highly sensitive to surface modifications as in case of shallow notches but is relatively insensitive to deeper defects. Hence, by judicious selection of the two modes, both surface and sub-surface notches in submerged plates could be easily discerned.

Mode shape of S_1 mode at 1 MHz indicates significant displacement and energy distribution near the surface as compared to the core of the plate. Hence, it should be more sensitive to shallow surface corrosion and is named as the *surface sensitive mode*. Similarly, the behaviour of S_0 mode at 0.5 MHz should be sensitive to deep pitting corrosion due to its wave structure that has more energy concentrated at the mid plane of the plate. Such a mode is referred to as *core sensitive* mode**.** In this work, **t**he S_0 and S_1 modes are investigated for their suitability for detecting surface and pitting corrosion in submerged plates.

To develop a corrosion monitoring strategy in submerged plates, scanning of the healthy plate in pulse transmission mode (PT) at selected modes is done to obtain the baseline signatures. Then the ultrasonic signatures of the plates undergoing accelerated corrosion are recorded. Comparison of the PT signatures vis-à-vis healthy plate helps to identify as well as quantify the extent of corrosion in the plate.

6.4 ACCELERATED CORROSION STUDIES

As indicated earlier, the general corrosion in plates remains on the surface while pitting tends to go deeper into the plate. The phenomenon of interaction of S_0 and S_1 modes differently with shallow and deep notches opens up a possibility of discerning the two types of corrosion by applying the two modes. This section explores the suitability of guided wave monitoring in a steel plate undergoing accelerated corrosion in chloride environment. Plates have been subjected to accelerated corrosion and monitored by the present technique utilizing selected Lamb wave modes.

6.4.1 Experimental Details

In natural environments, corrosion process takes several years to occur. Hence, the corrosion has been accelerated in this study by using the impressed current technique. Healthy mild steel plate specimen (600 mm x 250 mm x 4mm) in submerged state is scanned in PT using the selected surface and core sensitive modes at the marked locations. The initial mass of the plate is also recorded. The plate is then subjected to an impressed current corrosion. A bottomless acrylic tank with dimensions (200 mm x 40mm x 30 mm) is placed atop this steel plate for selective exposure of the specimen to corrosive environment. The tank is filled with 3.5% brine solution. A copper strip is dipped in the brine solution and is made cathode in the circuit while the plate acts as anode. A constant voltage of 30V was applied between the two terminals by means of a constant power supply device **(Figure 6.1)**. An external resistance (R) in series generated a current of 0.32 Amperes in the circuit.

After every 24 hours of exposure to accelerated chloride corrosion, the acrylic tank is dismantled. Ultrasonic scanning of the plate (in submerged condition) using both S_0 and S_1 modes is done to monitor the changes in the PT signatures. Mass of the plate is also recorded for ascertaining the mass loss due to corrosion after each day of exposure. After ultrasonic testing, the acrylic tank is again fixed on the plate and the accelerated corrosion process is continued. This procedure is repeated till the PT signal vanishes.

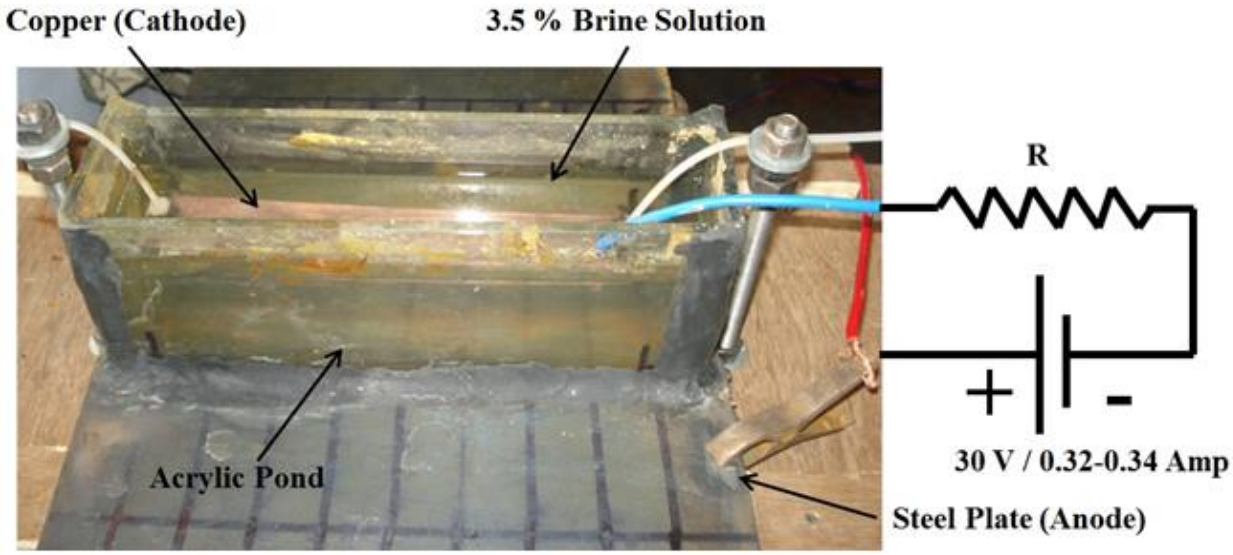

Figure 6.1: Accelerated Corrosion Set-Up

6.4.2 Results and Discussions

6.4.2.1 Visual Observations

Steel plates undergoing accelerated chloride corrosion showed blackish brown corrosion products floating in the acrylic tank within first 6 hours of exposure. The brine solution converted into a reddish brown liquid and was changed after every 12 hours in order to ensure consistent current level in the corrosion circuit. After 2 days of subjecting to accelerated corrosive environment, corrosion patches in the form of small pits were observed on the plate. The pits deepened and spread on the surface of the plate with increasing exposure. After 5 days, widespread corrosion areas were observed **(Figure 6.2a**).

A consistent loss in mass was observed after each day of corrosion. The process continued till 13 days and was stopped when pits gave way to two holes in the plate **(Figure 6.2b)**. At this stage, corrosion exposure could not be continued further as the brine solution leaked and the PT signals too almost vanished.

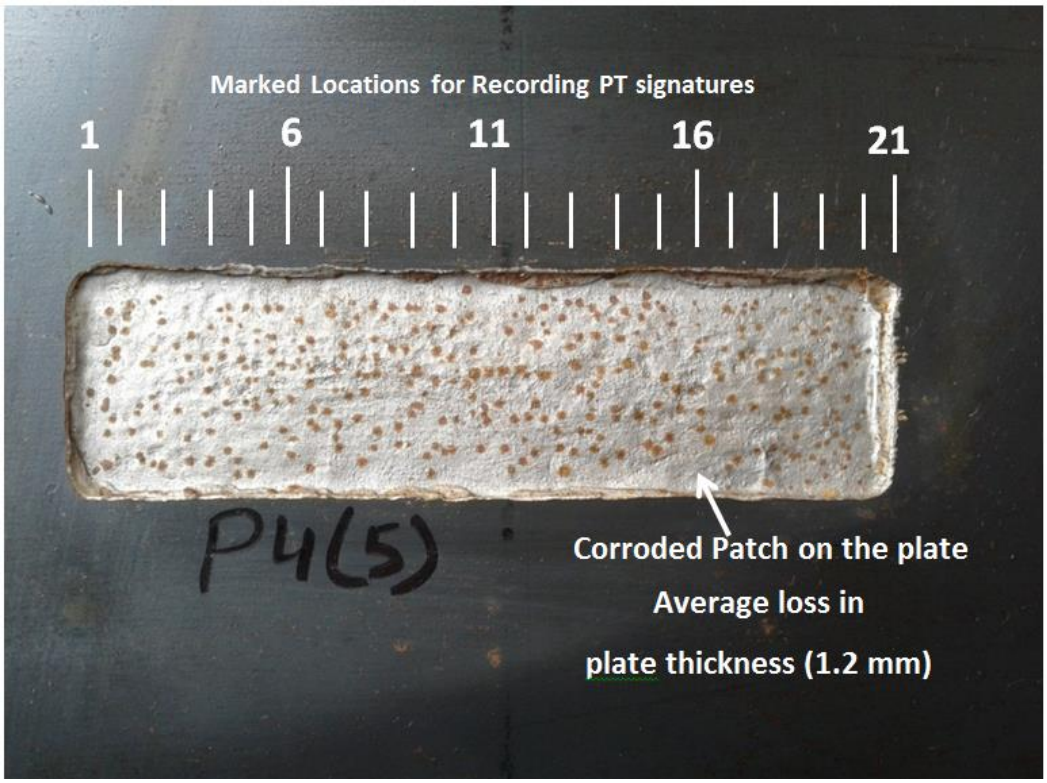

(a) 5 Days

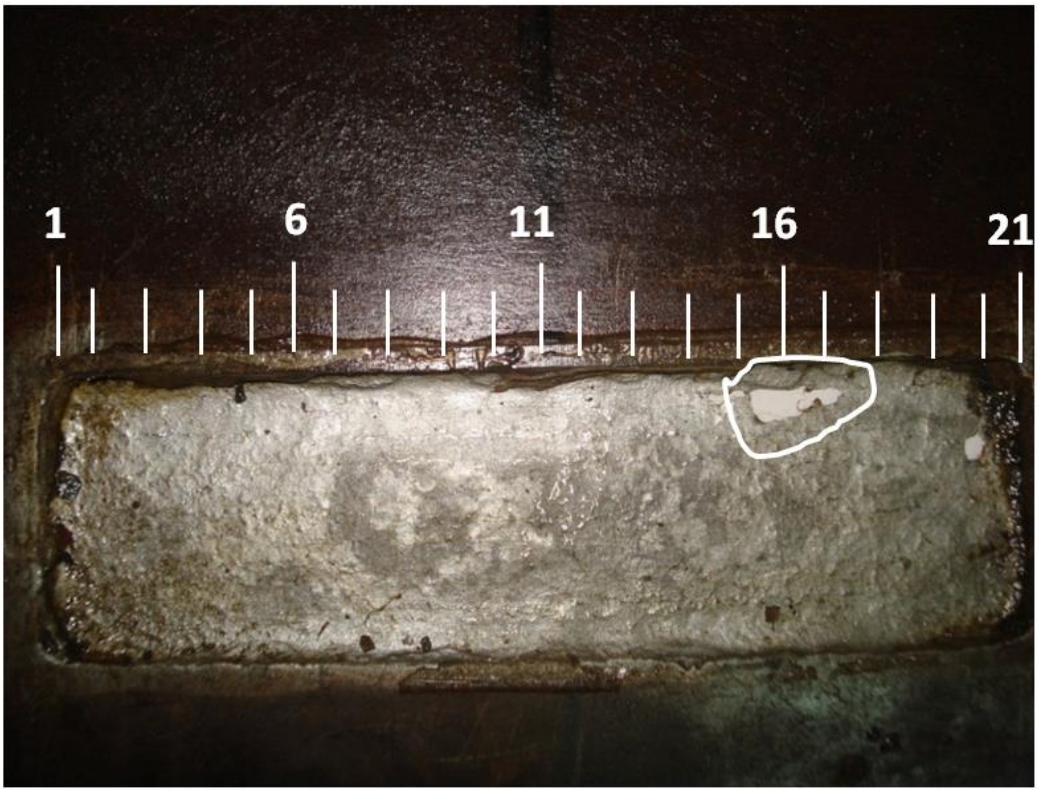

(b) 13 Days (Hole Formation)

Figure 6.2: Accelerated Corrosion in the plate

6.4.2.2 Monitoring with surface sensitive mode (S_1 mode at 1 MHz)

Ultrasonic PT signatures were recorded periodically at the marked locations on the plate using the surface sensitive S_1 mode at 1 MHz **(Figure 6.2a)** after every 24 hours of exposure**.** PT signatures for Location 16, where maximum material loss was observed due to corrosion are shown in **Figure 6.3.** Initially for the healthy plate, the signature is characterized by a strong pulse at all locations on the plate. With the onset of corrosion, changes are observed in PT signatures. Left peak representing fastest mode (S_1) at 1 MHz diminishes rapidly with the increasing exposure to corrosion. The decline in the signal amplitude is sharp in initial 6 days indicating its suitability to detect onset and initial phase of surface corrosion effectively. Further from 7-13 days, the signal drop is not very significant.

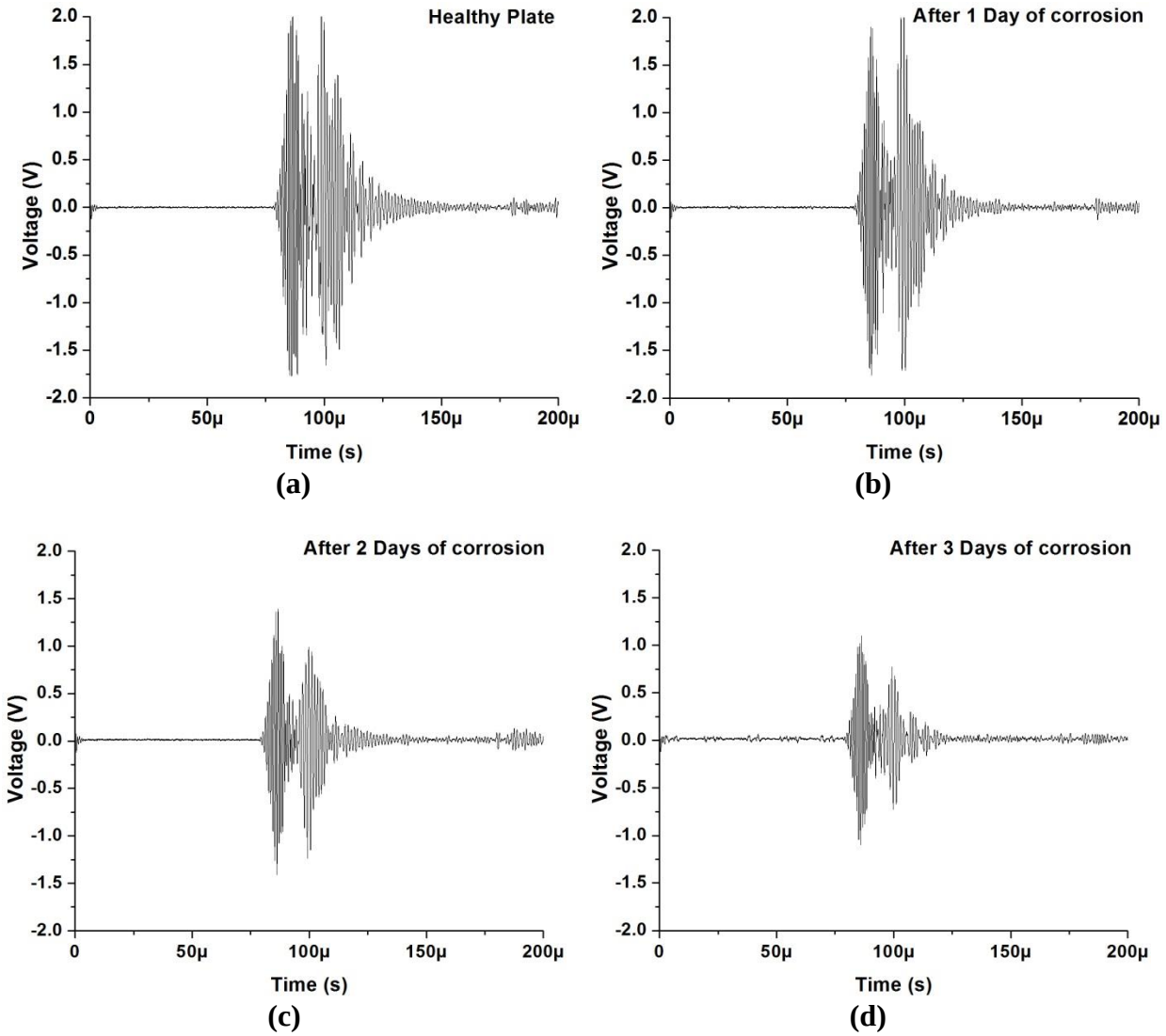

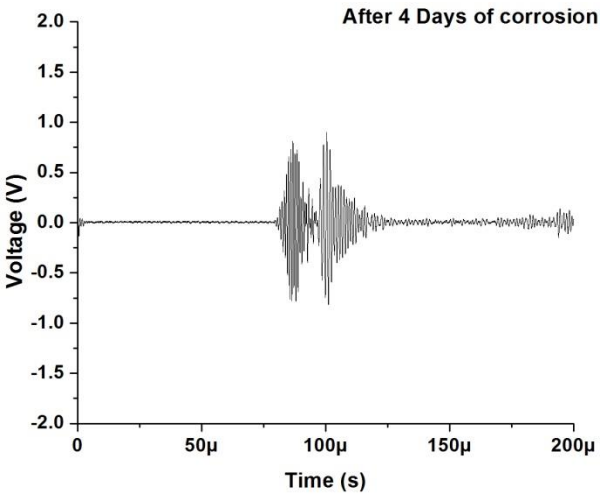
After 4 Days of corrosion
Voltage (V)
Time (s)
2.0
1.5
1.0
0.5
0.0
-0.5
-1.0
-1.5
-2.0
0
50µ
100µ
150µ
200µ

(e)

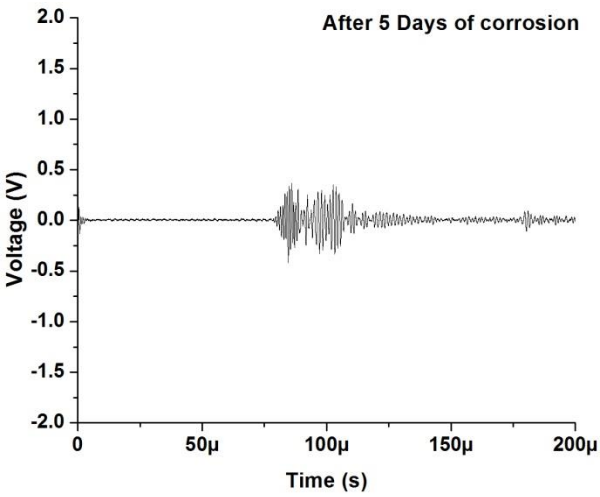
After 5 Days of corrosion
Voltage (V)
Time (s)
2.0
1.5
1.0
0.5
0.0
-0.5
-1.0
-1.5
-2.0
0
50µ
100µ
150µ
200µ

(f)

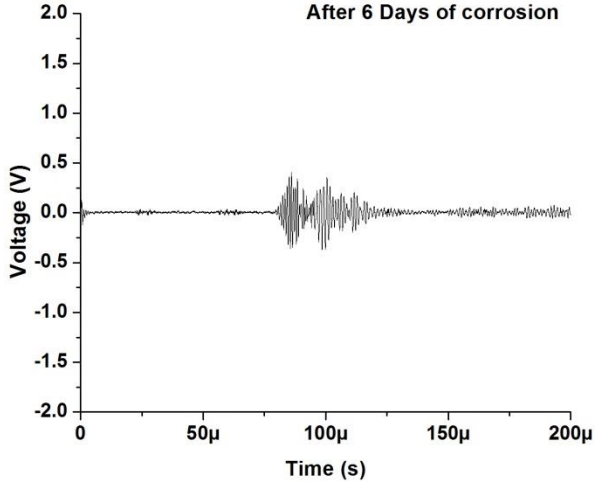
After 6 Days of corrosion
Voltage (V)
Time (s)
2.0
1.5
1.0
0.5
0.0
-0.5
-1.0
-1.5
-2.0
0
50µ
100µ
150µ
200µ

(g)

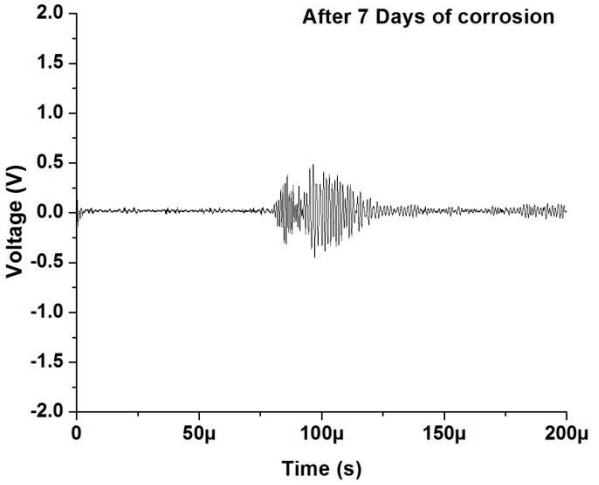
After 7 Days of corrosion
Voltage (V)
Time (s)
2.0
1.5
1.0
0.5
0.0
-0.5
-1.0
-1.5
-2.0
0
50µ
100µ
150µ
200µ

(h)

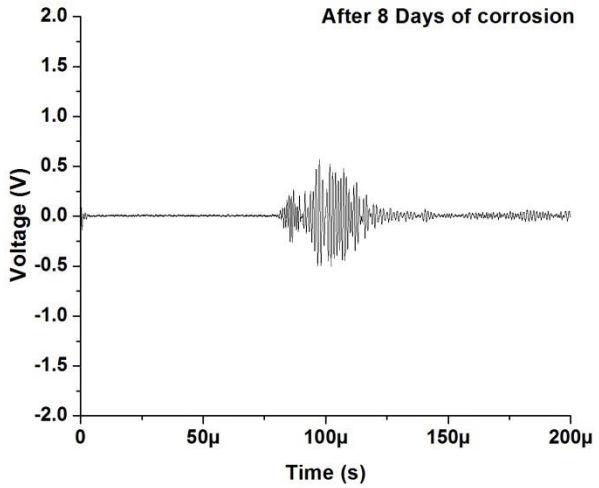
After 8 Days of corrosion
Voltage (V)
Time (s)
2.0
1.5
1.0
0.5
0.0
-0.5
-1.0
-1.5
-2.0
0
50µ
100µ
150µ
200µ

(i)

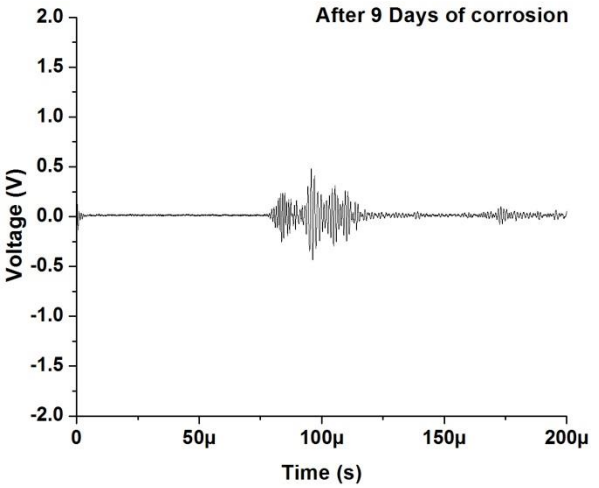
After 9 Days of corrosion
Voltage (V)
Time (s)
2.0
1.5
1.0
0.5
0.0
-0.5
-1.0
-1.5
-2.0
0
50µ
100µ
150µ
200µ

(j)

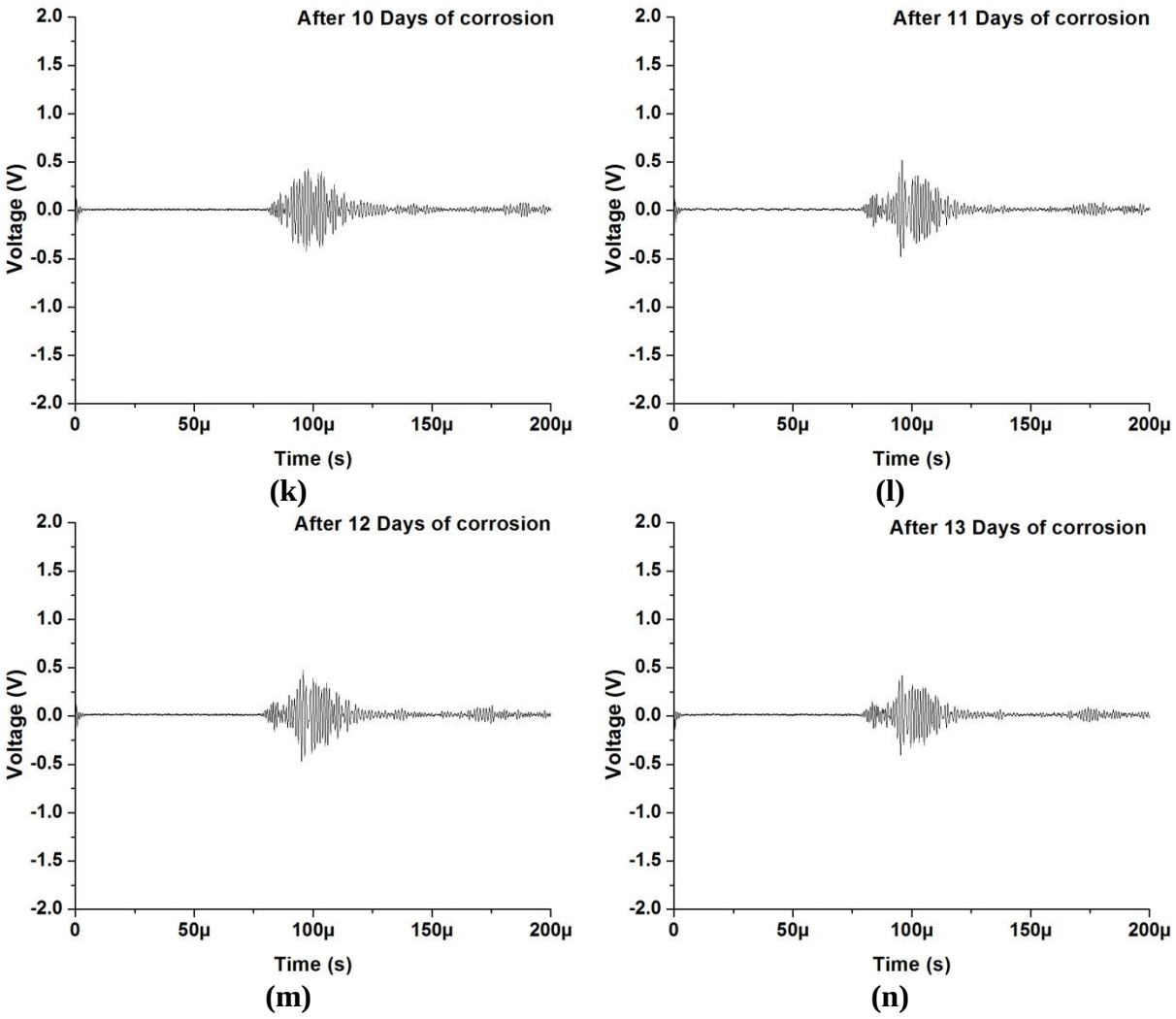

Figure 6.3: PT signatures using core sensitive mode at Location 16 in plate undergoing accelerated corrosion

The received peak to peak voltage amplitude of the transmitted pulse in the corroded plate is normalized with respect to the corresponding peak to peak voltage in the healthy plate and is refered to as V_n. Through V_n it is possible to compare different modes on the same scale.

Figure 6.4 shows V_n at various locations on the plate using the surface sensitive mode with increasing days of corrosion. The transmitted signal attenuates with increasing exposure to corrosive environment indicating material loss due to corrosion. Maximum drop in voltage amplitude is observed at locations marked 15-17 on the plate. It suggests significant localized corrosion in these regions leading to formation of holes after 13 days of corrosion **(Figure 6.2b)**.

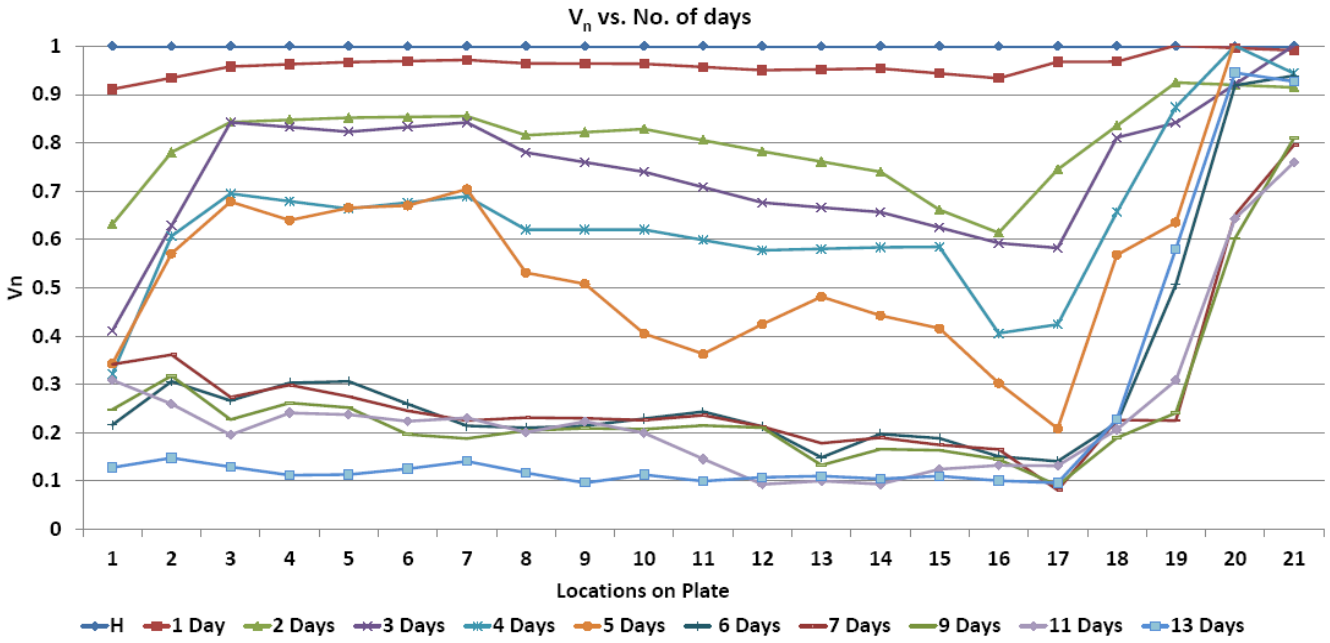

Figure 6.4: PT results (V_n) using surface sensitive S_1 mode at 1 MHz at all locations of plate with increasing exposure

The behavior of this mode can be explained by the mechanism of corrosion in the presence of chlorides. Corrosion in the presence of chlorides is characterized by pitting and localized loss of material. Due to non-uniform loss of material from the plate surface, the smooth waveguide in the healthy plate is disturbed resulting in scattering of the wave and hence, attenuation of the transmitted signal. Another observation is that the signal drops significantly only in first 6 days of corrosion. It drops to 20% of its original value in the first 6 days **(Figure 6.9**). As corrosion progresses (7-13 days), no significant attenuation in the signal is observed. This is due to the surface sensitive nature of the mode which picks up early surface modifications but is not responsive to deep pits with increasing exposure.

Comparison of actual corrosion with notches on the plate using this mode indicates a close match **(Figure 6.5)**. In notched specimens, with increase in the depth of the notch, drop in signal was observed up to 37.5% depth of the notch using the surface sensitive mode. But with further increase in depth of the notch, change in signal was relatively insignificant. Similar trends are observed with actual corrosion where the signal drops sharply during the first 6 days of corrosion, but subsequently this fall is not so prominent.

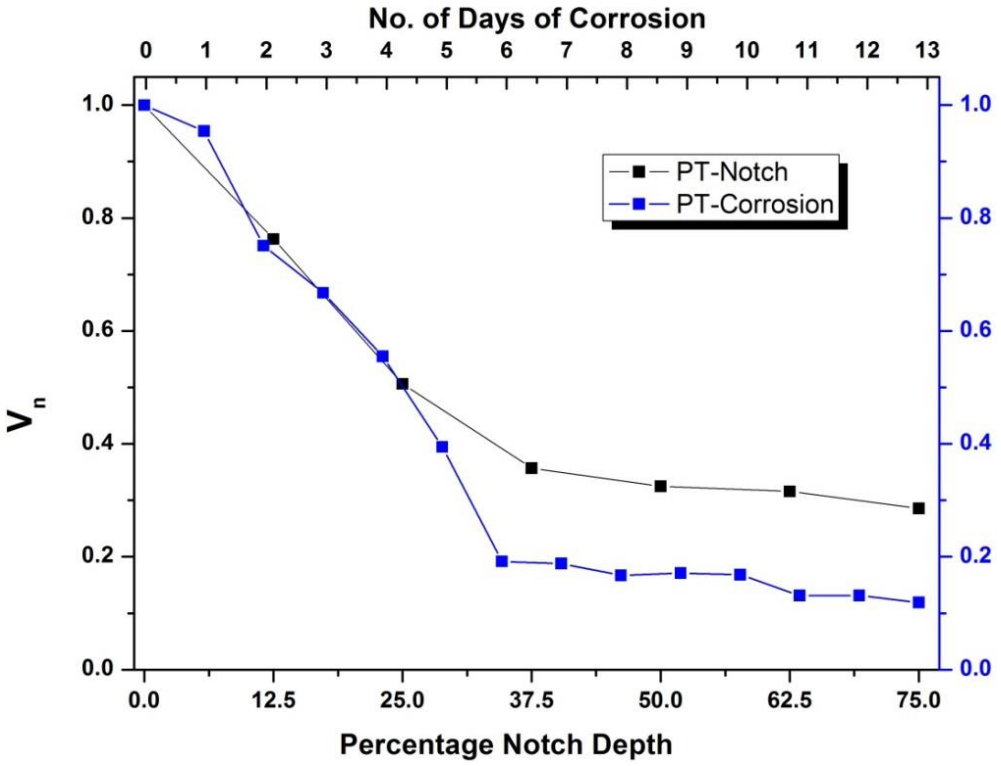

Figure 6.5: Comparison of Notch and Corrosion using surface sensitive S_1 mode

Hence, PT scanning of the submerged plate subjected to chloride corrosion with the surface sensitive mode is marked by rapid signal attenuation at the initial stages. To capture the complete corrosion process, combined effect on ultrasonic signal needs to be studied with both the surface and core sensitive modes.

6.4.2.3 Monitoring with core sensitive mode (S_0 at 0.5 MHz)

The PT signatures obtained using core sensitive mode at Location 16 of the plate are shown in **Figure 6.6** below.

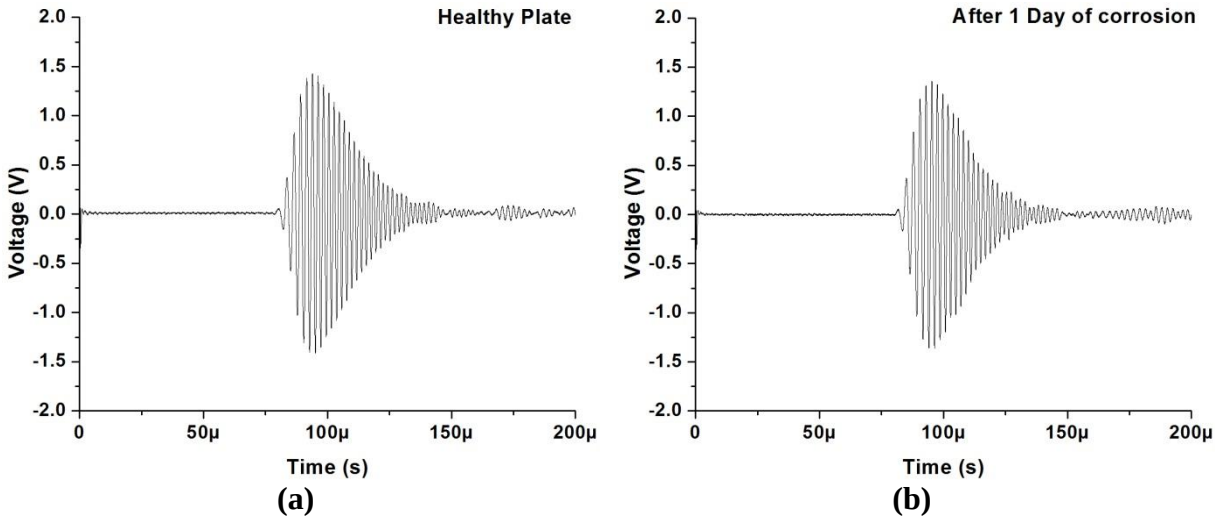

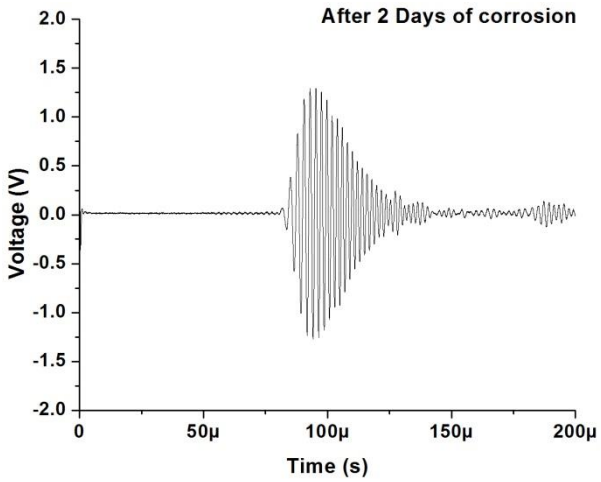
After 2 Days of corrosion
Voltage (V)
Time (s)
2.0
1.5
1.0
0.5
0.0
-0.5
-1.0
-1.5
-2.0
0
50µ
100µ
150µ
200µ

(c)

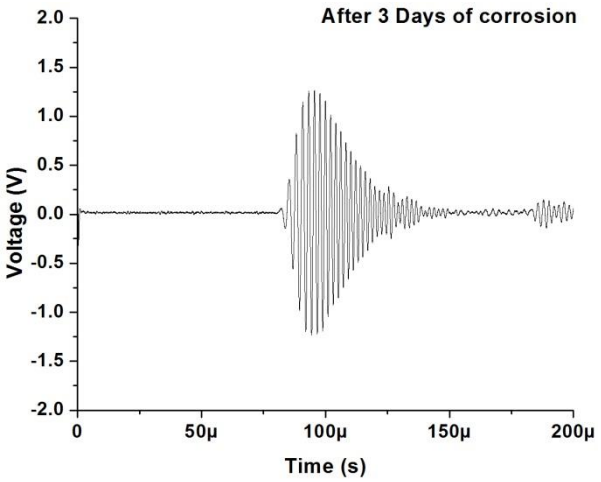
After 3 Days of corrosion
Voltage (V)
Time (s)
2.0
1.5
1.0
0.5
0.0
-0.5
-1.0
-1.5
-2.0
0
50µ
100µ
150µ
200µ

(d)

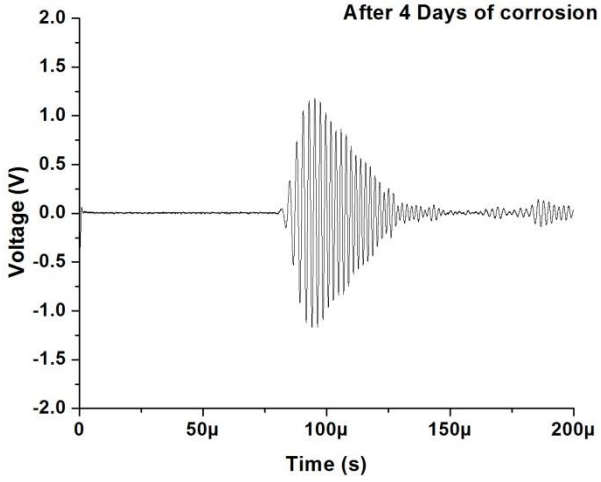
After 4 Days of corrosion
Voltage (V)
Time (s)
2.0
1.5
1.0
0.5
0.0
-0.5
-1.0
-1.5
-2.0
0
50µ
100µ
150µ
200µ

(e)

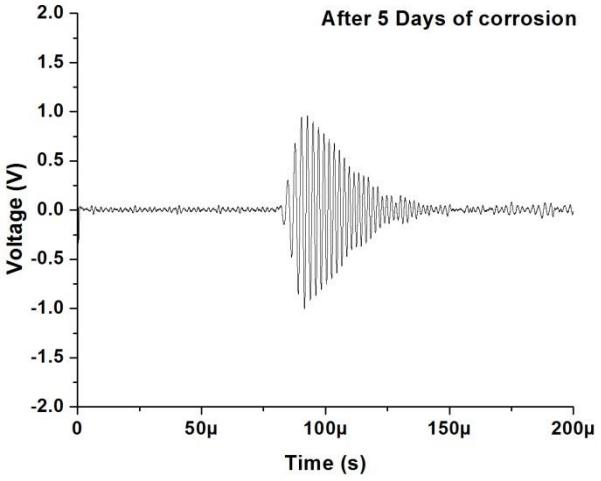
After 5 Days of corrosion
Voltage (V)
Time (s)
2.0
1.5
1.0
0.5
0.0
-0.5
-1.0
-1.5
-2.0
0
50µ
100µ
150µ
200µ

(f)

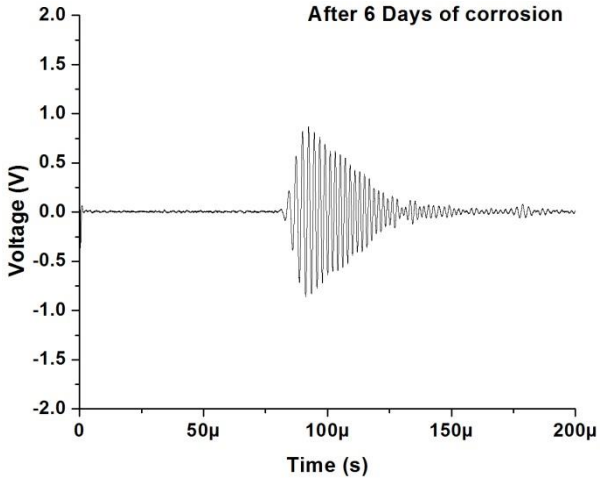
After 6 Days of corrosion
Voltage (V)
Time (s)
2.0
1.5
1.0
0.5
0.0
-0.5
-1.0
-1.5
-2.0
0
50µ
100µ
150µ
200µ

(g)

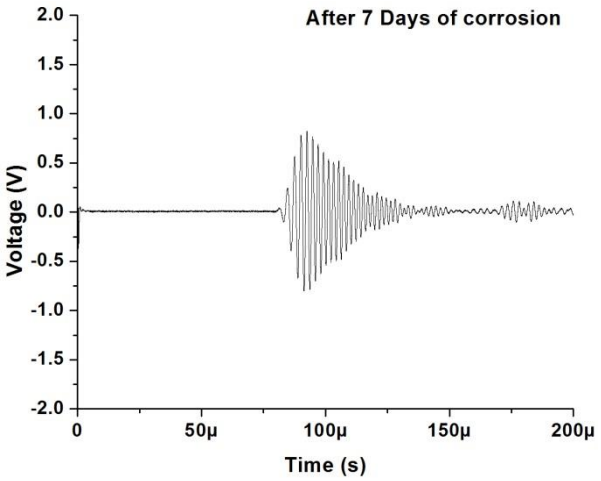
After 7 Days of corrosion
Voltage (V)
Time (s)
2.0
1.5
1.0
0.5
0.0
-0.5
-1.0
-1.5
-2.0
0
50µ
100µ
150µ
200µ

(h)

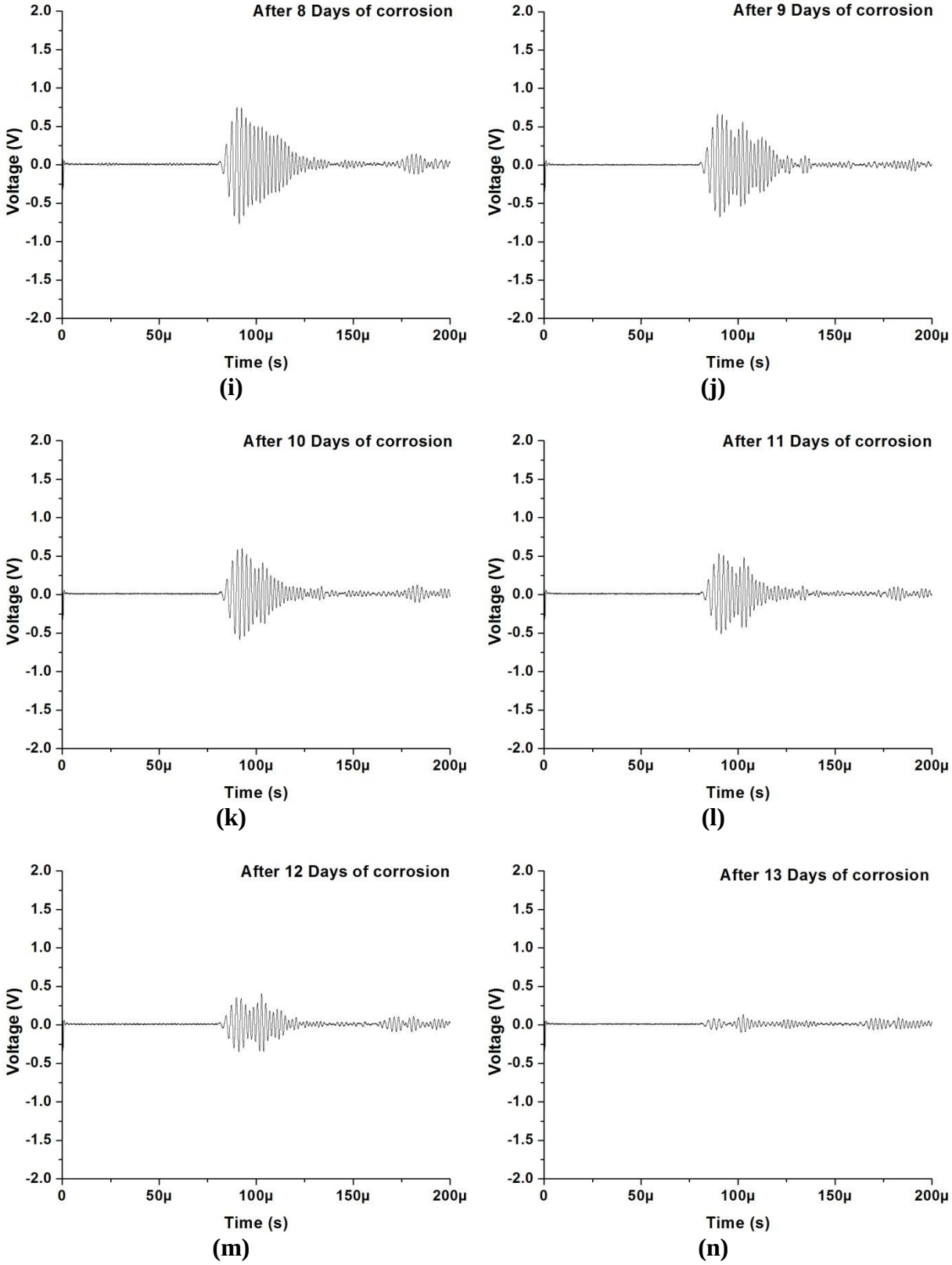

Figure 6.6: PT signatures using core sensitive mode at Location 16 in the plate undergoing accelerated corrosion

Figure 6.7 shows V_n values of the received signals using core sensitive S_0 mode at 0.5 MHz with progressive corrosion.

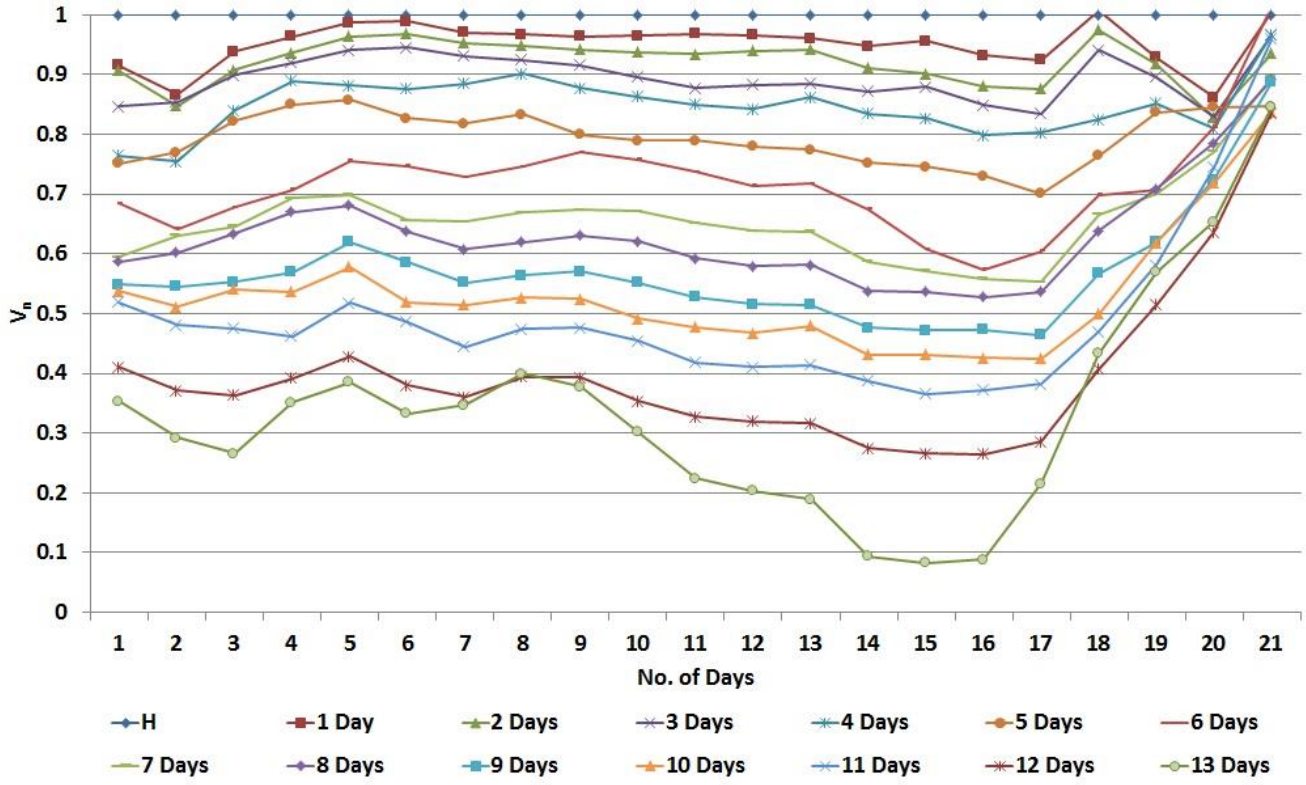

Figure 6.7: PT results (V_n) using core sensitive S_0 mode at 0.5 MHz at all locations of plate with increasing exposure

PT scanning of the plate using this mode exhibits relatively less changes in PT signatures **(Figure 6.6)** and the signal trends at all locations **(Figure 6.7)** during the initial 6 days in comparison to the surface sensitive S_1 mode. Drop in signal is only 40% using core sensitive mode as against 80% drop observed using surface sensitive mode during the initial 6 days **(Figure 6.9).** This mode does not sense surface deteriorations as effectively as S_1 mode does. As corrosion further progresses, consistent drop in voltage amplitude is observed with this mode throughout the corrosion period. This is due to the core sensitive nature of the mode. This mode picks and points towards massive non-uniform material loss in the form of pits. The widespread loss of material due to corrosion is also confirmed visually. As corrosion progresses, there is consistent increase in scattering and multiple reflections and it results in regular fall in received signal amplitude. Hence, it can be concluded that as the surface sensitive mode picks up the initial surface changes due to corrosion, the core sensitive mode is effective in picking up the progression of corrosion leading to pitting.

The behavior of core sensitive mode can be compared in cases of deep notches and pitting corrosion. The transmission of waves through the notched and in actually corroding plate had a close match **(Figure 6.8)**. In the notched specimens, drop in signal was observed with the increase in the depth of the notch (PT-notch). Similar trends are observed with corrosion studies where increase in exposure to corrosive environment also causes a continuous attenuation in PT-corrosion. Clearly, the results of notch specimens are in close agreement with the actual corrosion monitoring results taken with core sensitive mode S_0 at a frequency of 0.5 MHz throughout the period of corrosion. On the other hand, the surface sensitive mode is effective for monitoring onset of corrosion in the form of surface degradations quite like identifying shallow notches. Thus, surface corrosion and pitting corrosion can be discerned through the proposed method.

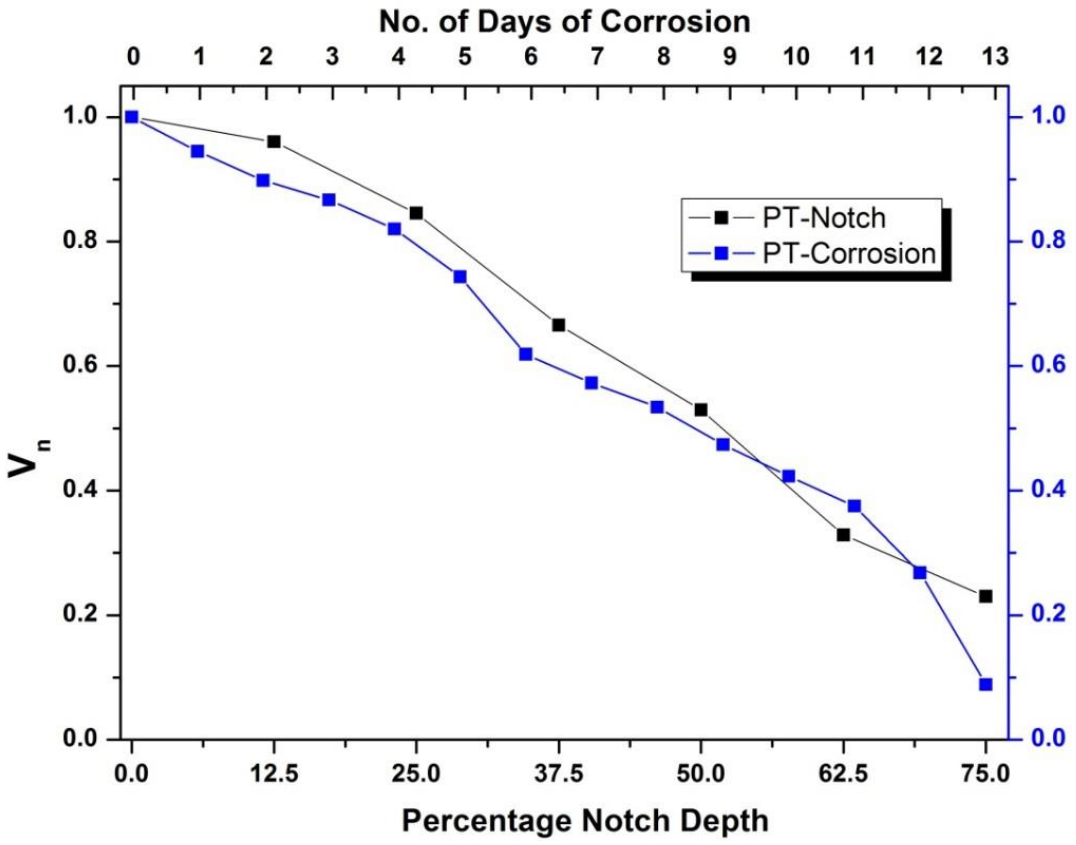

Figure 6.8: Comparison of Notch and Corrosion using core sensitive S_0 mode at 0.5 MHz

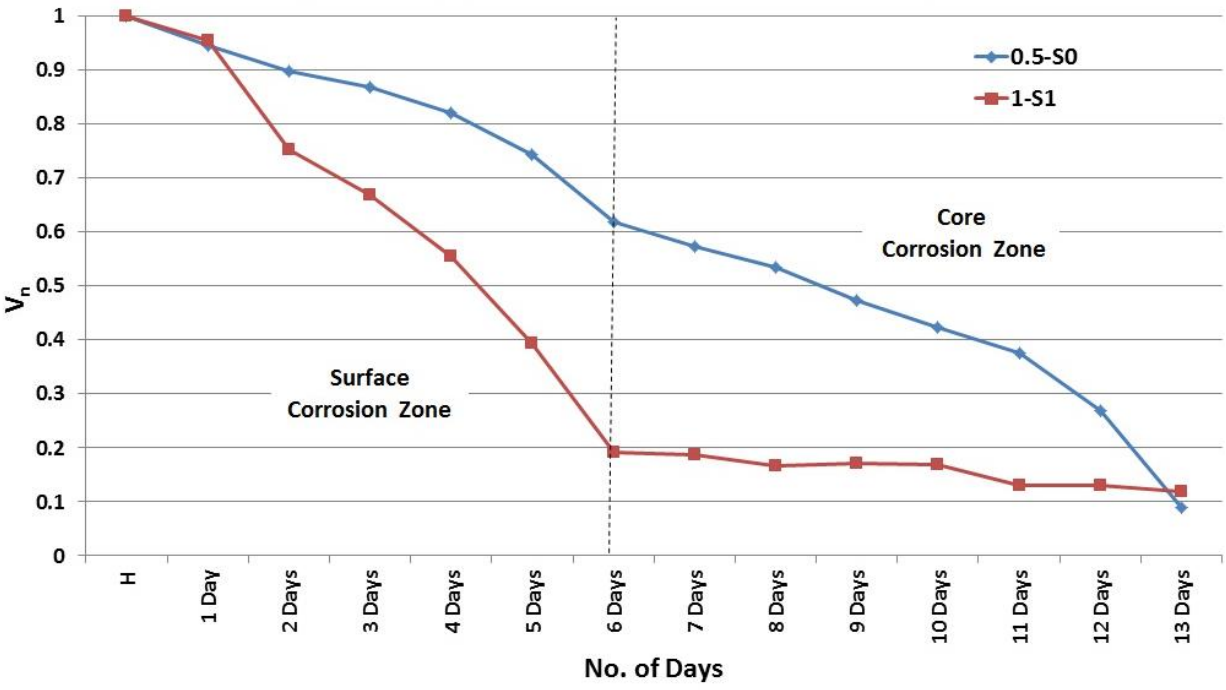

Figure 6.9: Trend of V_n with increasing exposure to corrosion

6.4.2.4 Corrosion Mechanism using Guided Waves

From the study of ultrasonic signal plots with surface and core sensitive modes, two distinct zones were observed (**Figure 6.9**):

- First six days had a rapidly falling PT signal using S_1 mode as compared to relatively lesser sensitive S_0 signal, indicating predominant surface changes taking place due to onset of corrosion but inappreciable core changes. This zone is referred as '*Surface corrosion zone*'.
- From seven to thirteen days, S_1 signal showed very sluggish changes with increasing exposure to chloride environment as against S_0 signal which dropped significantly. This indicates that the corrosion makes inroads deeper in the plate and it was not restricted to the surface only. This zone is referred as '*Core Corrosion Zone*'.

6.5 DESTRUCTIVE TESTS

6.5.1 Test Program

A destructive test program was developed for accelerated corrosion of different durations to facilitate a possible calibration of the ultrasonic signals with different ages and stages of corrosion. Mass loss and tensile strength of the plate were measured. Five steel plate

samples (600 mm x 250 mm x 4mm) were subjected to ultrasonic PT testing in submerged state in order to establish the baseline signature corresponding to the healthy state. Also the initial mass of these samples was recorded. Subsequently, these samples were exposed to accelerated corrosion of varying durations of 3, 5, 7, 10 and 13 days respectively. Parameters like current settings, brine solution concentration etc. were maintained constant for all samples undergoing accelerated corrosion. All plate samples were investigated using the selected modes after every 24 hours of accelerated corrosion. The experiment also allowed examination of repeatability of the proposed ultrasonic method.

Figure 6.10 and Figure 6.11 shows the variation in ultrasonic voltages at different days of corrosion using the surface and core sensitive modes respectively at a particular location. The trends of peak to peak voltage ratios were found to be the same in all the plate samples at different extents of corrosion using the surface sensitive mode (**Figure 6.10**). There is a rapid drop in signal strength in all corrosion samples with the surface sensitive mode up to 6 days of corrosion. It points towards the onset of corrosion with significant surface modification. The relatively insignificant drop in signal amplitudes beyond this point confirms the start of pitting phenomenon where the surface sensitive mode is less effective. All the samples show consistency in results and hence, ensure the repeatability in the methodology. The S_0 mode at 0.5 MHz that is more sensitive to profile changes in the plate also indicated repeatable trends for plate samples exposed to 3, 5, 7, 10 and 13 days of corrosion **(Figure 6.11)**. All samples exhibited drop in ultrasonic voltages with increasing exposure to chlorides.

6.5.2 Destructive Testing and Correlation with Ultrasonic Voltages

Mass loss in plates undergoing corrosion at different ages was measured along with the stress-strain behavior and tensile strength after the period of exposure was completed. After the specified exposure period, acrylic tank is removed from the plate specimen. The plate is cleaned with wire brush and rinsed with acetone to remove all the corrosion products. It is then weighed to evaluate its residual mass. This procedure is adopted for all samples after every 24 hours of accelerated corrosion exposure. For tensile strength measurement, strips of 60mm width by 600mm length were cut from the corrosion patch on the plate (**Figure 6.12**). These strips were then tested in UTM to determine their average residual tensile strength after specified period of exposure to corrosion.

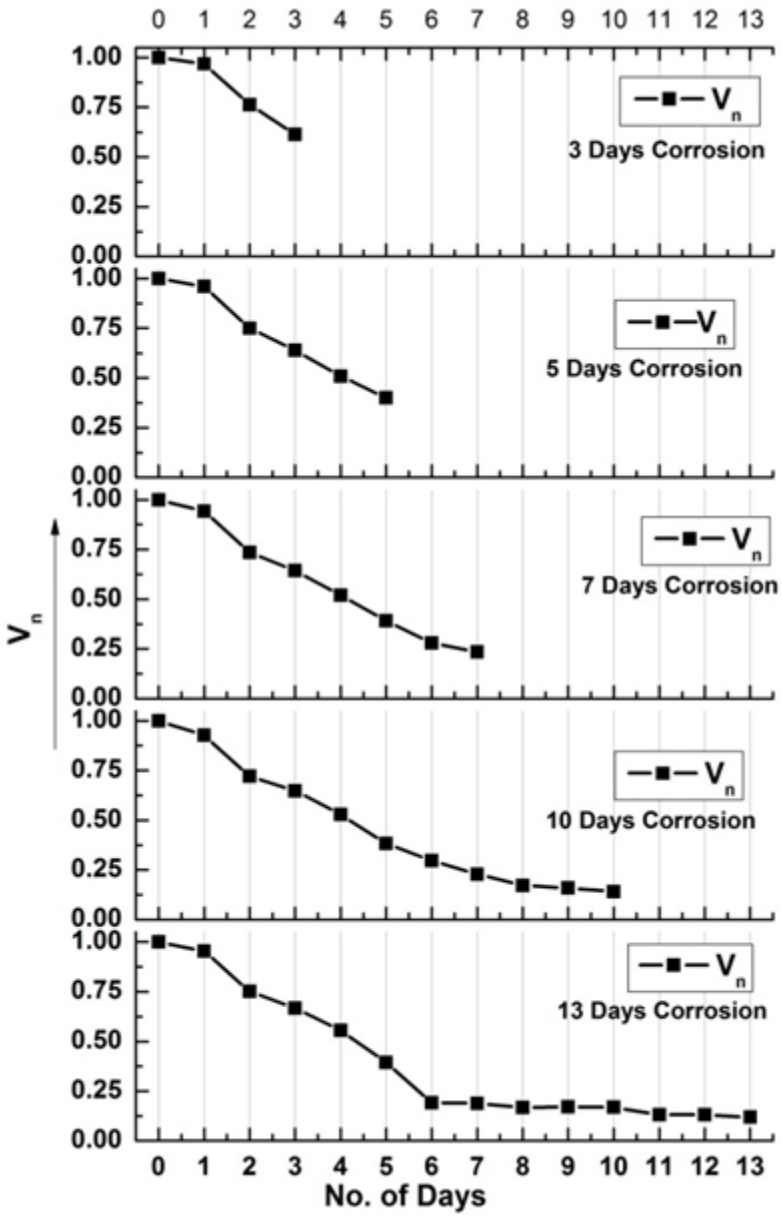

Figure 6.10: V_n for plates undergoing corrosion to different ages using S_1 mode at 1 MHz

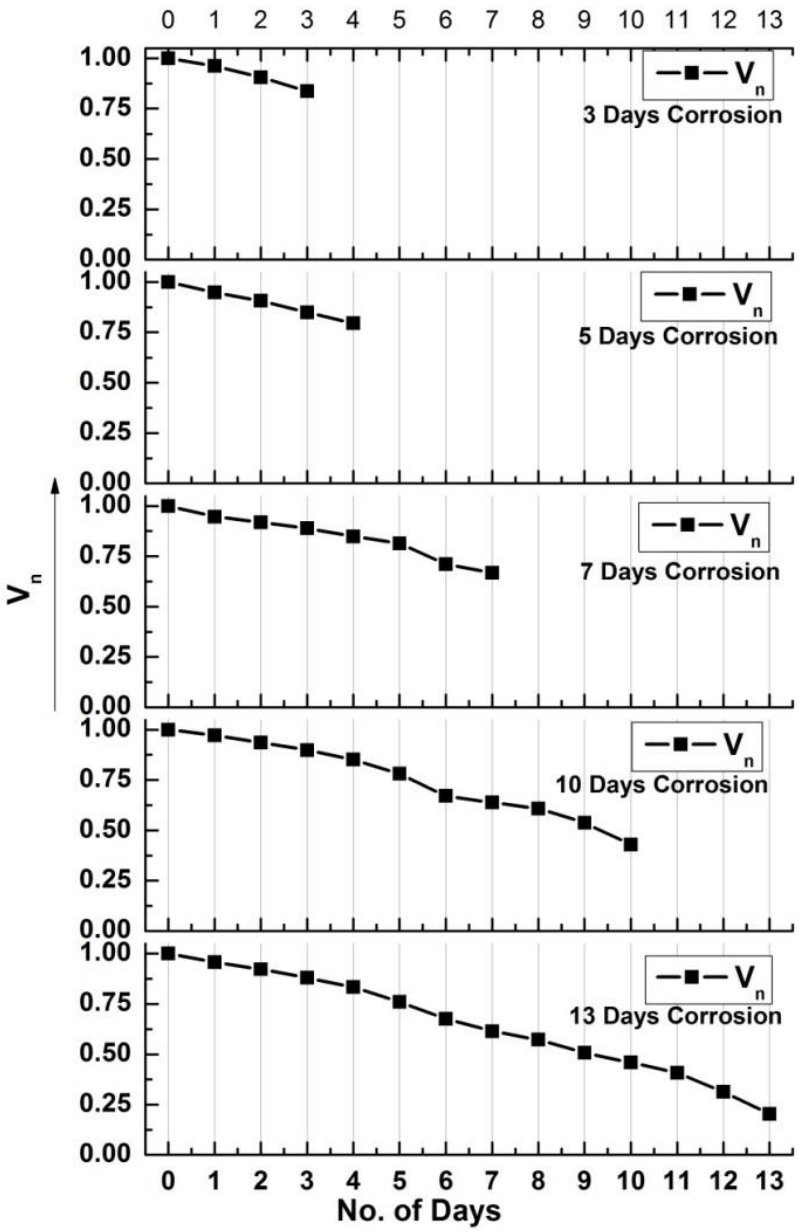

Figure 6.11: V_n for plates undergoing corrosion to different ages using S_0 mode at 0.5 MHz

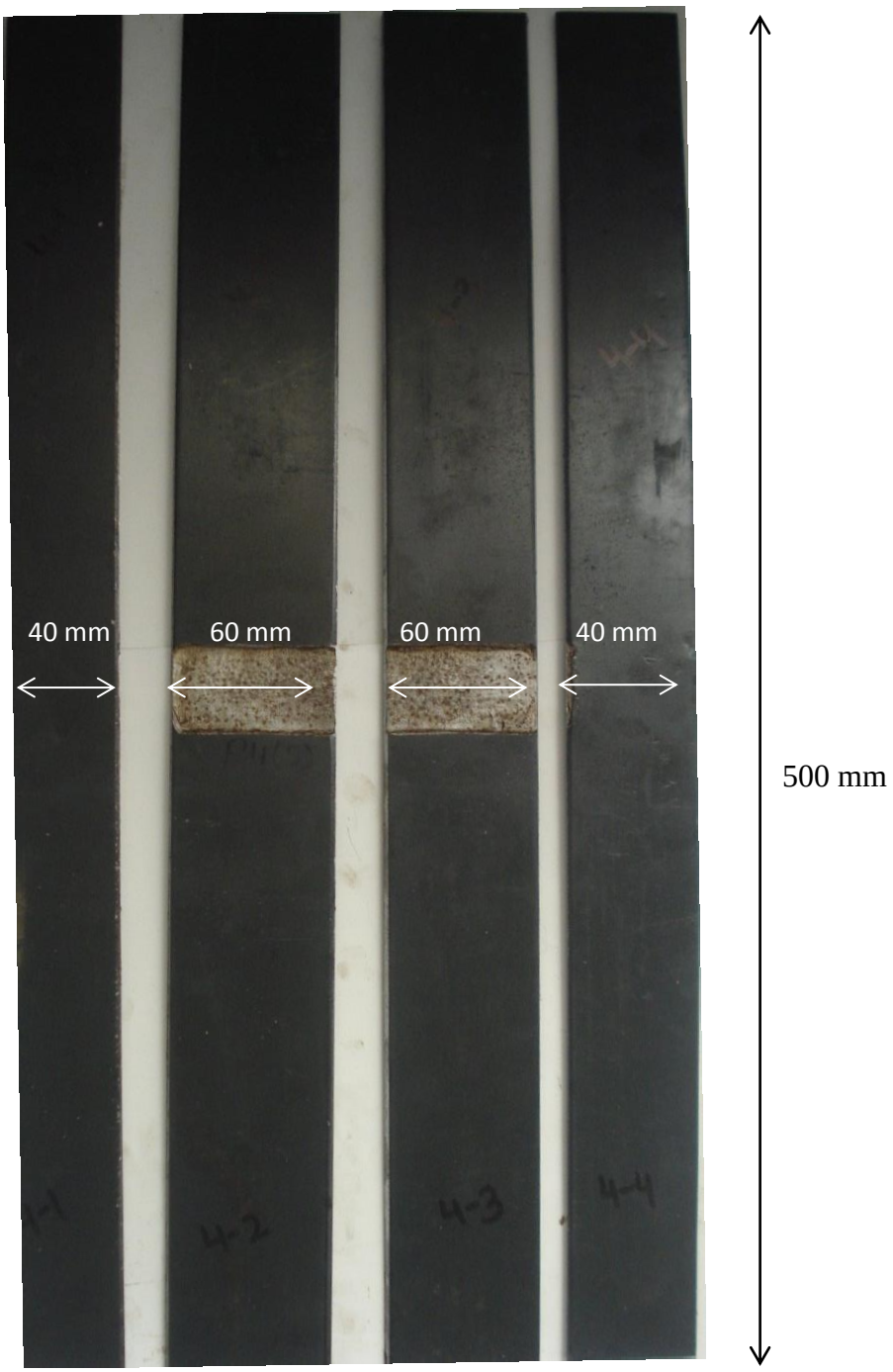

Figure 6.12 : Corroded plate specimen details for tensile testing

(a) Healthy

(b) 3 days

(c) 5 days

(d) 7 days

(e) 10 days

(f) 13 days

Figure 6.13 : Failed tensile test specimens at different ages of corrosion

Table 6.1 shows the variation in mass loss and tensile strength with increasing corrosion. After 13 days of corrosion, the plate had lost about 3% mass and about 90% of its thickness in comparison to the healthy plate. The observed loss in tensile strength after 13 days is 94.7%. High percentage loss in thickness and tensile strength is due to localized corrosion due to pitting caused by chlorides. The visual inspection also confirmed that the plate had experienced severe and widespread pitting in the exposed area. **Figure 6.13(a-f)** shows the failed plate specimens in tension at different ages of corrosion. With increasing corrosion exposure, failure mode of the plates changes from ductile to sudden and brittle.

Table 6.1: Variation in destructive test parameters with increasing exposure to corrosion

Exposure to corrosion (in Days)	**0**	**3**	**5**	**7**	**10**	**13**
Mass Loss (%)	0	0.6125	1.1375	1.575	2.25	2.9
Tensile strength (N/mm^2)	356.1	287.7	233.7	145.7	91.37	18.6
Loss in Tensile Strength (%)	0	21.3	34.1	59.1	74.3	94.7

The stress-strain curves of all the specimens are plotted and are shown in **Figure 6.14**. The stress has been calculated with respect to original cross-sectional area of the specimen and strain is measured between two points separated by 150mm using an extensometer. The healthy plate specimen shows a ductile behavior with well-defined elastic and plastic regions. On the other hand, as corrosion in samples increases, the plastic region in the stress–strain curves diminishes indicating brittleness in the samples.

An important observation is that although there is a huge loss of strength, the initial stiffness and the elastic modulus of the corroded samples remains largely unaffected. This is indicated by very little change in initial slopes of stress-strain curves with varying ages of corrosion. Thus, a corroded sample would behave more or less in the same way as a healthy plate at initial stages. However, they would fail suddenly at higher stresses. This illustrates the catastrophic effect of pitting corrosion.

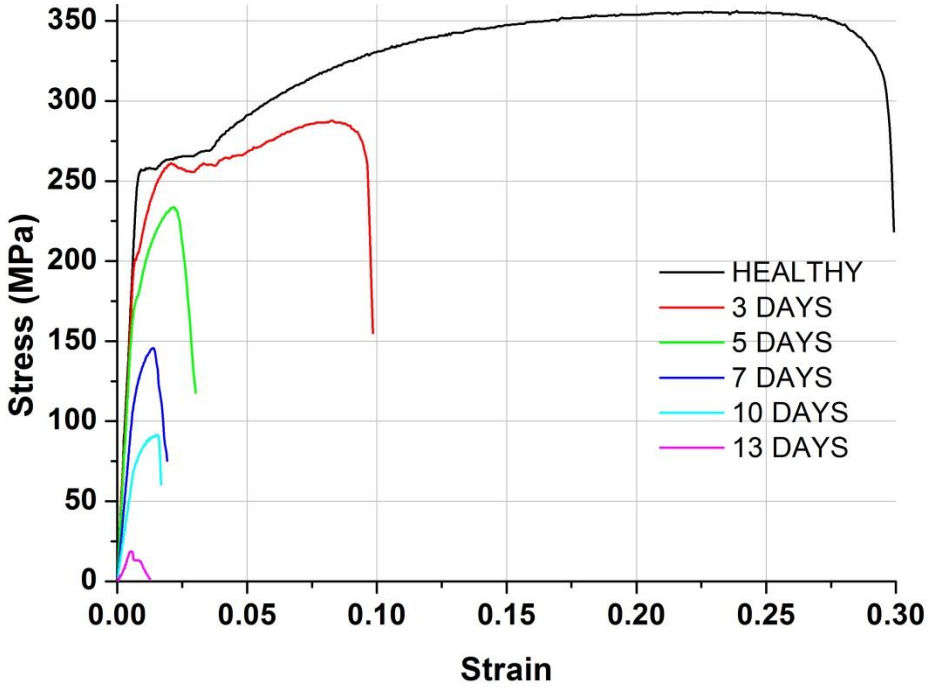

Figure 6.14 : Stress Strain curves for plate specimens at different ages of corrosion

Figure 6.15 (a-b) shows a consistent and rapid fall in ultimate stress and ultimate strain with increasing corrosion. There is a drastic fall in ultimate strength and ultimate strain with 3 days of corrosion pointing towards the catastrophic effect of even small corrosion damage. Rate of fall of ultimate strain with increasing exposure to corrosion is considerable. The fall in ultimate strain is more drastic in early stages of corrosion. The ultimate stress falls gradually with progression of corrosion.

Similar trend of fall in yield stress is indicated with increasing corrosion (**Figure 6.15c**). Mass loss is uniform and it linearly varies with time (**Figure 6.15d**). It may be noted that mass loss is recorded after every 24 hours so there are 13 days observations. Other destructive parameters i.e. ultimate stress, ultimate strain, yield stress have been recorded for five specimens exposed to 3,5,7,10,13 days of accelerated corrosion. It is evident that due to the localized nature of corrosion, even a moderate mass loss may affect the strength substantially. Loss in tensile strength with increasing corrosion indicates the loss of cross-sectional area of the plate due to pitting effect of chloride corrosion. The present monitoring system that uses ultrasonic guided waves to detect corrosion would be paramount in ensuring safety of the structure.

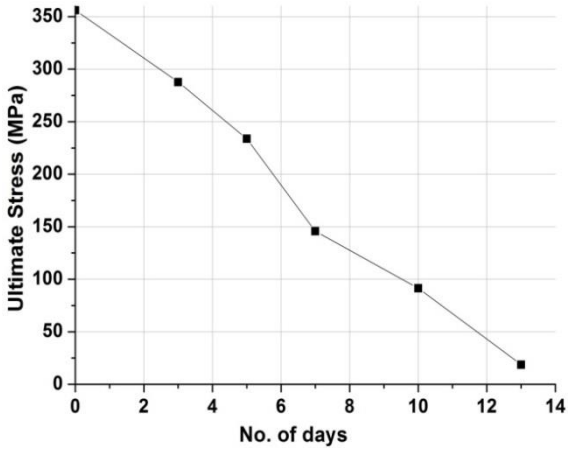

(a) Ultimate stress

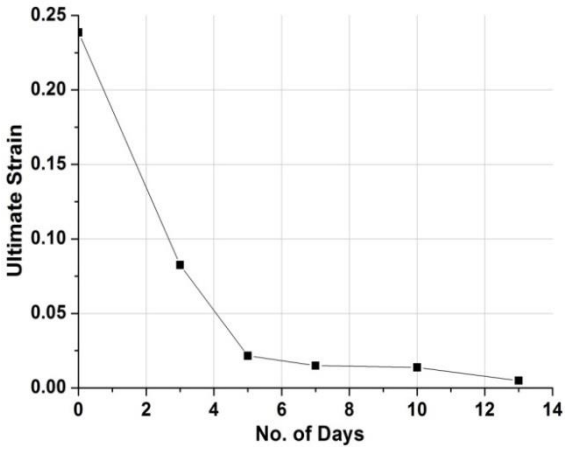

(b) Ultimate strain

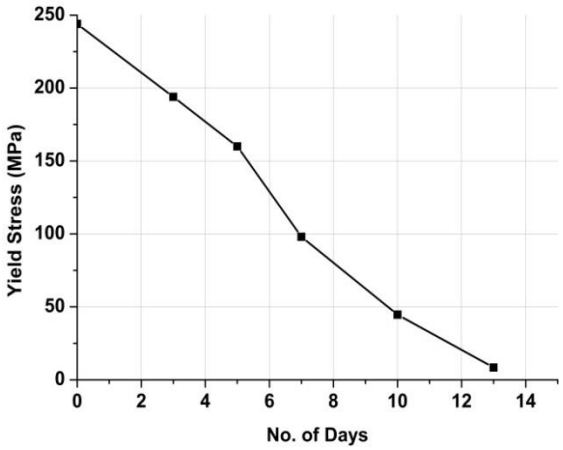

(a) Yield stress

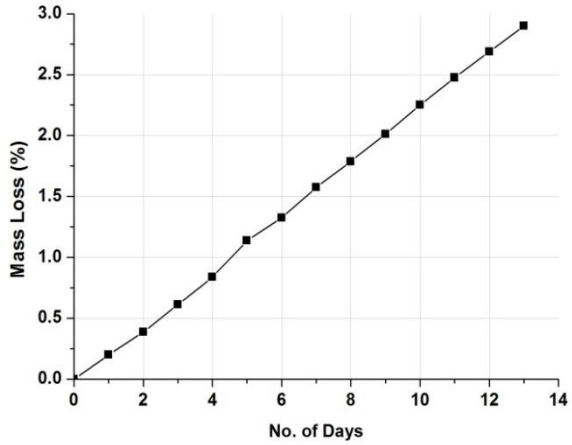

(d) Mass Loss

Figure 6.15: Variation in different destructive parameters with increasing exposure to corrosion

6.5.3 Correlation of Ultrasonic Voltages with Destructive Tests

A correlation was attempted to facilitate non-destructive estimation of the physical condition of the plate undergoing corrosion. It is important to choose the right mode of the guided waves for calibration of destructive parameters. It is indicated earlier that the surface sensitive mode S_1 at 1 MHz is capable of detecting corrosion at an early stage. However, it is not very suitable for mapping its output to the physical condition of the plate because the drop in voltage ratios is insignificant at later stages of corrosion. But in case of the core sensitive S_0

mode at 0.5 MHz, the signal decreases more uniformly with the deterioration of the plate due to corrosion. Thus, it can be used to calibrate the ultrasonic signal with the strength of the plate.

Figure 6.16 shows the comparison between ultrasonic signals with the core sensitive mode and destructive testing results of mass loss (ML) and tensile strength (f_t). It must be kept in mind that the calibrations are for the present system only and they may not be applied for a general case. However, they certainly capture the nature of the relationships.

Mass Loss (ML)

The signal strength was highest at the initial stages and it reduced sharply with the loss of mass as corrosion progressed. Thus, a linear graph has been fitted between normalized voltage ratio and mass loss given by Equation (4).

$$\text{Mass Loss (ML\%)} = 3.5(1-V_n) \quad (6.1)$$

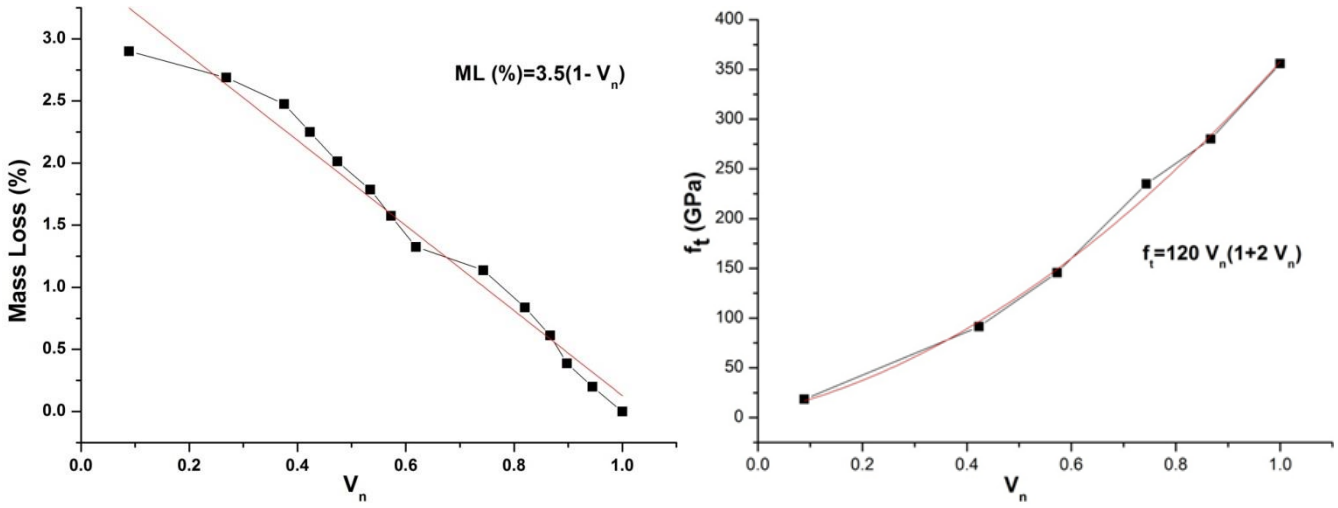

(a) Mass Loss vs V_n **(b) Tensile Strength Vs V_n**

Figure 6.16: Correlation between ultrasonic and destructive test parameters

Tensile Strength (f_t)

The tensile strength of the bar reduces monotonically with corrosion. Thus, a polynomial equation of 2nd order has been attempted for calibrating the residual strength with normalized voltage ratio as below

$$f_t = 120\ V_n\ (1+2\ V_n) \quad (6.2)$$

Where, f_t = Tensile Strength at any instant (MPa)

V_n = Normalized Voltage Amplitude Ratio

6.6 CLOSING REMARKS

This chapter illustrates a non-contact and in-situ corrosion monitoring methodology for submerged plates using specific Lamb wave modes. Specific surface sensitive and core sensitive guided wave modes are used for monitoring plates undergoing accelerated impressed current corrosion in presence of chlorides. A combination of the selected guided wave modes could effectively differentiate between various corrosion mechanisms occurring in plates. Along with the ultrasonic signals, mass loss, stress-strain behaviour and tensile strength of the plates at different stages of corrosion have been monitored. Algebraic relationships between the ultrasonic readings and other parameters have been developed. This investigation should be useful in developing a non-destructive technique for monitoring progressive corrosion in plates and assessing their deterioration in strength, stiffness and mass loss that would help in the estimation of residual life.

CHAPTER 7

HEALTH MONITORING METHODOLOGY

7.1 GENERAL

This chapter sums up the methodology established in this research endeavour for non-contact health monitoring of submerged plates using ultrasonic leaky Lamb waves. The methodology consists of testing of the plates in pitch –catch orientation using specific guided wave modes using combination of pulse transmission and pulse echo techniques. Presence and extent of damage in the plate is picked up by pulse transmission scanning of the plate and the exact localization of the damage is ascertained by pulse echo investigations. This chapter presents the application of this methodology to various cases. Different case studies presented includes plates with notches machined in random orientations (normal and oblique) to the direction of wave propagation, corroding plates (uniform and non-uniform corrosion) etc.

7.2 MONITORING METHODOLOGY

The step-wise procedure for monitoring of submerged plates for damage identification, its localization and assessment of extent is presented below. As already outlined in the previous chapters, testing of the plate is carried out in pitch catch configuration using the selected core sensitive and surface sensitive Lamb wave modes using pulse echo and pulse transmission methods.

7.2.1 STEP 1: PULSE TRANMSISSION (PT) MONITORING

Presence and Identification of notch in plate

The plate under investigation (500mm X 300 mm) with a single notch (180mm length, 2mm wide and 1.5 mm deep; **Figure 7.1a**) is scanned in Pulse Transmission mode keeping the transmitter and the receiver probes in pitch catch orientation as shown in **Figure. 7.1b** using the test-up as elaborated in Chapter 4 (Figure 4.1 and 4.2).

The pulse transmission scanning is done at marked locations on the plate at an interval of 10mm each keeping all the testing parameters like propagation distance (D_p), water path (D_w) and angle of probes as detailed in Chapter 4.

(a) Actual Plate with a Notch

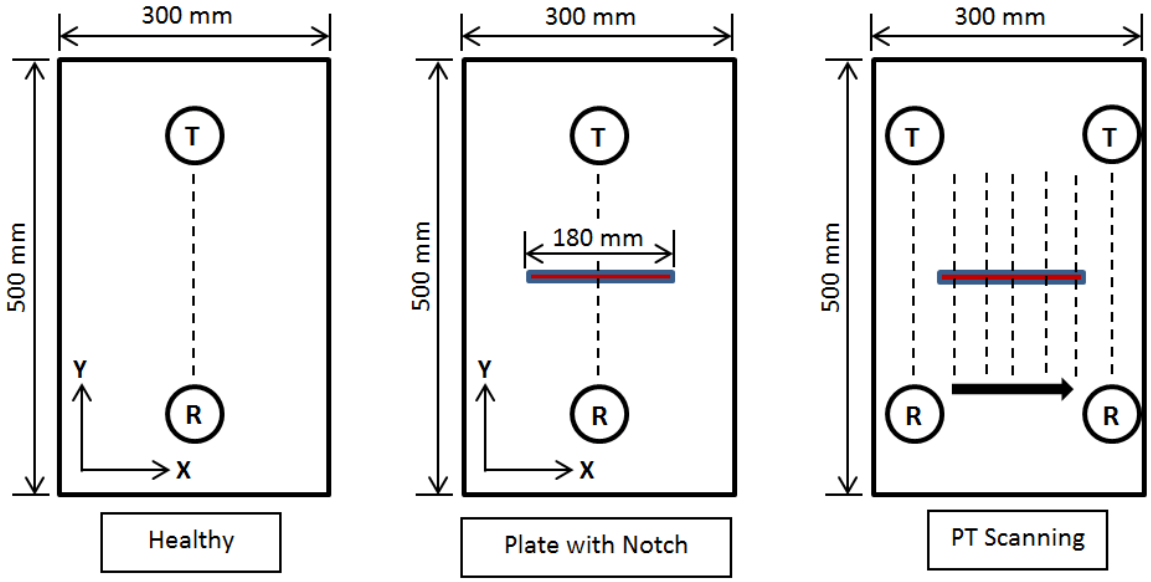

(b) Schematic of PT scanning (Top View)

Figure 7.1: Pulse Transmission Scanning of Plate with a Notch

Normalized peak to peak voltage ratio of the transmitted signals during pulse transmission scanning along the length of the plate at marked locations with a selected mode is shown in **Figure 7.2**.

These trends clearly indicate a drop in the transmitted signals as the probes interact with a 1.5mm deep notch along the locations 1-18 (180mm span of the notch) as against the signal in healthy zone of the plate (H_1,-H_5).

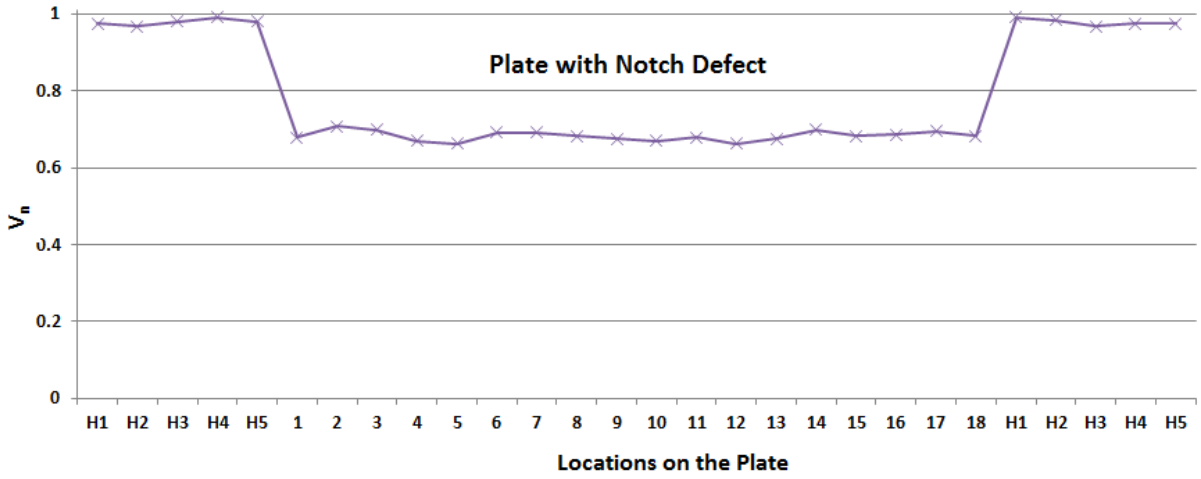

Figure 7.2: Trends of transmitted pulses along the plate in PT scanning (0.5 MHz S_0)

Hence, this step of PT scanning of the plate identifies the defect zone in the plate along the X-direction as indicated by dip in the PT trends **(Figure 7.2).**

Depth of Notch

PT scanning not only identifies the defect ridden zones but can also reveal the depth of notch across thickness of the plate. This is accomplished by making judicious selection of appropriate Lamb wave modes. Suitable specific core sensitive and surface sensitive Lamb wave modes can be selected based on study of mode shapes and characteristics of the available modes for effective diagnosis and quantification of notch damages using dispersion curves as per the procedure outlined in detail in Chapter 5. By analysing the relative fall of the PT pulse amplitude for the selected modes, depth of discontinuities can be effectively discerned as discussed in detail in Section 5.3.

Modes having specific core sensitive and surface sensitive features can be exploited to monitor and quantify the sub-surface and deep notches in the plates. A plate with multiple notches of varying depths as shown in **Figure 7.3a** is scanned in PT using typical core and surface sensitive modes. **Figure 7.3b** shows a comparison of quantitative changes in the

voltage amplitudes of the received signals using both the modes. These changes can be correlated to the presence, location and depth of the notches. It is well indicated that the surface sensitive mode is more effective in picking up initial surface modification up to 25% of notch depths whereas core sensitive mode is more suitable for diagnosing deeper notches. It is indicated by relatively higher drops in signal at larger depths of the notches with core sensitive mode. This clearly brings out the effectiveness of the core and surface sensitive modes in discovering the deeper and shallow notches respectively.

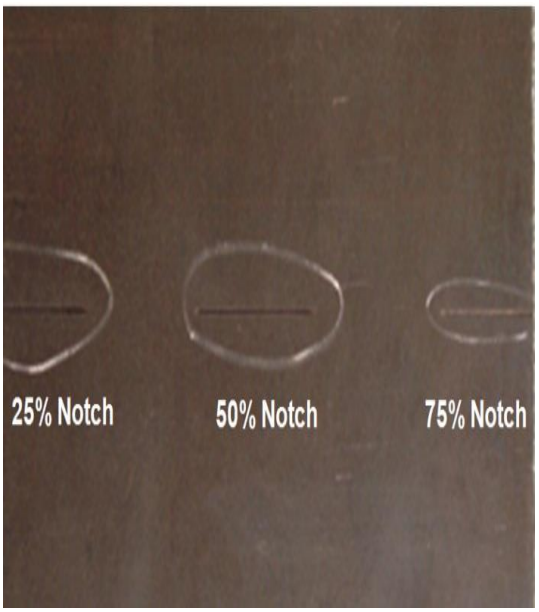

(a) Actual Plate

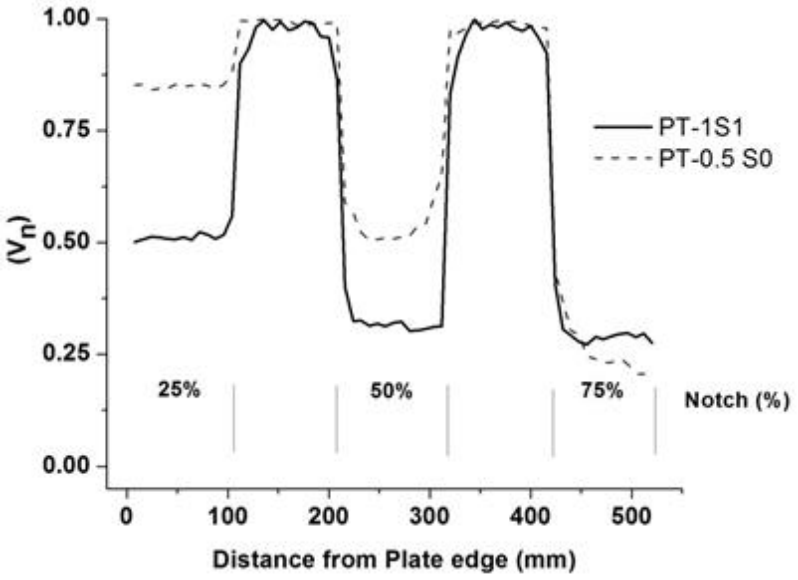

(b) PT Scanning of the plate using Core and Surface Sensitive Modes

Figure 7.3: PT scanning of the plate with multiple notches of varying depths

Hence the PT scanning of the plate using suitable Lamb wave modes successfully ascertains the presence and spread of damage zones (along X-direction) and is also well indicative of extent of damage in the plate across thickness of the plate i.e. Z- direction.

7.2.2 STEP 2: PULSE ECHO (PE) MONITORING

PT reveals the presence and extent of damage in the plate but in order to acquire the exact location and topology of the defect/notch Pulse Echo (PE) investigations and scanning is done. PT results shortlists the damage ridden domain that required PE scanning thus avoiding exhaustive PE scanning of the entire specimen resulting in quicker inspection time. PE scanning data is further processed to generate defects images depicting the location, shape and spread of the damage.

Another important consideration regarding PE scanning is that, core sensitive Lamb wave mode is preferred over surface sensitive Lamb wave mode as it exhibits consistent drop in signal with increasing depth of notch. Also PE signal of this Lamb wave mode is easy to interpret and analyse as core sensitive mode (0.5 MHz S_0) has a single sharp peak and is devoid of multimode behaviour. So, it is recommended to use core sensitive mode for defect localization using pulse echo (PE) scanning and defect map generation.

PE scanning is accomplished by moving one of the probes along Y direction **(Figure 7.4a)**. During this translation, the Y-coordinates of the probe and the corresponding PE signatures are simultaneously recorded. At a particular location (say Y_{i-1}), when it is quite far from the notch, a typical PE signature has two distinct peaks which are the first and second reflections from the plate. In the vicinity of the notch, another moving peak called as Defect Reflection Peak (DRP) is observed between first and second reflections. As the defect is approached (i.e. Y_i and $Y_{i+1.....}$), time of arrival of DRP reduces and its signal amplitude increases. When probe is very close to the notch, DRP with very strong amplitude coincides with first reflection peak. As a result, a sharp surge in amplitude of first reflection peak is observed. This step aims at monitoring this quantum jump in the signal amplitude along with the corresponding Y-coordinates. Also as the depth of the notch increases, the first reflection peak amplitude also rises.

The PE data (X and Y coordinates from DRO) along with PE signal amplitude is plotted in the form of defect map representing the defect terrain on the plate. Hence the location, spread (i.e. position and size) and magnitude (i.e. depth) of the notch in the plate is

characterized and indicated very well by the present methodology. Defects in the form of notches with varying depths are represented in the colour plots levels on the defect map.

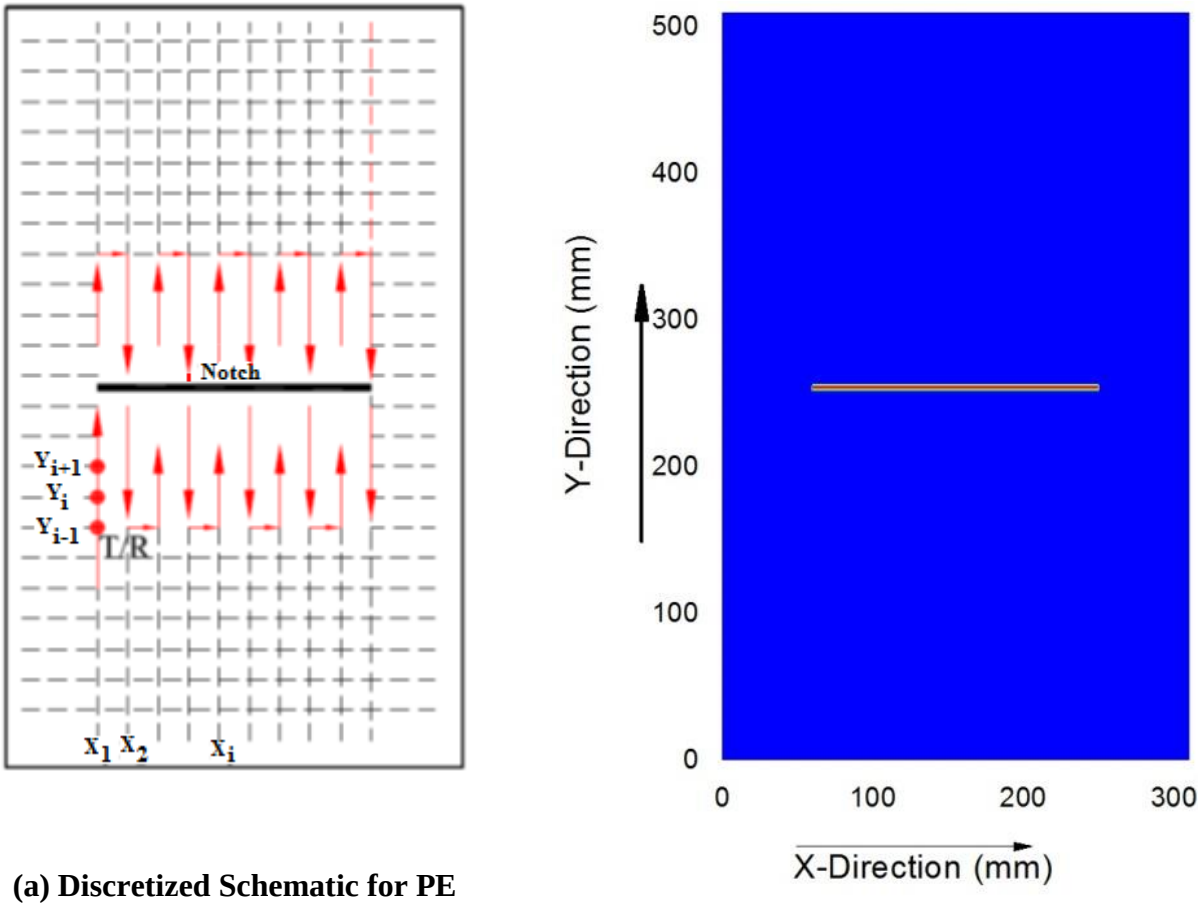

(a) Discretized Schematic for PE scanning

(b) Defect Map for notched plate

Figure 7.4: PE scanning of Plate for defect localization and defect map generation

It is observed that defect map generated in the plate with a single notch **(Figure 7.4b)** closely matches with the actual photographic image of the plate specimen **(Figure 7.1a)**. The photographic image although represents the spread and location of the defect, but it does not clearly show the depth of the notch. However, the defect map clearly represents location, spread and depth of the defects in the form of colour coding.

7.3 CASE STUDY 1: PLATE WITH OBLIQUE NOTCHES

7.3.1 Ultrasonic Pulse Transmission Monitoring

A hybrid defect map generation methodology comprising of PE and PT scanning of the submerged plate specimen has been established in the previous section and used successfully for the specimen having notch defects placed normal to the direction of wave propagation. But a plate specimen may not essentially have the defects placed in this

orientation always. So, this methodology is further applied to plate specimens (500mm X 300mm X 4mm) with oblique notches machined at varying inclinations of 15°, 30°,45°, 60°and 75° to the X-direction **(Figure 7.5)**. The notches are machined at the centre of the specimen in order to avoid reflections from the edges and are confined in a square patch of size 180mm. The effect of obliquity of the notch on PT signal of the propagating Lamb wave mode is first investigated.

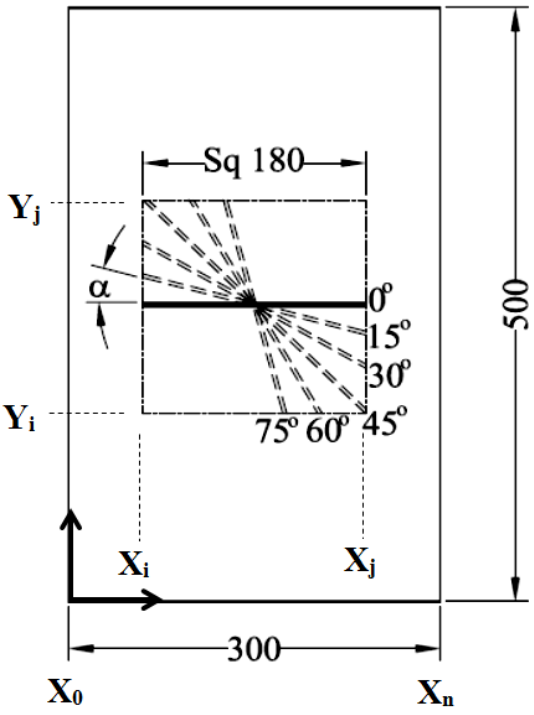

Figure 7.5: Schematic of the plates with oblique notches

Figure 7.6a shows the PT signatures obtained using S_0 mode at 0.5 MHz with oblique notches at varying angles ($\alpha = 0^o$ to 75^o). As expected, the PT signal amplitude falls due to presence of notch. But this fall in amplitude with same depth of notch is different depending upon the orientation of the notch with respect to the direction of wave propagation. From the PT signatures, it is observed that the transmitted signal strength continuously drops as the angle of the notch increases from 0^o to 75^o. This fall in amplitude is attributed to the reflection of incoming energy from the defect, thus leading to loss in transmitted energy **(Figure 7.6b)**. The normalized peak-peak voltage ratio trends with changing angle of the notch is shown in **Figure 7.7**.

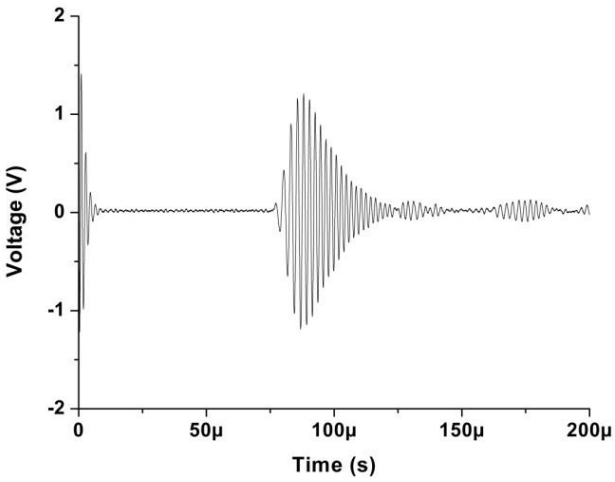

Healthy Plate Signal

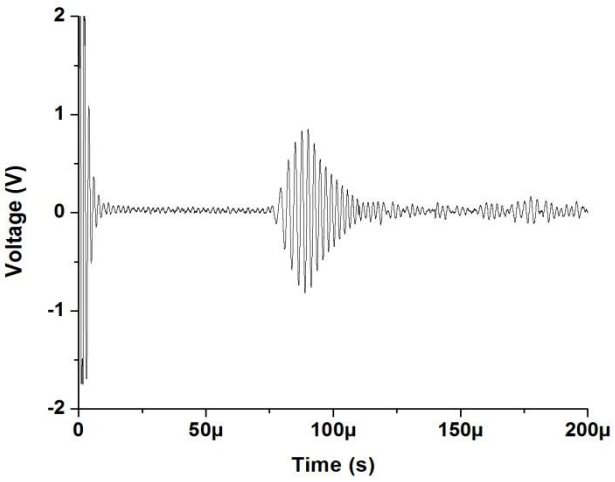

α = 0°

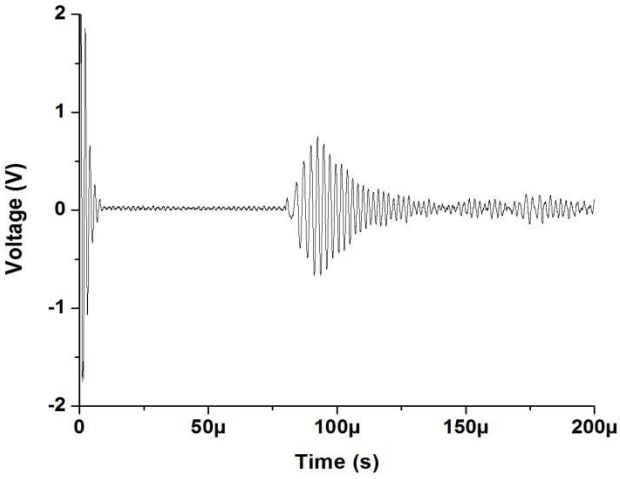

α = 15°

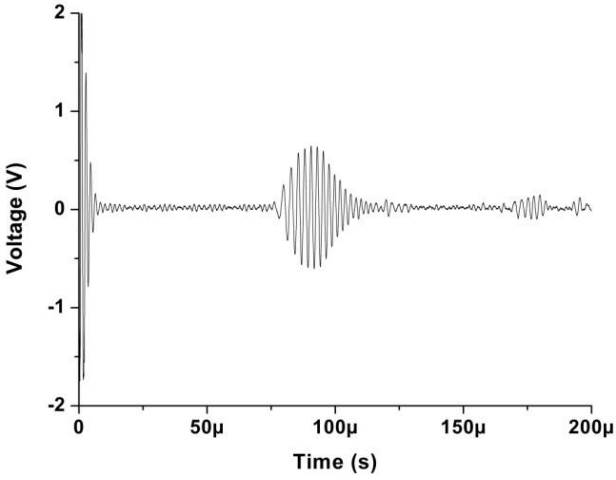

α = 30°

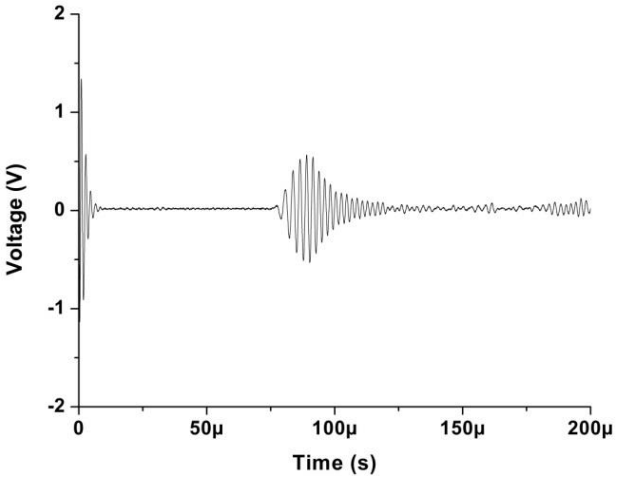

α = 45°

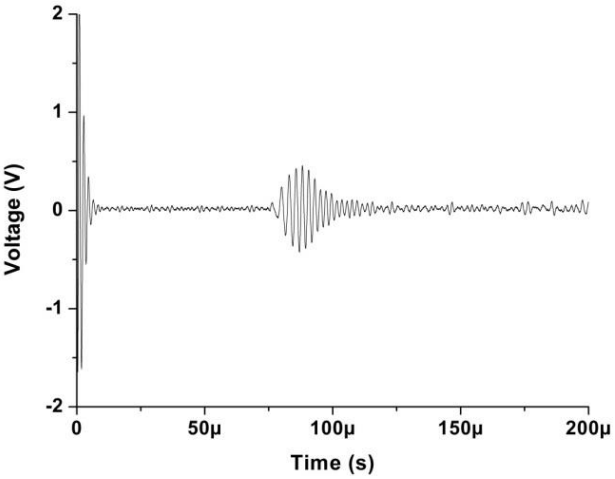

α = 60°

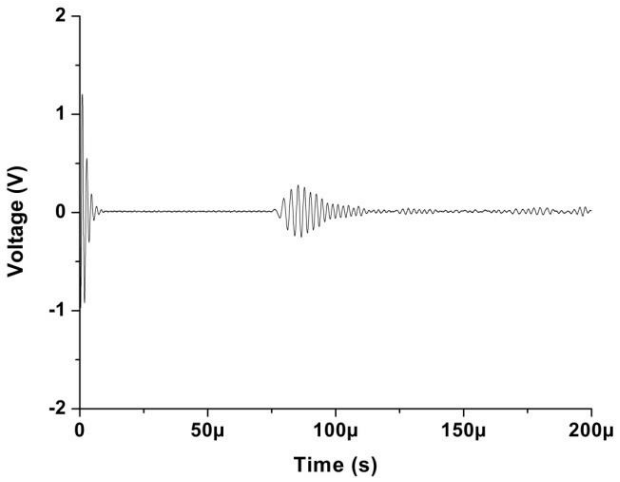

α = 75°

(a) PT signatures at a particular location with varying angle of notch

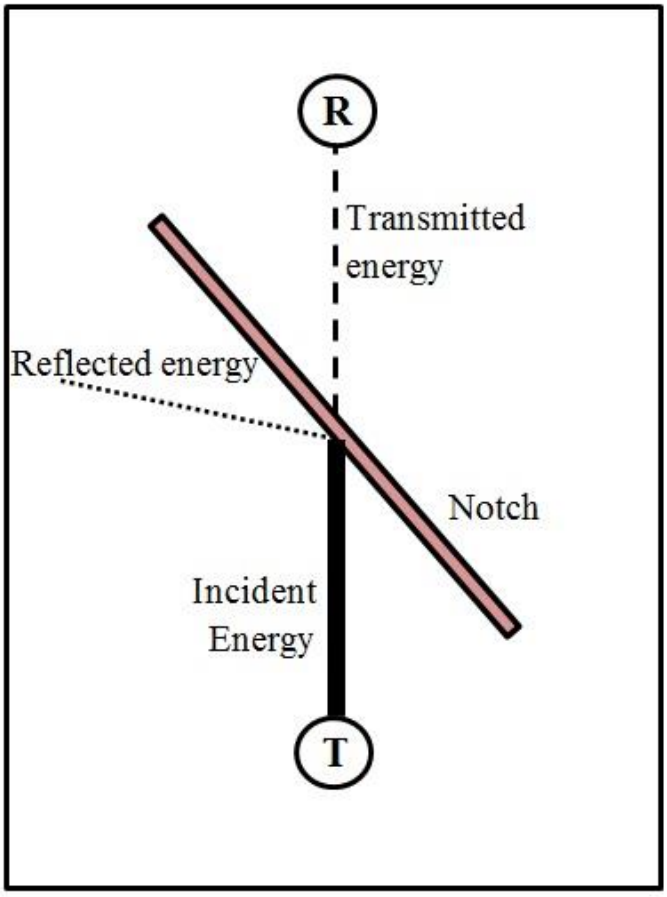

(b) Interaction of Lamb wave with oblique notch

Figure 7.6: Effect of inclination of notch

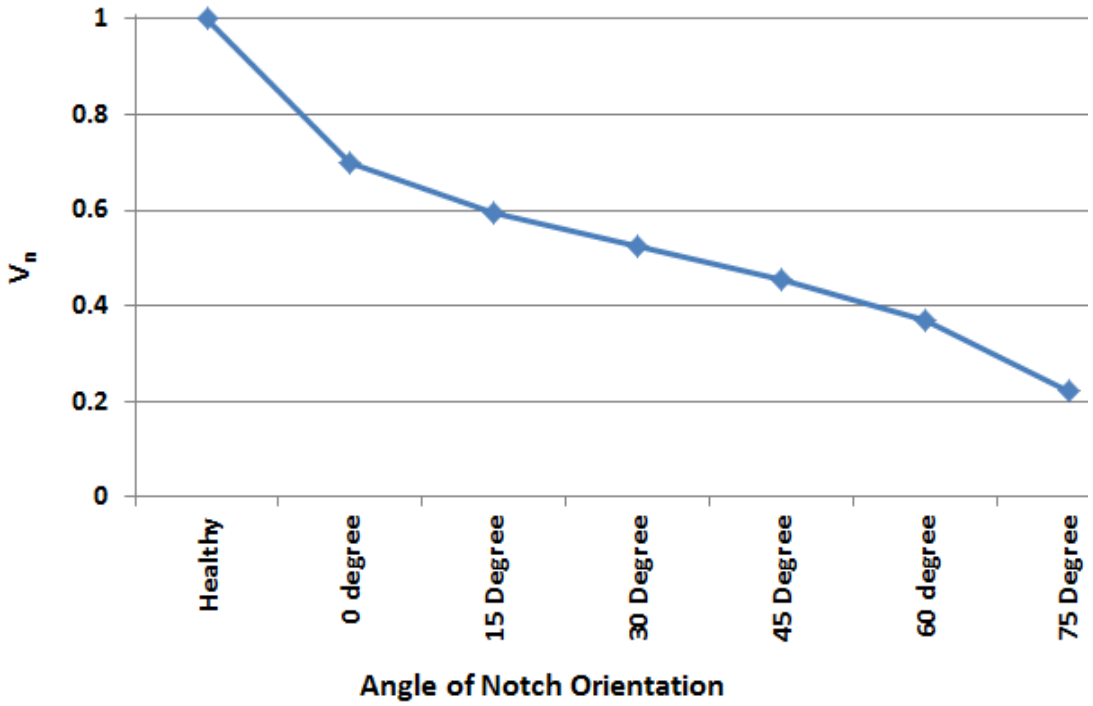

Figure 7.7: Trends of PT signal with increasing angle of notch at a particular location

PT scanning of the plate specimens is done at different locations along X-direction and the trends of peak-peak voltage amplitude ratios at all locations are shown in **Figure 7.8**. As already outlined, with the increasing angle of orientation of the notch (α), the signal continuously drops. Influence of the notch can be observed on PT signatures recorded along X-direction as shown in the range X_i to X_j **(Figure 7.5)**. This range X_i to X_j (the projected span of the notch along X-direction) is different for each specimen depending upon the obliquity of notch. Similar PT scan can also be implemented using S_1 mode at 1 MHz.

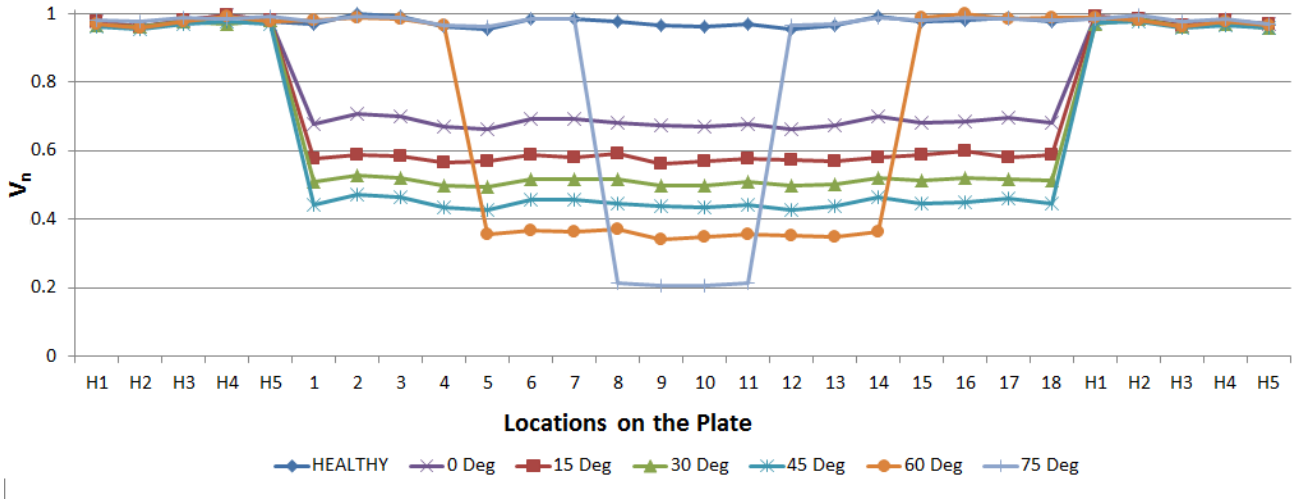

Figure 7.8: PT Amplitudes with Varying Angle of Notch at all Locations

7.3.2 Pulse Echo Monitoring

PE scanning is implemented only within zone (X_i-X_j) identified during PT scanning. The methodology for PE scanning along the Y-direction to obtain the defect maps is same as followed for straight notches **(Figure 7.4)**. Defect map is generated by using the locational data (from DRO) and corresponding PE signal amplitude. The defect maps for the plates with notches at different angles are shown below in **Figure 7.9**. PE scanning provides the limits of defect ridden zone along Y-direction represented by the range Y_i to Y_j (projected span of the notch along Y- direction). It is important to note that probes were incremented through 10mm along X- direction during two consecutive PT scans. However, in PE scan the probe was moved by 1mm step along Y- direction. Resolution of the defect maps can be further improved by reducing these increments. But it shall lead to longer inspection times.

It is observed that however topologically the defect maps match with the actual photographic images very closely but obliquity of the notches adversely affects the contrast of the defect map. For the same depth of notch, defect maps in **Figure 7.9 (a) and (j)** show different levels of contrast. It is due to the fact that defect maps rely on the PE signal strength at any given location. With increasing obliquity of the notch, the PE signal strength continuously falls due to reflection by the notch **(Figure 7.9 k)**. This effect is especially more prevalent when notch angle is more than 45^o and severely mars the contrast of the image obtained (**Figure 7.9 h and j**).

In order to improve visualization of the defect map, domain of the plate bounded by X_i-X_j and Y_i-Y_j limits is rescanned in PE mode by translating the probe along in X-direction (**Figure 7.10)**. Locational and signal amplitude data logged during two PE scans is superimposed and defect map is generated. The final improved defect map obtained by superposition of X and Y direction PE scanning of plate specimens are shown in **Figure 7.11**. These defect map images clearly reveal damage topology, position and extent. Improvement in the contrast level of the damage zone can also be very clearly noticed.

Hence, the combined PT and PE investigations of the submerged plates can be successfully applied for monitoring plates with oblique notches also. The methodology not only identifies the presence but also locates and quantifies the oblique notches in the submerged plates. A flow chart showing the step wise methodology is given in **Figure 7.12**.

(a) Actual Plate with 15° Notch

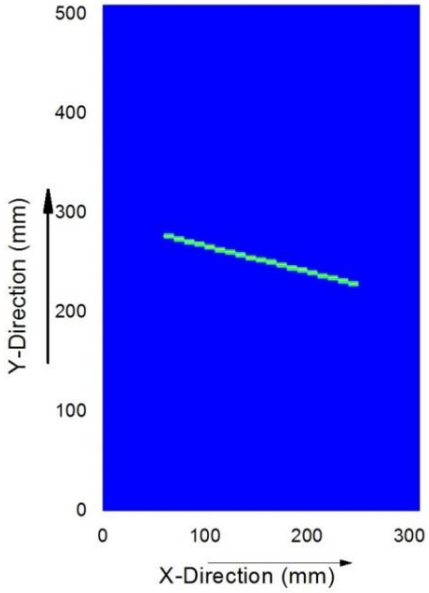

(b) Defect Map with 15° Notch

(c) Actual Plate with 30° Notch

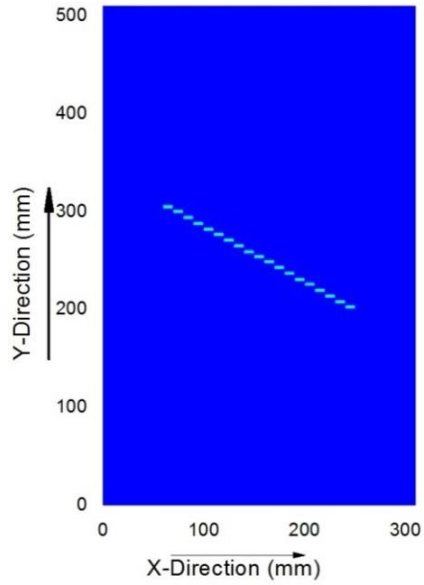

(d) Defect Map with 30° Notch

(e) Actual Plate with 45° Notch

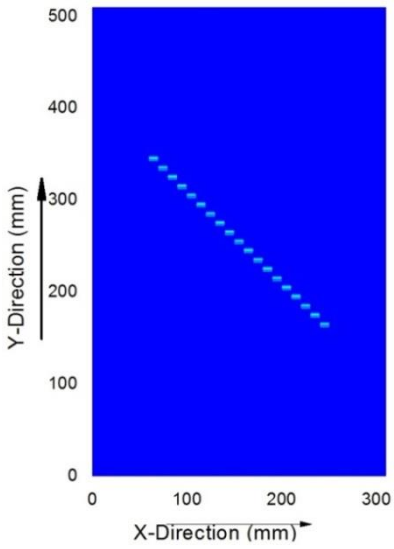

(f) Defect Map with 45° Notch

(g) Actual Plate with 60° Notch

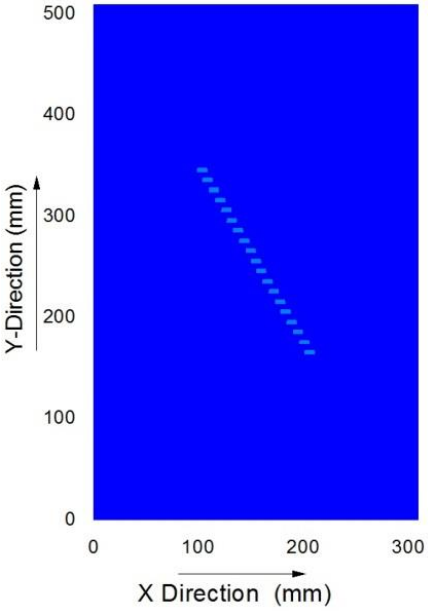

(h) Defect Map with 60° Notch

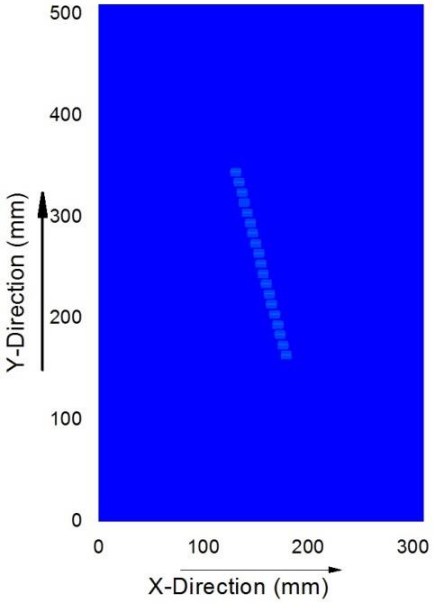

(i) Actual Plate with 75° Notch **(j) Defect Map with 75° Notch**

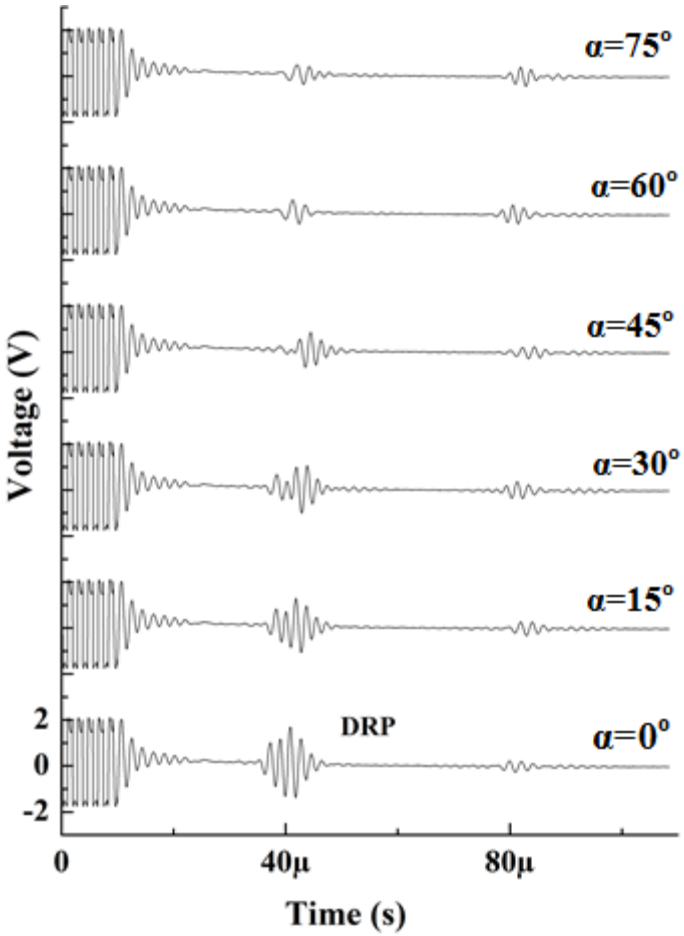

(k) DRP amplitude with varying notch orientation

Figure 7.9: Defect Map in plates with Oblique notches

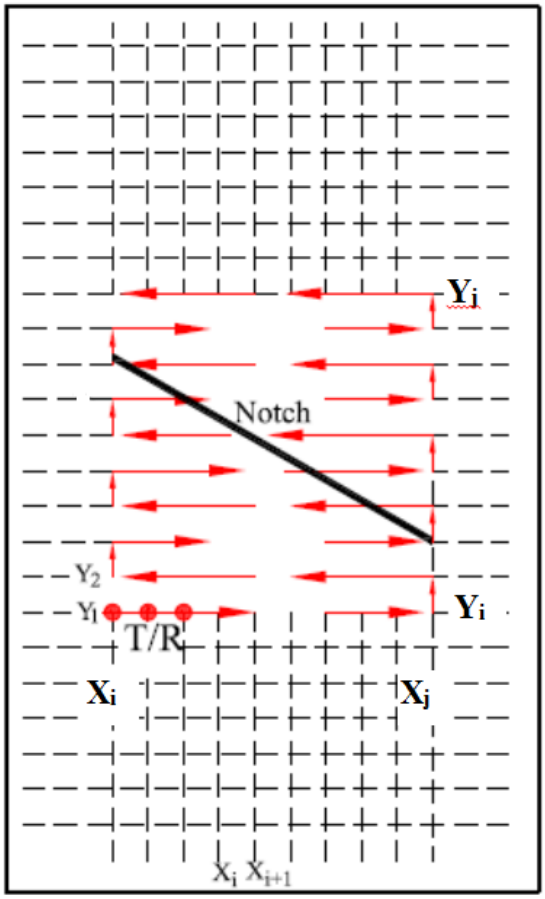

Figure 7.10: Schematic of PE scanning in X- Direction

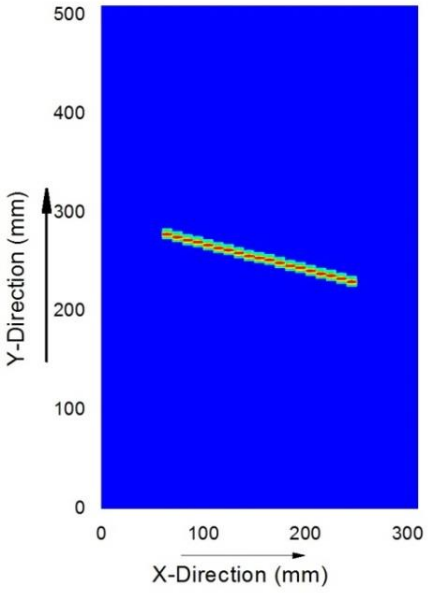

(a) 15° Notch

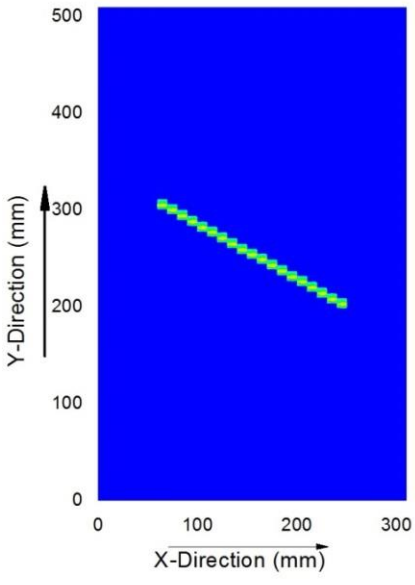

(b) 30° Notch

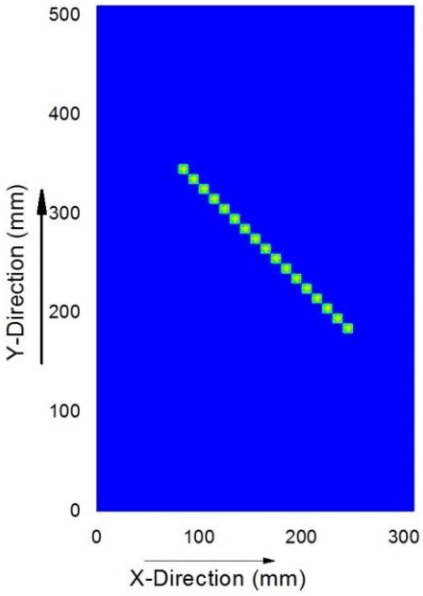

(c) 45° Notch

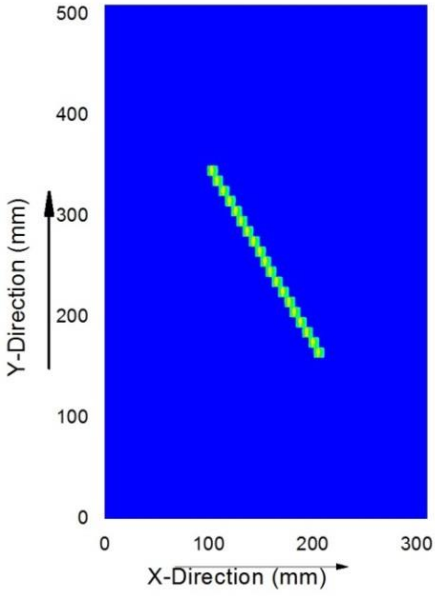

(d) 60° Notch

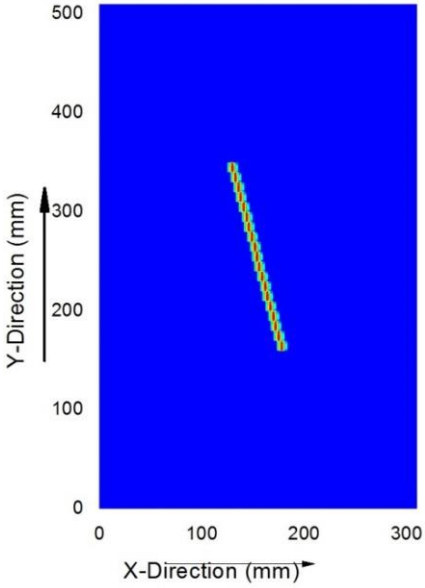

(e) 75° Notch

Figure 7.11: Defect Maps obtained by superimposition of PE data along X- and Y-directions

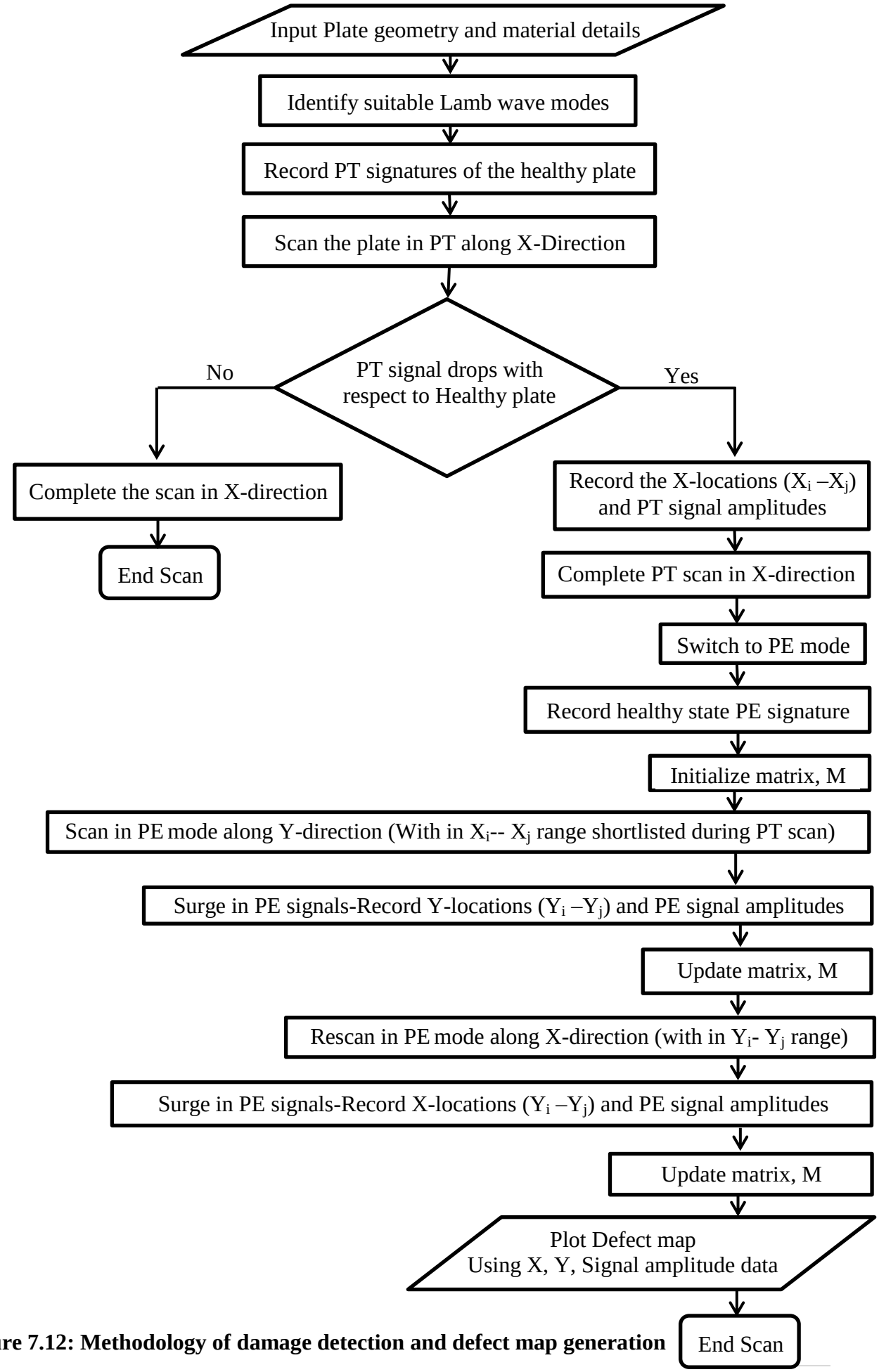

Figure 7.12: Methodology of damage detection and defect map generation

7.4 CASE STUDY 2: PLATE WITH ACCELERATED CORROSION (NON-UNIFORM CORROSION)

7.4.1 Pulse Transmission monitoring

The developed methodology is also applied to a plate subjected to accelerated impressed current corrosion as explained in Chapter 6. It yielded a corrosion patch with pits spread and distributed non-uniformly in the exposed area (**Figure 7.13a**). Ultrasonic PT signatures were recorded in the healthy zone of the plate as well as in the corroded patch at marked locations on the plate using 0.5 MHz probe. PT scan results are presented in the form of peak voltage amplitudes of the received signals **(Figure 7.13b).** These scan results are suggestive of random material loss at various locations on the plate. In the healthy plate, the signature is characterized by a strong pulse at all locations of the exposure area. In the corroded area, a significant drop in voltage of the transmitted signal is observed**.** It is noted that the maximum drop in voltage amplitude is observed at location 6. It suggests significant localized corrosion at this location. This can also be visually verified by formation of localized pits at the same location. Drop in transmitted signal strength can be attributed to the corrosion leading to the material loss in the form of pits on the steel plate. Due to this non-uniform loss of material from the surface, the smooth waveguide in the healthy plate is disturbed, resulting in scattering of waves and thus attenuation of transmitted signal. It is indicated by the fall in the voltage amplitudes of the transmitted pulses as observed in the notched plate specimens. Hence, PT scanning of the submerged plate with corrosion can bring out the existence of areas with substantial material loss.

7.4.2 Pulse Echo Monitoring

Depth of the prominent corrosion pits present on the plate is measured with the depth gauge. **Figure 7.14a** shows the depth of pits on the plate. To generate the defect map of the corrosion patch, ultrasonic pulse echo monitoring has been carried out. The voltages of the reflected pulses obtained were plotted in the form of defect map (**Figure 7.14b**). Pattern of the generated defect map shows a close resemblance to the corroded patch topology on the plate. This is particularly true for the deeper pits (depths 0.87 mm, 0.81 mm, 0.79 mm measured with dial indicator) which appear as bright spots in the defect map. Hence, the non-contact methodology established in the study can also be effectively employed for monitoring material loss in the form of corrosion in submerged plates.

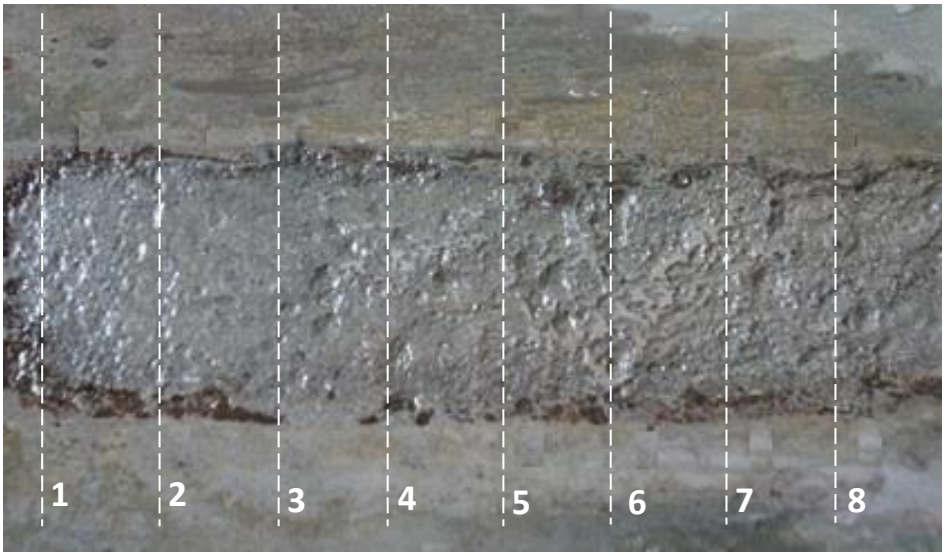

(a) Corroded patch on plate

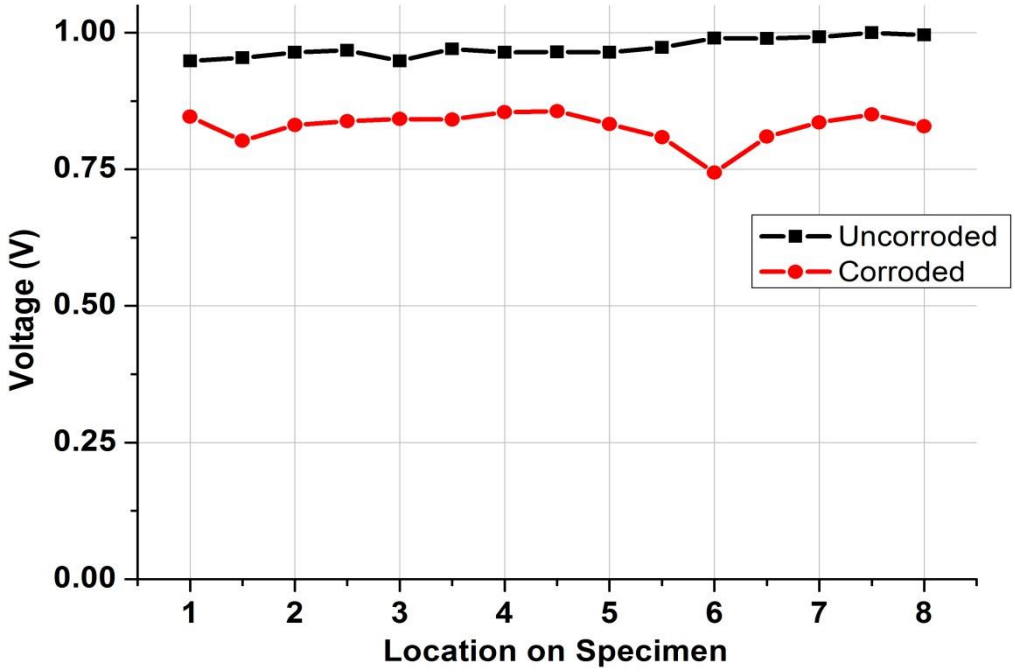

(b) Peak to peak voltage amplitude ratio at different locations

Figure 7.13: PT scanning of plate with corroded patch

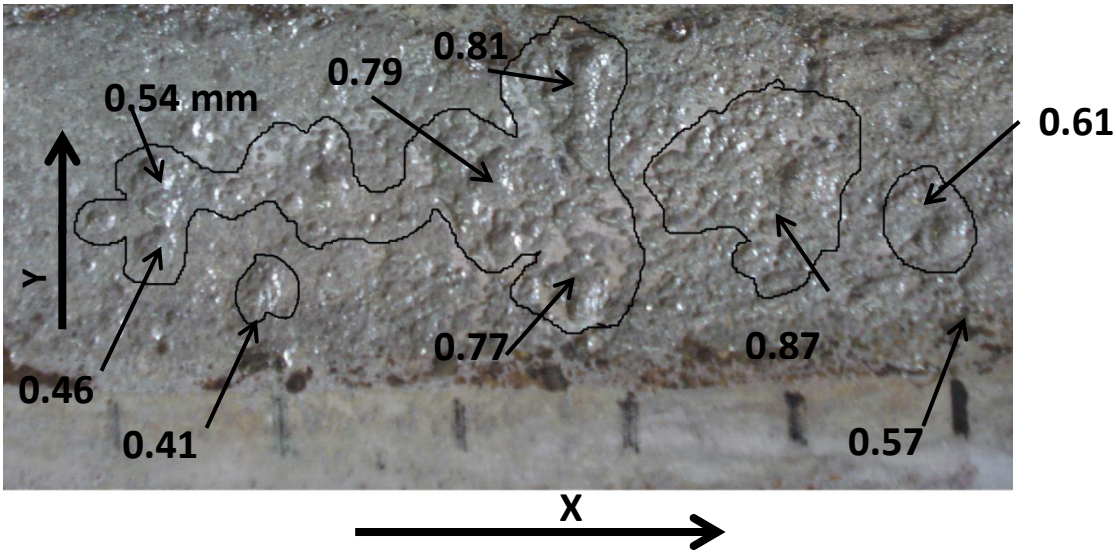

(a) Corroded patch on the plate– Depth of pits shown in mm

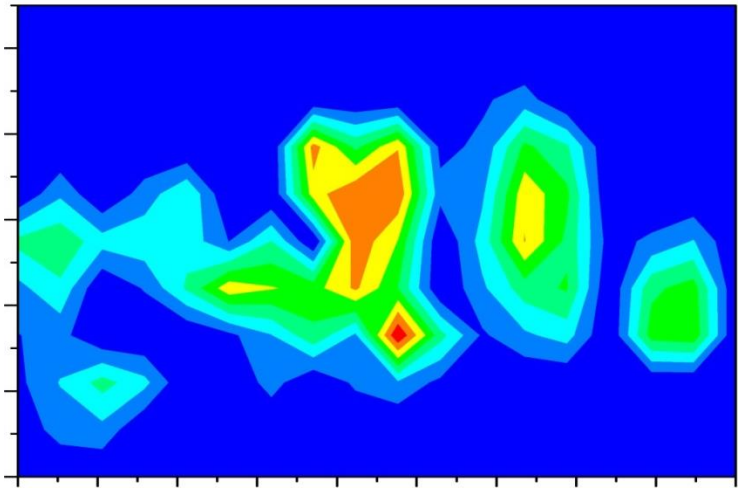

(b) Defect map

Figure 7.14: PE scanning of plate with a corrosion patch

7.5 CASE STUDY 3: PLATE SUBJECTED TO ACID ATTACK (UNIFORM CORROSION)

A plate specimen (500 mm X 300 mm X 4 mm) is exposed to chemical attack by mounting an acrylic pond (130mm X 40mm), containing concentrated nitric acid, on the top of the plate. The acid attack yielded a uniformly corroded patch which loses about 2mm depth in 4 days throughout the exposed area **(Figure 7.14).** The plate is scanned in X as well as Y direction to obtain the defect map **(Figure 7.15).**

Figure 7.15: Condition of Plate subjected to Acid Attack after 3 days

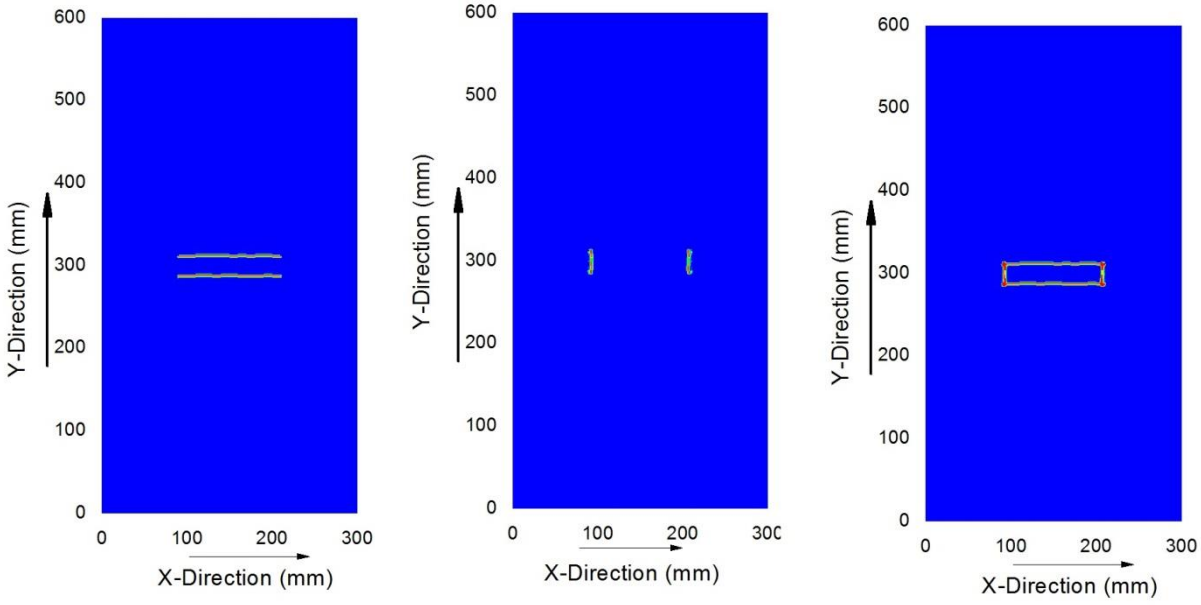

(a) PE Scanning along Y direction **(b) PE Scanning along X Direction** **(c) Superimposed scans**

Figure 7.16: Defect Map generation of a plate subjected to acid attack

7.6 CASE STUDY 4: PLATE WITH AN ENGRAVED IMAGE

Health monitoring methodology presented in flow chart (**Figure 7.12)** is also applied to a plate with an engraved image consisting of multiple milled notches in different orientations **(Figure 7.17a)**. The defect map of the plate is developed by carrying out PE

scanning along X and Y directions and matches with the actual photograph of the plate as shown in **Figure 7.17(b-d)**.

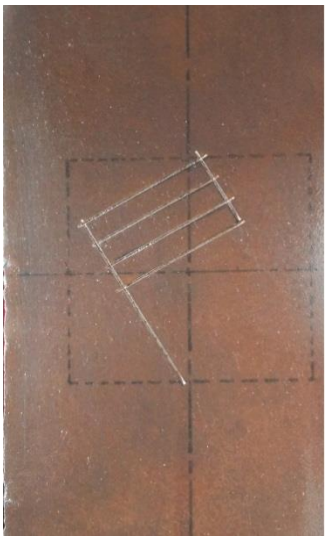

(a) Actual Plate

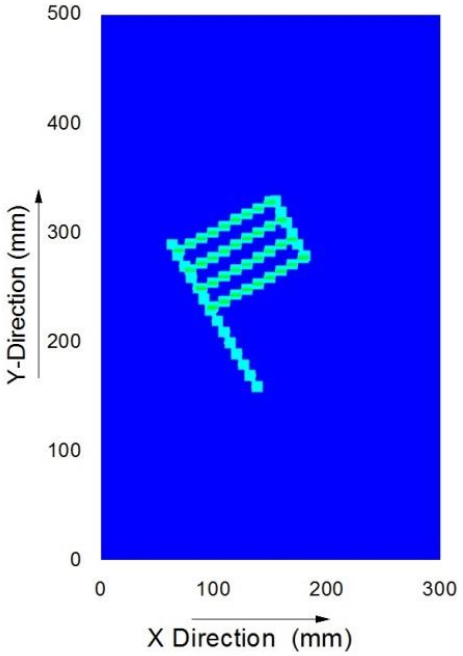

(b) PE scanning along Y-direction

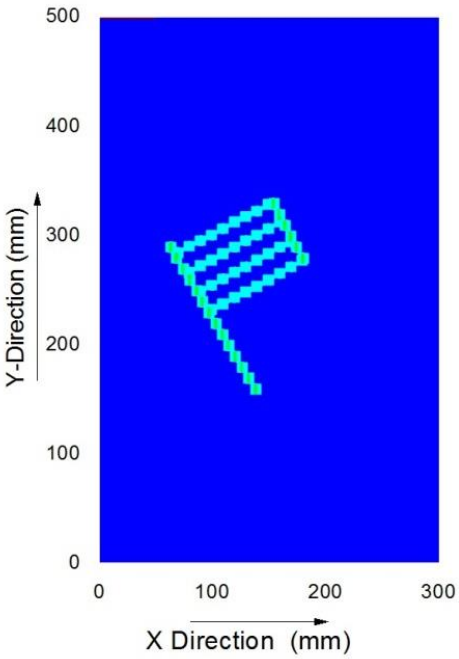

(c) PE Scanning along X-direction

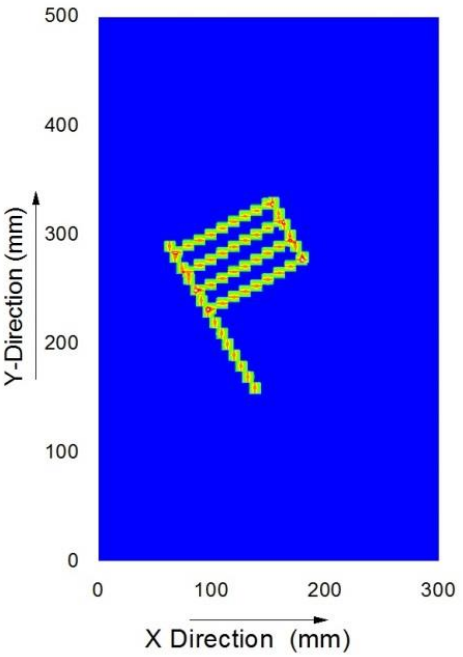

(d) Superimposed Defect Map

Figure 7.17: Plate with an engraved image

7.7 CLOSING REMARKS

This chapter summaries the damage monitoring methodology for submerged plates and is successfully implemented on plates subjected to various types of defects in the form of straight and oblique or inclined notches, uniform corrosion and non-uniform corrosion. Combined use of pulse transmission and pulse echo techniques in pitch-catch orientation of the probes can discern, localize as well as quantify the damages. The variation in the properties of the surrounding water media like density, salinity, temperature variations etc. does not affect the wave propagation characteristics of the Leaky Lamb wave travelling in the plate which have been used for characterization of damage in the submerged plate. The technique developed in this research effort has the potential to be developed as a commercially viable non-contact and in-situ damage monitoring methodology for submerged infrastructure components.

CHAPTER 8

CONCLUSIONS AND FUTURE SCOPE OF RESEARCH

8.1 INTRODUCTION

Present work is focused on developing a non-contact, cost effective health monitoring technique to quickly locate, quantify and map the material loss in the form of machined notches and corrosion as in ship hulls and other offshore infrastructures. These components are otherwise difficult to be monitored regularly by conventional techniques due to inaccessibility and economic constraints. In this work ultrasonic leaky Lamb waves have been identified and used as a potential and effective health monitoring tool for such cases. A pair of mobile probes arrange in Pitch-Catch orientation have been used to scan the submerged plate in both pulse echo (PE) and pulse transmission (PT) modes. Sensitivity of specific Lamb wave modes to the depth of damage has been exploited to discern the extent of damage. This methodology has been first developed for material loss idealized as machined notches. Subsequently the methodology is successfully applied to plates undergoing actual accelerated corrosion in chloride environments simulating marine saline conditions. The simulated and actual corrosion results are compared to study the effectiveness of simulation techniques. Effective combination of ultrasonic guided wave modes could identify the onset as well as progression of corrosion in plates. The ultrasonic signals are calibrated to estimate the physical condition of the plates in terms of residual tensile strength. The conclusions spread over the entire research have been summarized in the following sections.

8.2 LAMB WAVE PROPAGATION IN SUBMERGED PLATES

The propagation characteristics of various Lamb wave modes in submerged plate geometries was investigated to develop a damage monitoring strategy for plate assemblies as in ship hulls and marine structures. In such large structures, where the principal motive is detection of defect, this strategy is very promising and an experimental set-up was developed employing a mobile pair of immersion transducers. Specific ultrasonic guided wave modes with unique scanning capabilities have been identified and excited. Finally, the propagation of these selected modes through submerged plates would be further utilized for damage

detection in plates. Major conclusions drawn from the study of Lamb wave propagation in submerged plates can be summarized as:

- Different guided Lamb wave modes can be successfully generated in plates submerged in water by orienting the transducers at different incident angles (θ) in pitch – catch configuration.
- Mobile probes should be placed at an optimum distance from the immersed plate and making equal inclinations (θ) with vertical. If the distance of the probe from the plate is too large, it results in loss of incident energy to the surrounding water. On the other hand, if the probes are placed too close to the plate, field reflections from the solid interface overlaps with the initial pulse of the transducer. Also the near field effects influence the received signal.
- Probes are to be placed equidistant from the plate. This is confirmed from PE signatures by ensuring same time of flight in water (t_w) of the first reflection pulse from the specimen in both the probes.
- After setting the probes, ultrasonic testing of the immersed specimen is carried out in PT configuration. Guided waves propagating through the immersed plate continuously loose energy to the surrounding water and the optimum p*ropagation distance (D_p)* is set such that the signal fidelity is maintained for damage detection.
- The experimental generation of different modes was also confirmed from theoretical considerations using Dispersion curves.
- Different leaky Lamb wave modes exhibit unique propagation characteristics.
- Different symmetric and anti-symmetric modes can be generated by simply varying the angle of the transmitting and receiving probes but the selection of a particular mode for damage detection is based on the considerations of minimum attenuation for maximizing scanning distance, good signal fidelity and the energy distribution profile across the plate thickness.
- The effect of physical obstructions on the Lamb wave propagation through the submerged plate was done to ensure that PT signatures only depict the guided Lamb waves travelling through the submerged plate and to rule out any possibilities of any undesirable signals like reflections or transmission from other nearby interfaces like water surface in the tank, bottom of the tank etc.

8.3 PLATES WITH NOTCHES

Guided wave modes with unique scanning capabilities were identified by studying their interaction with the notch damages. These selected modes were employed to identify the problem areas in the plate. Attenuation of the received PT signal could relate to the extent of the damage due to notch. Subsequent PE scanning was done to localize the damages. Post processing of the PE data was pictorially represented in the form of defect maps. Following conclusions can be derived from the monitoring of a plate with machined notches:

- Lamb wave modes sensitive to near-surface and sub-surface damages have been identified as Surface Sensitive and Core Sensitive Modes.
- These specific ultrasonic Lamb wave modes are further utilized for non-contact scanning of the plates to identify the presence, location and extent of damage.
- Effective combination of these modes leads to comprehensive inspection of the submerged plate structures. Pulse Transmission scanning of the submerged plate specimen helps in identifying the problem areas in the plate due to the damage. Attenuation of the received PT signal could relate to the extent of the damage due to notch.
- Defect localization is done by carrying out PE investigations using core sensitive mode. This mode is preferred since it is more responsive to damages throughout the thickness of the plate in comparison to surface sensitive mode which only picks up initial degradations.
- Defect Reflection Peaks (DRP) obtained in PE indicated the exact position of the notch.
- Post processing of the information generated from PE scanning of the plate is pictorially represented in the form of defect maps or images or tomograms.
- The methodology is successfully applied to a plate with twin notches and multiple notches of varying depths.
- Effect of oblique notches on the wave propagation characteristics was also studied. Developed methodology was successfully implemented on plates having inclined notches and the corresponding defects images were generated.
- Defect maps were also successfully generated for plates with a uniform corrosion patch (chemical attack) and a non-uniform corrosion patch (due to chlorides). The defect maps highlight the affected areas very clearly.

8.4 ACCELERATED CORROSION STUDIES

The damage detection methodology developed for machined notches was extended to plates undergoing accelerated corrosion in chloride environments to simulate marine conditions. A combination of the selected guided wave modes could effectively discern various corrosion mechanisms occurring in plates. Along with the ultrasonic signals, destructive parameters of mass loss, tensile strength, ultimate strain etc. of the plates at different stages of corrosion have been monitored. Algebraic relationships between the ultrasonic readings and other parameters have been developed. Important conclusions derived from this study can be summarized as:

- The interaction of specific core and surface sensitive guided wave modes with plates undergoing accelerated progressive corrosion indicated similar pattern as with notches.
- Uniform and pitting corrosion could be discerned by the selected surface sensitive and core sensitive modes. The surface sensitive mode picks up the onset of corrosion and initial surface degradation very well. Further ingress and progression of corrosion deep in the plate is identified better by the core sensitive mode.
- Plates at different stages of corrosion were also ultrasonically monitored to explore the ability of ultrasonics to predict the level of deterioration of the plates. It was done by studying correlations between ultrasonic voltages and destructive parameters of mass loss and tensile strength. Thus, a mapping was established between the physical conditions of the plate and the voltage ratios in the form of algebraic equations.
- This should facilitate evaluation of fitness of plated structures for their intended purpose in immersed conditions.
- Through a judicious selection of ultrasonic guided wave modes complete corrosion mechanism occurring in marine environments in plate assemblies can be monitored using a pair of non-contact mobile immersion probes.

8.5 FUTURE SCOPE OF RESEARCH

Ultrasonic guided waves utilizing specific core and surface seeking modes can be successfully used for real time monitoring of damages in plates in submerged state. Through a judicious selection of specific Lamb wave modes, it is possible to distinguish between sub-surface and deep notches as well as the effect of chloride induced corrosion in submerged plates. The ability of ultrasonics to predict the level of deterioration in the submerged plates due to corrosion and to correlate with the physical condition of the plates at different stages of

corrosion is successfully explored. In the course of investigation, a few open issues have been identified. Ultrasonic guided waves can be implemented for health monitoring of infrastructure systems and there is a lot of potential future research in this area:

- Develop efficient numerical method to model propagation of Lamb waves through submerged plate considering the solid- fluid interaction.
- Study the effect of curvature in plate geometry and presence of structural features like weldments in actual submerged plates using the developed methodology.
- To study the effect of factors like turbulence, variations in temperature and properties of the couplant medium like salinity, density etc. on the healthy wave signatures.
- Implement suitable signal processing tools to aid the faster and efficient extraction of features from the signal.
- Develop an autonomous system involving robotic aids to carry out damage monitoring of a submerged plate structure.
- Application of surface sensitive modes to compare the effectiveness of prevalent protection techniques like paints, coatings etc.

8.6 CLOSING REMARKS

This investigation is a step forward and should be useful in developing a non-destructive, non-contact, in-situ and in-service damage monitoring technique for submerged plates and their assemblies for monitoring in-service defects in the form of cracks, notches, dents and progressive corrosion due to environmental effects in marine structures. It also successfully attempts to assess their deterioration in strength, stiffness and mass loss due to corrosion and correlates it with ultrasonic voltages that would help in the non-destructive estimation of residual life of structures in submerged state.

LIST OF REFERENCES

Achenbach, J.D., Wave Propagation in Elastic Solids, Amsterdam, North Holland (1973).

Agarwala, V.S. and Ahmad, S. (2000), Corrosion detection and monitoring: A review. Corrosion/2000, Paper No. 271, NACE International, Orlando, Florida.

Agarwala, V.S. and Fabiszewski, A.(1994), Thin film micro sensors for integrity of coatings, composites and hidden structures, Corrosion/1994, Paper No. 342, Houston, Texas.

Alleyne, D.N. and Cawley, P.(1991), A 2-dimensional Fourier transform method for the measurement of propagating multi-mode signals, Journal of Acoustical Society of America., 89(3), pp. 1159-1168.

Alleyne, D.N. and Cawley, P. (1992), Optimization of Lamb waves inspection techniques, NDT& E International, 25(1), pp. 1-22.

Alleyne, D.N. and Cawley, P.(1992), The interaction of Lamb waves with defects, IEEE Transactions on Ultrasonics, Ferroelectrics and Frequency Control, IEEE, New York, 39(3), pp. 381-397.

Alleyne, D.N., Cawley, P., Lank, A.M. and Mudge, P.J. (1997), The Lamb wave inspection of chemical plant pipe network, Review of Progress in QNDE, Plenum Press New York, 16, pp. 1269-1276.

Alleyne, D.N., Pavlakovic, B., Lowe, M.J.S. and Cawley, P. (2001), Rapid long-range inspection of chemical plant pipework using guided waves, Insight, 43, pp. 93-96.

Atalar, A., Koymen, H. and Degertekin, F.L. (1990), Characterization of layered materials by the Lamb wave lens, IEEE Ultrasonic Symposium., Proc. Pubs. IEEE Service Ctr., Piscataway, New Jersey, pp. 359-362.

Atalar, A., Koymen, H. and Degertekin, F.L. (1992), A Lamb wave lens for acoustic microscopy, IEEE Transactions On Ultrasonics, Ferroelectrics and Frequency Control, IEEE, New York, pp. 661-667.

Auld, B., Acoustic Fields and Waves in Solids, Krieger, Malabar, Florida (1990).

Ball, D.F. and Shewring, D. (1994), Some problems in the use of Lamb waves for the inspection of cold-rolled steel sheet coil, Non-destructive Testing, 6(3), pp. 138-145.

Banerjee, S. and Kundu, T. (2006), Elastic wave propagation in sinusoidally corrugated waveguides, Journal of Acoustical Society of America, 119 (4), pp. 2006-2017.

Banerjee, S., and Kundu, T. (2008), Semi-analytical modeling of ultrasonic fields in solids with internal anomalies immersed in a fluid, Wave Motion, 45, pp. 585-591.

Bayliss, M., Short D. and Bax, M. Underwater Inspection, London, E & FN Spon (1988)

Benz, R., Niethammer, M., Hurlebaus, S. and Jacobs, L.J. (2003), Localization of notches with Lamb waves, Journal of Acoustical Society of America, 114 (2), pp. 677-685.

Benmeddour, F., Grondel, S., Assaad, J. and Moulin, E. (2008a), Study of the fundamental Lamb modes interaction with asymmetrical discontinuities, NDT & E International., 41 (5), pp. 330–340.

Benmeddour, F., Grondel, S., Assaad, J. and Moulin, E. (2008b), Study of the fundamental Lamb modes interaction with symmetrical notches, NDT & E International., 41 (1), pp. 1–9.

Bijudas, C. R., Mitra, M. and Mujumdar, P. M. (2013), Time reversed Lamb wave for damage detection in a stiffened aluminium plate, Smart Materials and Structures, 22(10), pp. 105026-105033.

Bindal, V.N., Transducers for ultrasonic flaw detection, Narosa Publishing House (1999).

Bingham, J. and Hinders, M. (2009), Lamb wave detection of delaminations in large diameter pipe coatings, The Open Acoustics Journal, 2, pp. 75-86.

Brekhovskikh, L.M, Waves in layered media. Academic Press, New York (1980).

Brekhovskikh, L.M. and Goncharo, V., Mechanics of continua and wave dynamics, Springer- Verlag (1985).

Bridge, B. and Ramli, A. (1990) , Non-destructive evaluation of the quality (cure) of polymeric coatings on steel food cans by means of high frequency Lamb wave propagation: a preliminary study, Journal of Materials Science, 25 (3), pp. 1794-1802.

Cawley, P. and Alleyne, D. (1996), The use of Lamb waves for the long range inspection of large structures, Ultrasonics, 34, pp. 287-290.

Challis, R.E. and Bork, U. (1995), Artificial Neural Network processing of Lamb wave data for adhesive bond characterisation, Proc. Ultrasonic International 1993, Butterworth-Heinemann, Oxford, UK, pp. 775-778.

Chen, J., Su Z. and Cheng, L. (2010), Identification of corrosion damage in submerged structures using fundamental anti-symmetric Lamb waves, Smart Materials and Structures, 19, pp. 1-12.

Chimenti, D.E., and Nayfeh, A. H. (1985), Leaky Lamb waves in fibrous composite laminates,

Journal of Applied Physics, 58, pp.4531-4538.

Jones, D., Principles and Prevention of Corrosion, 2nd Edition, Upper Saddle River, NJ, Prentice-Hall (1996).

Dalton, R. P., Cawley, P. and Lowe, M. J. S. (2000), The Potential of guided waves for monitoring large areas of metallic aircraft fuselage structures, Journal of Non Destructive Evaluation, 20(1), pp. 29-46.

Datta, D. and Kishore, N.N. (1996), Features of ultrasonic wave propagation to identify defects in composite materials modelled by finite element method, NDT & E International, 29 (4), pp. 213–223.

Davis G. D., Dacres C. M. and Krebs, L. A. (2002), In-situ corrosion sensor for coating testing and screening, Materials Performance, pp. 46-50.

Deng, Q. and Yang, Z., (2012), Scattering of S_0 and A_0 Lamb modes in a plate with multiple damage, Journal of Vibration and Acoustics, 134 , pp. 011004-011009

Ditri, J.J. and Rose, J.L. (1992), Excitation of guided elastic wave modes in hollow cylinders by applied surface tractions, Journal of Applied Physics, 72(7), pp. 2589-2595.

Ditri, J.J. and Rose, J.L. (1994), Excitation of guided waves in generally anisotropic layers using finite sources, Journal of Applied Mechanics, 61, pp. 330-338.

Drinkwater, B.W., and Wilcox, P., (2006), Ultrasonic arrays for non-destructive evaluation: A review, NDT&E International, 39, pp. 525–541

Edalati. K., Kermani, A., Seiedi, M. and Movafeghi, M. (2005), Defect detection in thin plates by ultrasonic lamb wave techniques, 8th International Conference of the Slovenian Society for Non-Destructive Testing in Engineering, pp. 35-43.

Ewing, W.M., Jardetzky, W.S. and Press, F., Elastic waves in layered media, Mc Graw-Hill, (1957).

Farnell, G.W. and Adler, E.L. (1972), Elastic wave propagation in thin layers, In W.P. Mason and R.N. Thunston, Editors, Physical Acoustics - principles and methods, pp. 35–127.

Fromme, P. and Sayir, M.B. (2000a), Detection of cracks at rivet holes using guided waves, Ultrasonics, 40, pp. 199–203.

Fromme, P., Wilcox, P.D., Lowe, M.J.S and Cawley, P. (2004), On the sensitivity of corrosion and fatigue damage detection using guided ultrasonic waves, IEEE International Ultrasonics, Ferroelectrics and Frequency Control, Joint 50th Anniversary Conference, pp. 1203-1206.

Fromme, P. and Sayir, M.B. (2000b), Measurement of the scattering of a Lamb wave by a through hole in a plate, Journal of Acoustical Society of America, 111 (3), pp. 1165-1170.

Ghosh, T., Kundu, T. and Karpur, P. (1998), Efficient use of Lamb modes for detecting defects in large plates, Ultrasonics, 36, pp. 791-801.

Graff, K.F., Wave motion in Elastic Solids (Dover Publications, New York (1991).

Guang, D., Wei, L., Ying, Z. and Feifei, L. (2002), An acoustic emission method for the in service detection of corrosion in vertical storage tanks, Materials Evaluation, 21(8), pp. 976-978.

Guo, N. and Cawley, P. (1993), The interaction of Lamb waves with delaminations in composite laminates, Journal of Acoustical Society of America ,94 (4), pp. 2240-2246.

Guo, D. and Kundu, T. (2001), A new transducer holder mechanism for pipe inspection, Journal of Acoustical Society of America, 110(1), pp. 303-309.

Hay, T.R., Royer, R.L., Gao, H., Zhao X. and Rose, J. L. (2006), A comparison of embedded sensor Lamb wave ultrasonic tomography approaches for material loss detection, Smart Materials and Structures, 15, pp. 946-951.

Habib, K. and Al-Sabti, F. (1997), Monitoring pitting corrosion by holographic interferometry, Corrosion, 53, pp.688-692.

James, C.P., McKeon and Hinders, M. K. (1999), Parallel projection and cross hole Lamb wave contact scanning tomography, Journal of Acoustical Society of America, 106(5), pp. 2568-2577.

Janarthan, B., Mitra M., and Mujumdar, P.M. (2013), Lamb wave based damage detection in composite panel, Journal of the Indian Institute of Science, 93, pp. 715-734.

Jones D., Principles and Prevention of Corrosion 2nd Edition. Prentice-Hall, Upper Saddle River, New Jersey (1996).

Johnson, D. (1992), Aboveground storage tank floor inspection using magnetic flux leakage, Materials Performance, pp. 36-39.

Jenot F., Ouaftouh, M., Duquennoy, M. and Ourak, M. (2001), Corrosion thickness gauging in plates using Lamb wave group velocity measurements. Measurement Science and Technology, 12, pp. 1287-1293.

Kishore, N. N., Sridhar, I. and Iyengar, N.G.R. (2000), Finite element modelling of the scattering of ultrasonic waves by isolated flaws, NDT & E International, 33(5), pp. 297-305.

Kolsky. H., Stress waves in solids. Dover Publications, New York (1963).

Krautkramer, J. and Krautkramer. H., Ultrasonic testing of materials. Springer-Verlag (1983).

Kundu, T. Potel, C. and Belleval, J.F. (2001), Importance of Near lamb mode imaging in multilayered composite plates, Ultrasonics, 39, pp. 283-290.

Kundu, T. and Placko, D., Advanced ultrasonic methods for material and structure inspection, ISTE Ltd., Newport Beach, CA 92663, USA (2007).

Lamb, H. (1917), On waves in an elastic plate, Conference of the Royal Society, pp. 114–128.

Lehfeldt, E. and Ho11er, P., (1967), Lamb waves and lamination detection, Ultrasonics, 5, pp. 255-257.

Lee, B.C. and Staszewski, W.J. (2003a), Modelling of Lamb waves for damage detection in metallic structures: Part-1, Wave Propagation, Smart Materials and Structures, 12, pp. 804-814.

Lee, B.C. and Staszewski, W.J. (2003a), Modelling of Lamb waves for damage detection in metallic structures: Part-1, Wave Interactions with damage, Smart Materials and Structures, 12, pp. 815-824.

Lee, B.C., Staszewski, W.J. (2007), Lamb wave propagation modelling for damage detection. Part II: Damage Monitoring Strategy, Smart Materials and Structures, 16 (2), pp. 260-274.

Leleux , A., Philippe, M. and Castaings, M., (2013), Long range detection of defects in composite plates using Lamb waves generated and detected by ultrasonic phased array probes, Journal of Non-Destructive Evaluation, 32, pp. 200–214.

Leonard, K.R., Malyarenko E.V. and Hinders, M.K. (2002), Ultrasonic Lamb wave tomography, IOP Inverse Problems, 18, pp. 1795-1808.

Leonard, K.R. and Hinders, M.K. (2005), Multimode Lamb wave tomography with arrival time sorting, Journal of Acoustical Society of America, 117(4), pp. 2028-2038.

Ledesma, M. N., Baruch, E. P., Demma, A. and Lowe, M. J. S. (2009), Guided wave testing of an immersed gas pipeline, Materials Evaluation, 67(2), pp. 102–115.

Leduc, D., Morvan, B., Pariege, P. and Izbicki, J.L. (2004), Measurement of the effects of rough surfaces on Lamb waves propagation, NDT&E International, 37, pp. 207–211.

Love, A. E. H., Some problems of geodynamics. Cambridge University, London (1911).

Lowe, M.J.S. (1995), Matrix techniques for modeling ultrasonic waves in multilayered media, IEEE

Trans.,Ultrasonics, Ferroelectrics and Frequency Control, 42(4), pp. 525-542.

Lowe, M.J.S., Alleyne, D.N. and Cawley, P. (1998), Defect detection in pipes using guided waves, Ultrasonics, 36, pp. 147-154.

Lowe, M. J. S. and Diligent, O. (2001), Reflection of the fundamental Lamb modes from the ends of plates, Review of Progress in Quantitative Non-Destructive Evaluation, AIP Conference Proceedings, 557, pp. 89-96.

Lu, Y., Ye L., Su, Z. and Nao Huang, N. (2007), Quantitative evaluation of crack orientation in aluminium plates based on Lamb waves, Smart Materials and Structures,16, pp. 1907–1914

Mal, A.K. and Bar-Cohen, Y. (1990), Characterization of composites using combined LLW and PBS methods, Review of Progress in Quantitative NDE, 10, Eds. D.O. Thompson and D.E. Chimenti, Plenum Press, New York, pp. 1555-1560.

Mansfield, T.L. (1975), Lamb wave inspection of aluminium sheet, Materials Evaluation, 33, pp. 96-100.

Marinetti, S and Vavilov, V. (2010), IR thermographic detection and characterization of hidden corrosion in metals: General Analysis, Corrosion Science, 52(3), pp. 865-872.

Mazeika, L., Kazys, R., Raisutis R. and Sliteris, R. (2011), Ultrasonic guided wave tomography for the inspection of the fuel tanks floor, International Journal of Materials and Product Technology, 41, pp.128-139.

Mijarez, R., Gaydecki, P. and Burdekin, M., (2007), Flood member detection for real-time structural health monitoring of sub-sea structures of offshore steel oilrigs, Smart Materials and Structures, 16, pp. 1857–1869.

Mohan, R. and Mitra, M., (2011), Lamb wave based tomography for damage detection in aluminium plate, Singapore International NDT Conference & Exhibition.

Nagy, P.B., Rose, W. R. and Adler L., (1986), A single transducer broadband technique for Leaky Lamb wave detection, Review of Progress in NDE, Eds. D.O. Thompson and D.E. Chimenti, Plenum Press, New York.

Na, W. B. and Kundu, T. (2002), Underwater pipeline inspection using guided waves, Journal of Pressure Vessel Technology, 124, pp. 196–200.

Nagy, P. (1996), Longitudinal guided wave propagation in a transversely isotropic rod immersed in fluid, Journal of Acoustical Society of America, 98 (1), pp. 454- 457.

Nayfeh, A.H. and Chimenti**,** D.E.(1983), Propagation of guided waves in fluid-coupled plates of fibre-reinforced composites, Journal of Acoustical Society of America, 83(5), pp. 1736-1743.

Nayfeh, A. U. (1986), Acoustic wave reflection from water-laminated composite interfaces, Review of Progress in Quantitative NDE, Eds. D.O. Thompson and D. E. Chimenti, Plenum Press, New York, 5, pp.1119-1128.

Ni, X. and Rizzo, P. (2012), Highly nonlinear solitary waves for the inspection of adhesive joints, Experimental Mechanics,52, pp. 1493–1501.

Okada, K. (1986), Ultrasonic measurement of anisotropy in rolled materials using surface wave, Japanese Journal of Applied Physics, 25 (1), pp. 197-199.

Panova A.A., Pantano P. and Walt D.R. (1997), In-situ fluorescence imaging of localized corrosion with a pH sensitive imaging fiber, Analytical Chemistry, 69, pp. 1635-1641.

Pavlakovic, B.N. and Cawley, P., DISPERSE User's Manual Version 2.0.1.1, Imperial College, University of London, London (2000).

Pearson, L. H., and Murri, W. J. (1986), Review of Progress in Quantitative NDE, Eds. D.O. Thompson and D. E. Chimenti, Plenum Press, New York, Vo1.5, pp.1093- 1101.

Perez, I. and Kulowitch, P. (2000), Thermography for characterization of corrosion damage', Corrosion /2000, Paper No. 290, NACE International, Orlando, Florida.

Pilant, W.L. (1972), Complex roots of the Stoneley wave equation, Bulletin of the Seismological Society of America, 62, pp.285–299.

Pistone, E., Li, K. and Rizzo, P., (2013), Non-contact monitoring of immersed plates by means of laser-induced ultrasounds, Structural Health Monitoring, 12(5-6), pp. 549–565.

Poddar, B., Tiwari, A., Mitra, M. and Mujumdar, P. M. (2011), Time reversibility of a Lamb wave for damage detection in a metallic plate, Smart Materials and Structures, 20, pp. 025001-025010.

Rayleigh, L. (1885), On waves propagating along the plane of an elastic solid, Proc. London Math. Soc., 17.

Rizzo, P., Han, J. and Ni, X. (2010), Structural health monitoring of immersed structures by means of guided ultrasonic waves, Journal of Intelligent Materials Systems and Structures, 21, pp. 1397-1407.

Rokhlin, S.I. (1979), Interaction of Lamb waves with delaminations in thin sheets, International

Advanced Non-Destructive Testing, 6, pp. 263-285.

Rokhlin, S.I. and Bende¢, F. (1983), Coupling of Lamb waves with the aperture between two elastic sheets, Journal of Acoustical Society of America, 73, pp. 55-60.

Rose, J.L., Fuller, M.C., Nestleroth, J.B. and Jeong, V.H. (1983), An ultrasonic global inspection technique for an offshore K-Joint, Soc. Petro. Eng J., 23, pp. 358-364.

Rose, W. R., Rokhlin, S. I., and Adler, L. (1986), Review of Progress in Quantitative

NDE, Eds. D.O. Thompson and D. E. Chimenti, Plenum Press, New York, 5, pp. 1111-1117.

Rose, J.L., Rajana, K. and Hansch, M.K.T.(1995), Ultrasonic guided waves for NDE of adhesively bonded structures, Journal of Adhesion, 50, pp. 71–82 .

Rose, J.L., Pelts, S.P. and Quarry, M.J. (1997), A Comb transducer for mode control in guided wave NDE , IEEE Ultrasonics Symposium, pp. 1033- 1036.

Rose, J.L., Ultrasonic Waves in Solid Media, Cambridge University Press, Cambridge, UK (1999).

Rose, J. L. (2002a), Standing on the shoulders of giants – An example of guided wave inspection, Materials Evaluation, 60, pp. 53-59.

Rose, J.L. (2002b), A baseline and vision of ultrasonic guided wave inspection potential, Journal of Pressure Vessel Technology, 124, pp 273-282.

Rose, J.L. (2003), NDT Solution–Guided wave testing of water loaded structures, Materials Evaluation, 60, pp. 23.

Saidarasamoot, S., Olson, D.L., Mishra, B., Spencer, J.S., Wang, G., (2003), Assessment of the emerging technologies for the detection and measurement of corrosion wastage of coated marine structures, Proceedings of OMAE'03, The 22nd International Conference on Offshore Mechanics & Arctic Engineering, Cancun, Mexico.

Santos, M.J. and Perdiga, J. (2005), Leaky Lamb waves for the detection and sizing of defects in bonded aluminium lap joints, NDT &E International, 38, pp. 561-568.

Santos, M.J. and Faia, P., (2009), Propagation of ultrasonic Lamb waves in aluminium adhesively bonded lap joints and in single plates, Research in Non-Destructive Evaluation, 20(3), pp. 178-191.

Scholte, J.G. (1947), The range of existence of Rayleigh and Stoneley waves, Geophysics, 5, pp. 120–126.

Sicard, R., Chahbaz, A. and Goyette J. (2003), Corrosion Monitoring of airframe structures using

ultrasonic arrays and guided waves, CP657, Review of Quantitative Non-destructive Evaluation, 22, Eds. D. O. Thompson and D. E. Chimenti, pp. 806-813.

Sicard, R., Chahbaz, A. and Goyette J., (2004), Guided Lamb Waves and L-SAFT Processing Technique for Enhanced Detection and Imaging of Corrosion Defects in Plates with Small Depth-to-Wavelength Ratio, IEEE Transactions on Ultrasonics, Ferroelectrics, and Frequency Control, 51 (10), pp. 1285-1297.

Silk, M.G. and Bainton, K.F. (1979), The propagation in metal tubing of ultrasonic wave modes equivalent to Lamb waves, Ultrasonics, pp.11-19.

Singh, D., Castaings, M. and Bacon, C. (2011),Sizing strip-like defects in plates using guided waves, NDT&E International, 44, pp. 394–404

Song W. J., Rose, J. L. and Whitesel, H. (2002), An ultrasonic guided wave technique for damage testing in a ship hull, Materials Evaluation, 61, pp. 94-98.

Song W.J., Rose, J.L., Galan, J.M., Abascal R. and Whitesel, H. (2003), Transmission and reflection of A_0 mode Lamb wave in a plate overlap, Review of Quantitative Non-Destructive Evaluation, pp. 1088-1094.

Sharma, S. and Mukherjee, A. (2010), Longitudinal guided waves for monitoring chloride corrosion in reinforcing bars in concrete, Structural Health Monitoring, 9(6), pp. 555-567.

Sharma, S. and Mukherjee, A. (2011), Monitoring corrosion in oxide and chloride environments using ultrasonic guided waves, Journal of Materials in Civil Engineering, 23, pp. 207-211.

Sharma, S. and Mukherjee, A. (2013),Non- Destructive evaluation of corrosion in varying environments using guided waves, Research in Non-Destructive Evaluation, 24, pp. 63-88.

Staszewski, W.J., Boller, C., Grondel, S., Biemans, C., O'Brien, E., Delebarre, C. and Tomlinson, G.R., Damage detection using stress and ultrasonic waves in health monitoring of aerospace structures, John Wiley & Sons, Germany, pp. 125-162 (2004).

Stoneley, R. (1924), Elastic waves at the surface of separation of two solids, Conference of the Royal Society, pp.416–428.

Su, Z.Q., Ye, L. and Lu, Y. (2006), Guided Lamb waves for identification of damage in composite structures: A Review, Journal of Sound and Vibration, 295, pp. 753-781.

Tang, B., and Henneke, E G. (1989),Lamb wave monitoring of axial stiffness reduction of laminated composite plates, Material Evaluation, 47, pp.928-934.

Titcomb, A.N. (1982), Evaluation of internal tank corrosion and corrosion control alternatives, 14th Annual OTC, Houston, Texas.

Tuzzeo, D. and Scalea, F.L. (2001), Non -contact air-coupled guided wave ultrasonics for detection of thinning defects in aluminium plates , Research in Non-Destructive Evaluation, 13(2), pp. 61 – 77.

Worlton, D.C. (1961), Experimental confirmation of Lamb waves at megacycle frequencies, Journal of Applied Physics, 32, pp. 967-971.

Wilcox, P., Lowe, M. and Cawley, P. (2005), Omnidirectional guided wave inspection of large metallic plate structures using an EMAT array, IEEE Trans. on Ultrasonics, Ferroelectrics and Frequency Control, 52(4), pp. 653-665.

Yang, W. and Kundu, T. (1998), Guided waves in multi layered anisotropic plates for internal defect detection, Journal of Engineering Mechanics, 124(3), pp.311-318.

Yeo, F. and Fromme, P. (2006), Guided ultrasonic wave inspection of corrosion at ship hull structures, Quantitative Non Destructive Evaluation, AIP Proceedings 820, 25, pp. 202-209.

Vavilov, V.R. (2003), Non-contact one-sided evaluation of hidden corrosion in metallic constructions by using transient infrared thermography, Rev. Metal Madrid Vol Extr., pp. 235-242.

Viktorov, I. A., Rayleigh and Lamb waves. Plenum Press, New York (1970).

Volker, A., Mast, A. and Bloom, J.T. (2008), Permanent corrosion monitoring using guided waves, 17th World Conference on Non-destructive Testing, 25-28 Oct 2008, Shanghai, China.